Université de Montréal

Les coûts énergétiques de l'activité des juvéniles du saumon atlantique (*Salmo salar* L.) dans un écoulement turbulent

par

Eva C. Enders

Département de sciences biologiques

Faculté des arts et des sciences

Thèse présentée à la Faculté des études supérieures

en vue de l'obtention du grade de

Philosophiæ Doctor (Ph.D.)

en sciences biologiques

Décembre 2003

Université de Montréal

Faculté des études supérieures

Cette thèse intitulée :

Les coûts énergétiques de l'activité des juvéniles du saumon atlantique (*Salmo salar* L.) dans un écoulement turbulent

présentée par

Eva C. Enders

a été évaluée par un jury composé des personnes suivantes :

Pierre Legendre
président-rapporteur

Daniel Boisclair
directeur de recherche

James W.A. Grant
membre du jury

John D. Armstong
examinateur externe

Anne Bourlioux
représentante du doyen de la FES

Thèse acceptée le :

SOMMAIRE

Plusieurs espèces de poisson sont en déclin. Ce déclin est causé entre autre par une diminution de la quantité et de la qualité de l'habitat fluvial. Les modèles bioénergétiques peuvent être utilisés afin d'assurer la protection, la restauration et la gestion des habitats des espèces menacées. Dans les modèles bioénergétiques, le gain énergétique net des poissons est utilisé pour décrire la qualité de l'habitat. Le métabolisme d'activité des poissons constitue l'une des variables clés de la modélisation bioénergétique. Conséquemment, les prédictions justes du modèle bioénergétique reposent sur des quantifications adéquates du métabolisme d'activité. On utilise généralement des modèles de nage forcée pour estimer le métabolisme d'activité des poissons en rivière. Ces modèles sont issus d'expériences où les poissons doivent nager dans un écoulement ayant une vitesse constante. Seulement, dans leur milieu naturel, les poissons sont confrontés à des écoulements turbulents où les vitesses fluctuent. On connaît peu l'influence que peut avoir la turbulence sur le comportement et sur le métabolisme d'activité des poissons.

Les objectifs de cette étude sont 1) d'analyser le comportement des juvéniles du saumon atlantique en relation avec les structures turbulentes des rivières, 2) de mesurer l'effet de la turbulence de l'écoulement sur les coûts énergétiques de nage en laboratoire et de comparer les résultats avec les prédictions des modèles existants de nage forcée et d'activité spontanée, 3) de comparer le métabolisme d'activité des juvéniles sauvages avec le métabolisme d'activité des juvéniles piscicoles et

domestiques ainsi que 4) de développer un modèle des coûts énergétiques de nage des juvéniles du saumon atlantique dans un écoulement turbulent.

Afin de répondre au premier objectif, nous avons développé une stratégie d'échantillonnage permettant d'observer le comportement des juvéniles et de mesurer simultanément la vitesse de l'écoulement en rivière. Les résultats de ces observations indiquent que les poissons ne semblent pas préférer les périodes de faibles vitesses pour initier leurs mouvements alimentaires. Cependant, les résultats révèlent que le temps alloué aux comportements alimentaires varie en fonction des caractéristiques de l'écoulement turbulent.

Pour répondre aux autres objectifs, nous avons développé une installation expérimentale permettant de mesurer l'effet de la turbulence sur les coûts énergétiques de nage. Nos premiers résultats démontrent que les coûts énergétiques de nage sont affectés par la vitesse moyenne et par l'intensité de la turbulence. Les coûts énergétiques de nage augmentent selon un facteur de 1.3 à 1.6 lorsque l'écart type de la vitesse augmente de 5 à 8 $cm \cdot s^{-1}$. Nous avons ensuite comparé les coûts énergétiques de nage mesurés aux prédictions obtenues à l'aide des modèles de nage forcée et d'activité spontanée. Les modèles de nage forcée sous-estiment de 1.9 à 4.2 fois les coûts effectifs de nage en écoulement turbulent alors que les modèles d'activité spontanée les surestiment de 2.8 à 6.6 fois. Une seconde série de résultats nous a permis de montrer que les coûts énergétiques de nage des poissons sauvages et piscicoles ne sont pas significativement différents. Les coûts énergétiques de nage des juvéniles piscicoles peuvent donc être utilisés pour estimer adéquatement les coûts énergétiques de nage des juvéniles sauvages. Les juvéniles domestiques

consomment de 12 à 29% plus d'oxygène que les juvéniles sauvages et piscicoles. Enfin, une troisième série de résultats mène à des modèles des coûts énergétiques de nage en fonction de la température de l'eau, de la masse corporelle, de la vitesse moyenne, de l'écart type de la vitesse et de l'énergie turbulente cinétique.

Cette étude contribue à augmenter nos connaissances sur les relations entre le comportement des poissons et la structure turbulente de l'écoulement en milieu naturel. Elle nous permet également de mieux comprendre l'influence d'un écoulement turbulent sur les coûts énergétiques de nage. Ces résultats ont des conséquences concrètes pour la modélisation des coûts énergétiques de nage des poissons évoluant dans les systèmes fluviaux. Nous devrons également en tenir compte dans la modélisation bioénergétique utilisée dans la restauration et la gestion des habitats ainsi que dans la conception d'ouvrages tels que des passes migratoires.

Mots clés: comportement du poisson; mouvement alimentaire; écoulement turbulent; turbulence; consommation d'oxygène; métabolisme d'activité; modèle de coûts énergétiques de nage; respirométrie; domestication; juvénile du saumon atlantique; *Salmo salar*.

SUMMARY

The activity metabolism of fish plays a key role in bioenergetics modeling. Consequently, the precise quantification of the activity metabolism is crucial to generate appropriate predictions from bioenergetics models. Generally, forced swimming models are used to estimate the activity metabolism of stream-dwelling fish. These models are developed from experiments in which fish swim in flows of constant velocities. However, in their natural environment stream-dwelling fish are confronted to highly fluctuating flows. Little is known on the effects of turbulent flows on fish behavior and fish energetics. The objectives of this thesis are 1) to analyze the behavior of juvenile Atlantic salmon (JAS) in relation to turbulent flow structures in gravel-bed rivers, 2) to measure the effect of turbulent flow on the swimming costs in the laboratory and to compare the results with predictions of existing forced and spontaneous swimming models, 3) to compare the swimming costs of wild JAS to those of farmed and domesticated JAS, and 4) to develop swimming costs models for JAS swimming in turbulent flows.

We developed a sampling strategy that allowed us to observe fish behavior and to measure simultaneously the flow velocity. Resulting from these observations, it seemed that JAS did not prefer low-speed flow events to undertake their feeding motions which would have led to a decrease in swimming costs. However, our findings indicated that the proportion of time fish allocated to motions varied according to characteristics of turbulent flow.

We developed an experimental design that allowed us to measure the effect of turbulence on the energetic cost of swimming. Our first series of experiments showed that the swimming costs increased with both mean flow velocity and standard deviation of flow velocity. Swimming costs increased by 1.3- to 1.6-times with an increase in the standard deviation of flow velocity of 5 and 8 $cm \cdot s^{-1}$. We compared the observed swimming costs to predictions of forced and spontaneous swimming models. The forced swimming model underestimated the actual swimming costs in turbulent flow by 1.9- to 4.2-fold. The spontaneous swimming model in opposite overestimated the actual swimming costs by 2.8- to 6.6-fold. In a second series of experiments, we showed that swimming costs of wild JAS were not significant different from farmed JAS. Swimming costs estimated from farmed JAS can therefore be applied to estimate adequately the swimming costs of wild JAS. However, domesticated JAS consumed 12.0 to 29.2% more oxygen than wild and farmed JAS swimming in turbulent flow. Finally, we developed swimming cost models for JAS swimming in turbulent flow using water temperature, body mass, mean flow velocity, standard deviation of flow velocity and turbulent kinetic energy as independent variables.

This study contributes to our comprehension off the relations between fish behavior and turbulent flow structures. We also improved our understanding off the effects of turbulent flow on the swimming costs of fish. These results have concrete consequences for the modeling of the swimming costs of stream-dwelling fish. They may equally be applied in bioenergetics modeling used in the restoration and the management of fish habitats as well as in the conception of migratory pass ways.

Keywords: fish behaviour; feeding motion; turbulent flow; turbulence; oxygen consumption rates; activity metabolism; swimming costs model; respirometry; domestication; juvenile Atlantic salmon; *Salmo salar*.

TABLES DES MATIÈRES

LISTE DES TABLEAUX

LISTE DES FIGURES

LISTE DES SYMBOLES

A	Amplitude d'un mouvement
ADV	Vélocimètre Doppler acoustique
BOD	Demande biologique d'oxygène
C	Consommation
C_A	Coûts énergétiques reliés à l'activité
C_R	Moyenne de coûts énergétiques totaux
χ^2	Khi carré
ΔO_2	Différence dans la concentration d'oxygène
δ	Distance
ECM	Courantomètre électromagnétique
F	Perte fécales
F1, F7	Première génération, septième génération
GEN	Gain énergétique net
IPH	Indices probabilistes de qualité d'habitat
IQH	Indices de qualité d'habitat
JAS	Juvéniles du saumon atlantique
l	Longueur caractéristique
L_t	Longueur totale
M	Masse corporelle de poisson
max	Dénote une valeur maximale
mean	Dénote une valeur moyenne
min	Dénote une valeur minimale
N, n	Nombre

p	Probabilité
P	Production de biomasse (croissance somatique et gonadique)
PC	Composante principale
R_e	Nombre de Reynolds
r	Corrélation linéaire de Pearson
R	Respiration
R_A	Métabolisme d'activité
R_S	Métabolisme standard
R_{SDA}	Métabolisme lié à la digestion
ρ	Densité de l'eau
SMR	Taux métabolique standard
SD	Écart type
SQRT	Racine carré
t	Temps
TI	Intensité turbulente
TKE	Énergie turbulente cinétique
U	Pertes d'excrétion
U	Vitesse dans la composante longitudinale de l'écoulement
u'	Fluctuation de vitesse longitudinale
$\bar{u}$	Valeur moyenne de la vitesse dans la composante longitudinale
V	Vitesse de nage
V	Vitesse dans la composante verticale de l'écoulement
v'	Fluctuation de vitesse verticale
$\overline{v}$	Valeur moyenne de la vitesse dans la composante verticale
ν	Viscosité cinématique
Vo_2	Consommation d'oxygène du poisson

V_W	Volume d'eau dans le respiromètre
W	Vitesse dans la composante latérale de l'écoulement
w'	Fluctuation de vitesse latérale
$\overline{w}$	Valeur moyenne de la vitesse dans la composante latérale

Der Salm

Ein Rheinsalm schwamm den Rhein
bis in die Schweiz hinein.
Und sprang den Oberlauf
von Fall zu Fall hinauf.
Er war schon weißgottwo,
doch eines Tages - oh! -
da kam er an ein Wehr:
das maß zwölf Fuß und mehr !
Zehn Fuß - die sprang er gut !
Doch hier zerbrach sein Mut.
Drei Wochen stand der Salm
am Fuß der Wasser-Alm.
Und kehrte schließlich stumm
nach Deutsch- und Holland um.

Christian Morgenstern

REMERCIEMENTS

Je tiens d'abord à remercier mon directeur, Daniel Boisclair, pour m'avoir donnée l'opportunité de faire ce doctorat à l'Université de Montréal, m'avoir fait confiance et m'avoir laissée une grande liberté pendant cette période doctorale. Je te remercie aussi pour avoir partagé ta vision sur la science appliquée et pour tes conseils, ta rigueur, tes commentaires judicieux lors de la rédaction des articles.

J'aimerais remercier chaleureusement André Roy de m'avoir accueillie au sein de ton équipe. Ton encouragement a été une source principale de motivation pour moi. Merci également pour l'initiation au monde de la géomorphologie fluviale, les discussions enrichissantes sur les articles, affiches et conférences et pour avoir partagé ton enthousiasme et ton dynamisme pour la recherche.

Je remercie John Armstrong et James Grant d'avoir accepté de faire parti du comité d'évaluation de cette thèse. J'aimerais également remercier Pierre Legendre pour sa participation en tant que président du jury ainsi que pour l'aide et les judicieux conseils statistiques.

Je tiens à remercier Thomas Buffin-Bélanger pour l'enthousiasme que tu as toujours apporté à mon projet. Je ne m'étendrai pas sur ta compétence, ta simplicité, ta disponibilité et les nombreuses discussions sur la turbulence. Je voudrais également te remercier pour ton aide toujours efficace et précise avec les problèmes de turbulence que j'ai pu avoir pendant mon doctorat.

Je remercie également Jean-Pierre Martin et Guillaume Guénard pour la conception et la construction de la « Magic Turbulence Box ». Merci à Emilie Pelletier, Anne Oberle, Sébastien Dupuis et Judith Bouchard pour l'aide apportée sur le terrain et en laboratoire.

J'exprime aussi toute ma gratitude vers le CIRSA qui m'a permis d'aller travailler à la rivière Sainte-Marguerite, ce paysage splendide. Un grand merci aux laboratoires de Julian Dodson, Joe Rasmussen et Normand Bergeron pour tous les instruments que je vous ai empruntés. Je dois un grand merci à André Boivin, Francis Bérubé, Mylène Levasseur, Geneviève Morinville, Véronique Thériault et Sophie Lenormand. Merci à Pascale Biron pour le prêt de l'ADV.

J'aimerais remercier la Pisciculture de Tadoussac et la Station NINA à Ims, Norvège de m'avoir accueillie pour effectuer les expériences respirométriques dans vos installations et pour avoir fourni les juvéniles du saumon atlantique. Je remercie vivement Dan Joseph de la Station gouvernementale de pisciculture à Dor, Israël qui m'a enseigné tout ce qu'il faut savoir sur la manipulation des poissons.

Un merci tout spécial à mes collègues et amis du laboratoire d'écologie des poissons, Nathalie Gaudreau, Jérôme Gingras, Frédéric Burton, Anik Brind'Amour, Jean-Cristophe Guay, et du laboratoire de géomorphologie fluviale, Antoine Richer, Claudine Boyer, Bruce MacVicar, Hélène Lamarre, Jay Lacey, pour votre complicité. Merci à tous ceux qui ont partagé mes heures de labo, merci pour les blagues et les rires que nous avons partagés et qui ont garanti le plaisir de chaque journée en votre compagnie. J'ai apprécié toutes vos contributions directes et indirectes. Je désire souligner ma reconnaissance envers tous mes amis de la « gang de Géo ». Merci beaucoup David Fortin, Geneviève Lapointe, Sandrine Solignac, Sonya Banal et Sylvie Manna.

Je remercie aussi Claudette Blanchard, secrétaire du GRIL, ainsi que les secrétaires du Département de sciences biologiques de l'Université de Montréal, spécialement Diane Lacasse et Joanne Noiseaux qui ont fait un grand effort de comprendre mon français des premières heures. Un grand merci à Ginette Méthot, Hélène Lavigne, Louise Pelletier et Louise Cloutier pour votre amabilité, disponibilité et efficacité.

Dankeschön de tout mon cœur à ma famille, mes parents Karl-Heinz et Doris, ainsi que mes grands-parents Heinrich et Ilse, j'ai toujours senti vos encouragements et votre confiance en moi, ce support a joué un grand rôle tout au long de mon parcours. Vielen Dank mon frérot Martin pour toutes tes recherches et tes petits programmes informatiques et pour être un merveilleux coéquipier dans le pool de Formule 1.

Tout spécialement, je désire remercier, François, pour ta foi en moi et ton soutien inconditionnel, pour tous les dimanches matins où nous sommes allés nourrir les poissons, pour toutes les traductions dans un français propre. Je te remercie pour ta patience, pour m'avoir écouté si attentivement et pour ta tendresse.

Je remercie les Fonds du Département de sciences biologiques et de la Faculté des études supérieures de l'Université de Montréal, la Fondation J.-A. Paulhus (Université de Montréal), la Groupe de Recherche Interuniversitaire en Limnologie ainsi que mon directeur de recherche Daniel Boisclair pour les bourses d'étude qui m'ont été accordées.

Et finalement, j'aimerais dire merci à tous les juvéniles du saumon atlantique qui ont posés devant la caméra dans la rivière Sainte-Marguerite et à ceux qui ont nagés en laboratoire dans les expériences respirométriques.

1 INTRODUCTION GÉNÉRALE

1.1 Les coûts énergétiques de l'activité

La locomotion est une caractéristique très largement répandue dans le règne animal. Contrairement au règne végétal, la plupart des animaux sont capables de se déplacer activement (Wehner et Gehring 1990). Ces déplacements sont nécessaires pour la quête de nourriture, la fuite face aux prédateurs et la migration entre les sites d'engraissement et de reproduction. La locomotion est cependant coûteuse au plan énergétique (Webb 1997). Par exemple, environ 40% du bilan énergétique des poissons est attribué au métabolisme relié à la locomotion (Brett et Groves 1979; Boisclair et Leggett 1989). C'est ce qui explique l'intérêt porté à l'étude des coûts énergétiques reliés aux déplacements. Ceci s'inscrit dans une approche écophysiologique où nous tentons de comprendre l'effet des facteurs biotiques et abiotiques sur les coûts énergétiques liés aux déplacements. Nous savons déjà que de nombreux facteurs comme la masse corporelle de l'organisme ou la vitesse des déplacements interviennent dans l'augmentation des coûts énergétiques (Winberg 1956; Brett 1973). Cependant, l'avancement des connaissances sur la turbulence des fluides en milieu fluvial (Roy et Buffin-Bélanger 2001), lié notamment à l'utilisation de nouvelles techniques de mesure, nous incite également à approfondir notre compréhension des interactions entre la turbulence et l'animal (Vogel 1994; Boisclair 2001). Nous savons déjà que plusieurs espèces ont des systèmes sensoriels bien adaptés au fluide en mouvement. Par exemple, l'oreille intérieure, la ligne latérale, le neuromaste ou la moustache, permettent de percevoir et d'interpréter les changements dans les caractéristiques des fluides ambiants (Northcutt 1997; Montgomery et al. 2000; Rinberg et Davidowitz 2000; Fraser et Shelmerdine 2002).

Ainsi, on a démontré que les phoques (*Phoca vitulina* L.) étaient particulièrement doués pour détecter avec leur moustache la turbulence dans le sillage des poissons (Dehnhardt et al. 2001). Ils réussissent ainsi à suivre précisément la trace hydrodynamique générée par une proie. McLaughlin et Noakes (1998) ont également montré que certains poissons réagissent à la turbulence. Ainsi, les coûts énergétiques de nage des juvéniles de l'omble de fontaine (*Salvelinus fontinalis* MITCHELL) varient en fonction de l'hétérogénéité spatiale de l'écoulement. Une étude récente a montré que les truites arc-en-ciel *(Oncorhynchus mykiss* WALBAUM) profitent des vortex de l'écoulement turbulent afin de minimiser les coûts énergétiques de nage (Liao et al. 2003). Nous ne savons cependant pas encore si les poissons réagissent aussi à l'hétérogénéité temporelle de l'écoulement. Dans cette perspective, nous tenterons de déterminer si les poissons utilisent l'hétérogénéité temporelle de l'écoulement pour minimiser leurs coûts énergétiques de nage. De plus, nous quantifierons les coûts énergétiques de nage dans un environnement turbulent. Il sera ensuite possible d'appliquer ces connaissances à la modélisation bioénergétique des poissons. Les modèles bioénergétiques pourront quant à eux être utilisés pour décrire la qualité de l'habitat et la distribution des poissons. L'approche bioénergétique s'applique à des problèmes reliés à la conservation d'espèce et à la gestion de la pêche et des habitats (Nislow et al. 2000). Ces connaissances pourront ultérieurement servir dans l'élaboration de projets de restauration d'habitat fluvial ou dans la conception de passes migratoires.

1.2 Sujet et structure de la thèse

Cette thèse se penche sur l'analyse de la relation entre le comportement des juvéniles du saumon atlantique et la structure turbulente de l'écoulement dans lequel

ils évoluent. Nous quantifierons aussi les coûts énergétiques de nage en relation avec l'écoulement turbulent. Nous comparerons de plus les coûts énergétiques de nage dans un écoulement turbulent pour des poissons sauvages, piscicoles (première génération en pisciculture) et domestiques (septième génération en pisciculture). Ensuite, nous estimerons les effets de facteurs comme la température et la masse corporelle sur les coûts énergétiques de nage. Finalement, nous développerons un modèle des coûts énergétiques de nage en milieu turbulent chez les juvéniles du saumon atlantique.

La thèse comporte sept chapitres. Afin de cerner la problématique et d'identifier les objectifs spécifiques de cette thèse, le deuxième chapitre présente d'abord une mise en contexte de la problématique à partir des connaissances et des limites actuelles des connaissances. Ce chapitre introduit ensuite l'espèce choisie, son comportement et son environnement, suivi des objectifs de l'étude et d'une description des méthodes utilisées. La présentation des observations de terrain et des expériences en laboratoire s'organise autour de quatre articles en préparation, soumis ou publié dans des revues scientifiques avec comité de lecture (Chapitres 3 à 6). Le troisième chapitre présente une analyse du comportement des juvéniles du saumon atlantique en relation avec les caractéristiques de l'écoulement turbulent en rivière. Cette étape permet de déterminer si le comportement des juvéniles du saumon atlantique varie en fonction des caractéristiques de l'écoulement turbulent. Les résultats indiquent que la proportion de temps que le juvénile alloue à ses mouvements varie avec les caractéristiques de l'écoulement turbulent. Cependant, les juvéniles du saumon atlantique ne semblent pas préférer les périodes de faibles vitesses pour entreprendre leurs attaques, ce qui n'est pas une stratégie optimale sur

le plan énergétique. Le chapitre 4 montre l'effet de la vitesse moyenne et de la turbulence de l'écoulement sur les coûts énergétiques de nage des juvéniles du saumon atlantique. Dans ce chapitre, comme dans les deux suivants, l'approche repose sur des expériences respirométriques menées en laboratoire. Les résultats confirment que les coûts de nage sont affectés par l'intensité de la turbulence. Pour une vitesse moyenne donnée de l'écoulement, les coûts de nage augmentent selon un facteur de 1.3 à 1.6 avec un accroissement de l'écart type de la vitesse de 5 à 8 $cm \cdot s^{-1}$. Ceci montre que des modèles où figurent explicitement la moyenne et l'écart type de la vitesse de l'écoulement sont nécessaires pour estimer les coûts de nage dans un écoulement turbulent. Le cinquième chapitre compare les coûts énergétiques de nage dans un écoulement turbulent des juvéniles du saumon atlantique sauvages, piscicoles et domestiques. Les résultats indiquent que dans un écoulement turbulent, les juvéniles sauvages et piscicoles consomment moins d'oxygène que les juvéniles domestiques. Les coûts énergétiques de nage des juvéniles piscicoles de première génération peuvent être utilisés pour estimer adéquatement les coûts énergétiques de nage des juvéniles sauvages. Le chapitre 6 porte plus particulièrement sur les facteurs influençant les coûts énergétiques de nage tels que la température, la masse corporelle, la vitesse moyenne et la turbulence de l'écoulement. Les résultats confirment que les coûts énergétiques de nage sont affectés par la température de l'eau, la masse corporelle, la vitesse moyenne et le niveau de turbulence. La conclusion générale de la thèse met en évidence la contribution originale de cette dernière aux connaissances.

2 LES COÛTS ÉNERGÉTIQUES DE L'ACTIVITÉ DES JUVÉNILES DU SAUMON ATLANTIQUE (*SALMO SALAR* L.) DANS UN ÉCOULEMENT TURBULENT

2.1 Contexte et problématique

Nous observons dans le monde entier un déclin alarmant des populations de plusieurs espèces de poissons (Kerr et Ryder 1997; Parrish 1999; Pauly et al. 2002). Les populations de prédateurs piscivores sont particulièrement en déclin (Christie 1972; Casey et Myers 1998). Ce phénomène est provoqué par une combinaison de plusieurs facteurs. Voici un aperçu des principaux facteurs susceptibles de causer la diminution des populations de grands poissons prédateurs piscivores.

La pêche commerciale joue un rôle clé dans la diminution ainsi que dans l'extinction des populations de poissons (Myers et Worm 2003; Pauly et Watson 2003). Les pêcheries ont atteint une ampleur industrielle au début du XIX^{ième} siècle lorsque les pêcheurs commencèrent à opérer des bateaux à vapeur. Les bateaux sont ensuite devenus de plus en plus efficaces grâce aux moteurs diesel et à l'équipement sophistiqué dont ils disposent (treuils, sonars, radars) (Pitcher et Hart 1982). L'évolution de l'équipement a permis aux pêcheries d'accroître l'effort de pêche et d'augmenter le nombre de captures même si les populations étaient déjà en baisse. Suite à l'effondrement d'une espèce, l'industrie de la pêche a tendance à cibler une nouvelle espèce et à concentrer ses efforts de pêche sur celle-ci. Le phénomène se répétant, nous observons que les espèces ciblées se retrouvent de plus en plus basses dans le réseau trophique (Pauly et al. 1998).

De même, la perturbation des habitats provoque aussi une diminution de l'abondance des populations (Berst et Spangler 1972; Christie 1972; Wells et McLain 1972). L'altération des habitats est causée par de multiples changements environnementaux de source naturelle et/ou anthropique. Ces changements sont fréquemment interreliés. Pour ces raisons, l'impact d'un facteur individuel est généralement difficile à évaluer. Au début de la civilisation, le déboisement et le brûlis des terres ont causé de l'érosion ainsi que l'affinement des sédiments dans les frayères de choix. Les migrations ont été bloquées par les digues de moulins et plus tard par des barrages hydroélectriques (Hartman 1972; Wilzbach et al. 1998). Le déboisement et le ralentissement des cours d'eau par les barrages ont provoqué une augmentation de la température de l'eau. L'utilisation accrue des substances nutritives et d'engrais par l'agriculture a contribué à l'accroissement des solides dissous dans l'eau de ruissellement, ce qui entraîne une eutrophisation des cours d'eau et des lacs (Regier et Hartman 1973). Pour sa part l'eutrophisation a provoqué une sérieuse désoxygénation, particulièrement des hypolimnions des lacs profonds (Christie 1972). L'eutrophisation et les contraintes dues à la pollution industrielle ont un impact négatif sur la survie des populations de poisson. Plus récemment, le réchauffement climatique est soupçonné d'avoir des effets négatifs sur la quantité et la qualité des ressources halieutiques (Schindler 2001). Les populations de poisson se trouvant déjà à leur limite de tolérance de température sont particulièrement en danger (Schindler 2001; Friedland et al. 2003). Finalement, l'invasion des espèces exotiques dans certains habitats a également provoqué le déclin des populations (Christie 1974). Les navires, de plus en plus rapides, transportent accidentellement dans les eaux de ballast différents organismes et les redistribuent partout sur la planète. Les espèces colonisatrices ainsi transportées mettent alors en danger des

écosystèmes établis souvent fragilisés par les facteurs nommés précédemment (Mills et al. 1994). En plus de ces espèces indésirables, l'ensemencement d'espèces non indigènes perturbe les populations autochtones. Plusieurs chercheurs soupçonnent même que des effets négatifs sur la survie des populations de poisson indigène sont causés par l'ensemencement d'individus provenant des piscicultures (Noakes et al. 2000; Jutila et al. 2003; Weber et Fausch 2003).

2.1.1 Contrôle et gestion de la ressource

De nombreux organismes se sont donné pour mission de gérer l'impact de la pêche au niveau international (FAO, ICES), national (DFO) et régional (ZEC). Les méthodes de contrôle des prises varient selon la stratégie de gestion et l'état des populations (restriction de la taille des poissons, quota sur certaines espèces, fermeture périodique de la pêche, moratoire sur la pêche).

La perte des habitats fluviaux est considérée comme l'un des principaux facteurs qui limitent le maintien des populations de poissons en rivière. Devant la diminution des populations survenue au cours des deux dernières décennies, nous avons vu une intensification de la recherche portant sur les relations entre la distribution des poissons et l'habitat fluvial. Dans le but de mettre en place des programmes efficaces de restauration et d'aménagement des rivières, il est impératif d'améliorer nos connaissances sur ces habitats. Ceci est d'autant plus essentiel qu'elles serviront aux gestionnaires de rivières pour évaluer et quantifier l'impact potentiel des projets de développement sur l'habitat des poissons.

2.1.2 Modélisation de l'habitat et de la distribution des poissons

De nombreux modèles d'habitat et de distribution des poissons ont été utilisés comme outils de gestion afin d'assurer la protection, la restauration et la gestion des habitats. Bien que quelques modèles aient été développés pour le milieu marin (Pauly et al. 2002), la plupart des modèles sont conçus pour les milieux fluviaux. Les intérêts multiples que peuvent représenter ces milieux expliquent cette attention particulière. Citons en exemple les nombreux ouvrages hydroélectriques construits en milieu fluvial, ces derniers nécessitent une gestion des débits et des niveaux d'eau des rivières.

Dans ce contexte, des modèles d'habitat physique tels que le *Physical Habitat Simulation* PHABSIM (Bovee 1982), le modèle d'Evaluation d'Habitats EVHA (Ginot et Souchon 1995) et les modèles numériques d'habitat (Leclerc et al. 1995; Guay et al. 2000) ont été développés afin de simuler la qualité de l'habitat. Les approches utilisées se fondent sur la modélisation de l'habitat physique et sur l'établissement d'indices de qualité d'habitat (IQH) ou d'indices probabilistes de qualité d'habitat (IPH). Ces indices sont généralement établis à partir trois variables : la vitesse moyenne, la profondeur de l'eau et le substrat. La distribution des poissons, en relation avec les variables physiques du milieu, est utilisée pour évaluer la qualité des microhabitats (point focal) ou des macrohabitats (tronçon de la rivière; Figure 2.1). L'efficacité des modèles d'habitat physique a cependant été critiquée (Orth et Maughan 1982; Mathur et al. 1985). À titre d'exemple, l'impact des variables biotiques comme la compétition intra- ou interspécifique et le risque de prédation n'est pas considéré dans ces modèles. De plus, on ne tient pas compte des variables physiques tels que la température, qui joue un rôle déterminant dans la

bioénergétique du poisson (Brett et Groves 1979; Ebersole et al. 2003). Par conséquent, dans le but d'optimiser les prédictions des modèles, plusieurs chercheurs ont proposé d'utiliser l'approche bioénergétique. On peut ainsi mieux lier la modélisation d'habitat avec les mécanismes biologiques (Fausch 1984; Hughes 1992; Van Winkle et al. 1998).

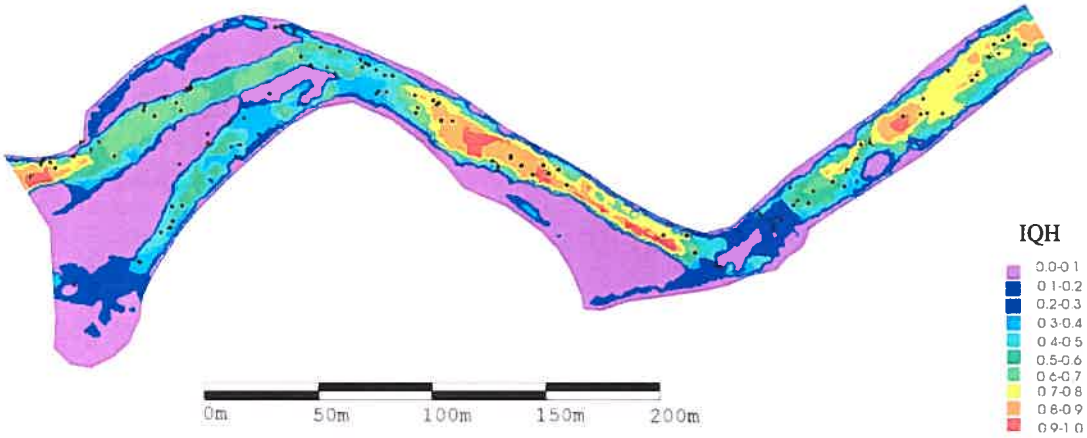

Figure 2.1 Évaluation de la qualité de l'habitat des juvéniles du saumon atlantique dans un tronçon de la rivière Sainte-Marguerite à l'aide d'un indice de qualité d'habitat (IQH). Le développement de l'IQH repose sur le patron d'utilisation de la profondeur, de la vitesse moyenne de l'écoulement et du substrat par les juvéniles du saumon atlantique. Les valeurs prédites d'IQH varient entre 0 (mauvais habitat) et 1 (excellent habitat). La distribution observée des poissons est présentée par les points noirs. Chaque point représente un poisson individuel (d'après Guay et al. 2000).

2.1.3 Modélisation bioénergétique

Dans les modèles bioénergétiques, on utilise le gain énergétique net (GEN) des poissons pour décrire la qualité de l'habitat (Hill et Grossman 1993; Sabo et al. 1996; Nislow et al. 2000; Vehanen et al. 2000). On suppose que les habitats de meilleure qualité sont situés là où le gain énergétique net est le plus élevé (Fausch 1984). Celui-ci est basé sur le bilan entre les gains et les dépenses énergétiques du poisson. Le modèle bioénergétique s'exprime comme suit (Winberg 1956) :

(2.1) $$C = P + R + F + U$$

où la consommation C est l'énergie consommée (nourriture absorbée), la production de biomasse P est l'énergie utilisée pour la croissance somatique et gonadique, la respiration R est l'énergie perdue sous forme de chaleur, F et U représentent respectivement les pertes fécales et les pertes d'excrétion (Wootton 1990; Figure 2.2). La respiration R se divise ensuite en trois composantes : le métabolisme standard, le métabolisme d'activité et le métabolisme relié à la digestion.

Les modèles bioénergétiques sont généralement utilisés pour estimer la dynamique des populations et/ou le taux de croissance des poissons (Stewart et al. 1983; Krohn et al. 1997; Bevelhimer 2002). Ils sont basés sur les estimations de toutes les composantes du budget énergétique. Chaque composante du modèle est estimée par un sous-modèle empirique ayant comme variables indépendantes la température de l'eau et la masse corporelle. La difficulté de la modélisation bioénergétique demeure la paramétrisation de ces variables, notamment les dépenses associées à l'activité des poissons. Les sous-modèles sont dérivés d'une multitude de méthode calorimétrique et respirométrique. Les paramètres sont souvent estimés en empruntant des données obtenues pour d'autres espèces. Par exemple, les modèles empiriques du métabolisme du saumon sockeye (*Oncorhynchus nerka*), qui a été intensivement étudié (Brett 1963; Brett 1964; Brett 1965), sont régulièrement appliqués afin d'estimer les métabolismes d'autres saumons pacifiques, par exemple le saumon chinook (*O. tshawytscha*), le saumon chum (*O. keta*),

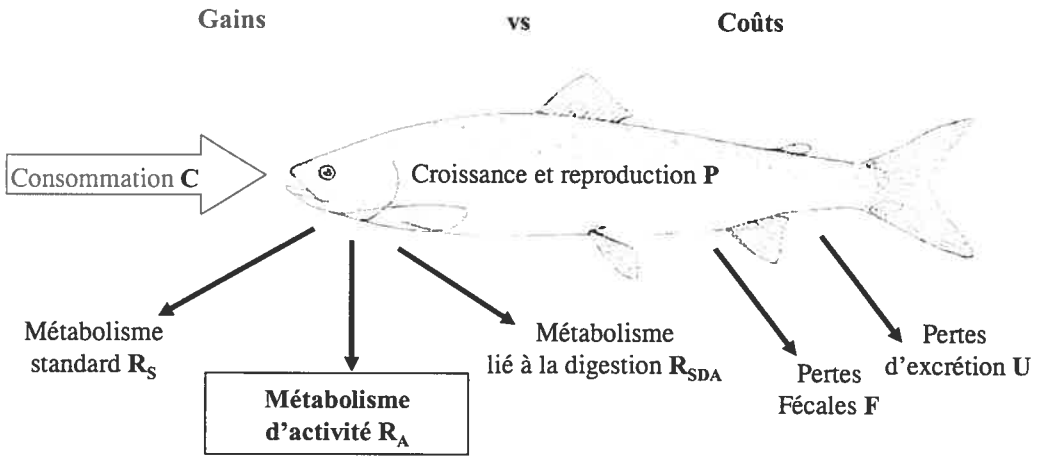

Figure 2.2 Modèle schématique de la répartition des gains et des coûts énergétiques d'un poisson. Les gains énergétiques sont acquis par la consommation C. Les coûts énergétiques incluent la production P (la croissance et la production), le métabolisme R, les pertes fécales F et les pertes d'excrétion U. Les coûts énergétiques reliés au métabolisme (respiration R) se divisent en métabolisme standard R_S, métabolisme d'activité R_A et métabolisme relié à la digestion R_{SDA}.

le saumon coho (*O. kisutch*) et le saumon rose (*O. gorbuscha*) (Stewart et Ibarra 1991; Davis et al. 1998; Rand et Stewart 1998). Ce qui nous amène à se poser la question de la transférabilité des modèles (Trudel et al. sous presse). Rappelons qu'une présomption inadéquate influence la précision de la prédiction générée par le modèle bioénergétique (Ney 1993). Parmi les composantes, le métabolisme d'activité est le plus variable et le plus important puisqu'il peut contribuer jusqu'à 40% du bilan énergétique (Brett et Groves 1979; Boisclair et Leggett 1989). Par conséquent, la quantification précise des coûts liés au métabolisme d'activité est d'une importance cruciale pour obtenir une prédiction juste du budget énergétique (Boisclair et Leggett 1989; Hansen et al. 1993; Ney 1993).

2.1.4 Modélisation des coûts énergétiques de nage

L'énergie utilisée par le poisson pour nager (migration, prédation et fuite) représente les coûts du métabolisme d'activité. Trois approches sont utilisées pour quantifier les coûts énergétiques de nage. Dans la première approche, le métabolisme

d'activité est défini comme un facteur fixe, généralement de deux à trois fois plus élevé que le métabolisme standard (Winberg 1956; Kitchell et al. 1977). Par contre, dans la deuxième approche (l'approche indirecte), le métabolisme d'activité représente la différence entre l'énergie consommée et l'énergie utilisée pour la croissance, le métabolisme standard, le métabolisme relié à la digestion, les pertes fécales et les pertes d'excrétions (Boisclair et Leggett 1989). Ceci s'applique dans la mesure où l'on a quantifié précisément les autres coûts énergétiques. La troisième approche, celle que nous avons choisie, mesure directement le métabolisme d'activité. Dans cette approche, nous devons d'une part connaître la quantité et l'intensité des mouvements du poisson dans son milieu naturel et d'autre part, les coûts énergétiques associés à ces mouvements. Les coûts énergétiques par unité de mouvement sont mesurés en laboratoire grâce à des expériences respirométriques.

Plusieurs méthodes ont été développées pour quantifier et décrire les mouvements du poisson dans son milieu naturel. On compte parmi celles-ci les expériences de marquage et de recapture (Arnold et Holford 1995), de pistage de banc de poissons avec un ultra sonar (Misund et Beltestad 1996; Pedersen 1996) ou de poisson individuel par radio-télémetrie (Diana 1980; Moore et al. 1990; Ovidio 1999). Les mouvements du poisson peuvent également être estimés en utilisant un indice de mouvement tel que les électrocardiogrammes (Wardle et Kanwisher 1974; Priede et Young 1977; Armstrong 1986; Sureau et Lagardere 1991; Lucas et al. 1993; Armstrong 1998), les électromyogrammes (Kaseloo et al. 1992; Briggs et Post 1997; Økland et al. 1997), ainsi que par l'enregistrement obtenu par des cameras stéréocinématographiques submersibles (Ménard 1991; Boisclair 1992). Toutes ces méthodes permettent d'analyser les mouvements du poisson à des échelles

temporelles et spatiales différentes. Les études télémétriques enregistrent l'activité du poisson durant des semaines ou des années dans un tronçon ou sur la totalité de la rivière tandis que la méthode vidéo donne des informations de l'activité pendant quelques heures ou une journée dans le microhabitat.

Une fois le patron d'activité établi, nous devons connaître les relations entre les caractéristiques des mouvements et les dépenses énergétiques afin de transformer ces mouvements en coûts énergétiques d'activité. Les relations sont généralement développées à partir d'expériences respirométriques en laboratoire. Deux types d'approche sont utilisés à cette fin. Dans la première approche, le métabolisme d'activité est mesuré alors que le poisson est forcé de nager contre un écoulement dans un chenal expérimental (Brett 1964; Brett 1965; Fry 1971; Beamish 1978; Brett et Groves 1979; Schurmann et Steffensen 1994). Les expériences de nage forcée ont montré que les coûts énergétiques de nage augmentent de façon exponentielle avec la vitesse de l'écoulement (Figure 2.3). La nage à vitesse soutenue n'étant qu'une infime partie du patron d'activité du poisson, il serait important de tenter d'obtenir des mesures quantitatives des coûts énergétiques associés à d'autres phases de nage du poisson (accélération, virage et changement de direction). On définit généralement ces patrons comme « l'activité spontanée » du poisson. Les mesures basées sur l'activité spontanée du poisson représentent la deuxième approche. Ici, contrairement aux expériences de nage forcée, le poisson nage librement dans un respiromètre sans être soumis à un écoulement. Auparavant, les coûts énergétiques de l'activité spontanée étaient évalués à partir (1) d'enregistreurs d'activité mécanique (Spoor 1946), (2) de senseurs de chaleur (Kausch 1968) ou (3)

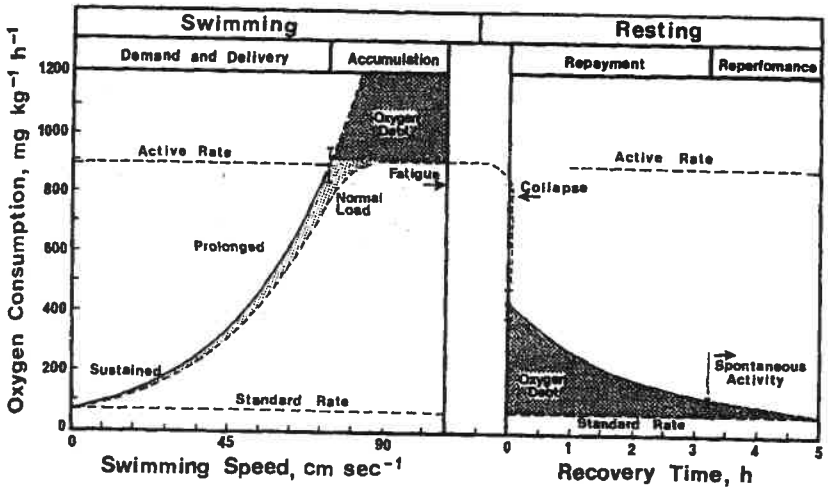

Figure 2.3 La consommation d'oxygène du saumon sockeye en relation avec la vitesse de la nage à 15°C (d'après Brett 1964).

de cellules photographiques (Smit .1965). Aujourd'hui, les expériences respirométriques nous permettent d'estimer les coûts énergétiques de l'activité spontanée en enregistrant simultanément l'activité du poisson avec un appareil vidéo (Koch et Wieser 1983; Krohn et Boisclair 1994; Tang et Boisclair 1995).

La comparaison des résultats des deux approches montre que les coûts énergétiques de nage avec une vitesse constante (expérience de nage forcée) sont significativement moins élevés que ceux de l'activité spontanée (Boisclair et Tang 1993). Pour des poissons ayant une même masse corporelle et nageant à la même vitesse moyenne, les coûts énergétiques associés à l'activité spontanée sont de 3 à 22 fois plus élevés que les coûts énergétiques associés à la nage forcée (Tang et al. 2000). La différence est attribuée aux coûts énergétiques engendrés par les virages et les accélérations (Enders et Herrmann 2003). Ces derniers n'existent pas dans les expériences de nage forcée (Forstner et Wieser 1990; Boisclair et Tang 1993). L'augmentation des coûts énergétiques lors de l'activité spontanée s'explique par l'utilisation des muscles blancs qui ne sont pas sollicités pour la nage forcée à vitesse

constante. Lorsque les poissons nagent à vitesse constante, ils se servent du métabolisme aérobique (muscles rouges). Par contre, lors des mouvements plus complexes, comme les virages et les accélérations, ils utilisent le métabolisme anaérobique (muscles blancs). Le métabolisme anaérobique étant moins efficace, le poisson doit dépenser plus d'énergie (Goolish et Adelman 1987).

Plusieurs études portant sur les poissons en rivière s'appuient sur un modèle bioénergétique basé sur l'estimation des coûts d'activité à partir de modèles de nage forcée. Dans ces modèles, les coûts énergétiques sont estimés à partir de la vitesse moyenne de l'écoulement. On présume donc que les poissons, dans leur milieu, nagent contre une vitesse constante d'écoulement (Hughes et Dill 1990; Vehanen et al. 2000). Nous tenterons de vérifier la validité de ces postulats. Pour y arriver, nous allons d'abord présenter l'espèce choisie afin de tester les présomptions préalablement mentionnées.

2.2 Le saumon atlantique (*Salmo salar* L.)

2.2.1 Choix de l'espèce

Dans le contexte de l'analyse du comportement et des coûts énergétiques de nage des poissons vivant en rivière, nous avons choisi le saumon atlantique pour faire notre étude. C'est une espèce qui vit, dans son stade juvénile, dans des habitats fluviaux caractérisés par une grande variabilité de la vitesse d'écoulement. Dans cet environnement, les juvéniles exécutent des déplacements intermittents afin de se nourrir de la dérive. Les mouvements intermittents augmentent généralement les coûts énergétiques à cause des accélérations et des décélérations (Krohn et Boisclair 1994; Tang et al. 2000; Kramer et McLaughlin 2001). Selon la théorie de quête

alimentaire optimale, les juvéniles devraient être sensibles à la variabilité des coûts énergétiques de nage dans un fluide où les vitesses changent dans le temps et l'espace. De plus, plusieurs études ont récemment démontré que les salmonidés modifient leur quête alimentaire en fonction de la disponibilité de nourriture, de la compétition et de la présence de prédateurs (Höjesjö et al. 1999; Johnsson 2003). Les salmonidés considèrent donc instinctivement les coûts énergétiques d'une quête alimentaire, les coûts associés à la compétition ainsi que le risque de prédation avant d'amorcer un mouvement de quête alimentaire qui mènera à un gain énergétique (Vehanen 2003). Le recours à une stratégie alimentaire qui minimise les coûts énergétiques de nage dans un écoulement variable et turbulent ne serait en conséquence pas étonnant pour les juvéniles du saumon atlantique. Ces caractéristiques font en sorte que le saumon atlantique est une espèce appropriée pour répondre aux objectifs de cette étude. De plus, le saumon atlantique à l'état sauvage est considéré comme une espèce menacée ayant d'ailleurs disparu de plusieurs rivières d'Europe et d'Amérique du Nord (Bardonnet et Baglinière 2000; COSEWIC 2002). À l'origine, la distribution du saumon atlantique s'étendait à toutes les rivières appropriées qui coulent vers l'Atlantique Nord, la mer du Nord et la mer Baltique (MacCrimmon et Gots 1979). En France, par exemple, le nombre de rivières dans lesquelles se trouvent les saumons atlantiques a fortement diminué depuis le milieu du XVIII^{ième} siècle (Figure 2.4). Aujourd'hui, on retrouve encore des populations de saumon atlantique dans la Loire et dans quelques rivières de Bretagne, de Normandie et du Pays Basque français. La complexité de son cycle de vie rend le saumon atlantique davantage vulnérable aux changements anthropiques. Pour mieux comprendre, nous allons d'abord décrire le cycle de vie du saumon atlantique.

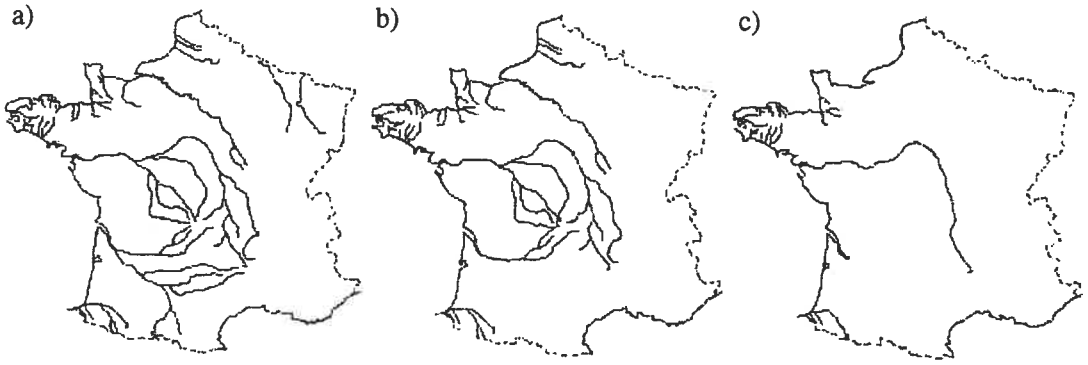

Figure 2.4 Changement temporel du nombre des rivières colonisées par le saumon atlantique en France. a) Au milieu du XVIII^{ième} siècle, b) à la fin du XIX^{ième} siècle, c) à la fin du XX^{ième} siècle (d'après Bardonnet et Baglinière 2000).

2.2.2 Le cycle de vie du saumon atlantique

Le saumon atlantique (*Salmo salar* LINNAEUS, 1758) est une espèce anadrome qui partage sa vie entre l'eau douce et l'eau salée (Figure 2.5). Quelques populations de saumons atlantiques peuvent aussi réaliser l'ensemble de leur cycle de vie en eau douce, on l'appelle alors « ouananiche ». Cependant, la plupart des populations doivent évoluer dans deux environnements distincts afin de compléter leur cycle de vie. Premièrement, en rivière, où les saumons adultes frayent et les juvéniles s'alimentent et deuxièmement, en mer, où a lieu la phase adulte des saumons (Mills 1989). Après avoir passé de deux à quatre ans en mer, les saumons adultes remontent leurs rivières natales (montaison) pour s'y reproduire. Lors de la montaison, les saumons arrêtent de se nourrir jusqu'à leur retour en mer, six mois ou un an plus tard. La fraie débute tard à l'automne (mi-octobre à mi-novembre). Les frayères optimales se caractérisent par un substrat graveleux sans limon (Moir et al. 2002). Considérant leur masse corporelle, les femelles produisent relativement peu d'œufs, entre 2,000 et 15,000. Elles creusent un nid et y déposent les œufs. Les mâles fécondent ensuite ces œufs avant que les femelles ne les recouvrent de graviers afin d'assurer une aération adéquate et une bonne protection. Une fécondité élevée n'est

donc pas nécessaire puisque les œufs sont bien protégés dans le substrat; ils y restent pendant tout l'hiver. Contrairement aux saumons pacifiques (*Oncorhynchus* spp.), environ 40% des saumons atlantiques survivent à la fraie et peuvent se reproduire plusieurs fois. Ils hivernent dans les fosses de la rivière et dévalent vers la mer au printemps suivant. La période d'éclosion des œufs s'étend de la fin mars au début avril. Suite à l'éclosion, les alevins vésiculés absorbent leur sac vitellin en progressant vers la surface du substrat. Après quatre à cinq semaines, les alevins émergent du substrat et se nourrissent dans les zones peu profondes caractérisées par un écoulement de faible vitesse. Après un an, les juvéniles atteignent le stade de tacon. Les tacons présentent des marques verticales foncées sur les flancs ainsi qu'une rangée de points rouges le long de la ligne latérale. Pendant la phase de vie en eau douce, les tacons sont territoriaux, ils ont des exigences très précises quant au choix de leur microhabitat. Ils se nourrissent alors principalement d'invertébrés. Puis, au printemps de la deuxième ou troisième année de vie, les tacons passent par un ensemble de modifications qui vont leur permettre de pouvoir vivre et croître en milieu marin. Ce phénomène de smoltification entraîne des changements morphologiques (forme du corps, livrée), comportementaux (abandon du comportement territorial) et physiologiques (osmorégulation, excrétion) complexes. Les saumoneaux présentent une pigmentation argentée. En mai ou en juin, les saumoneaux dévalent les rivières et entreprennent une migration vers la mer. L'empreinte olfactive de la rivière se produit à ce stade, ce qui permettra aux saumons de retrouver leur rivière natale. En mer, les saumons gagnent des zones d'engraissement parfois éloignées. Par exemple, la plupart des populations de saumon atlantique des rivières d'Amérique du Nord migrent vers les Grands Bancs de Terre-Neuve et la mer du Labrador (Friedland et al. 2000). Cependant, quelques

saumons atlantiques d'Amérique du Nord traversent l'Atlantique Nord et joignent les saumons atlantiques d'Europe dans les zones d'engraissement situées autour des Iles Féroé ainsi que dans la mer de Norvège (Hansen et Jacobsen 2003). Aussi, 25 à 66% des saumons atlantiques de la côte ouest du Groenland proviennent de rivières européennes (Reddin et Friedland 1999). Les saumons se nourrissent principalement de poissons et de crustacés. Après être restés en général de deux à quatre ans en mer, les saumons retournent dans leur rivière natale pour frayer à leur tour; c'est ainsi que se ferme le cycle de vie du saumon atlantique (Figure 2.5). Le saumon atlantique fait preuve d'une considérable plasticité phénotypique et peut avoir, selon les individus, un cycle biologique variable (Klemetsen et al. 2003). Par exemple, pour atteindre leur maturité, les saumons doivent généralement séjourner en mer pour une période de deux à quatre ans. Cependant, certains individus, nommés madeleineaux, séjournent en mer pendant seulement une année et reviennent en rivière beaucoup plus petits que les grands saumons. Le ratio du nombre de madeleineaux versus le nombre de grands saumons varie selon les années et les rivières. Par exemple, dans la rivière Miramichi Nord-Ouest, on compte en moyenne 4 saumons adultes pour 100 madeleineaux. Par contre, dans la Miramichi Sud-Ouest, en moyenne 182 saumons adultes remontent la rivière pour 100 madeleineaux (ICES 2003). D'autres poissons deviennent matures sans jamais quitter la rivière (tacons précoces). Le pourcentage de tacons mâles précoces peut être très important. Dans la rivière Sainte-Maguerite, par exemple, entre 39% à 45% des tacons atteignent leur maturité à l'âge d'un an, 71% à 80% des tacons sont mature à l'âge de deux ans (Aubin-Horth 2002). De façon similaire, dans la rivière Imsa en Norvège, environ 82% des tacons atteignent leur maturité à l'âge d'un an en rivière (Bohlin et al. 1986).

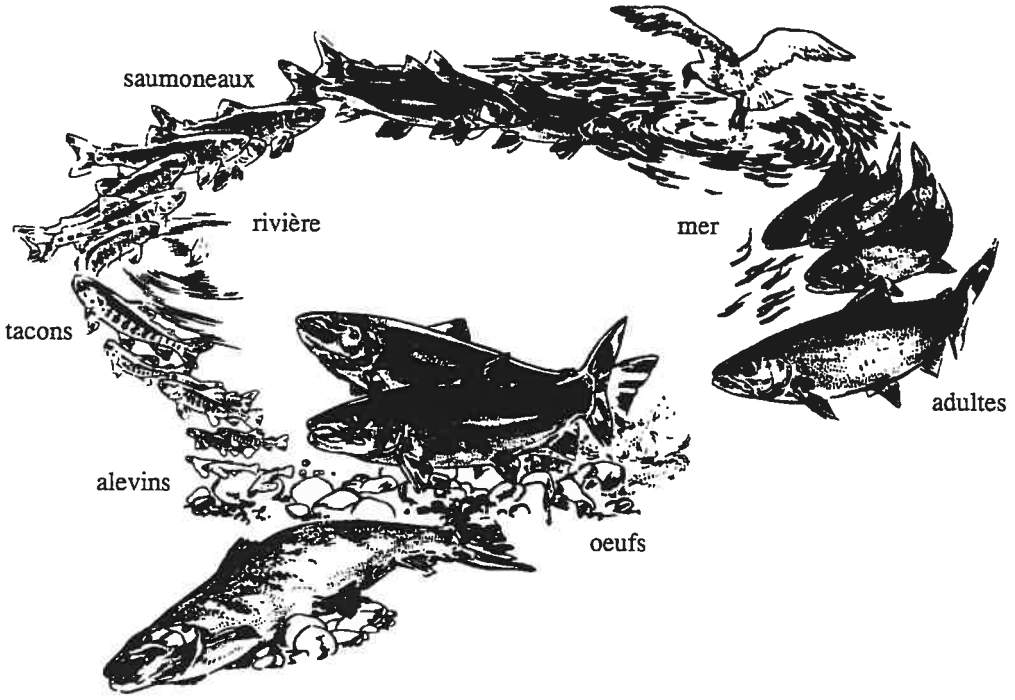

Figure 2.5 Cycle de vie du saumon atlantique (d'après Mills 1989).

2.2.3 Les périls pour la survie des populations du saumon atlantique

Nous avons vu que plusieurs populations d'espèces de poissons prédateurs piscivores sont en déclin. Le saumon atlantique est une de ces espèces. Nous avons également présenté les facteurs causant le déclin et nous allons maintenant discuter des facteurs qui s'appliquent spécifiquement au saumon atlantique. Premièrement, la pêche du saumon atlantique est une tradition profondément ancrée dans la culture occidentale. Dans le passé, la pêche commerciale à grande échelle du saumon atlantique a contribué au déclin de cette espèce (Dempson et al. 2001; Figure 2.6). Depuis 1992, la pêche commerciale du saumon atlantique est interdite au Canada (ICES 2003). Cependant, les pêcheurs sportifs exercent encore une pression sur les populations affaiblies de saumon atlantique. Une gestion efficace des populations du saumon atlantique est donc nécessaire afin d'assurer la pérennité de cette ressource.

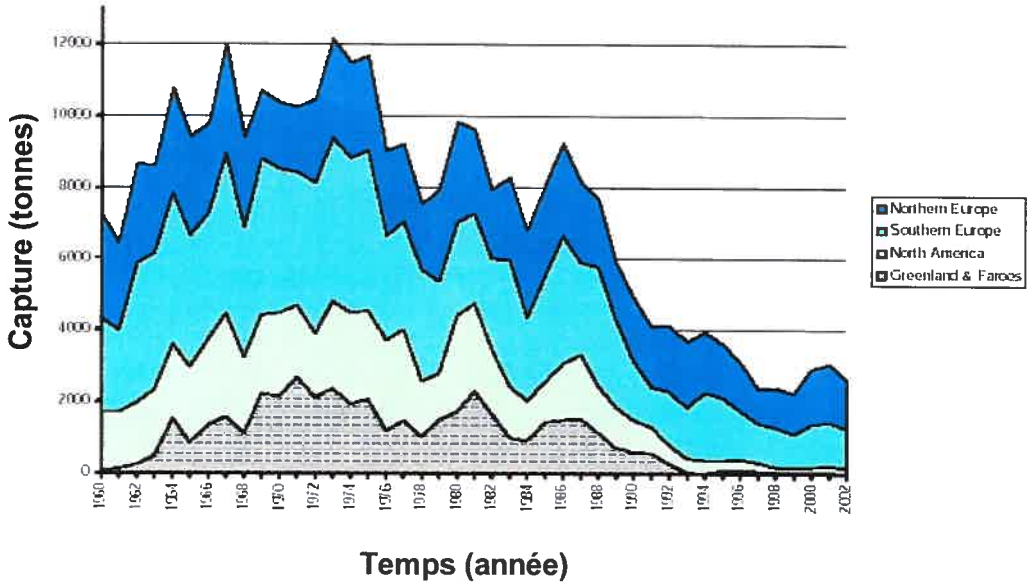

Figure 2.6 Capture de saumons atlantiques dans l'Atlantique du Nord entre 1960 et 2002 (d'après ICES 2003).

Deuxièmement, la diminution du nombre de rivières appropriées pour la fraie et la croissance des juvéniles a aussi un effet négatif sur la survie du saumon atlantique. Nous observons effectivement une forte diminution de la quantité ainsi qu'une importante dégradation de la qualité des habitats fluviaux. Cette diminution est largement attribuable aux changements anthropiques (Mills 1989).

En troisièmement lieu, le saumon atlantique a besoin de se déplacer librement entre deux habitats distincts afin de compléter son cycle biologique. Ainsi, les saumoneaux doivent pouvoir descendre les rivières vers la mer et les remonter pour aller frayer lorsqu'ils sont adultes. Les écluses de navigation et les barrages hydroélectriques représentent souvent des barrières insurmontables pour la migration des saumoneaux et des saumons adultes. Au Québec, on a d'abord installé des digues de moulin, puis des barrages hydroélectriques sur plusieurs rivières à saumon, ce qui a conduit au déclin et même à l'extinction des populations de saumon atlantique de ces rivières. Par contre, l'espèce a été restaurée grâce à des campagnes d'ensemencements de saumons provenant des pisciculture de Tadoussac et de

Gaspé. De plus, des passes migratoires furent construites pour que les saumons puissent remonter les rivières.

Quatrièmement, les conditions océaniques telles que la température et la disponibilité de la nourriture jouent un rôle important dans l'abondance et la qualité des géniteurs ainsi que pour le maintient de l'espèce en mer (Scarenecchia 1984; Friedland et al. 1998). Le taux de croissance et la survie des adultes en mer augmentent avec la température de l'eau de surface. L'augmentation de la température de l'eau exerce également un effet positif sur l'abondance de nourriture dans les zones d'engraissements des saumons atlantiques (Friedland et al. 2000), ceci favorise à son tour le taux de croissance et conséquemment la survie des saumons. Friedland et al. (2000) mentionnent cependant que des changements climatiques drastiques qui pourraient mener à une augmentation prononcée de la température de l'eau pourraient avoir des conséquences néfastes sur la survie des saumons en mer.

Enfin, l'introduction de saumons provenant de pisciculture semble avoir un effet négatif sur les populations sauvages (Gross 1998). Les populations de saumon atlantique ne sont pas seulement confrontées aux poissons piscicoles ensemencés mais aussi aux individus domestiques qui s'échappent des pisciculture commerciales. Fleming et al. (1994) ont montrés que les saumons domestiques provenant de la pisciculture ont subi des changements morphologiques et comportementaux importants et qu'ils diffèrent à plusieurs égards de leurs ancêtres sauvages. Le nombre des saumons atlantiques en pisciculture a connu une croissance exponentielle depuis les années 80 (Figure 2.7). L'invasion de saumons domestiques échappés des pisciculture en milieu naturel pourrait non seulement augmenter la

compétition pour les ressources naturelles mais aussi résulter en des changements génétiques; ceci pourrait mener à un déclin de la fitness des populations sauvages (Noakes et al. 2000; Jutila et al. 2003; Weber et Fausch 2003).

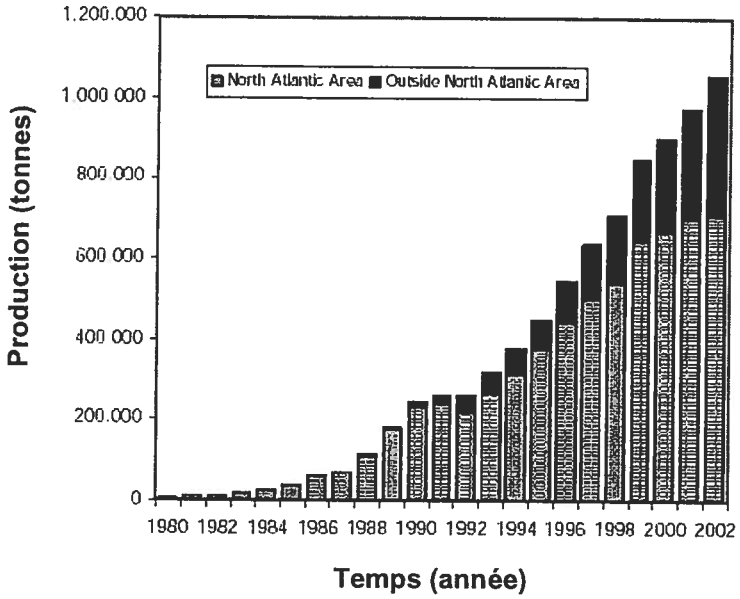

Figure 2.7 Production de saumons atlantiques en pisciculture entre 1980 et 2002 (d'après ICES 2003).

2.2.4 Le comportement des juvéniles du saumon atlantique

Les saumons atlantiques juvéniles vivent dans des rivières à lit de gravier où ils exercent un patron d'activité complexe qui varie sur plusieurs échelles temporelles (saisonnière et journalière). En été, les juvéniles sont principalement actifs durant la journée et ils se cachent dans les interstices du substrat pendant la nuit (Gries et Juanes 1998). Par contre, l'hiver, ils sont exclusivement actifs durant la nuit. Ce changement de comportement répond aux variations de la température de l'eau. Quand l'eau est froide, généralement en dessous de 8°C, les juvéniles sont plutôt nocturnes, ce qui leur permet d'éviter les prédateurs diurnes au moment où la température froide de l'eau ralentit leur vitesse de nage. Cependant, étant des prédateurs visuels, il devient alors plus difficile pour les juvéniles de détecter leur nourriture étant donné les conditions de faible luminosité (Fraser et Metcalfe 1997).

Dans les rivières subarctiques, où la température de l'eau demeure sous 8°C durant l'été, on observe également des habitudes nocturnes chez les juvéniles (Rimmer et al. 1983; Fraser et al. 1993; Fraser et al. 1995). Durant l'été, lorsque la température de l'eau excède 8°C, les juvéniles s'alimentent principalement durant la journée. Ils se nourrissent d'invertébrés aquatiques tels que les éphéméroptères, trichoptères, plécoptères, chironomides, diptères, annélides et mollusques (Rader 1997). Selon le stade de vie et le moment de la journée, ces organismes se trouvent en dérive dans l'écoulement ou sur le substrat de la rivière. Les invertébrés sont plus actifs la nuit afin d'éviter les prédateurs visuels comme les juvéniles du saumon atlantique (Rader 1997). Pendant les journées ensoleillées, 75% de l'alimentation des juvéniles se fait par capture d'invertébrés à la dérive (Stradmeyer et Thorpe 1987a). Par faible luminosité, durant la nuit ou lors de journées nuageuses, l'alimentation benthique peut aussi être importante (Nislow et al. 1998; Armstrong et al. 1999; Amundsen et al. 2000).

Les juvéniles du saumon atlantique sont territoriaux. Ils défendent leur site d'alimentation contre leurs congénères qui s'y introduisent (Kalleberg 1958; Keenleyside et Yamamoto 1961). Lorsque l'espace est limité et que la densité des juvéniles est élevée, une compétition intraspécifique pour les meilleurs sites s'établit. Lors des périodes d'alimentation, les juvéniles du saumon atlantique se positionnent au-dessus d'une roche-mère qui leur sert d'abri. Le comportement alimentaire des juvéniles est représenté par une succession de mouvements allant de la roche-mère vers la surface de la rivière pour capturer les invertébrés transportés par l'écoulement (Figure 2.8).

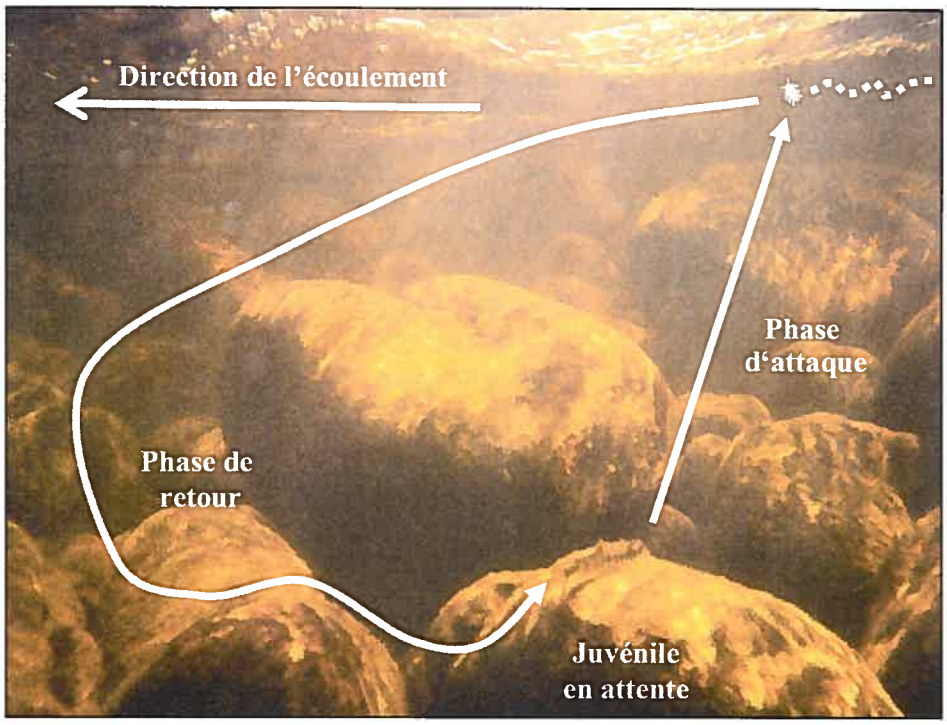

Figure 2.8 Mouvement alimentaire des juvéniles du saumon atlantique capturant les invertébrés transportés par l'écoulement.

Si les proies sont suffisamment proches, les juvéniles peuvent aussi les capturer par un simple mouvement latéral de la tête (Stradmeyer et Thorpe 1987b). Lorsque le juvénile se tient en position sur sa roche-mère, il déploie ses nageoires pectorales de façon à ce que l'écoulement de l'eau exerce une pression sur les nageoires et pousse le corps du juvénile vers le substrat de la rivière (Figure 2.9). Bien que plusieurs auteurs soupçonnent que les coûts énergétiques liés à cette position sont équivalents aux coûts énergétiques de nage forcée (Fausch 1984; Hughes et Dill 1990), il est généralement admis que se maintenir dans cette position n'entraîne aucune augmentation du taux métabolique (Facey et Grossman 1992; Johnston 2002). L'utilisation du contre-courant situé derrière la roche-mère et la force qui agit sur les nageoires pectorales permettent aux juvéniles de réduire les coûts énergétiques reliés au maintien de la position d'attente.

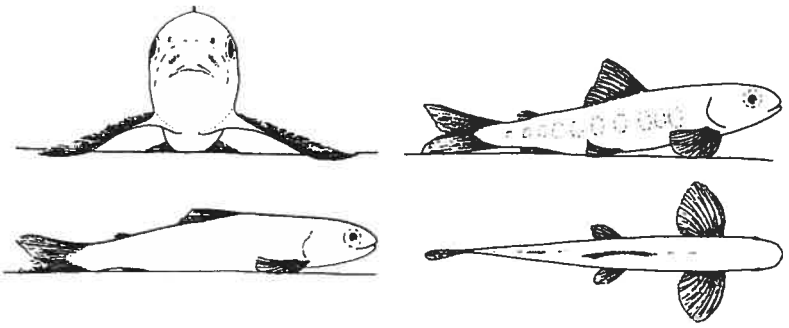

Figure 2.9 Position d'attente des juvéniles du saumon atlantique (d'après Arnold et al. 1991).

Comme nous avons déjà vu, on estime dans les modèles bioénergétiques le métabolisme d'activité en utilisant un modèle de nage forcée basé sur la vitesse moyenne de l'écoulement (Hughes et Dill 1990; Guensch et al. 2001). Les mouvements d'attaque vers la surface entrepris par le saumon pour se nourrir étant d'une toute autre nature, nous devons nous questionner quant au modèle qui sera le plus approprié pour évaluer les dépenses énergétiques : le modèle de nage forcée (Brett, 1964), le modèle de l'activité spontanée (Tang et Boisclair, 1995) ou éventuellement un nouveau modèle. Les mouvements d'alimentation peuvent être scindés en trois phases : une accélération vers la surface de l'eau, un virage brusque et une phase de nage continue pour retourner à la roche-mère. Les dépenses énergétiques des phases d'accélération et de virage peuvent être évaluées par le modèle de l'activité spontanée. Cependant, ce modèle ne prend pas en compte l'écoulement auquel le jeune saumon est constamment confronté en rivière. D'autre part, les dépenses énergétiques de la phase de retour peuvent être évaluées par le modèle de nage forcée mais ce modèle serait inapproprié pour évaluer les dépenses liées aux accélérations et aux virages. La combinaison de la complexité des mouvements entrepris par les poissons et des conditions naturelles dynamiques de leur milieu de vie, rend difficile le choix du modèle le plus approprié pour réaliser une estimation juste des coûts énergétiques. En effet, les juvéniles du saumon

atlantique vivent dans des écoulements turbulents où des écarts importants de la vitesse et du cisaillement surviennent à des échelles de temps très fines. Conséquemment, il semble qu'il soit nécessaire de développer un nouveau modèle pour évaluer les dépenses énergétiques de nage des juvéniles du saumon atlantique. Nous remettons également en question le fait que la vitesse moyenne, plutôt qu'une variable liée à la turbulence de l'écoulement, soit utilisée dans les modèles bioénergétiques. On postule que le comportement du saumon peut être influencé par les fluctuations de vitesse typiques d'un écoulement turbulent. Une compréhension des processus par lesquels l'eau s'écoule en rivière est donc requise. Ainsi, nous ferons une incursion dans le monde de la dynamique des fluides en rivière graveleuse où nous présenterons l'habitat physique du poisson ainsi que quelques variables importantes pour la description de la dynamique d'écoulement dans cet habitat.

2.3 Structure turbulente dans un écoulement à lit de gravier

Les caractéristiques physiques variées des rivières à saumon permettent à ces derniers d'y trouver différents types d'habitats : frayères, habitats d'alimentation d'été et habitats hivernaux pour les juvéniles. Ces rivières sont généralement graveleuses et caillouteuses et elles sont caractérisées par des séquences de mouille et de seuil (Figure 2.10; Knighton 1998). Wolman (1955) a décrit les mouilles comme étant des sections où les profondeurs sont importantes et les vitesses d'écoulement sont plus lentes comparativement à celles que l'on observe dans les sections de seuil. Les mouilles correspondent à des creux topographiques où le matériel du lit est en général plus fin. Les seuils sont moins profonds et le substrat est fait d'accumulations de particules grossières (Richards 1976).

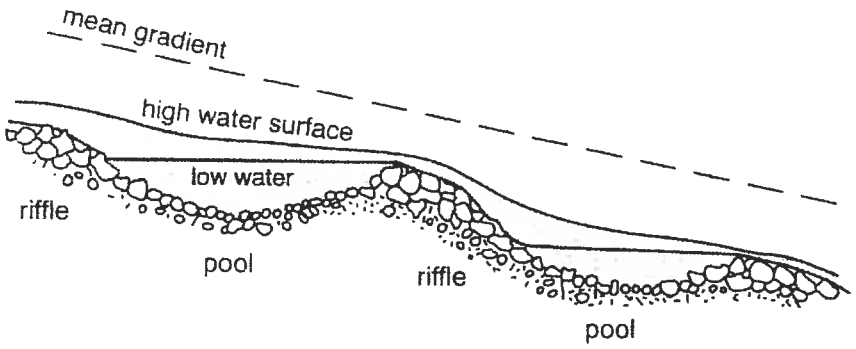

Figure 2.10 Succession de sections de mouille (*pool*) et de seuil (*riffle*). Les mouilles sont caractérisées par un substrat généralement plus petit, par un écoulement moins rapide et par une plus grande profondeur que les seuils (d'après Knighton 1998).

Les amas de galets et les blocs que l'on retrouve à la surface du substrat des rivières à lit de gravier sont utilisés par les juvéniles du saumon atlantique comme roche-mère. Les amas de galets se composent d'une accumulation de galets dont les plus gros sont situés sur le côté amont de l'accumulation et les plus petits se situent dans la zone d'abri, à l'aval (Figure 2.11). Les amas de galets se retrouvent souvent dans les sections de seuil, là où l'intensité turbulente est plus élevée (Brayshaw et al. 1983; Hassan et Reid 1990). Leur présence favorise la stabilité du lit et l'imbrication des particules retarde la mise en transport des sédiments car elle augmente les forces de résistance à l'écoulement (Church et al. 1998).

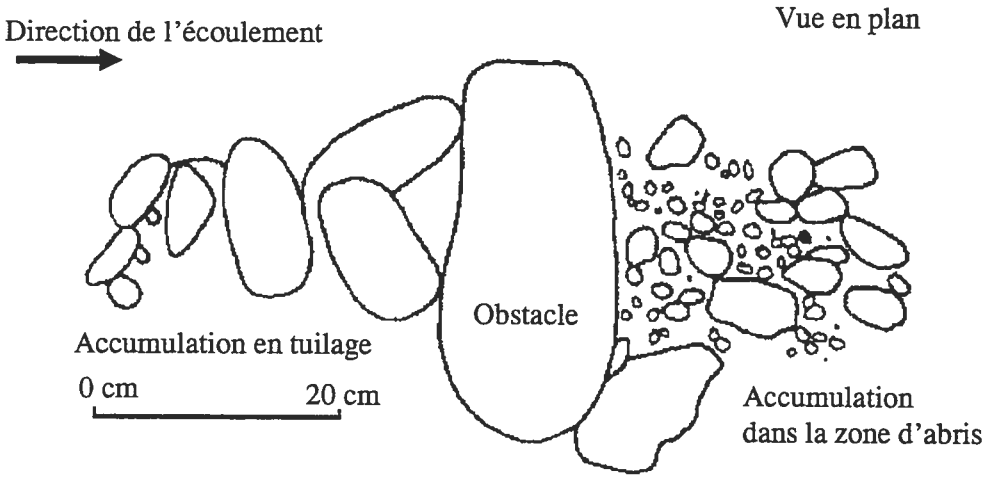

Figure 2.11 Les composantes d'un amas de galets dans un cours d'eau à lit de gravier : obstacle principal, zone d'accumulation de galets en amont et dépôt en aval (d'après Brayshaw et al. 1983).

En période d'alimentation, l'été, les juvéniles fréquentent les seuils où l'écoulement est rapide (DeGraaf et Bain 1986). Ils choisissent fréquemment des endroits où les vitesses moyennes d'écoulement sont de 5 à 70 $cm \cdot s^{-1}$ et les profondeurs d'eau de 20 à 80 cm (Morantz et al. 1987). Typiquement, le substrat dans ces sections est constitué de graviers (2-64 mm), de cailloux (64-256 mm) et de quelques blocs (256-1000 mm; Guay et al. 2000). L'écoulement auquel les juvéniles sont confrontés, est soumis à deux principaux types de forces : la force gravitationnelle, qui permet au fluide de s'écouler et d'accélérer en fonction de la pente du chenal, et les forces de friction, qui s'opposent au mouvement de l'écoulement provoqué par la gravité. Nous pouvons classifier l'état de l'écoulement selon deux formes : laminaire ou turbulent (Figure 2.12). Reynolds (1883), qui a décrit ces deux états, a noté que la nature de l'écoulement découle de la viscosité, de la vitesse du liquide et du diamètre du chenal. L'influence de ces facteurs est représentée dans un simple rapport sans dimension appelé le nombre de Reynolds (R_e).

$$R_e = V \cdot l / \nu \tag{2.2}$$

où V est la vitesse moyenne d'écoulement, l une longueur caractéristique (par exemple la profondeur de l'écoulement) et ν la viscosité cinématique. Cette équation exprime essentiellement l'importance relative des forces visqueuses par rapport aux forces turbulentes qui agissent sur un corps submergé. Si R_e est petit (R_e <500), les forces visqueuses prédominent et l'écoulement est laminaire. Dans un écoulement laminaire il n'y a pas d'échanges latéraux ni verticaux de parcelles de fluide et le fluide se déplace en couches parallèles (Figure 2.13). Si le nombre de Reynolds

augmente ($500 < R_e < 2000$), les forces turbulentes deviennent plus importantes. L'écoulement n'est plus strictement laminaire, nous appelons cet état transitionnel. Lorsque le nombre de Reynolds est élevé ($R_e > 2000$), les forces turbulentes prédominent et l'écoulement devient turbulent. En rivière, le nombre de Reynolds peut facilement atteindre 100,000 ou plus, ce qui correspond à un écoulement fortement turbulent.

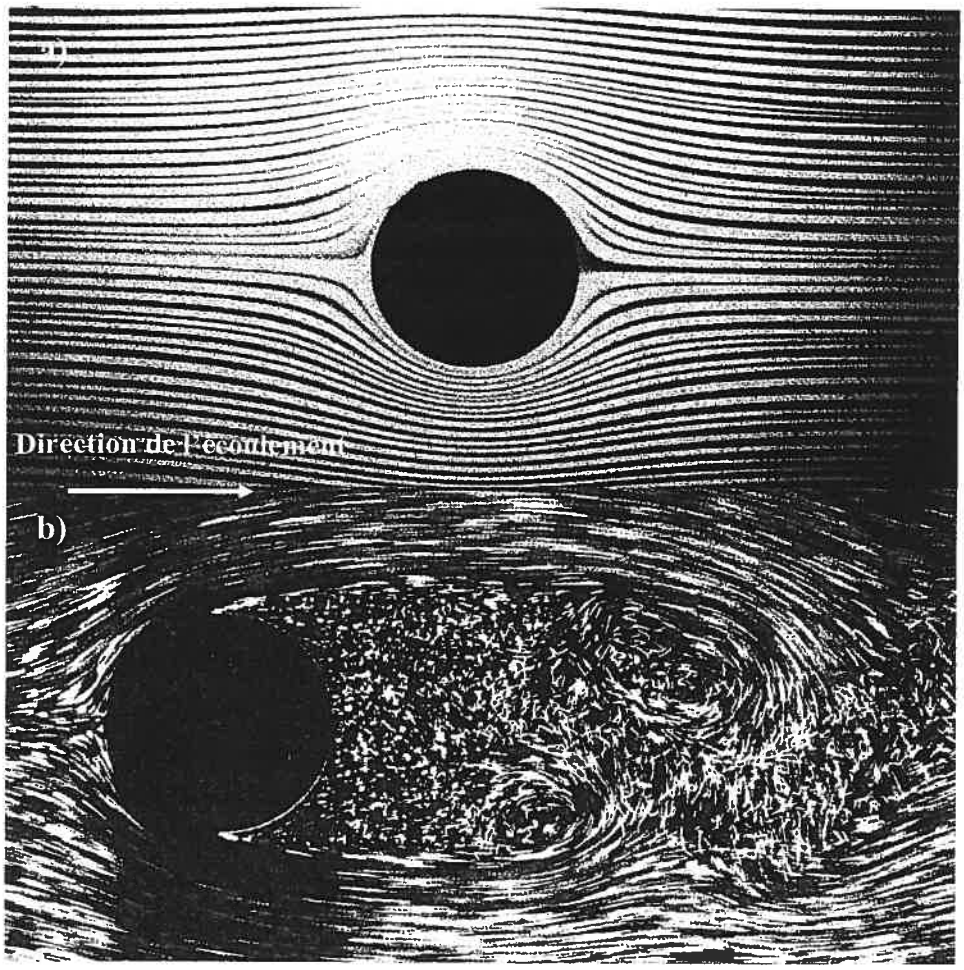

Figure 2.12 Vue en plan d'un écoulement a) laminaire et b) turbulent (d'après Allen 1997).

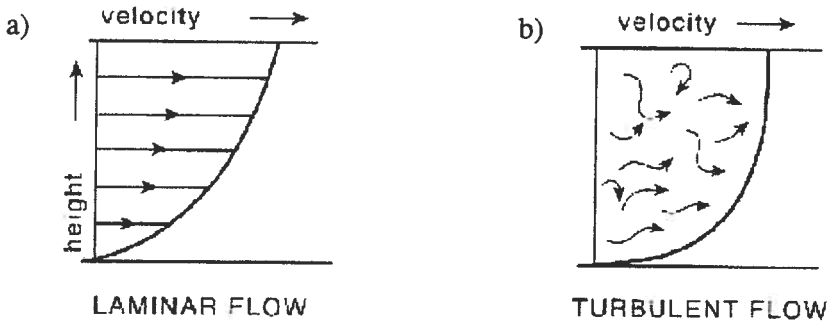

Figure 2.13 a) Écoulements laminaires constitués par le glissement des tranches d'eau les unes sur les autres et par le ralentissement des vitesses près du lit. b) Les écoulements turbulents sont quant à eux caractérisés par des échanges d'énergie entre les tranches d'eau (d'après Knighton 1998).

La turbulence est un état d'instabilité du fluide qui se traduit par un mouvement tridimensionnel variant dans l'espace et le temps (Tritton 1988). Elle se traduit par des variations de la vitesse instantanée du fluide et constitue l'un des plus importants états d'un fluide en mouvement dans la nature (Bradshaw 1985). La visualisation et les instruments de mesure de vitesse nous permettent de décrire les variations et les structures turbulentes d'un écoulement. Malgré l'hétérogénéité et la rugosité du milieu, il apparaît de plus en plus évident que l'écoulement dans une rivière à lit de gravier est organisé dans l'espace et le temps (Buffin-Bélanger et al. 2000a). La compréhension des structures d'écoulement est fondamentale lorsqu'on s'intéresse à l'écologie des juvéniles du saumon atlantique. Les deux caractéristiques suivantes doivent être considérées dans la description de l'organisation spatiale de l'écoulement : (1) la couche-limite et (2) le profil de vitesse.

2.3.1 Structure de la couche-limite

Un fluide qui est en contact immédiat avec une surface solide, dans notre cas le lit de la rivière, a la même vitesse que la surface. C'est la propriété de non-glissement de l'eau causée par l'adhérence des molécules d'eau avec la surface qui dicte cette règle. La distance δ à laquelle la vitesse approche celle de l'écoulement libre

représente l'extension verticale de la couche-limite (Figure 2.14). Cette couche correspond à la tranche d'eau affectée par la résistance exercée par le lit. Dans un écoulement turbulent, la vitesse du fluide dans la couche-limite suit un gradient marqué. Dans cette couche, la distribution des vitesses permet de définir, en fonction des forces dominantes, trois sous-couches distinctes: visqueuse, transitionnelle et turbulente.

La sous-couche visqueuse, autrefois appelée laminaire, est située près du lit et elle se caractérise par des vitesses et un nombre de Reynolds relativement faibles. Nous observons la sous-couche visqueuse au-dessus d'un lit lisse ou composé de particules homogènes. Elle tend à disparaître sur les lits plus rugueux. Dans les sous-couches visqueuses, on observe des manifestations turbulentes intermittentes mais intenses. C'est dans cette région qu'on a observé l'initiation des structures turbulentes qui forment le cycle d'égestion-incursion (Kline et al. 1967; Grass 1971). Nous discuterons de cet aspect ultérieurement. La sous-couche transitionnelle joue un rôle intermédiaire entre les sous-couches visqueuse et turbulente; ici, les forces turbulentes deviennent plus importantes. Enfin, comme son nom l'indique, la sous-couche turbulente est entièrement caracterisée par un écoulement turbulent. La hauteur de la couche-limite est exprimée par la distance δ qui est égale à la distance entre le lit de la rivière et la position où la vitesse de la couche limite diffère de 1% de l'écoulement libre. Dans les rivières à lit de gravier, la couche limite turbulente occupe presque toujours toute la colonne d'eau puisqu'on atteint rarement la vitesse d'un écoulement libre. Le profil vertical des vitesses longitudinales dans la sous-couche turbulente prend une forme logarithmique. Ce profil de vitesse exprime la variabilité de la vitesse longitudinale en fonction de la profondeur de l'écoulement.

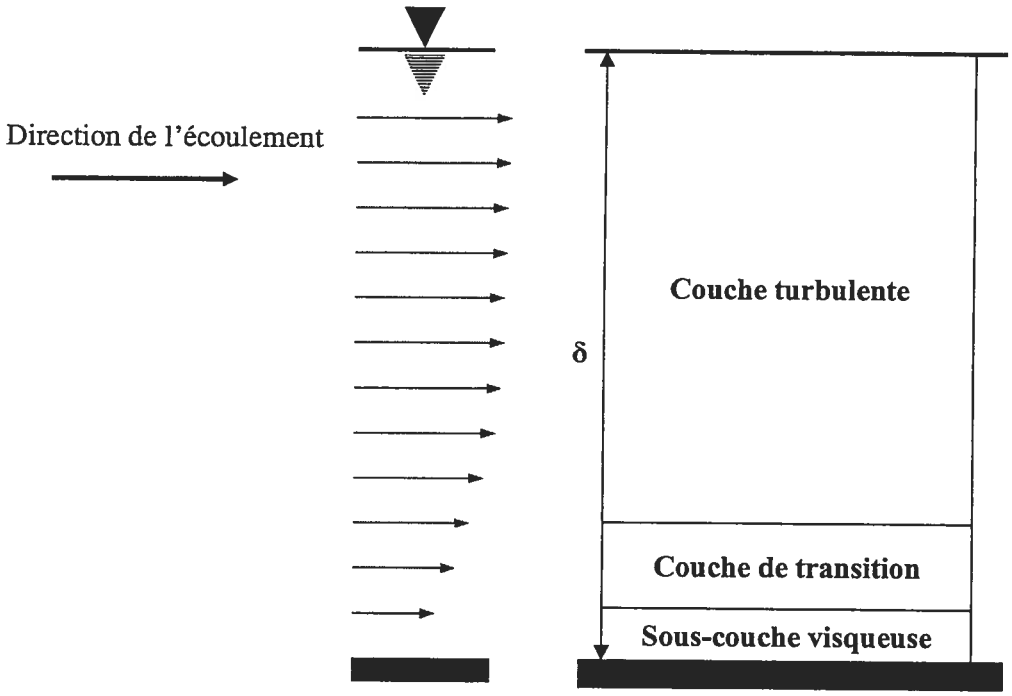

Figure 2.14 Profil vertical de vitesse d'un écoulement et stratification utilisée pour décrire les couches-limites turbulentes. A la distance δ, la vitesse approche celle de l'écoulement libre (d'après Dingman 1984).

2.3.2 Structures turbulentes

L'écoulement turbulent sur lit de gravier n'est pas un phénomène stochastique; on y observe différentes structures turbulentes qui se définissent comme étant une organisation d'une portion de fluide avec une certaine cohérence spatiale et temporelle (Buffin-Bélanger et al. 2000b). Nous décrirons trois types de structures turbulentes présentes dans des écoulements à lit de gravier : (1) les structures d'éjection (*bursting motion*), (2) les structures d'échappement (*shedding motion*) et (3) les structures à grande échelle (*large-scale flow structures*).

La formation des structures d'éjection, proches du lit, est associée à la présence de traînées longitudinales de faibles vitesses dans la sous-couche visqueuse d'un écoulement turbulent (Theodorsen 1952; Kline et al. 1967; Grass 1971). Ces traînées se définissent comme des filaments de fluide longs et étroits qui restent stables sur

une certaine distance et qui se tordent lorsqu'ils s'échappent vers la couche supérieure de l'écoulement (Figure 2.15). Ils montent lentement et s'alignent dans le sens de l'écoulement. Les structures d'éjection sont souvent suivies par des incursions de forte vitesse dans la sous-couche visqueuse provenant de la zone supérieure. Ainsi, à une micro-échelle, on observe dans l'écoulement turbulent un cycle continu mais non périodique de structure d'éjection et d'incursion. Cependant, l'existence du cycle d'éjection et d'incursion des écoulements sur des lits de gravier n'a pas été observée en milieu naturel.

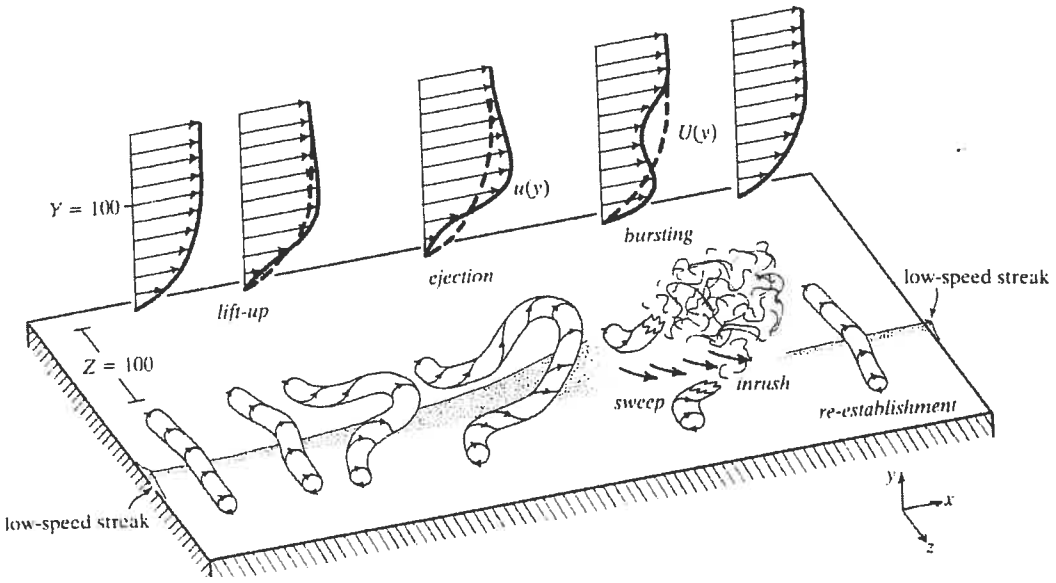

Figure 2.15 Modèle du cycle d'éjection-incursion (*burst-sweep cycle*). Le développement, à partir d'une traînée longitudinale, d'une éjection vers la couche supérieure de l'écoulement suivie d'une incursion de fluide qui se dirige vers la surface du lit. Les profils de vitesse sont également présentés pour chacune des étapes du cycle (d'après Allen 1997).

La deuxième structure turbulente, la structure d'échappement, se développe par la présence d'une hétérogénéité du lit qui entraîne une modification de la force de résistance, de la pression et conséquemment de l'organisation de l'écoulement autour d'un obstacle (Brayshaw et al. 1983). Acarlar et Smith (1987) ont proposé un modèle décrivant la formation d'une structure d'échappement autour d'un obstacle hémisphérique (Figure 2.16). La structure d'échappement prend une forme de fer à

cheval se développant en aval d'un obstacle et s'échappant de la zone de recirculation. La structure en fer à cheval diminue la pression en aval de l'obstacle. Pour un nombre de Reynolds élevé, le patron d'écoulement est caractérisé par deux lignes de vortex qui tournent rapidement. Le vortex de chacun des côtés tourne dans une direction opposée de l'autre côté. La structure d'échappement a d'abord été identifiée en laboratoire sur des lits lisses et homogènes, mais elle est également observée sur des lits rugueux en milieu naturel (Kirkbride 1993; Roy et Buffin-Bélanger 2001).

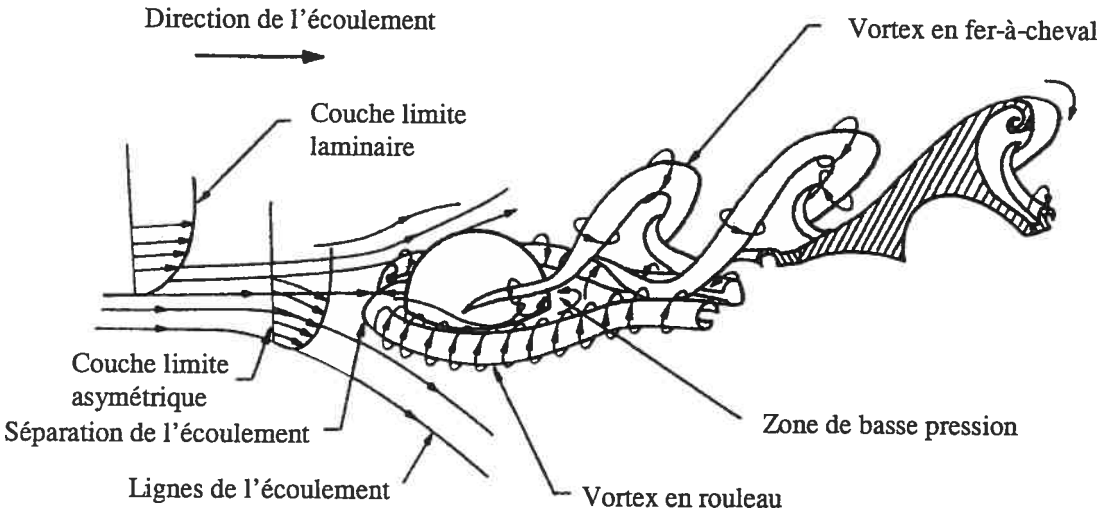

Figure 2.16 Modèle de l'effet d'un obstacle hémisphérique sur la structure de l'écoulement (d'après Acarlar et Smith 1987).

Troisièmement, les structures turbulentes à grande échelle sont constituées de portions rapides d'écoulement des fluides entrecoupées de portions plus lentes (Kirkbride et Ferguson 1995; Ferguson et al. 1996; Buffin-Bélanger et al. 2000a). Dans une rivière à lit de gravier, les structures turbulentes à grande échelle occupent toute la colonne d'eau (Figure 2.17). Les zones plus lentes d'écoulement tendent à se diriger vers la surface de l'eau et les zones plus rapides vers le lit (Nezu et Nakagawa 1993). Pour la première fois en milieu naturel, Buffin-Bélanger et al. (2000a) ont

caractérisé en détail les structures turbulentes à grande échelle dans une rivière à lit de gravier à partir d'analyses de séries temporelles de vitesse. Ces auteurs confirment la présence de périodes de fortes et de faibles vitesses en utilisant un système de matrice représentant les fluctuations de vitesse de l'écoulement à trois hauteurs au-dessus du lit (Figure 2.18). Les matrices illustrent l'existence des périodes de fortes et de faibles vitesses dans une rivière à lit de gravier. Le patron des périodes de fortes et de faibles vitesses est quasi-périodique. Les événements reviennent dans des intervalles de 5 à 30 s (Roy et al. 1999). La longueur des structures est de 3 à 5 fois plus grande que la profondeur de l'écoulement et leur largeur varie entre 0.5 et 1 fois la profondeur de l'écoulement (Roy et al. 2004).

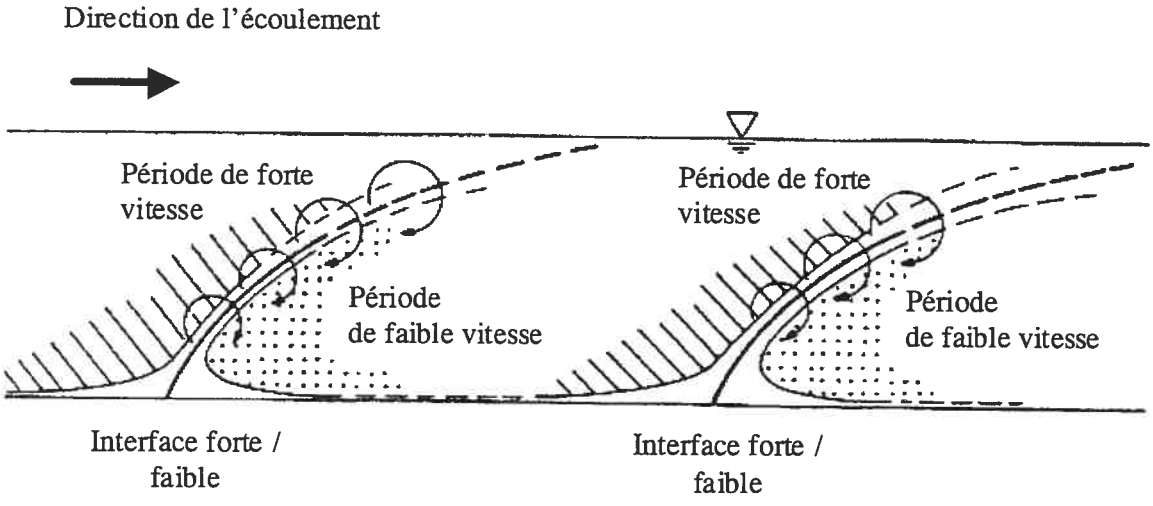

Figure 2.17 Présentation des périodes de fortes et de faibles vitesses (d'après Nakagawa et Nezu 1981).

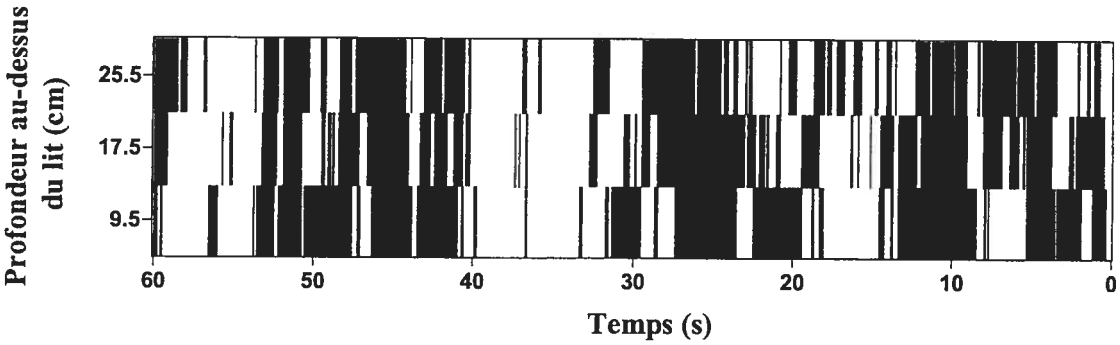

Figure 2.18 Matrices d'une série temporelle de vitesse longitudinale *U* montrant les périodes de fortes et de faibles vitesses. Les portions noires représentent les vitesses supérieures à la vitesse moyenne d'écoulement tandis que les portions blanches représentent les vitesses inférieures à la vitesse moyenne (d'après Buffin-Bélanger et al. 2000a).

Dans une rivière à lit de gravier, les trois différents types de structures turbulentes décrits précédemment sont non seulement présentes à différentes échelles, mais il est possible qu'elles interagissent les unes avec les autres. Buffin-Bélanger et al. (2000b) ont créé un schéma qui intègre les mécanismes à l'origine des structures et les interactions entre les structures d'éjection, les structures d'échappement et les structures à grande échelle (Figure 2.19). À partir de ces nouvelles connaissances, nous étudierons les effets de la turbulence sur le comportement et la physiologie des juvéniles du saumon atlantique.

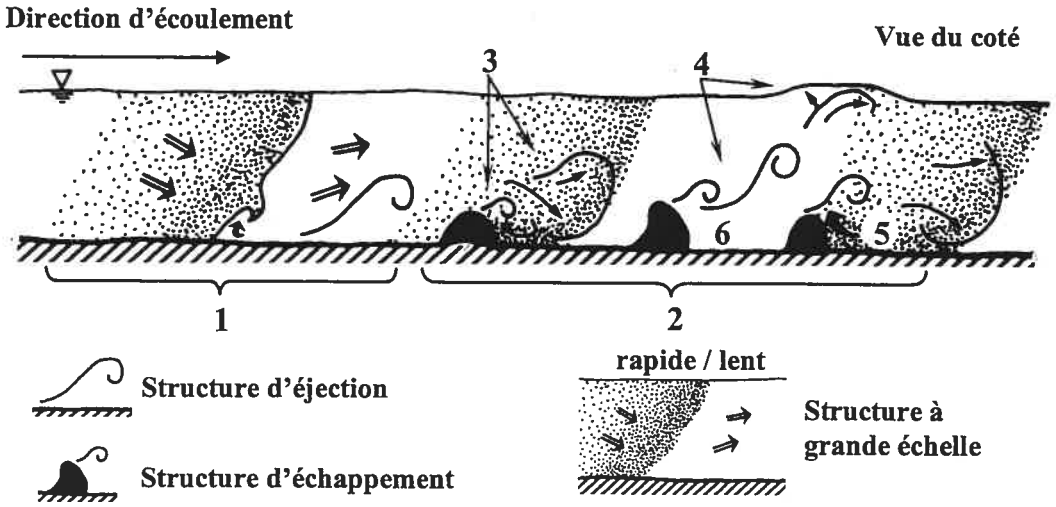

Figure 2.19 Modèle d'une intégration de trois types de structures turbulentes dans une rivière à lit de gravier. (1) La dynamique des structures d'éjection et des structures à grande échelle dans la portion où il y a peu d'obstacles protubérants et (2) la dynamique des structures d'échappement et des structures à grande échelle là où se trouvent des obstacles protubérants. Les structures d'échappement: (3) lors du passage d'une période de vitesse forte, l'échappement se produit à la fois vers la surface et vers le lit alors que (4) lors du passage d'une période de vitesse faible, l'échappement s'élève vers la surface. Ces différentes manifestations peuvent en partie être associées à la dynamique de la zone de recirculation qui devient (5) plus active et donne naissance à un mouvement vers le haut le long de l'obstacle suite au passage d'une période de vitesse forte alors que (6) ce mouvement est moins prononcé lors du passage d'une période de faible vitesse (d'après Buffin-Bélanger et al. 2000b).

2.4 Limite des connaissances et intégration de la thèse

Nous avons vu plus haut que la distribution et l'abondance des poissons peuvent être estimées à partir de modèles bioénergétiques (Hayes et al. 2000; Nislow et al. 2000). Cependant, la précision des modèles bioénergétiques est dépendante de l'exactitude des sous-modèles décrivant les composantes du bilan énergétique du poisson. Nous sommes particulièrement intéressés par la composante qui correspond au métabolisme d'activité d'une part parce qu'elle est importante sur le plan physiologique et d'autre part parce qu'elle se fonde présentement sur trois suppositions ambiguës :

(1) Utilisation de la vitesse moyenne – Il est connu que les juvéniles du saumon atlantique vivent dans des rivières à lit de gravier caractérisées par un écoulement turbulent (Keenleyside et Yamamoto 1961). Néanmoins, plusieurs études estiment les coûts énergétiques de nage des poissons en rivière à l'aide de la vitesse moyenne sans tenir compte de la turbulence (Hughes 1992; Guensch et al. 2001). L'écoulement en rivière à lit de gravier est dominé par des structures turbulentes à grande échelle qui occupent toute la colonne d'eau (Kirkbride et Ferguson 1995; Buffin-Bélanger et al. 2000a; Roy et al. 2004). Afin de déterminer si l'utilisation de la vitesse moyenne est appropriée pour l'estimation du métabolisme d'activité, nous devons d'abord explorer comment les juvéniles s'adaptent à leur environnement hydraulique. Si les juvéniles du saumon atlantique réagissaient à la variabilité temporelle de l'écoulement et utilisaient les périodes de faibles vitesses pour amorcer leurs attaques, ils minimiseraient ainsi leurs coûts énergétiques de nage. Advenant qu'une telle hypothèse soit vraie, l'utilisation de la vitesse moyenne surestimerait les coûts énergétiques. Ce type d'adaptation comportementale aux conditions variables du milieu naturel est possible et a été démontrée dans des études sur le comportement d'autres espèces (Stephens et Krebs 1986). Il est aussi connu que les animaux sont capables d'utiliser leurs sens pour extraire des informations de leur environnement fluvial (Rinberg et Davidowitz 2000). À cet effet, Northcutt (1997) a montré que les poissons peuvent percevoir les changements de la vitesse et de pression de l'écoulement en utilisant leurs neuromastes. Les juvéniles du saumon atlantique évoluent et se nourrissent à l'intérieur d'une gamme étendue de vitesse d'écoulement (Wankowski 1979; Grant et Noakes 1987). De plus, l'alimentation à la dérive est coûteuse (Puckett et Dill 1984; Puckett et Dill 1985) et représente de 10 à 20% du budget du temps (Bachman 1984; Puckett et Dill 1985). Une adaptation à la

turbulence de l'écoulement serait donc favorable à la croissance des juvéniles du saumon atlantique.

(2) Estimation à partir d'un modèle de nage forcée – Pour les poissons vivant dans les systèmes fluviaux, les coûts énergétiques de nage sont estimés à partir des modèles de nage forcée. Les modèles de nage forcée sont basés sur un mouvement continu dans un fluide à vitesse constante. Ils ne tiennent pas compte des mouvements intermittents ou des mouvements complexes comme les changements de la vitesse et de la direction. Les accélérations et les décélérations du poisson ainsi que les virages entraînent une augmentation des coûts énergétiques par un facteur de 3 à 22 fois par rapport aux estimations obtenues des modèles de nage forcée (Boisclair et Tang 1993; Tang et al. 2000). Dans les rivières à lit de gravier, il existe des variations considérables des vitesses de l'écoulement turbulent (Roy et Buffin-Bélanger 2001). Les poissons doivent constamment ajuster leur vitesse de nage lorsqu'ils évoluent dans ce type d'écoulement. Ces mouvements brusques engendrent des coûts énergétiques (Webb 1983; Krohn et Boisclair 1994). Les coûts énergétiques de ces mouvements ne sont pas considérés par les modèles de nage forcée. Nous supposons donc que les modèles de nage forcée sous-estiment les coûts énergétiques réels des poissons en rivière.

(3) Estimation à partir de poissons piscicoles – Dans les expériences, les variables physiologiques sont souvent estimées à l'aide de poissons élevés en pisciculture. Cependant, les travaux de Fleming et al. (2000) ont montré que les poissons de pisciculture diffèrent des poissons sauvages d'un point de vue morphologique, comportemental et physiologique. Les juvéniles de saumon

atlantique provenant de la pisciculture ont une tête et des nageoires plus petites (Fleming et al. 1994). Ils sont également plus agressifs et plus dominants que leurs congénères sauvages. On doit donc se demander si les résultats d'expériences en laboratoire obtenus en utilisant des poissons provenant de la pisciculture s'appliquent aux poissons sauvages. Ceci a une forte influence sur la précision des prédictions des gains énergétiques nets générés par les modèles bioénergétiques (Ney 1993).

2.5 Objectifs de la recherche

En vue d'élaborer de meilleures modèles bioénergétiques, cette étude vise à analyser la relation entre le comportement d'alimentation des juvéniles et la structure d'un écoulement turbulent et à modéliser les coûts énergétiques de nage des juvéniles du saumon atlantique dans un écoulement turbulent.

Les objectifs spécifiques de cette thèse sont les suivants :

1. analyser le comportement des juvéniles du saumon atlantique en relation avec les structures turbulentes à grande échelle dans la rivière (Chapitre 3);
2. mesurer l'effet de la turbulence de l'écoulement sur les coûts énergétiques de nage en laboratoire et de comparer les résultats avec les prédictions des modèles de nage forcée et de l'activité spontanée (Chapitre 4);
3. comparer le métabolisme d'activité des juvéniles sauvages avec le métabolisme d'activité des juvéniles de la première génération de pisciculture (F_1) et de la septième génération de pisciculture (F_7) (Chapitre 5);
4. estimer l'influence de la température de l'eau et de la masse corporelle du poisson sur le métabolisme d'activité (Chapitre 6).

Le comportement des juvéniles du saumon atlantique en relation avec les structures turbulentes à grande échelle – Notre hypothèse est que les juvéniles du saumon atlantique réagissent à la turbulence. Plus spécifiquement, nous pensons que les juvéniles minimisent les coûts énergétiques de nage en ajustant leur activité de déplacement à l'intensité turbulente et en choisissant les périodes de faible vitesse d'écoulement pour amorcer leurs déplacements. Ces stratégies comportementales auraient des conséquences importantes sur le bilan énergétique, le taux de croissance et la survie des juvéniles du saumon atlantique. Nous avons testé cette hypothèse lors d'une étude *in situ*.

L'effet de la turbulence de l'écoulement sur les coûts énergétiques de nage en comparaison avec les prédictions obtenues des modèles de nage forcée – Notre hypothèse est que les coûts énergétiques de nage dans un écoulement sont plus élevés que ceux estimés par les modèles de nage forcée. Dans un écoulement turbulent, les poissons doivent constamment ajuster leur position à l'aide de leurs nageoires. Nous supposons que les coûts énergétiques de nage augmentent avec une augmentation de la turbulence à cause des coûts énergétiques reliés aux mouvements des nageoires (Gauthier 1998; Enders et Herrmann 2003). En laboratoire, nous avons mesuré les coûts énergétiques de nage des juvéniles du saumon atlantique dans un écoulement turbulent. Les résultats ont ensuite été comparés avec les prédictions des modèles de nage forcée.

La comparaison des coûts énergétiques de nage des juvéniles sauvages, piscicoles et domestiques – Notre hypothèse est que les coûts énergétiques de nage dans un écoulement turbulent diffèrent entre les poissons sauvages, piscicoles et

domestiques. Plusieurs études ont démontré que les poissons sauvages, piscicoles et domestiques diffèrent quant à leurs aspects comportementaux, morphologiques et physiologiques (Fleming et al. 1994; Einum et Fleming 1997; Johnsson et al. 2001). Nous émettons l'hypothèse que ces changements entraînent des différences dans les coûts énergétiques de nage parce qu'ils modifient l'habilité des poissons à nager. Nous avons mesuré et comparé les coûts énergétiques de nage dans un écoulement turbulent pour des poissons sauvages, piscicoles de première génération et domestiques de septième génération en pisciculture.

La modélisation des coûts énergétiques de nage dans un écoulement turbulent en relation avec la température de l'eau et la masse corporelle – Dans le cadre du modèle bioénergétique, nous voulons finalement développer un modèle complexe qui estime les coûts énergétiques de nage des juvéniles du saumon atlantique. Notre hypothèse est que les coûts énergétiques de nage varient en fonction de la température, de la masse corporelle, de la vitesse moyenne de l'écoulement et de l'intensité de la turbulence de l'écoulement. Nous avons donc mesuré en laboratoire les coûts énergétiques de nage en considérant plusieurs températures, masses corporelles, vitesses de l'écoulement et intensités de la turbulence.

Chaque objectif mène à un article qui présente des résultats originaux. Ces quatre articles constituent le corps de la thèse. Le premier article se base sur l'analyse des données échantillonnées directement dans la rivière; les trois autres se basent sur des expériences respirométriques réalisées en laboratoire.

2.6 Plan expérimental et méthodologie

Nous décrirons brièvement les approches choisies afin d'atteindre nos objectifs. Nous avons choisi une approche *in situ* afin de répondre à notre première hypothèse; les juvéniles du saumon atlantique profitent des périodes de faible vitesse pour amorcer leurs déplacements. L'avantage des observations en milieu naturel est qu'elles permettent d'examiner le comportement naturel des juvéniles du saumon atlantique dans leur environnement; on évite ainsi que le saumon ait un comportement modifié par un milieu artificiel. Le même phénomène s'applique aux mesures des structures turbulentes à grande échelle.

Cependant, on ne peut contrôler les variables environnementales lorsqu'on fait des observations en milieu naturel. Les fluctuations des variables physiques (température, débit) ou biotiques (présence de prédateur, abondance de nourriture) pourront affecter le comportement; il sera donc difficile de retracer l'effet des variables explicatives. Une autre problématique du milieu naturel est que, dans notre étude, la vitesse moyenne et la turbulence de l'écoulement sont des variables qui peuvent être interdépendantes. Cela amène des problèmes dans l'interprétation de l'effet individuel de chacune des variables sur le comportement du poisson. Un troisième inconvénient des observations en milieu naturel est que leur réussite est souvent tributaire des conditions météorologiques. L'ensemble de ces contraintes explique le fait que nos observations de terrain sont seulement basées sur un petit nombre de poissons (n =8 en tout).

Afin d'estimer les coûts énergétiques de nage en relation avec la turbulence de l'écoulement, nous avons donc décidé de faire des expériences en laboratoire, dans le but de contrôler toutes les variables environnementales, ce qui nous a permis de nous

concentrer sur l'effet explicite de chacune des variables d'intérêt. Des informations détaillées concernant les observations de terrain et les expériences en laboratoire seront données dans les chapitres suivants. Nous discuterons également de la méthodologie utilisée dans chacun des chapitres.

2.6.1 Observations de terrain

Deux campagnes d'observation du comportement des juvéniles du saumon atlantique ont été réalisées dans la rivière Sainte-Marguerite, un tributaire du Saguenay, Québec, Canada. Nous avons filmé individuellement le comportement de huit juvéniles pendant 30 min à l'aide de deux caméras submersibles. Simultanément, nous avons mesuré les fluctuations de la vitesse de l'écoulement à partir de courantomètres placés à proximité de chacun des poissons. Nous avons utilisé deux types de courantomètre: (1) Trois courantomètres électromagnétiques (ECM) fixés sur une tige au-dessus du lit de gravier et (2) un vélocimétre Doppler acoustique (ADV; Figure 2.20). Nous présenterons cette étude au chapitre 3.

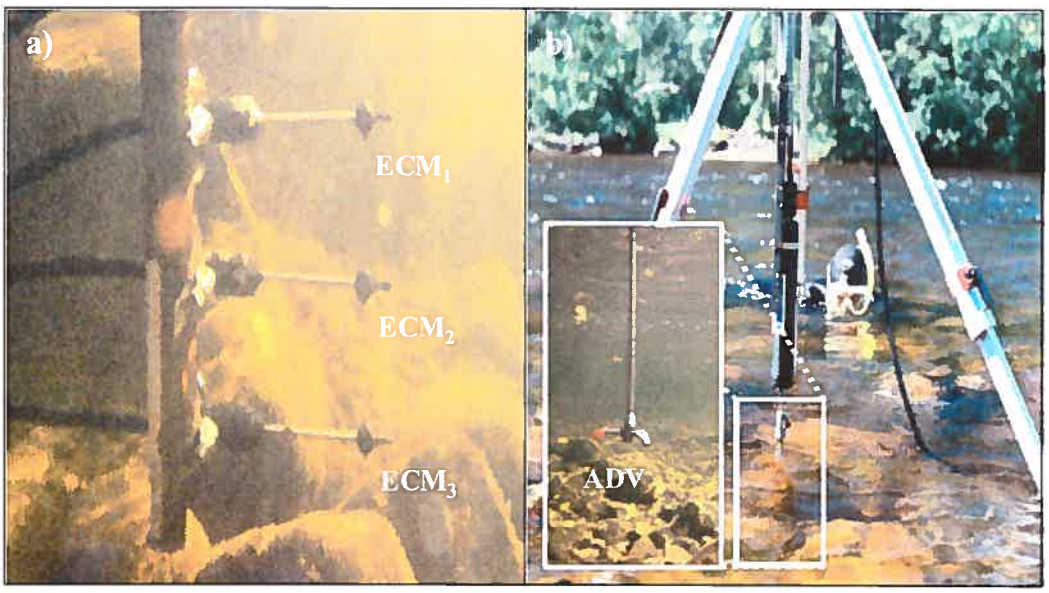

Figure 2.20 Deux types de courantomètre ont été utilisés: a) Trois courantomètres électromagnétiques de Marsh-McBirney (ECM) fixés sur une tige au-dessus du lit de gravier et b) un vélocimétre Doppler acoustique de Sontek (ADV).

2.6.2 Expériences en laboratoire

Nous avons évalué l'effet de la turbulence sur les coûts énergétiques de nage en exécutant une série de vingt expériences respirométriques pendant lesquelles nous avons soumis les poissons piscicoles à quatre types de conditions turbulentes différentes (une combinaison de deux moyennes et deux écart types de la vitesse de l'écoulement). Nous avons fait cinq expériences par condition turbulente à une température de l'eau de 15 °C avec des poissons de 10 g. Les taux de respiration des poissons obtenus pour chacune des conditions turbulentes ont été comparés avec les prédictions des modèles de nage forcée et de l'activité spontanée développés par Boisclair et Tang (1993). Cette partie de l'étude est présentée au chapitre 4.

Nous avons ensuite comparé les coûts énergétiques de nage dans un écoulement turbulent des juvéniles du saumon atlantique sauvages provenant de la rivière Sainte-Marguerite à ceux obtenus en utilisant des saumons piscicoles de première génération provenant de géniteurs sauvages et des saumons domestiques de septième génération provenant de géniteurs du programme national d'élevage du saumon atlantique pour l'aquaculture commercial à Sunndalsøra, Norvège. Les coûts énergétiques de nage ont été analysés à partir d'une vitesse moyenne d'écoulement et de deux écart types de la vitesse d'écoulement. Les expériences respirométriques ont été réalisées à une température de 15 °C avec des poissons ayant une masse corporelle variant de 4.0 à 16.1 g. Les résultats sont présentés au chapitre 5.

Pour estimer l'effet de la température de l'eau et de la masse corporelle sur le métabolisme d'activité, nous avons mené des expériences respirométriques à des températures de 10, 15 et 20 °C avec des poissons piscicoles de 4.3 à 17.6 g, à trois

moyennes et trois écart types de la vitesse d'écoulement. À l'aide de ces données, nous avons développé des modèles de nage en écoulement turbulent pour les juvéniles du saumon atlantique. Cette recherche fait l'objet du chapitre 6.

3 THE FEEDING BEHAVIOR OF JUVENILE ATLANTIC SALMON IN RELATION TO TURBULENT FLOW[1]

Abstract

The feeding behavior of juvenile Atlantic salmon (JAS; *Salmo salar*) in the Sainte-Marguerite River, Québec, Canada varied with the characteristics of turbulent flow. Fish in 1.7-fold more turbulent flow undertook significantly fewer motions of high amplitude and spent less time for motions. The proportion of time used for motions by fish decreased with an increase of mean and standard deviation of the flow velocity. However, JAS did not seem to prefer low-speed flow events or low fine scale flow velocities when initiating their motions. No relationship was found between the occurrence of motions and low-speed flow events. The frequency distributions of fine scale flow velocities during the initiation of motions did not differ from the frequency distributions of fine scale flow velocities selected at random. The frequency distributions of the duration of the inter-departure time were described by an exponential model indicating a random process. However, simulations indicated that JAS would decrease their swimming costs during motions by 19.8% in low and by 31.1% in high turbulent conditions by initiating motions in low-speed flow events. The real swimming costs did not differ from the swimming costs estimated for a scenario where fish initiate their motions at randomly selected flow velocities.

[1] Enders, E.C., T. Buffin-Bélanger, D. Boisclair & A.G. Roy. The feeding behavior of juvenile Atlantic salmon in relation to turbulent flow. *Journal of Fish Biology*. Submitted.
Contribution to the program of CIRSA (Centre Interuniversitaire de Recherche sur le Saumon Atlantique).

3.1 Introduction

Bioenergetics models may be used to quantify fish habitat quality by assigning values of the net energy gain to specific habitats which fish are expected to obtain while using these habitats (Fausch 1984; Sabo et al. 1996; Vehanen et al. 2000). Fish growth is expected to occur only in habitats with positive values of net energy gain because in these habitats fish feeding rates are presumed to surpass their energy expenditures. Therefore, it has been hypothesized that stream salmonids select microhabitats characterized by the presence of low flow velocities to minimize the energy spent swimming and the proximity of swift flow velocities providing invertebrate drift (Everest and Chapman 1972; Fausch and White 1986). Hence, the balance between the benefits and the costs of habitat utilization allows one not only to predict fish growth under specific environmental conditions but also to predict their spatial distribution (Fausch 1984; Hughes and Dill 1990; Guensch et al. 2001).

Swimming costs may be estimated by combining observations on fish behavior under given flow conditions and models that adequately represent the cost of performing specific behaviors. However, the estimation of the costs of habitat utilization in rivers is impeded by the lack of knowledge about the cost of swimming against turbulent flows (but see Enders et al. 2003) and about the effects of flow turbulence on fish behavior (McLaughlin and Noakes 1998). Generally, the cost of performing a specific movement is obtained as the product of fish swimming speed, the cost of swimming at that speed, and the time spent swimming (Hughes and Dill 1990; Guensch et al. 2001). The effective swimming speed is taken as the sum of fish apparent movement (relative to the river bed) and the average flow velocity at the location of the fish (Hinch and Rand 2000). However, in gravel-bed rivers stream-

dwelling fish live in highly turbulent flows. The structure of turbulence in gravel-bed rivers is dominated by a temporal succession of large-scale flow structures, which extend over the entire water column (Kirkbride and Ferguson 1995; Ferguson et al. 1996; Buffin-Bélanger et al. 2000a). Large-scale flow structures consist of quasi-periodic successions of high- and low-speed flow events of a duration ranging from 0.5 to 5 s (Roy and Buffin-Bélanger 2001). Measurements of these turbulent flow structures suggest that the flow velocity can change 3- to 8-fold relative to average flow velocity within 1 to 5 s (Roy et al. 1999). Detection and use by fish of low-speed flow events could greatly minimize their costs of habitat utilization. If fish take advantage of low-speed flow events, the use of the average flow velocity at the location of the fish to estimate their effective swimming speed could cause an overestimation of the costs of habitat utilization. Such a behavioral adaptation can be expected because it has been shown that fish can perceive changes in flow velocities with the use of one class of lateral line receptors, the neuromasts, which detect pressure changes (Northcutt 1997).

The objectives of this study were (1) to describe the behavior of a stream-dwelling fish in relation to the flow characteristics, (2) to test the hypothesis that fish use low flow velocities when undertaking their motions, and (3) to estimate the potential energetic advantage of using low-speed flow events.

3.2 Material and methods

The objectives were attained by simultaneously filming the behavior of stream-dwelling fish and recording the structures of the flow they experienced under natural conditions. This was performed for eight individual fish under a range of flow

characteristics. Each series of observations consisted in the recording of fish behavior and of flow characteristics during 30 min.

3.2.1 Species for study

Juvenile Atlantic salmon (*Salmo salar* L.) were selected for this study because their natural habitat encompasses gravel-bed rivers characterized by highly turbulent flows. The behavior of juvenile Atlantic salmon (JAS) comprises so-called 'sit-and-wait' phases during which JAS swim just above the substrate, often at the downstream edge of a rock, used as a protection against the turbulent flow. The rock preferentially used by a territorial JAS is referred to as its 'home-rock'. The sit-and-wait behavior represents the largest part of the time budget of JAS ($\geq$80%; Bachman 1984; Puckett and Dill 1985). JAS intermittently perform 'attacks' which are motions from the river bed towards the water surface, or in the water column, in which they capture drifting invertebrates (Kalleberg 1958). JAS forage in a wide range of flow velocities (Wankowski 1979; Grant and Noakes 1987) and experience, during these motions, rapid changes in the structure of flow. Thus, JAS live under conditions where it may be energetically advantageous to use low-speed flow events. Furthermore, drift feeding is expected to be energetically expensive and time consuming (commonly 10-20% of the time budget; Bachman 1984; Puckett and Dill 1985). Therefore, the preferential use of low-speed flow events may have important consequences for the energy budget, the growth rate, and the survival of JAS. As JAS may be sensitive to variations in the benefits and the costs of feeding in running water, they may modify their foraging behavior accordingly.

JAS were also used for this work because the abundance of the wild form of Atlantic salmon is decreasing (Bardonnet and Baglinière 2000). This situation is alarming particularly considering that these fish supported an extensive and valuable commercial and recreational fishery. It is expected that an improved assessment of the costs of habitat utilization for JAS would contribute to the development of models and management strategies of riverine environments better adapted to protect this species.

Eight juvenile Atlantic salmon were observed during this study. They showed the for salmon parr typical vertical markings on their flank. The total body length of the observed fish ranged from 8.3 to 11.6 cm which corresponds to body mass of 5.7 to 14.5 g.

3.2.2 Sampling site

Observations of fish behavior and flow characteristics were made on the main branch of the Sainte-Marguerite River in the Saguenay region of Quebec, Canada (Figure 3.1). Observations were made during two periods (11.-12.9.1999 and 26.-28.7.2000) further defined as Sampling periods I and II, respectively. The sampling site consisted in a 500 m^2 riffle located approximately 4 km from the junction of the Sainte-Marguerite River and the Saguenay River (48°15' N, 69°55' W). This site was selected because it was sufficiently large and diversified to observe the behavior of numerous fish under a wide range of flow characteristics. The river section at our sampling site had a width of 50 m at bankfull condition. The water depth at the home-rocks where fish were observed ranged from 26 cm to 45 cm. The substrate of the river bed at the sampling site ranged from pebble to boulder. The substrate

composition quantified as the median diameter axis (D_{50}) of substrate components was 6 cm. The water temperature was 19°C during the observations in 1999 and 22°C in 2000. All observations were made between 10:00 h and 17:00 h under sunny conditions (less than 20% cloudiness).

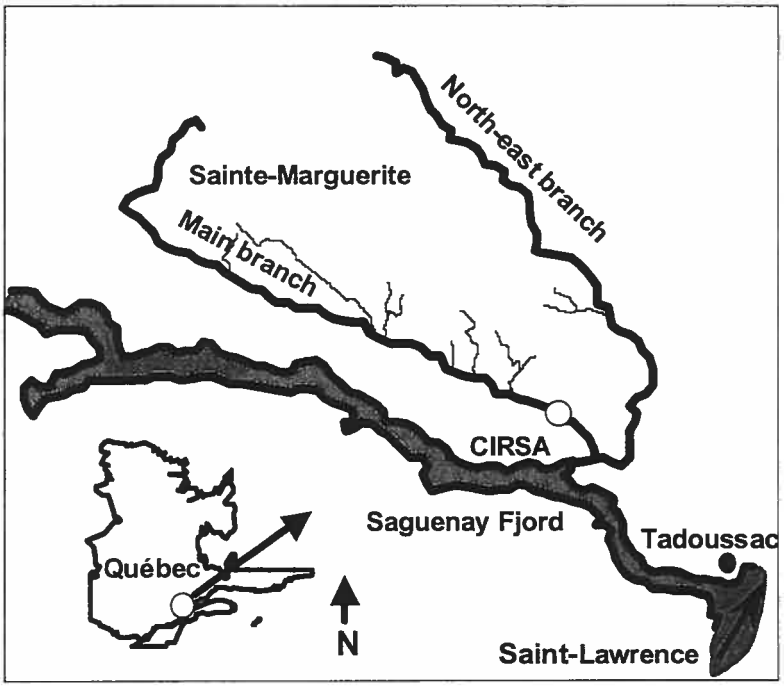

Figure 3.1 The study site at the Sainte-Marguerite River located at the Northern shore of the Saint-Lawrence River, Québec, Canada.

3.2.3 Sampling procedure

The observations aimed at documenting the behavior of JAS with simultaneous measurements of flow velocity fluctuations at a high temporal resolution. The behavior of JAS was recorded using a submersible stereocinematographic video system (Ménard 1991; Boisclair 1992). The underwater cameras were installed where a snorkeller observed JAS displaying intermittent feeding behavior (Figure 3.2 a). The cameras were installed at 0.5 to 1 m from the location of the fish. This range

of distance allowed the cameras to be sufficiently close to the fish to precisely record their motions and sufficiently far from the fish to film their complete trajectory during their largest motions. Fish were filmed for 30 min. The exact time of recording (hours-minutes-seconds-milliseconds) was assigned to each frame filmed by a time and day camera titler (TDCT, WJ-410, Panasonic Canada Inc., Lachine, Québec) for the later synchronization of the behavior records with the corresponding flow velocity time series. Velocity measurements were carried out simultaneously to the recording by positioning the currentmeters at distances ranging from 4 to 9 cm to the fish (Figure 3.2 b). To ensure the synchronization of the behavior records with the corresponding flow velocity time series, the currentmeters were turned on as the time code of the TDCT was initialized.

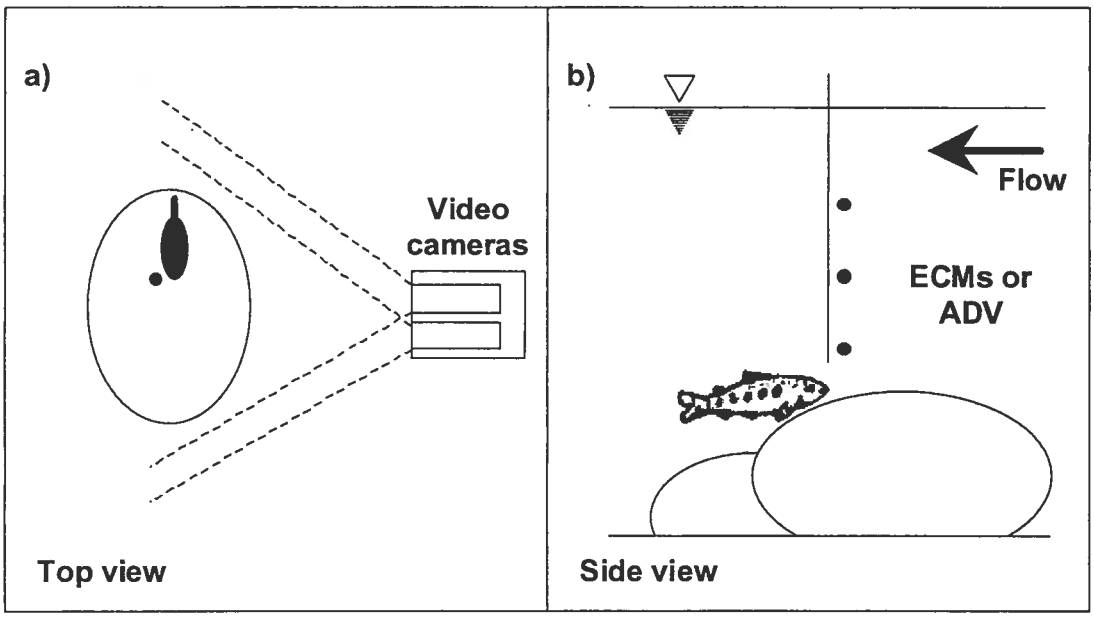

Figure 3.2 Experimental set-up for the analysis of fish behavior in relation to turbulent flow of juvenile Atlantic salmon. a) Fish were filmed with a stereocinematographic video camera system in their sit-and-wait position undertaking motions in irregular time intervals. b) Simultaneously flow velocity was measured with a currentmeter close to the fish position.

Two different types of currentmeters were used for the two sampling periods. During Sampling period I, three bi-directional Marsh-McBirney Electromagnetic Currentmeters (ECMs; Frederick, Maryland USA) were deployed to measure the flow velocity in the vicinity of the fish. The three ECMs were mounted vertically to detect the advection of high- and low-speed flow events (Buffin-Bélanger et al. 2000a). The ECM sensor head is 1.3 cm in diameter and allow velocity sampling at a 20 Hz frequency. The diameter of the sampling volume is three times that of the sensor head (sampling volume $=31.1$ cm^3). The ECMs were set 8 cm apart on a wadding rod. The lowest ECM was situated 4 cm above the fish's sit-and-wait position. Hence, the lowest ECM was able to record the focal point velocity of the fish as suggested by DeGraaf and Bain (1986) and Morantz et al. (1987). The setup did not disturb the fish. JAS stayed on their home-rock during the installation of the cameras and currentmeters or came back to their home-rocks within a few minutes. The fish subsequently showed the same frequency of motions than before the installation of the instruments (Table 3.1, Chi^2-Test, $0.41 < \chi^2 < 1.42$, $0.48 < p < 0.81$). Using this setup, the motions of two fish (hereafter referred to as fish #1 and fish #2) were recorded for 30 min each. During Sampling period II, a Sontek Field Acoustic Doppler Velocimeter (ADV; Sontek, San Diego, California, USA) was used. The ADV has the advantage of having a smaller sampling volume (0.25 cm^3) located 5 cm away from the probe. Therefore, the focal point velocity of the fish was measured more precisely at a frequency of 25 Hz. Using this setup, a second series of observations was carried out and six films of 30 min were obtained from six different fish (hereafter referred to as fish #3 to fish #8) with synchronous flow velocity measurements.

Table 3.1 Number of motions per amplitude (A1 motions do not extend further than 4 cm from original fish position; A2 motions range from 4 to 20 cm, and A3 motions are longer than 20 cm) and total number of motions in a 30 min period before and during the installation of the currentmeters. The fish were not disturbed by the setup, as they showed the same frequency of motions before and during the installation of the measuring devices.

Fish	#1		#2	
No. of motion	before	during	before	during
A1	48	50	37	40
A2	36	34	18	13
A3	27	32	8	11
total	111	116	63	64
motions·min^{-1}	3.7	3.9	2.1	2.1
χ^2	0.41		1.42	
p	0.81		0.49	

3.2.4 Characteristics of fish behavior

Each video-recording was visually analyzed to detect and describe all motions undertaken by JAS. For each motion, the time at which the fish initiated the motion and that at which fish returned to its initial location were noted ($\pm$0.03 ms). Each motion was then divided into two phases: (1) the phase of attack (forward movement) and (2) the phase of return (return movement to the initial location). The exact time of the beginning and the end of each phase was noted. Each motion was also classified according to its amplitude (further referred to as amplitude class): amplitude A1 described motions towards the river bed that do not extend further than 4 cm from original fish position; amplitude A2 described motions towards the mid-water which expand up to 20 cm; and amplitude A3 described motions reaching water surface (motions of more than 20 cm). Consequently, in this study, fish behavior was defined by the number and the duration of motions per amplitude class, the proportion of time used for these motions, and the time interval between two consecutive motions for the entire 30 min of sampling.

The total number of motions per amplitude class was counted for every fish. The duration of the complete motion was calculated by subtracting the exact time of the end of the returning phase from the time of the beginning of the attacking phase. The proportion of time spent for motions (%) was calculated by adding the duration of all motions and dividing this sum by the duration of the recording. The time interval from the end of the returning phase of a motion to the beginning of the attack phase of the next motion (hereafter referred to as inter-departure time) was calculated to obtain the time interval between two consecutive motions.

3.2.5 Characteristics of flow structures

For each time series of flow velocity, five flow characteristics were described that differed in terms of the temporal scales used for their calculations. Two global scale characteristics were calculated using the velocity time series we recorded. The two global scale characteristics estimated were the mean flow velocity $\bar{u}$ (arithmetic mean) and the standard deviation of flow velocity u_{SD}. The two intermediate scale characteristics were defined using events occurring at a temporal scale ranging from 1 to 4 s: the number of flow events in the time series and the duration of flow events. Time intervals during which flow velocity measures were continuously faster than $\bar{u}$ over a time period longer than 1 s were defined as high-speed flow events. Uninterrupted time intervals during which flow velocity values were slower than $\bar{u}$ over a time period longer than 1 s were defined as low-speed flow events (Figure 3.3 a). The time intervals in between high- and low-speed flow events were defined as medium-speed flow events. This technique is a modification of the U-Level detection technique (Lu and Willmarth 1973). It has been used to characterize the turbulent flow structures found in gravel-bed rivers (Roy et al. 1996). Using this modified U-

Level detection technique, high-, medium-, and low-speed flow events were located within the time series and their duration determined (Figure 3.3 b). For further analyses of flow events, this specific data set (pairs of feeding motion and flow event) was classified in three sets: low (fish #1 to #3), medium (fish #4 and #5), and high (fish #6 to #8) flow velocity conditions using the mean flow velocity $\bar{u}$. The fine scale characteristic was a 0·2 s moving average flow velocity (arithmetic mean). This variable was estimated using the mean flow velocity over a time interval of 0.2 s. This time interval corresponds to 4 and 5 consecutive velocity measurements by the ECM (20 Hz) and by the ADV (25 Hz), respectively. This procedure was used to homogenize to 0.2 s the temporal scale at which fine scale observations were measured for the two types of currentmeters used during the study. The standard deviation was also analyzed at a fine temporal scale. However, analyses with these standard deviation values did not unveil any significant pattern. This situation may be related to the fact that a sample size of four or five may not be sufficient to estimate statistically useful standard deviation values in the context of this study. Analyses based on fine scale values of standard deviations are not discussed further.

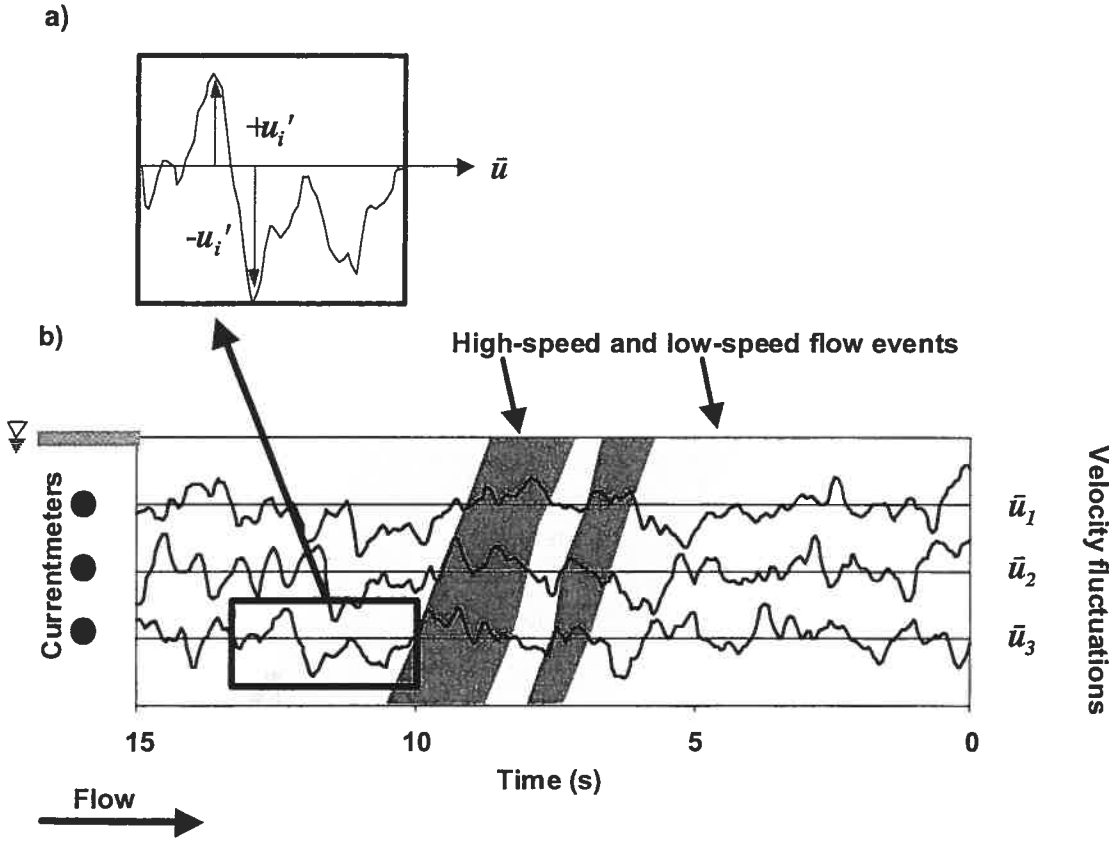

Figure 3.3 ECM velocity time series. a) Illustration of the fluctuating proportion u_i' and the average proportion $\bar{u}$ of the velocity signal. b) Velocity time series at three heights over the gravel-river bed measured synchronously with three ECMs. The light gray areas represent low-speed flow events stretching out over the entire water column. The dark gray areas represent high-speed flow events.

3.2.6 Energetic benefits of the use of low-speed flow events

The key hypothesis underlying this work is that JAS may obtain important energetic benefits by using low-speed flow events during their feeding behavior. It is theoretically conceivable that JAS displaying an intermittent feeding behavior (suite of sit-and-wait and attacks) under harsh flow conditions that fluctuate at temporal scales similar to those used to perform their motions may benefit by using low-speed flow events. However, no data are available to support such hypothesis. The hypothesis was tested by comparing the energy expenditures associated with fish movements as they occur under field situations (with regards to the number of motions, the amplitude of motions, the temporal arrangement of the motions relative

to the fluctuations of flow velocities) to the energy expenditures that may occur under two hypothetical scenarios. In the first hypothetical scenario, the fish would initiate its motions, only and always, at the beginning of a low-speed flow event. In the second hypothetical scenario, fish would perform its motions at randomly chosen times. Expected energy expenditures for motions as they occur under field situations and for both hypothetical scenarios were simulated using the data for the fish #1 and #2 because velocity data at three points over the water column were available for these fish (see ECM data; Table 3.2). In summary, three simulations based on observations made with fish #1 and #2 were performed. First, one for which fish initiated their motions as observed under field conditions. Second, one for which a hypothetical fish initiated its motions only in low-speed flow events. Third, one for which a hypothetical fish initiated its motions at randomly chosen times and flow velocities. For every simulation, the number of motions and their amplitudes were identical to the number of motions and their amplitudes observed under field conditions. Flow conditions were also kept constant for any given fish. Only the temporal arrangement of the motions relative to flow conditions was modified among the simulations to correspond to the desired scenario.

The energy expenditures simulated according to the three scenarios were estimated only for the attack phase of the fish. The calculations focused only on the swimming costs of the attack phase because it is during this phase that fish must swim against the flow whereas, during the return phase, JAS could profit from the recirculating zones created by the river-bed heterogeneity to return to the initial position (McLaughlin and Noakes 1998). Furthermore, in the simulations, only motions of amplitudes A2 and A3 were considered because it was presumed that the

motions of amplitude A1 are too short and too small for fish to profit from a low-speed flow event. Swimming costs were estimated using the distance and the duration of fish motions and the average flow velocity during the attack phase. The distance of the fish motion was estimated from the stereocinematographic recordings. The apparent swimming speed of the fish (V_1; $cm \cdot s^{-1}$) was calculated by dividing the distance fish swam during the attack phase by the duration of the attack phase. The effective swimming speed of the fish (V_3; $cm \cdot s^{-1}$) was calculated as the vectorial sum of the apparent swimming speed of the fish (V_1) and the average flow velocity during the attack phase (V_2; $cm \cdot s^{-1}$)

(3.1) $$V_3 = SQRT\ (V_1^2 + V_2^2)$$

The oxygen consumed for every motion was estimated using the duration of the motion t_a, the effective swimming speed V_3, and the multispecies respirometry model of Boisclair and Tang (1993). This model was selected because when swimming under turbulent flows fish perform swift changes in speed and direction. The model of Boisclair & Tang (1993) is the only model currently available to estimate the net swimming costs C_A for fish displaying changes in speed and direction.

(3.2) $$\log_{10} C_A = 0.54 \cdot \log_{10} M + 1.09 \cdot \log_{10} S - 0.93 \qquad (R^2 = 0.76,\ p < 0.0001)$$

where C_A are the net swimming cots ($mg\ O_2 \cdot h^{-1}$), M the fish mass (g), and S ($cm \cdot s^{-1}$). The fish length was estimated from the stereocinematographic recordings and converted to fish body mass with the following length-mass relationship of JAS

(3.3) $$M = 0.02 \cdot L_t^{2.79} \qquad (n = 50, r^2 = 0.82, p < 0.001)$$

where M is the body mass (g) and L_t the total length of the fish (E.C. Enders & D. Boisclair, unpublished data). Swimming costs (mg $O_2 \cdot h^{-1}$) over 30 min periods were estimated as the sum of the costs of the individual motions (attacks of amplitudes A2 and A3) recorded by our cameras. The same approach was used to estimate fish swimming costs according to the three scenarios.

3.2.7 Statistical analyses

Statistical analyses consisted in testing six hypotheses related to potential relationships between descriptors of fish behavior and characteristics of flow structure at different temporal scales. First, the existence of a relationship between the amplitude of fish motions and the turbulence of the flow was tested. More specifically, the hypothesis was tested that fish living in more turbulent conditions undertake fewer motions of high amplitude (A2, A3) than fish living in less turbulent flow. This hypothesis was tested using fish #1 and fish #2 because these fish were found in environments with the same mean flow velocity (27.8 and 26.8 $cm \cdot s^{-1}$, respectively) but with different standard deviations of flow velocity (4.3 and 7.7 $cm \cdot s^{-1}$, respectively). However, due to possible intra-specific variations and unknown differences in food availability, the data only allows us to speculate that the potentials differences are due to differences in the turbulence. The frequency distributions of motions of amplitudes A1, A2, and A3 for fish #1 and #2 were compared using a Chi^2-Test.

Second, the hypothesis was tested that the proportion of time used by fish to perform motions is related to the mean flow velocity $\bar{u}$ and the standard deviation of the flow velocity u_{SD}. This was done using linear regression analysis with data from fish #3 to #8. The data from fish #1 and #2 were not included because these fish spent relatively less time for motions than fish #3 to #8 which might be due to different environmental conditions during the two sampling periods.

Third, the hypothesis was tested that the occurrence of motions of any given amplitude is related to low-, medium-, and high-speed flow events. This was achieved by constructing a contingency table based on the frequency of motions of amplitudes A1, A2, and A3 under three classes of flow velocity conditions (low: fish #1 to #3, medium: fish #4 and #5, and high flow velocity condition: fish #6 to #8). The Freeman-Tukey deviate statistics was applied with a significance level of $p < 0.05$ (Legendre and Legendre 1998).

Fourth, the hypothesis was tested that the initiation of a motion is related to the occurrence of low flow velocities. This hypothesis was tested by assessing the statistical significance of the difference between the frequency distribution of flow velocities occurring when a given fish (fish #1 to #8) initiated a motion (mean of 0.2 s prior to the initiation of a motion) to the frequency distribution randomly sampled within all the flow velocities experienced by that fish (moving average of 0.2 s) with a Kolmogorov-Smirnov test.

Fifth, the hypothesis was tested that the initiation of motions is randomly distributed through time. Random processes are often described using exponential models (Scherrer 1984). In the context of the present hypothesis, it was presumed that the initiation of motions could be considered to occur at random if the frequency distribution of inter-departure time (time period during two consecutive motions,

from return to the next departure) follows an exponential model. Frequency distributions were developed by grouping all inter-departure times in classes of 10 s (0-9.9 s; 10-19.9 s; 20-29.9 s, etc.). One frequency distribution was obtained for each fish (fish #1 to #8). Each frequency distribution was compared to an exponential model using a Kolmogorov-Smirnov test.

Sixth, the hypothesis was tested that fish swimming costs under turbulent conditions are affected by the temporal arrangement of fish motions and flow velocities using data from fish #1 and fish #2. In particular, the hypothesis was tested that swimming costs estimated using combinations of fish motions and flow velocities observed in the field are statistically different from swimming costs estimated for a hypothetical fish which would perform motions only during low-speed flow events. Similarly, the hypothesis was tested that swimming costs estimated using combinations of fish motions and flow velocities observed in the field are statistically different from swimming costs estimated for a hypothetical fish which would perform motions at randomly chosen flow velocities. Comparisons between real conditions and the two hypothetical scenarios were performed using t-tests.

3.3 Results

3.3.1 Characteristics of fish behavior

Important differences were found between the behaviors of the two fish observed during Sampling period I (Table 3.2). Fish #1 performed 116 motions per 30 min compared to 64 motions during an equal time period for fish #2. Furthermore, fish #1 performed 1.3-times more motions of amplitude A1, 2.6-times more motions of amplitude A2, and 2.9-times more motions of amplitude A3, than fish #2. Fish #1

performed significantly more motions of amplitude A2 and A3 than fish #2 (Table 3.3, Chi^2-Test, χ^2 =6.25, p <0.05). The mean duration of the motions performed by fish #1 (2.2 s) was not significantly different from the motions of fish #2 (2.3 s, p = 0.80). Fish #1 allocated 13.4% of its time budget for motions compared to 8.1% for fish #2. The mean inter-departure time between two consecutive motions for fish #1 (11.7 s) was significantly shorter than for fish #2 (22.2 s, p <0.001).

Table 3.2 Mean flow velocity $\bar{u}$ and standard deviation of the flow velocity u_{SD} measured simultaneously at three heights over two fish positions in the Sainte-Marguerite River. The mean flow velocity over the whole water column $\bar{U}_{column}$ was calculated.

Fish	Currentmeter	Height (cm)	$\bar{u}$ (cm·s^{-1})	u_{SD} (cm·s^{-1})
#1	ECM_1	20	29.5	4.4
	ECM_2	12	29.7	4.1
	ECM_3	4	27.8	4.3
	$\bar{U}_{column}$		29.0	4.3
#2	ECM_1	20	37.6	7.7
	ECM_2	12	35.4	6.4
	ECM_3	4	26.8	7.7
	$\bar{U}_{column}$		33.3	7.3

Table 3.3 Mean flow velocity $\bar{u}$, standard deviation of flow velocity u_{SD}, number and percentage of motion separated by their amplitude. Data are shown for JAS (fish #1 and #2) in two contrasting turbulent flows.

Fish	#1		#2	
	$\bar{u}$	u_{SD}	$\bar{u}$	u_{SD}
(cm·s^{-1})	27.8	4.3	26.8	7.7
Motion	N	%	N	%
A1	50	43.1	40	62.5
A2	34	29.3	13	20.3
A3	32	27.6	11	17.2
total	116	100	64	100

The range of behavior noted during Sampling period II was wider than that during Sampling period I (Table 3.4). The number of motions observed during 30 min intervals of the Sampling period II varied 3.8-fold among fish and ranged from 50 for the least active fish (fish #6) to 188 for the most active fish (fish #3). The percentage of motions of amplitude A1 decreased as the total number of motions per 30 min increased ($n = 6, r^2 = 0.78, p = 0.02$). The opposite trend was observed for the percentage of motions of amplitude A3 that increased as the total number of motions per 30 min increased ($n = 6, r^2 = 0.79, p = 0.02$). However, no relationship was found between the percentage of motions of amplitude A2 and the total number of motions ($n = 6, r^2 = 0.13, p = 0.49$). The mean duration of the motions performed by fish during Sampling period II differed significantly between the six fish observed (1.8 – 2.5 s, $p = 0.02$). Fish #3, which was the most active fish, used 4.3-fold more time for motions (23.7% of its time budget) than fish #6 (5.5% of its time budget). The time used for motions increased significantly with the total number of motions ($n = 6, r^2 = 0{\cdot}96, p = 0.001$). The mean inter-departure time between two consecutive motions decreased significantly as the total number of motions increased. The relation between the mean inter-departure time and the total number of motions could be described well by a power function ($n = 6, r^2 = 0.99, p < 0.001$). The mean inter-departure time of 7.0 s for fish #3 was significantly shorter than for fish #6 of 31.8 s ($p < 0.001$).

Table 3.4 Univariate statistics summarizing the number of motions per amplitude and the total number of motions per 30 min of observation, the proportion of time used for motions, the mean, maximum and minimum inter-departure time compiled for each individual fish.

Characteristics of fish behavior	Fish	#1	#2	#3	#4	#5	#6	#7	#8
Number of motions	A1	50	40	76	69	55	25	42	48
	A2	34	13	86	71	53	22	37	38
	A3	32	11	26	23	14	4	4	6
	total	116	64	188	162	123	50	83	92
Mean duration of feeding motions (s)		2.2	2.3	2.3	2.1	2.4	2.0	2.5	1.8
Proportion of time used for motions (%)		13.4	8.1	23.7	18.9	16.4	5.5	11.1	9·1
Inter-departure time (s)	mean	11.7	22.2	7.0	8.6	11.0	31.8	16.2	16.6
	max	53.7	94.0	132.9	69.3	59.1	153.3	69.5	126.3
	min	0.1	0.7	0.0	0.1	0.1	2.8	2.0	0.2

3.3.2 Characteristics of flow structures

The structure of the time series of flow velocity was described at three temporal scales (global, intermediate, and fine). The global scale analysis of the recordings performed during Sampling period I (Table 3.2) indicated that fish #1 and fish #2 were swimming against mean flow velocities that differed only by 4% ($\bar{u}$ = 27.8 cm·s^{-1} and 26.8 cm·s^{-1}, respectively). However, the standard deviation of the flow velocity experienced by fish #1 (u_{SD} =4.3 cm·s^{-1}) was 44% lower than in the microhabitat occupied by fish #2 (u_{SD} =7.7 cm·s^{-1}, p <0.001). The analysis of the flow events occurring at an intermediate temporal scale indicated that, fish #1 was subjected to 1.8-fold fewer high-speed flow events that fish #2 (Table 3.5). Fish #1 also experienced 1.4-fold fewer low-speed flow events than fish #2. Hence, global and intermediate scale analyses led to conclude that fish #2 experienced more turbulent hydrodynamic conditions than fish #1. High-speed flow events lasted from 1.0 s to 2.9 s while low-speed flow events lasted from 1.0 s to 2.8 s. The standard deviation of high- and low-speed flow events covered the same range (0.1 to 0.5 s).

The mean duration of high-speed flow events (1.2 s) was significantly shorter ($p = 0.04$) than the duration of low-speed flow events (1.8 s). The duration of flow events also differed among fish ($p = 0.03$). The interaction term between the intensity of flow events (high, medium, or low) and locations occupied by fish (#1 and #2) was not statistically significant ($p = 0.11$). Moving average of flow velocity calculated at a fine temporal scale (0.2 s) ranged from 12.2 to 42.0 $cm \cdot s^{-1}$ for fish #1 and from 4.7 to 54.1 $cm \cdot s^{-1}$ for fish #2.

Table 3.5 Water depth, currentmeter used, mean flow velocity $\bar{u}$, standard deviation of the flow velocity u_{SD}, number, mean and standard deviation of the duration of high- and low-speed flow events, minimum and maximum 0.2 moving average velocity in the focal point for eight JAS in the Sainte-Marguerite River during observation.

Flow characteristics:			Global scale		Intermediate scale						Fine scale	
			Flow velocity		High-speed flow events			Low-speed flow events			0.2 moving average velocity	
Fish	Depth (cm)	Currentmeter	$\bar{u}$ ($cm \cdot s^{-1}$)	u_{SD} ($cm \cdot s^{-1}$)	n	mean (s)	SD (s)	n	mean (s)	SD (s)	min ($cm \cdot s^{-1}$)	max ($cm \cdot s^{-1}$)
#1	26	ECM	27.8	4.3	120	1.2	0.1	150	1.5	0.3	12.2	42.0
#2	28	ECM	26.8	7.7	210	1.5	0.4	216	1.8	0.5	4.7	54.1
#3	40	ADV	25.1	4.3	90	1.4	0.4	84	1.4	0.3	9.3	39.9
#4	30	ADV	32.0	10.3	114	1.5	0.3	150	1.3	0.3	4.8	57.5
#5	45	ADV	34.6	8.2	138	1.6	0.7	156	1.7	0.5	6.8	61.8
#6	35	ADV	46.1	10.7	102	1.3	0.3	78	1.3	0.3	15.2	78.2
#7	28	ADV	49.2	13.4	60	1.3	0.2	66	1.2	0.2	12.2	108.2
#8	32	ADV	49.2	10.7	102	1.4	0.3	132	1.4	0.3	19.0	79.7

During Sampling period II, the mean flow velocity ranged from 25.1 $cm \cdot s^{-1}$ (fish #3) to 49.2 $cm \cdot s^{-1}$ (fish #8; Table 3.5). Hence, in contrast to the fish observed during Sampling period I, for which mean flow velocity was rather constant, the mean flow velocity experienced by fish #3 to fish #8 during Sampling period II varied 2.0-fold. The standard deviation of the flow velocity at the six different fish locations ranged from 4.3 $cm \cdot s^{-1}$ (fish #3) and 13.4 $cm \cdot s^{-1}$ (fish #7). This represented a 3.1-fold difference between the lowest and highest standard deviation of flow

velocity. Both the mean flow velocity ($p < 0.001$) and the standard deviation of flow velocity ($p < 0.001$) varied significantly among the six microhabitats surveyed during the Sampling period II. The analysis of the flow events indicated a 2.3-fold difference in number of high-speed flow events and a 2.4-fold difference in number of low-speed flow events among the six JAS observed during Sampling period II. The longest observed high-speed flow event lasted 4.0 s. The corresponding value for low speed flow events was 3.3 s. The minimum duration of high- and low-speed flow events was 1.0 s. The standard deviation of the duration of high- and low-speed flow events ranged between 0.2 to 0.5 s. The mean duration of high-speed flow events (1.4 s) was not significantly different ($p = 0.72$) from the mean duration of low-speed flow events (1.2 s). Similarly, the mean duration of flow events did not differ among fish ($p = 0.97$). The interaction term was not statistically significant ($p = 0.81$). Fine scale average flow velocity ranged from 4.8 $cm \cdot s^{-1}$ (fish #4) to 108.2 $cm \cdot s^{-1}$ (fish #7).

3.3.3 Relationship between fish motions and flow characteristics

During sampling period I, the fish swimming in the less turbulent flow (fish #1, $u_{SD} = 4.3$ $cm \cdot s^{-1}$) performed 1.8-times more motions per 30 min than the fish swimming in the more turbulent flow (fish #2, $u_{SD} = 7.7$ $cm \cdot s^{-1}$). Fish #1 also performed 2.8-times more motions of amplitudes A2 and A3 (combined) than fish #2. Hence, the fish #1 did not only perform more motions than the fish #2 but it also made proportionally more high amplitude motions. The fish living under a less turbulent flow seemed to be more active than the fish living under more dynamic conditions. These behavioral differences may be related to the difference in turbulent conditions observed for the two fish. The mean duration of the motions was

relatively unaffected by turbulence (1.2-fold difference) but the time allocated for performing motions was 1.7-fold longer for fish #1 than for fish #2. The mean inter-departure time was also 1.9-fold shorter for the fish living under less turbulent flow.

During sampling period II, the total number of motions performed by JAS decreased with an increase in mean flow velocity (linear regression analysis, $n = 6$, $r^2 = 0.74$, $p = 0.03$). The percentage of motions of amplitude A1 increased with increasing mean flow velocity (linear regression analysis, $n = 6$, $r^2 = 0.96$, $p = 0.001$). The opposite trend was observed for the percentage of motions of amplitude A3 that decreased with increasing mean flow velocity (linear regression analysis, $n = 6$, $r^2 = 0.91$, $p = 0.003$). However, no relationship was found between the percentage of motions of amplitude A2 and mean flow velocity (linear regression analysis, $n = 6$, $r^2 = 0.23$, $p = 0.33$). Hence, the fish swimming in the less rapid flow performed more motions than the fish living in faster flow and they made proportionally more motions of high amplitude. The mean duration of the motions performed by fish during Sampling period II differed significantly between the six fish observed (1.8 – 2.5 s, $p = 0.02$). However, no relationship was found between the mean duration of the motions and mean flow velocity (linear regression analysis, $n = 6$, $r^2 = 0.07$, $p = 0.62$). The proportion of time used for motions by fish #3 to #8 was related to the mean flow velocity (Figure 3.4). JAS adjust the proportion of time used for motions to the mean flow velocity (linear regression analysis, $n = 6$, $r^2 = 0.77$, $p = 0.02$). The proportion of time used for motions decreased as mean flow velocity increased. However, no significant linear relationship was found between the proportion of time used for motions and the standard deviation of flow velocity (linear regression analysis, $n = 6$, $r^2 = 0.59$, $p = 0.08$). No significant relation was observed between the

mean inter-departure time obtained for fish #3 to #8 and mean flow velocity and standard deviation of flow velocity (linear regression analysis, n =6, r^2 =0.36, p = 0.21, r^2 =0.29, p =0.28, respectively).

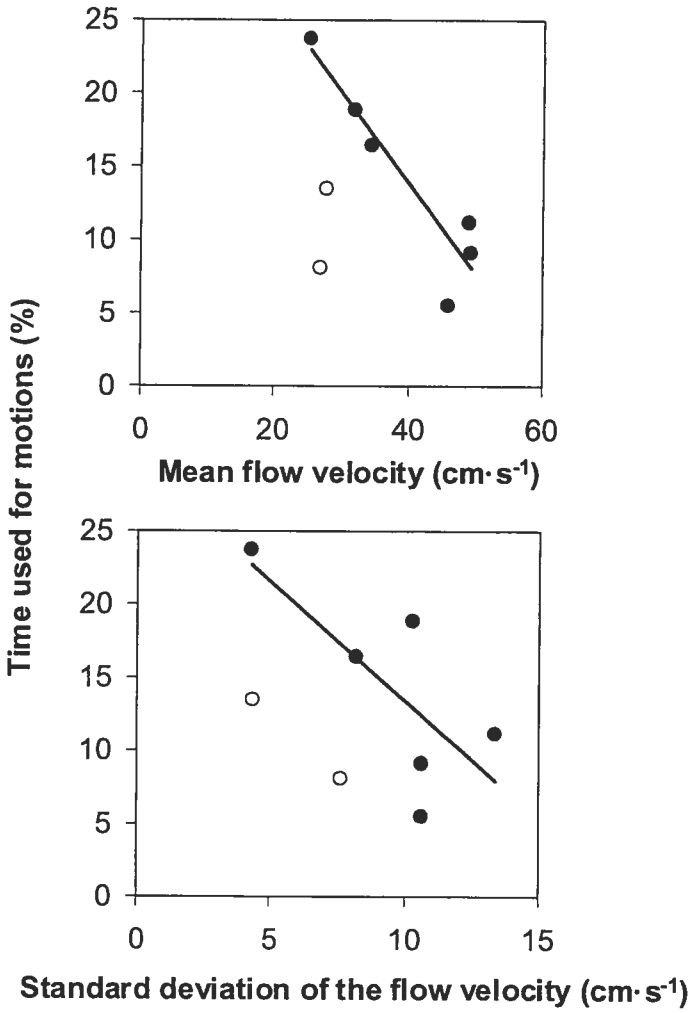

Figure 3.4 Proportion of time used by the fish for motions in relation to mean flow velocity $\bar{u}$ and standard deviation of the flow velocity u_{SD}. In open circles the measurements of Sampling period I and in solid circles the measurements obtained during the Sampling period II. For the linear regression only the data of Sampling period II were considered.

The hypothesis was tested that the occurrence of motions of specific amplitudes may be related to the occurrence of low-, medium-, or high-speed flow events using contingency table analysis. The data employed to test this hypothesis was divided in three classes of mean flow velocity conditions: low flow velocity (n = 3, $\bar{u}$ ranged from 25.1 to 27.8 cm·s^{-1}), medium flow velocity (n =2, $\bar{u}$ ranged from

32.0 to 34.6 $cm \cdot s^{-1}$), and high flow velocity (n =3, $\bar{u}$ ranged from 46.1 to 49.2 $cm \cdot s^{-1}$) conditions (Table 3.6). The occurrence of motions of amplitudes A1, A2 and A3 were not related to the occurrence of low-, medium-, or high-speed flow events for fish living in areas characterized by low flow velocity condition (χ^2 =2.30, p >0.05). However, the occurrence of motions of different amplitudes was related to the occurrence of specific flow events in medium (χ^2 =14.17, p <0.05) and high flow velocity conditions (χ^2 =12.83, p <0.05).

A *posteriori* test indicated that fish performed significantly fewer motions of amplitude A3 in medium (Freeman-Tukey deviate =3.89, p <0.05) and high flow velocity conditions (Freeman-Tukey deviate = 3.20, p < 0.05) than expected by chance.

Table 3.6 a) Observed frequency distribution of the motions classified by their amplitude and the occurrence in a specific flow event in i) low flow velocity, ii) medium flow velocity, and iii) high flow velocity conditions. b) Expected frequency distribution of the motions with the contingency table analysis.

a)

Obs. (%)	High-speed flow event	Medium-speed flow event	Low-speed flow event
A1	7.3	29.2	9.1
A2	6.5	23.0	5.9
A3	2.6	12.3	4.1

i) for fish in slow

Obs. (%)	High-speed flow event	Medium-speed flow event	Low-speed flow event
A1	11.6	23.2	11.6
A2	9.6	23.2	9.6
A3	0.9	7.9	2.3

ii) for fish in medium

Obs. (%)	High-speed flow event	Medium-speed flow event	Low-speed flow event
A1	6.1	31.6	8.8
A2	3.5	32.9	7.8
A3	0.0	7.7	1.5

iii) for fish in fast flow.

b)

Exp. (%)	High-speed flow event	Medium-speed flow event	Low speed flow event
A1	7.5	29.4	8.7
A2	5.8	22.8	6.7
A3	3.1	12.3	3.6

Exp. (%)	High-speed flow event	Medium-speed flow event	Low-speed flow event
A1	10.3	25.3	11.0
A2	9.4	23.0	10.0
A3	2.4	6.0	2.6

Exp. (%)	High-speed flow event	Medium-speed flow event	Low-speed flow event
A1	4.5	33.7	8.4
A2	4.3	32.0	8.0
A3	0.9	6.7	1.7

The possibility that fish initiate a motion preferentially during low flow velocities as estimated at a fine temporal scale (moving average of 0.2 s) was assessed using a Kolmogorov-Smirnov test. The means of the frequency distributions of fine scale flow velocities when fish initiated a motion (average 38.9 $cm \cdot s^{-1}$) were, on average 4.0% lower (range =-0.4% to 8.1%) from the mean of the frequency distributions of fine scale flow velocities selected at random. The frequency distributions of fine scale flow velocities during the initiation of a motion did not differ from the frequency distributions of fine scale flow velocities selected at random (Kolmogorov-Smirnov test, p-values range from 0.31 to 0.94). Consequently, the analyses suggest that JAS do not have a predilection for low fine scale flow velocities when initiating a motion (Figure 3.5).

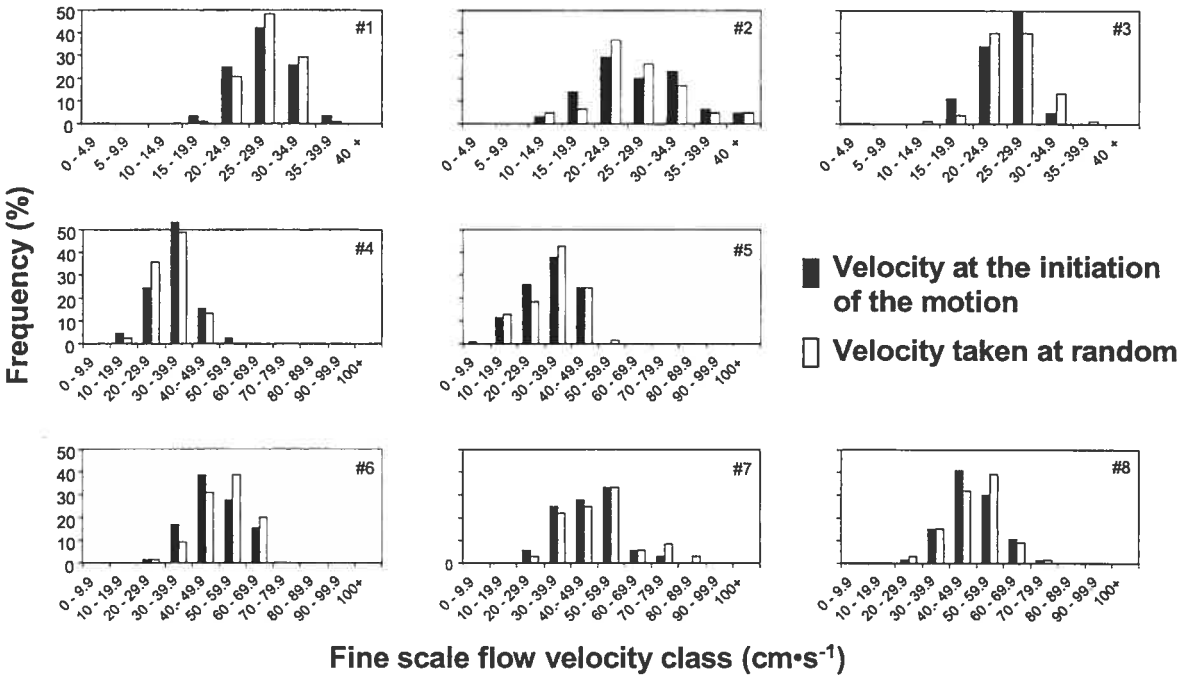

Figure 3.5 Distribution of the fine scale flow velocities at the moment of the initiation of the motion in solid bars and taken at random in open bars were compared for the eight fish. No preference of the use of low fine scale flow velocities for the initiation of fish motions could be observed.

Further, the ability of fish to select particular hydrodynamic conditions when initiating a motion was tested by comparing their inter-departure time to those expected from a random process. For that purpose, the frequency distributions of the duration of the inter-departure time was compared to those predicted by an exponential model (Figure 3.6). The frequency distribution of the observed inter-departure time did not significantly differ from the predicted frequency distribution of the exponential model (Kolmogorov-Smirnov test, p-values range from 0.23 to 0.91).

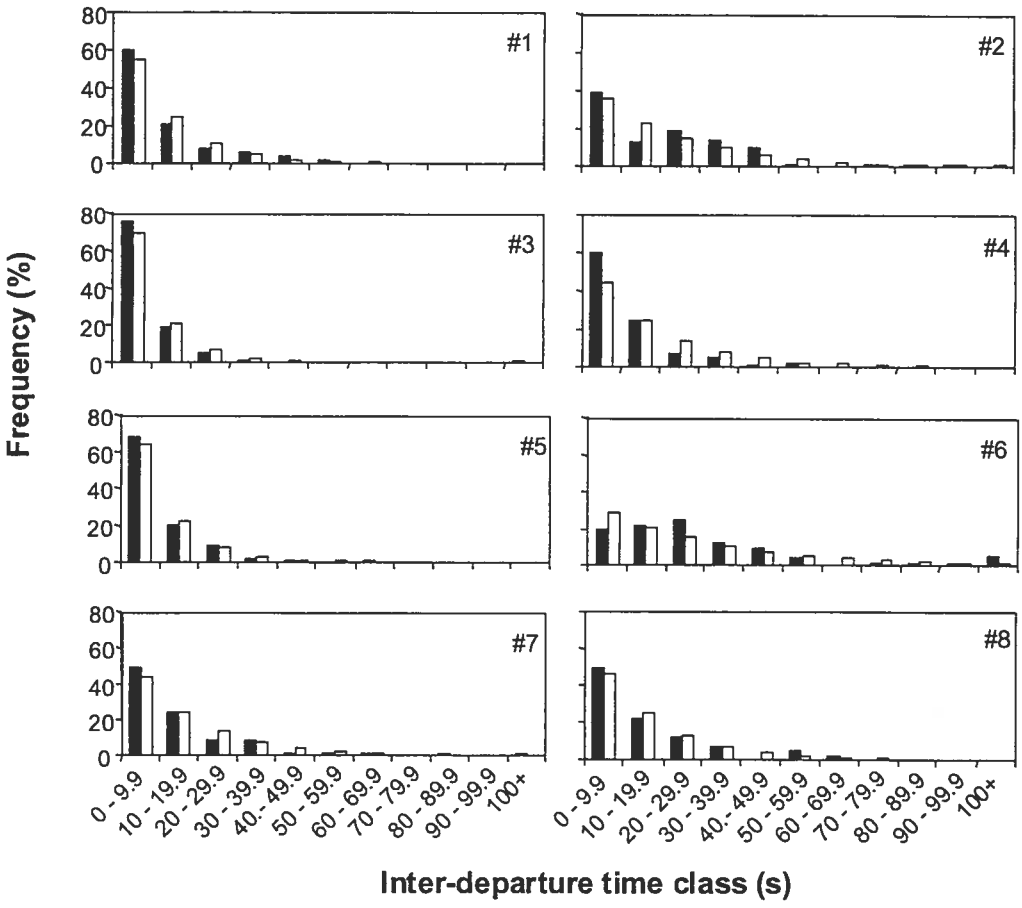

Figure 3.6 Comparison of the frequency distribution of the observed inter-departure time in solid bars and the predicted frequency distribution by an exponential model in open bars. A good coherence between observed and predicted distribution is observed.

3.3.4 Energetic benefits of the use of low-speed flow events

The energy expenditures of the attack phase of fish motions as they occur in the field were compared to those that may be incurred by fish under two hypothetical scenarios using fish #1 (9.0 g) and fish #2 (10.7 g). Although both fish lived in microhabitats characterized by similar flow velocities (27.8 $cm \cdot s^{-1}$ for fish #1 and 26.8 $cm \cdot s^{-1}$ for fish #2), the standard deviation of flow velocity was 1.8-times larger for fish #2 (u_{SD} =4.3 $cm \cdot s^{-1}$) than for fish #1 (u_{SD} =7.7 $cm \cdot s^{-1}$). Hence, fish #2 was observed under more turbulent flow conditions than fish #1. Swimming costs estimated for the attack phase of fish motions as they occur in the field ranged from 0.34 mg $O_2 \cdot h^{-1}$ (fish #2) to 0.62 mg $O_2 \cdot h^{-1}$ (fish #1). As expected, the more active fish #1 spent significantly more energy performing attacks than the less active fish #2 ($p < 0.001$). Under the first hypothetical scenario tested, fish #1 observed in a less turbulent flow would decrease its swimming costs during attacks by 19.8% (to 0.49 mg $O_2 \cdot h^{-1}$) by initiating all its motions in low-speed flow events. Adoption of this scenario to the fish #2 living in a more turbulent flow would decrease its swimming costs by 31.1% (to 0.23 mg $O_2 \cdot h^{-1}$). For both levels of turbulence, the swimming costs estimated with the scenario that fish use only low-speed flow events were statistically smaller than the swimming costs of the attacks as they occur in the field ($p < 0.01$). The costs of attacks obtained under the scenario that fish initiate their motions at flow velocities selected at random (0.61 mg $O_2 \cdot h^{-1}$ and 0.35 mg $O_2 \cdot h^{-1}$ for fish #1 and #2, respectively) were not significantly different from the costs estimated for attacks as they occur in the field (t-test; $0.28 < t < 0.20$, $0.78 > p > 0.84$).

3.4 Discussion

The analyses indicated that the behavior of stream-dwelling fish such as JAS may be affected by flow characteristics. Observations performed during Sampling period I indicated that the number of motions, and in particular the number of high amplitude motions, together with the proportion of the time budget allocated to motions were significantly lower for a fish subjected to high turbulence than for a fish living under more stable conditions. The fact that both fish (fish #1 and #2) were observed under very similar mean flow velocities ($\bar{u}$ = 27.8 and 26.8 $cm \cdot s^{-1}$, respectively) but different standard deviations of flow velocity (u_{SD} =4.3 and 7.7 $cm \cdot s^{-1}$, respectively) may suggest that studies of fish behavior under turbulent flow may require the assessment of these two variables. However, this conclusion is drawn from only two individual JAS.

Observations performed during Sampling period II confirmed that, the number of motions performed by JAS, and in particular the number of high amplitude motions, decreased in faster and more turbulent flow. Furthermore, fish subjected to 2.0-fold faster and 2.4-fold more turbulent flow allocated a 4.3-times smaller proportion of the time budget to motions than fish in slower and less turbulent flow. These observations demonstrated that, in a natural situation under turbulent flow, salmonids decrease the amplitude of the motions to intercept drifting prey particles as flow velocity increases. As such our field observations supported laboratory studies of Godin and Rangeley (1989) and O'Brien and Showalter (1993). Furthermore, our analyses showed that the amplitude of a motion and its occurrence in a specific flow event were independent for fish in low flow velocity conditions. However, for fish swimming in medium and high flow velocity conditions the amplitude of a motion and its occurrence in a specific flow event were related. The

statistical analysis based on a contingency table indicated that fish performed significantly fewer high amplitude motions in high-speed flow events than expected by the contingency tables analysis in medium and high flow velocity conditions. The biological significance of these results is difficult to assess since the frequency of high amplitude motions differed by only 1.5% (0.9% observed versus 2.4% predicted) at medium flow velocity conditions and 0.9% (0.0% observed versus 0.9% predicted) at high flow velocity conditions. These very small differences appear not be biologically meaningful. Similarly, JAS did not show any disposition for low fine scale flow velocities when initiating their motions. McLaughlin and Noakes (1998) analyzed the behavior of young-of-the-year brook charr (*Salvelinus fontinalis* MITCHELL) in their natural habitat and stated that the swimming motions may be influenced by the temporal and spatial heterogeneity of the flow. They showed that young-of-the-year brook charr use spatial flow velocity refuges to reduce their swimming costs. These authors could not analyze the relationship between short-term fluctuations and behavior as the velocity measurements were taken as averages over 60 s. However, they supposed that fish might react to temporal heterogeneity of the flow. In our study, the flow velocity was measured at high temporal resolutions of 20 and 25 Hz, respectively. Therefore, the relationship between the initiation of the motions and a fine scale characteristic such as the 0.2 s moving average velocities at the focal point of fish could be analyzed. However, in our study, JAS did not appear to use low fine scale flow velocities when initiating a motion. Furthermore, the frequency distributions of the inter-departure times of the eight JAS were not significant different from the frequency distribution of an exponential model which may signify that the inter-departure time can be reduced to a random variable. The fact that JAS initiate their motions not preferential in low-speed flow events or low

fine scale flow velocities and the fact that the inter-departure time can be seen as random variable may lead to conclusion that the JAS observed initiated their motions according to a temporal sequence that may be independent from hydrodynamic conditions and that may not be statistically different from a purely random process.

The fact that JAS initiate their motions independently of hydrodynamic conditions is surprising since the simulations of three hypothetical scenarios indicated that fish may benefit from an energetic advantage by using low-speed flow events. Fish #1 in less turbulent flow would decrease its swimming costs by 19.8% by undertaking all its motions in low-speed flow events. Fish #2 staying in more turbulent flow would even decrease the swimming costs by 31.1%. According to optimal foraging theory (Krebs 1978), JAS should be sensitive to variations in swimming costs when taking foraging decisions. One hypothesis that may explain why JAS may not initiate their motions only during low-speed flow events may be that other criteria co-determine this decision. For instance, fish may not decide to initiate a motion in a low-speed flow event when no drifting food particles are available during that specific time period. Hence, fish motions may not only be related to the occurrence of a specific flow event but more likely to a combination of the occurrence of potential food particles and flow velocity. Drift particle density has been shown to be positively related to flow velocity (Elliott 1967). However, on a smaller temporal scale drift might not be equally distributed. There are three contradictory hypothesis regarding drift distribution in relation to short term flow events: (1) Low-speed flow events, which are ejection of slow moving fluids developing towards the water surface, may cause uplifts of deposited particles in the water column. Therefore, low-speed flow events may contain a higher amount of

suspended particles per unit of time (Lapointe 1992). (2) High-speed flow events may be argued to contain more food particles because there is a larger water volume passing by in a given time interval resulting in a higher food particle concentration per time, or (3) particles may accumulate at the limit between high- and low-speed flow events – a process similar to the accumulation of particles between the front of two water masses (Ott 1988). However, in this study drifting prey particles could not be tracked either visually or on the video recordings, therefore the capture efficiency can not been addressed. Further studies of simultaneous measurements of drift, flow velocity, and feeding behavior at high temporal and spatial resolution are needed to verify these hypotheses.

Nevertheless, the present study contributes to approaches to study fish behavior under turbulent flows. Numerous aspects of fish behavior such as the proportion of the time budget used for activity, the number of motions performed per unit of time, the time between two consecutive motions, and the amplitude of motions were affected by the flow. More importantly, observations performed during this study indicated that fish subjected to similar mean flow velocities but different standard deviation of flow velocities may have a different behavior. The data do not allow us to assess the ultimate cause of the differences we observed (energetics of swimming against a turbulent flow or the quantity of the drift within the flow) but the study suggests that both the mean flow velocity and the standard deviation of flow velocity should be quantified when studying fish behavior under turbulent flows.

The present study also contributes to approaches to estimate the swimming costs of fish under turbulent flows. Bioenergetics models commonly estimate the

cost of swimming against a turbulent flow using a combination of respirometry models and the body mass of the fish, the effective swimming speed of the fish, and the time fish spend swimming at that speed (Hughes and Dill 1990; Guensch et al. 2001). The effective swimming speed of the fish is taken as the sum of the apparent speed of the fish (relative to the river bed) and the mean flow velocity. Because turbulent flow consists of a suite of high- and low-speed flow events (Kirkbride and Ferguson 1995; Ferguson et al. 1996; Buffin-Bélanger et al. 2000a) and because fish possess organs that may allow them to identify these structures (Northcutt 1997), it is possible that fish living in turbulent flows would perform their motions preferentially during low-speed flow events in order to minimize their energy expenditures. The selection by fish of low-speed flow events would cause the measures of mean flow velocity to overestimate the flow velocities against which fish actually swim. This, in turn, would cause the overestimation, by common modeling approaches, of the costs of habitat utilization by fish living under turbulent conditions. Consequently, the estimation of the costs of habitat utilization by fish that select low-speed flow events would require synchronized and detailed recordings of the fish behavior and the turbulent flow structure. Our study is, to our knowledge, the first attempt to estimate the potential energetic benefits of selecting low-speed flow events. Our calculations, which are based on *in situ* observations of the fish behavior and the turbulent flow structure, suggest that fish may decrease their activity rates 19.8% to 31.1% by performing their motions only and always in low-speed flow events. Despite this potential energy gain, our work showed that fish do not truly take advantage of low-speed flow events (other attributes such as the density of insects in the drift may affect the fish behavior). The only statistically significant relationship between the fish behavior and the turbulent flow structure was that fish tended to perform fewer

high amplitude motions during high-speed flow events when swimming under medium and high flow velocity conditions. Presumably, more energy may be saved when trying to avoid high-speed flow events under the more intense velocity conditions. However, this tendency was very subtle with fish performing high amplitude motions during high-speed flow events at a frequency only 0.9% to 1.5% lower than expected by chance. No significant preferential use of low-speed flow events was observed. Hence, for all practical purposes, fish can be presumed to make biologically insignificant use of low-speed flow events. This interpretation is confirmed by our finding that the time intervals between motions may be taken as a variable that is randomly distributed. One direct consequence of this finding is that fish may be presumed to swim against mean flow velocity during their motions. In this respect, the study suggests that estimates of fish apparent swimming speed (obtained, for instance, by video observations) and estimates of mean flow velocity encountered by fish may be sufficient to assess the mean effective swimming speed. This, however, should not be taken as an indication that the standard deviation of flow velocity is not required to assess fish energy expenditures. Recent studies suggest that the standard deviation of flow velocity affects the cost of swimming against turbulent flows. As such, it is possible that respirometry models developed to estimate the cost of swimming in turbulent flows may not only require the fish body mass and the mean fish swimming speed as independent variables but also the standard deviation of fish swimming speed (Enders et al. 2003). In contrast, the present study does suggest that the detailed examination of the temporal synchrony between fish behavior and occurrence of high- and low-speed flow events may not be required to estimate the effective swimming speed of fish that allows the estimation of the cost of swimming in turbulent flows.

4 THE EFFECT OF TURBULENCE ON THE COST OF SWIMMING FOR JUVENILE ATLANTIC SALMON (*SALMO SALAR*)[2]

Abstract

Fish activity costs are often estimated by transforming their swimming speed to energy expended using models developed from fish forced to swim against a flow of constant velocity. Forced swimming models obtained using a procedure that minimizes flow heterogeneity may not represent the cost of swimming in rivers characterized by turbulence and by a wide range of instantaneous flow velocities. We assessed the net swimming costs of juvenile Atlantic salmon (*Salmo salar*) in turbulent flows using two means (18 $cm \cdot s^{-1}$ and 23 $cm \cdot s^{-1}$) and two standard deviations of flow velocity (5 $cm \cdot s^{-1}$ and 8 $cm \cdot s^{-1}$). Twenty respirometry experiments were conducted at 15°C with fish averaging 10 g. Our results confirmed that net swimming costs are affected by the level of turbulence. For a given mean flow velocity, net swimming costs increased 1.3- to 1.6-fold as turbulence increased. Forced swimming models underestimated actual net swimming costs in turbulent flow by 1.9- to 4.2-fold. Spontaneous swimming models overestimated the real cost of swimming in turbulent flow by 2.8- to 6.6-fold. Our analyses suggest that models in which both the mean and the standard deviation of flow velocity are explicitly represented are needed to adequately estimate the cost of swimming against turbulent flows.

---

[2] Enders, E.C., D. Boisclair & A.G. Roy (2003) The effect of turbulence on the cost of swimming for juvenile Atlantic salmon (*Salmo salar* L.). *Canadian Journal of Fisheries & Aquatic Sciences*. 60, 1149-1160.
Contribution to the program of CIRSA.

4.1 Introduction

Bioenergetics models can be applied to quantify aspects fish habitat quality using the net energy gain obtained by a fish under specified environmental conditions (Hayes et al. 2000). In suitable habitats, fish have a positive balance between the energy acquired from their environment and that required for metabolic expenditures and physiological maintenance (Fausch 1984). Bioenergetics modeling involves the estimation of consumption, growth, metabolism, excretion, and egestion. Although activity metabolism is the least understood component of fish bioenergetics models, it has been argued to represent a large and variable proportion of fish energy budget (Boisclair and Leggett 1989; Boisclair and Sirois 1993; Rowan and Rasmussen 1996). Hence, inappropriate assumptions about activity metabolism may have a strong influence on the accuracy of the predictions of net energy gain and habitat quality values generated by bioenergetics models (Ney 1993; Boisclair 2001).

Fish activity metabolism may be estimated by quantifying fish behavior and transforming the characteristics of fish behavior (types and numbers of movements) in energy expenditures. This approach has been used to estimate the activity metabolism of fish in lakes (Lucas et al. 1991; Sirois and Boisclair 1995; Briggs and Post 1997). Estimation of activity metabolism for fish living in rivers represents a particular challenge because of the unknown metabolic consequences for fish of having to swim against a turbulent flow (Roy et al. 1999; Boisclair 2001). The cost of performing feeding motions from the river bed towards the water surface to capture prey items drifting in the water flow is often estimated using forced swimming models (Puckett and Dill 1985; Sabo et al. 1996). These models are obtained using flume respirometers designed to minimize flow heterogeneity

(Bainbridge 1958; Brett 1964; Beamish 1978). The experimental conditions used to develop forced swimming models resemble the conditions found in rivers because fish swim against a flow. However, these models focus on steady swimming and do not account for the costs of performing changes of speed and direction. Changes of speed and direction have been suggested to incur a 3- to 22-fold increase in fish respiration rates relative to predictions made by forced swimming models (Boisclair and Tang 1993; Tang et al. 2000). Spontaneous swimming models adequately account for the costs of performing accelerations and turns but they have been developed and used with fish swimming in absence of flow (Trudel and Boisclair 1996; Aubin-Horth et al. 1999; Tang et al. 2000).

Turbulence is the state of a flow characterized by the superposition of intense small-scale motions in all directions on a main large-scale flow (Vogel 1994). Turbulence may be perceived as a partly random, partly structured, temporal variation of flow velocity at one point in space (Kirkbride 1993). Turbulence may also be perceived as the spatial heterogeneity of flow velocities at a given time (Bradshaw 1985). As such, the description of turbulence depends on the temporal and spatial scales at which it is observed. Turbulence, and in particular, its descriptor, turbulence intensity (standard deviation of the flow velocity divided by the mean flow velocity), may be expected to vary with the temporal scale (e.g. ms or min) used to measure flow velocity and standard deviation of flow velocity at one point in space. Similarly, because of the spatially heterogeneous nature of turbulent flow, turbulence intensity estimated at a small spatial scale (1 cm^3) may be different from that estimated at a larger spatial scale (1 dm^3).

The turbulence of the flow in rivers may be an important factor influencing the activity costs of fish in these environments (Fausch 1993; McLaughlin and Noakes 1998). However, turbulence is not taken into account by either forced or by spontaneous swimming models. The objectives of this study were (1) to determine the effect of turbulence on net swimming costs, (2) to compare the cost of swimming in turbulent flow to the costs predicted by forced and spontaneous swimming models, and (3) to propose a new model to estimate the energetic cost of swimming in a turbulent flow.

4.2 Material and methods

We attained our objectives by performing twenty respirometry experiments during which we subjected individual fish to four types of turbulent conditions (a combination of two means and two standard deviations of the flow velocity). We performed five experiments per flow condition at a water temperature of 15°C. Fish respiration rates obtained under the different turbulent conditions were compared to predictions made by forced and spontaneous swimming models (Boisclair and Tang 1993). This strategy was adopted because our experimental set-up was not designed to provide and does not allow laminar flow or flow without turbulence. As such, we preferred to use as a reference for comparisons, the 40 years of data on forced and spontaneous swimming available in the literature and used by Boisclair and Tang (1993) to develop general forced and spontaneous swimming models.

4.2.1 Fish

Juveniles of Atlantic salmon (age-1+; *Salmo salar*; JAS) were selected for our study because their natural habitat encompasses gravel-bed rivers characterized by

highly turbulent flows. The behavior of JAS comprises so-called 'sit-and-wait' periods in which JAS swim just above the substrate, often at the downstream edge of a rock, used as a protection against the turbulent flow. The rock preferentially used by a territorial JAS is referred to as its 'home-rock'. The sit-and wait behavior represents the largest part of the time budget of JAS (>80%; F. Burton and D. Boisclair, unpublished data). JAS also perform 'attacks' which are feeding motions from the river bed towards the water surface, or in the water column, in which they capture drifting invertebrates (Kalleberg 1958). During these motions, JAS experience rapid changes in the structure of flow. JAS were also used for our work because the abundance of the wild form of Atlantic salmon is decreasing (Bardonnet and Baglinière 2000). This situation is alarming particularly considering that these fish supported an extensive and valuable commercial and recreational fisheries. It is expected that an improved assessment of the costs of habitat utilization for JAS would contribute to the development of models and management strategies of riverine environments better adapted to protect this species.

The Pisciculture de Tadoussac (operated by the Société de la Faune et des Parcs du Québec, Canada) provided the JAS used for our experiments. These were F_1 generation fish from the crossing of wild genitors that originated from the Sainte-Marguerite River (Saguenay Region, Québec, Canada). The juveniles were transferred to the Université de Montréal and kept in a 500 L Living Stream aquarium (Frigid Units Inc.; Toledo, Ohio, USA; model LSW 700) at 15°C for a period of one month before beginning the experiments. This temperature was selected because it corresponded to the mean summer temperature of the Sainte-Marguerite River (F. Burton and D. Boisclair, unpublished data). The pH of the

water was 7.8. Total hardness was 116 $mg \cdot L^{-1}$ $CaCO_3$ and water alkalinity was 83 $mg \cdot L^{-1}$ $CaCO_3$. The water was kept oxygen-saturated by airstones. Fish were fed daily with commercial food pellets (Corey Feed Mills Ltd., Fredericton, New-Brunswick). The mean mass of the fish used for our respirometry experiments was 10.09 g wet (total number of fish used in our experiments, N = 20; standard deviation, S.D. =0.33 g wet; mean total length, TL =10.8 cm, S.D. =0.4 cm).

4.2.2 Experimental design

The respirometer consisted of a Plexiglas® box having a volume of 24 L (60 cm x 20 cm x 20 cm) with a lid that could be hermetically sealed. The respirometer was placed in a 500 L Living Stream aquarium to maintain a water temperature of 15°C during the experiments. The respirometer contained two pumps and a bottle-shaped swimming chamber. The size of the respirometer was dictated by the size of the two pumps and the swimming chamber we used. The pumps were inserted in the respirometer to ensure that oxygen could not be introduced in the respirometer by the water flowing in the pumps. The size and the shape of the swimming chamber were selected to ensure that fish could not avoid the flow and to minimize the influence of wall effects on our fish. Such wall effects may, at times, create vortices or more laminar flows near solid surfaces. Hence, flow structure closer to walls may be different from that in the center of a swimming chamber. Using a much smaller swimming chamber would have meant that fish would have been closer to the walls of the swimming chamber and more prone to wall effects difficult to describe or quantify. The narrow neck of the swimming chamber was connected to a pump (model 1750, Jacobs Canada Inc., Mississauga, Ontario) that generated the turbulent flow in the swimming chamber by recirculating water within the respirometer

(Figure 4.1). This pump is hereafter refereed to as pump 1. Another pump (Model 402, Powerhead, Montréal, Québec; hereafter referred to as pump 2) served two purposes. Before an experiment, pump 2 was used to create a water exchange between the respirometer and the aquarium, and hence, to provide oxygenated water to the respirometer. During an experiment, pump 2 was used to transfer water from the respirometer to the oxygen meter. The swimming chamber contained two grids. The grids consisted of nylon mesh of 9 cm in diameter perforated with 2 mm x 2 mm holes. The grids were located in the 'upstream' and 'downstream' sections of the swimming chamber. The 'upstream' grid was used to produce a spatially uniform fine turbulence flow structure within the swimming chamber (Tritton 1988). The 'downstream' grid was designed to force the fish to remain in the swimming chamber without interfering with the flow.

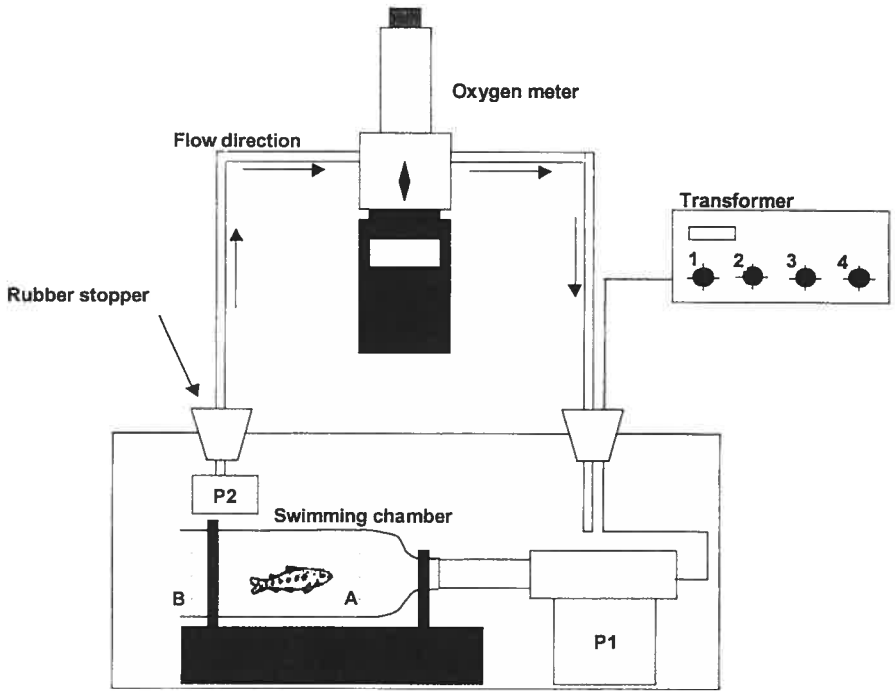

Figure 4.1 Schematic representation of the experimental set-up used during the respirometry experiments performed to estimate the cost of swimming in a turbulent flow. A transformer modulated the electric current that powered a pump (P1), which created a turbulent flow in the swimming chamber against which a fish would swim. A second submerged pump (P2) continuously transferred water from the swimming chamber to the oxygen meter to measure the oxygen uptake by a fish. The swimming chamber contained two grids. The 'upstream' grid (A) was used to produce a spatially uniform fine turbulence flow structure within the swimming chamber and the 'downstream' grid (B) was designed to force the fish to remain in the swimming chamber.

Turbulence in the swimming chamber was created by modulating the electric current that powered pump 1. Four components of the electric current were adjustable: (1) the maximal electric current which determines the maximal flow velocity, (2) the minimal electric current which determines the minimal flow velocity, (3) the frequency of pulsation between a reduction of the electric current to introduce a pulsation of the water flow, and (4) the duration of the reduction of the electric current to manipulate the duration of low- and high-speed flow conditions. Flow structures were quantified using an Acoustic Doppler Velocimeter (ADV; Sontek, San Diego, California, USA). The ADV allowed us to record the three orthogonal velocity components of the flow (streamwise, U; vertical, V; lateral, W) at a frequency of 25 Hz. The volume sampled by the ADV (0.25 cm^3) is located 5 cm away from its probe so that the perturbation of the measured flow by the probe is minimized. This volume (cylinder of 0.9 cm horizontally and a radius of 0.6 cm) was judged appropriate for our purposes because it resembled the product of the surface area of the cross section of the head and the length of the head of the fish we used. The volume sampled by the ADV was therefore similar to the volume of the head of the fish we used. The ADV permitted us to define the settings of the components of the electric current that could create four different flow conditions determined by two mean streamwise flow velocities $\bar{u}$ (low flow condition $= 18$ $cm \cdot s^{-1}$; high flow condition $=23$ $cm \cdot s^{-1}$) and two standard deviations of the streamwise flow velocity u_{SD} (low turbulence $=5$ $cm \cdot s^{-1}$; high turbulence $=8$ $cm \cdot s^{-1}$). The four experimental flow structures were selected for our experiments because they corresponded to flow conditions commonly used by JAS in the Sainte-Marguerite River (Guay et al. 2000; E.C. Enders and D. Boisclair, unpublished data). Fish activity costs were quantified

by measuring the oxygen depletion over time with an oxygen meter (model 565, Intab, Stenkullen, Sweden; ± 0.005 mg $O_2 \cdot L^{-1}$).

4.2.3 Experimental procedure

4.2.3.1 Characteristics of flow structures

Turbulence was quantified at the beginning and the end of the suite of experimental observations (five experiments) aimed at testing the effect of one of the four specific flow conditions on fish respiration rates. Turbulence was quantified in the absence of fish to avoid interference caused by fish on our recordings. For every flow condition, six velocity time series (three at the beginning and three at the end of a suite of experimental observations) were recorded for a period of 5 min. Between each velocity time series, the apparatus used to create the turbulent flow was completely shut down. This strategy was adopted to verify the repeatability and the stability of the flow structures created by our apparatus for given settings of the electric current that powered the pump.

4.2.3.2 Respirometry

Respirometry experiments were performed using a single fish at a time. A fish was selected at random from our stock of experimental fish, kept separately, and not fed for two days before the experiment to avoid increased metabolic rates resulting from digestion (Brett and Groves 1979). Twenty-four hours before the beginning of an experiment, the fish was introduced into the swimming chamber to allow it to adapt to the experimental conditions. After this introduction, the respirometer was sealed without residual air bubbles. During this adaptation phase, pump 2 generated a water exchange between the respirometer and ambient water of the aquarium. At the

beginning of the experiment, pump 2 was connected to the oxygen meter preventing an external water supply and pump 1 was started to create the turbulent flow structures in the swimming chamber. Oxygen concentration was measured at the beginning of the experiment, after which it was measured every 30 min for the duration of the experiment (6 h) for a total of 13 oxygen concentration measurements.

We monitored fish behavior during each experiment to ensure that they were continuously swimming. Every 10 min an image of the position held by the fish within the swimming chamber was automatically registered with a web cam (Sony Electronics Inc., Oradell, New York). In addition, during the last 30 min of the experiment, the fish was continuously filmed by a video camera (WV-BL602; Panasonic Canada Inc., Lachine, Québec). Hence, our procedure presumes that if a fish is always in a swimming position in a series of images registered at 10 min intervals, and if it swims continuously during the last 30 min of an experiment, it was continuously swimming during the 6 h of the experiment. Analysis of the images and of the films collected during our twenty experiments indicated that fish were always swimming in the central section of the swimming chamber. No fish settled at the bottom of the swimming chamber or was observed against the 'upstream' or 'downstream' grid of the swimming chamber. Consequently, we are proceeding with the assumption that, during our experiments, fish were continuously swimming against the flow structures created by our apparatus.

An experiment always ended after 6 h. This 6 h period was chosen because performing longer (few hours but without provoking fatigue; see Discussion) rather

than shorter experiments (few minutes) may allow oxygen depletion estimated during the respirometry experiments to include the repayment of an oxygen debt incurred by the recourse by fish to anaerobic metabolism. No observation was made below 7.6 mg $O_2 \cdot L^{-1}$ to minimize the influence of low oxygen concentration on the fish behavior (Beamish 1978). At the end of an experiment the fish was removed from the respirometer, anaesthetized (clove oil; 0.6 mg$\cdot L^{-1}$), weighed (g wet), and measured (TL cm). The biological oxygen demand (BOD) was determined within 6 h of an experiment using the same procedure but without fish.

4.2.3 Computations

We estimated the cost of swimming against a turbulent flow in three steps. Firstly, we estimated the total metabolic rate of fish (Vo_2; mg $O_2 \cdot h^{-1}$) as

$$Vo_2 = \Delta O_2 / \Delta t \cdot V_W - BOD \quad (4.1)$$

where ΔO_2 is the difference in oxygen concentration between two consecutive oxygen concentration measurements (mg $O_2 \cdot L^{-1}$), Δt is the time interval of 0.5 h between two consecutive oxygen concentration measurements, V_W is the volume of water in the respirometer excluding the solid volume of our pumps, swimming chamber, and fish, the and BOD is the biological oxygen demand by micro-organisms in the water (mg $O_2 \cdot h^{-1}$). BOD ranged from 0.001 to 0.004 mg $O_2 \cdot h^{-1}$. Because we measured oxygen concentration within the swimming chamber at 30 min intervals over 6 h, we obtained 12 Vo_2 values per experiment. Secondly, we calculated the mean (further referred to as C_R; mg $O_2 \cdot h^{-1}$) and the standard deviation

of the 12 Vo_2 values obtained for each experiment. Thirdly, the net swimming costs against a turbulent flow (C_A; mg $O_2 \cdot h^{-1}$) was estimated as

$$C_A = C_R - SMR \quad (4.2)$$

where SMR is the standard metabolic rate of a fish (mg $O_2 \cdot h^{-1}$). The standard metabolic rate was determined by a model that we developed using data from Brett and Glass (1973) on the standard metabolism of juvenile sockeye salmon (*Oncorhynchus nerka*) weighing 4 to 10 g and held at a water temperature of 15°C

$$SMR = 0.227 \cdot M^{0.653} \quad (n = 5; r^2 = 0.86; p < 0.05) \quad (4.3)$$

where M is the body mass of the fish (g wet). SMR values were obtained by extrapolating the relationship between oxygen consumption and mean flow velocity from forced swimming experiments to zero velocity. According to Equation 3, SMR for the fish used in our experiments ranged from 1.00 - 1.07 mg $O_2 \cdot h^{-1}$.

4.2.4 Statistical analysis

The repeatability of each of the four experimental flow structures created by our apparatus was tested using one-way analysis of variance (ANOVA). Such ANOVA was performed to compare the mean streamwise flow velocities during the three times series recorded before a suite of experimental observations. The analysis was also done for the three velocity time series obtained after a suite of experimental observations. The stability of the turbulent flow structures was tested using a one-way ANOVA comparing the mean flow velocities before to those after a suite of

experimental observations. During this analysis, the three velocity time series obtained before or after a suite of experimental observations were used as replicates. The repeatability and the stability of the standard deviations of the flow velocities were tested using the same approach with Levene's test of the homogeneity of variance. This test was selected because it has been argued to be more robust and not dependent on the assumption of normality compared with, for example the Bartlett's test of homogeneity of variance (Scherrer 1984).

We confirmed the periodicity of the pulsating flow using a power spectrum analysis (Lapointe et al. 1996). Each 5 min velocity time series measured with the ADV were filtered using a Gausian filter. The filtered time series was decomposed in frequencies using a Fourier transformation (Legendre and Legendre 1998). The power spectrum analysis measures the variance contributions from different frequencies within the velocity time series. The total variance of the time series is presented as the area under a relationship between the variance associated to a frequency and the frequency (referred to as a power spectrum). Spikes in the power spectrum indicate a periodicity with the corresponding frequency. Low- and high-speed flow events within the velocity time series were identified using conditional analysis. These events were defined as velocity fluctuations above or below the mean streamwise velocity that lasted more than 0.75 s (Lu and Willmarth 1973).

Net swimming costs were compared among the four different flow structures with a two-way ANOVA using mean flow velocity and standard deviation of flow velocity as classification variables. The five replicates of net swimming costs for

each flow structure allowed us to test the statistical significance of the interaction term of this analysis (mean flow velocity x standard deviation of flow velocity).

The net swimming costs we estimated while fish were swimming against a turbulent flow were compared to predictions made by the forced and the spontaneous swimming models developed by Boisclair and Tang (1993). The predictions of the forced and the spontaneous swimming models were obtained considering the fish body mass and the mean flow velocity used during our experiments. Net swimming costs predicted by the forced or spontaneous models were compared to observed net swimming costs using model II regression analysis. The null hypothesis in this analysis was that there is no statistically significant difference between predicted and observed net swimming costs. The slope of the regression line was tested against an expected value of unity and the intercept was tested against an expected value of zero. The 95% confidence intervals were computed for the slope and intercept parameters. The significance of the slope of the major axis was estimated using a permutation test (Legendre and Legendre 1998).

4.3 Results

4.3.1 Characteristics of flow structures

The means and the standard deviations of the streamwise flow velocities recorded were consistent with the targeted values (Table 4.1). The mean streamwise flow velocities ranged from 18.02 to 18.32 $cm \cdot s^{-1}$ for the low flow condition (target = 18 $cm \cdot s^{-1}$) and from 23.02 to 23.09 $cm \cdot s^{-1}$ for the high flow condition (target =23 $cm \cdot s^{-1}$). The standard deviation of the streamwise flow velocity under the low turbulent conditions ranged from 5.06 to 5.16 $cm \cdot s^{-1}$. Corresponding values under the

high turbulent conditions ranged from 7.92 to 8.27 $cm \cdot s^{-1}$ (Table 4.1). The mean vertical flow velocities ranged from -0.70 to 0.44 $cm \cdot s^{-1}$ for low flow velocities, and from -0.10 to 0.12 $cm \cdot s^{-1}$ for high flow velocities. The standard deviation of the vertical flow velocity under the low turbulent conditions ranged from 4.79 to 5.04 $cm \cdot s^{-1}$ and from 6.93 to 7.64 $cm \cdot s^{-1}$ under high turbulent conditions. Corresponding values for the mean lateral flow velocities ranged from -0.45 to 0.49 $cm \cdot s^{-1}$ for low flow and from 0.20 to 0.32 $cm \cdot s^{-1}$ for high flow conditions. The standard deviation of the velocities under the lateral flow ranged from 5.41 to 5.62 $cm \cdot s^{-1}$ under low turbulence and from 7.50 to 7.71 $cm \cdot s^{-1}$ under high turbulence conditions.

Table 4.1 Ranges of the mean flow velocity and the standard deviation of the flow velocity ($cm \cdot s^{-1}$) during the six 5-min velocity time series. Ranges of minimum and maximum flow velocity ($cm \cdot s^{-1}$) for the streamwise U (u_{min}, u_{max}), vertical V (v_{min}, v_{max}), and lateral W (w_{min}, w_{max}) velocity components in the four different flow conditions, and the ranges of their standard deviations (u_{SD}, v_{SD}, w_{SD}, respectively) are also presented.

Velocity component	Low velocity low turbulence	Low velocity high turbulence	High velocity low turbulence	High velocity high turbulence
Range $\bar{u}$	18.02 - 18.18	18.26 - 18.32	23.02 - 23.08	23.02 - 23.09
Range u_{SD}	5.06 - 5.16	8.16 - 8.27	5.07 - 5.15	7.92 - 8.08
u_{min}	3.11 - 4.63	0.27 - 1.64	3.47 - 5.64	0.35 - 0.90
u_{max}	34.21 - 35.36	36.34 - 38.94	34.47 - 36.88	42.24 - 44.85
Range $\bar{v}$	-0.70 - 0.34	-0.42 - 0.44	-0.10 - 0.10	-0.10 - 0.12
Range v_{SD}	4.79 - 4.94	6.93 - 7.05	4.81 - 5.04	7.14 - 7.64
v_{min}	-23.02 - -18.74	-25.83 - -22.04	-29.77 - -27.35	-31.41 - -28.39
v_{max}	20.61 - 22.95	21.52 - 24.26	27.84 - 31.45	29.20 - 30.65
Range $\bar{w}$	0.15 - 0.19	-0.45 - 0.49	-0.20 - 0.10	0.30 - 0.32
Range w_{SD}	5.41 - 5.57	7.50 - 7.69	5.42 - 5.62	7.53 - 7.71
w_{min}	-26.27 - -20.38	- 27.49 - -22.31	-21.71 - -35.37	-24.95 - -30.61
w_{max}	22.64 - 23.82	25.08 - 28.23	29.62 -33.31	29.04 - 35.74

For any given flow condition, the mean streamwise flow velocity $\bar{u}$ and the standard deviation of streamwise flow velocity u_{SD} did not vary significantly among the three recordings performed before (variation = 0.1-1.8%) or after (variation =

0.1-1.8%) a suite of experimental observations (Repeatability test; $\bar{u}$: 0.656 <p < 0.998; u_{SD}: 0.196 <p <0.989). Similarly, for any given flow condition, the mean streamwise flow velocity $\bar{u}$ and the standard deviation of streamwise flow velocity u_{SD} obtained before a suite of experimental observations did not vary significantly (variation = 0.0-2.0%) from values estimated after a suite of experimental observations (Stability tests; $\bar{u}$: 0.917 <p <0.998; u_{SD}: 0.464 <p <1.000). These results suggest that the flow structures created by our apparatus were repeatable and stable.

The spike at 0.17 Hz in the power spectrum analysis confirmed the presence of a dominant period of 6 s within the velocity time series (Figure 4.2). However, the power spectra also showed the occurrence of a variety of frequencies signifying the presence of a fully developed turbulent flow. The examination of the velocity time series allowed me to identify from two to five low-speed flow events/min and five high-speed flow events/min. The mean duration of the flow events was 1.0 s. The standard deviation of the duration of the flow events ranged from 0.20 to 0.29 s (Table 4.2).

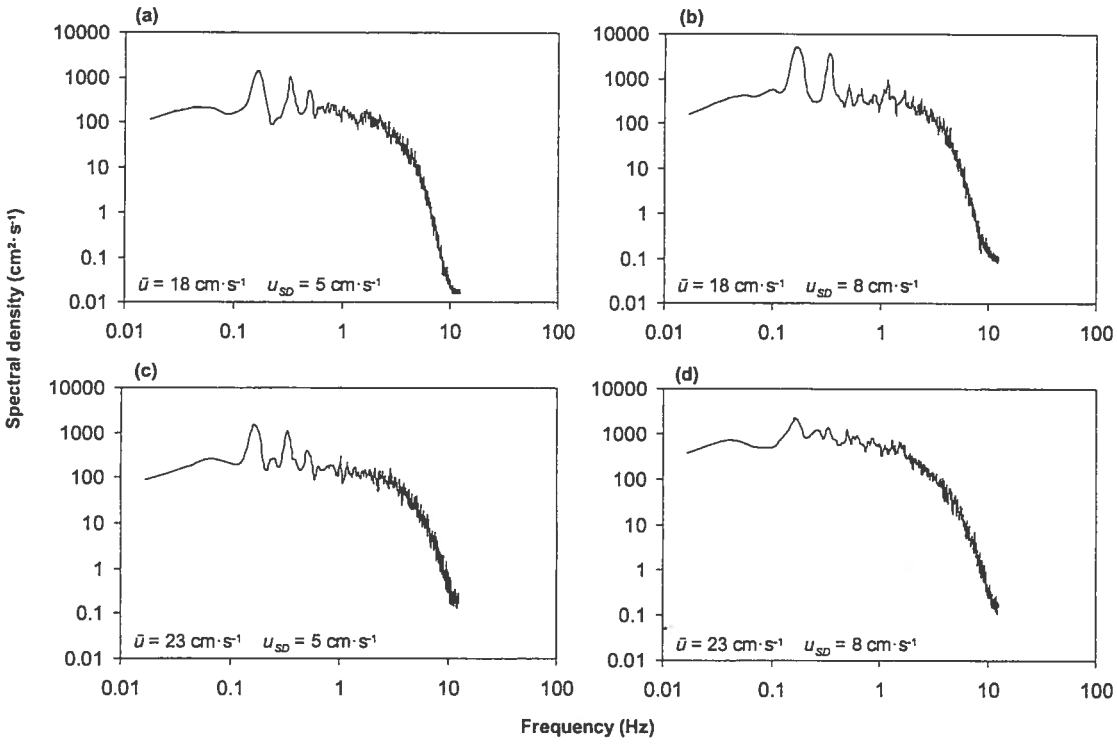

Figure 4.2 Relationship between the spectral density and the frequency of the streamwise velocity component U of the time series for four different flow conditions (two mean water velocities $\bar{u}$ of 18 and 23 cm·s^{-1} and two standard deviations u_{SD} of 5 and 8 cm·s^{-1}).

Table 4.2 Number and duration of low- and high-speed flow events for each of the four turbulent conditions.

	Low velocity low turbulence	Low velocity high turbulence	High velocity low turbulence	High velocity high turbulence
N of low-speed flow events/min	2	3	2	5
N of high-speed flow events/min	5	5	5	5
Mean duration (s)	1	1	1	1

4.3.2 Net swimming costs

Net swimming costs varied three-fold among our experiments ranging from 1.46 mg O_2·h^{-1} ($\bar{u}$ =18 cm·s^{-1}; u_{SD} =5 cm·s^{-1}) to 4.42 mg O_2·h^{-1} ($\bar{u}$ =23 cm·s^{-1}; u_{SD} = 8 cm·s^{-1}; Figure 4.3). These values corresponded to a factor ranging from 1.4 to 4.3 times SMR. Net swimming costs tended to increase with mean flow velocity ($p <$

0.01) and with the standard deviation of the flow velocity ($p < 0.01$). The interaction between the mean and the standard deviation of flow velocity was also significant ($p < 0.01$) indicating that an increase of standard deviation of flow velocity did not have the same effect for the low and the high flow conditions.

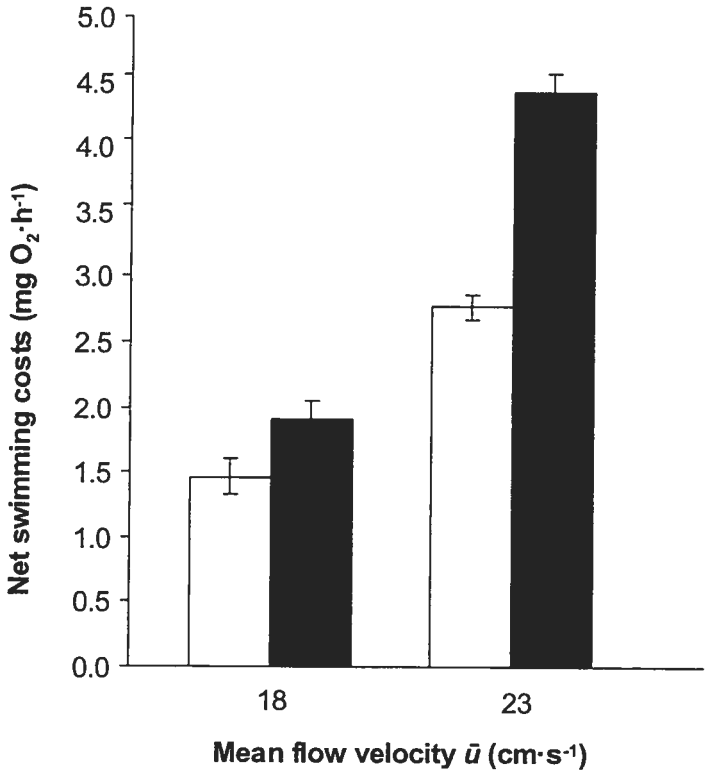

Figure 4.3 Net swimming costs of juvenile Atlantic salmon (*Salmo salar*) under four turbulent conditions defined by the mean flow velocity ($\bar{u}$) and the standard deviation of flow velocity (u_{SD}). Low turbulence conditions (u_{SD} of 5 $cm \cdot s^{-1}$) are represented by open bars and high turbulent conditions (u_{SD} of 8 $cm \cdot s^{-1}$) are represented by solid bars. Vertical lines represent 95% confidence intervals.

An increase of the standard deviation of flow velocity from 5 to 8 $cm \cdot s^{-1}$ increased net swimming costs by factor of 1.3 at a low flow conditions. This factor was 1.6 at high flow conditions (Table 4.3).

Table 4.3 Number of respirometry experiments (n) per flow condition (combinations of mean flow velocity $\bar{u}$ and standard deviation of the flow velocity u_{SD}), mean fish mass (M), net swimming costs (C_A) in the corresponding turbulent flow condition, and standard deviation (SD) of C_A among the five experiments.

n	$\bar{u}$ ($cm \cdot s^{-1}$)	u_{SD} ($cm \cdot s^{-1}$)	M (g)	C_A ($mg\ O_2 \cdot h^{-1}$)	SD of C_A ($mg\ O_2 \cdot h^{-1}$)
5	18	5	10.01	1.46	0.17
5	18	8	10.15	1.91	0.08
5	23	5	10.09	2.77	0.12
5	23	8	10.13	4.42	0.15

4.3.3 Comparison between observed net swimming costs and predictions by forced and spontaneous swimming models

Predictions of net swimming costs obtained using forced swimming model tended to underestimate observed activity costs. At low flow conditions, the forced swimming model underestimated the observed net swimming costs of JAS subjected to turbulent flows by a factor ranging from 1.9 (u_{SD} =5 $cm \cdot s^{-1}$) to 2.4 (u_{SD} =8 $cm \cdot s^{-1}$). Corresponding values at high flow conditions ranged from 2.6 (u_{SD} =5 $cm \cdot s^{-1}$) to 4.2 (u_{SD} =8 $cm \cdot s^{-1}$; Table 4.4). The 95% confidence interval of the intercept of the regression model between observed and predicted net swimming costs ranged from 0.55 to 0.74. This intercept was statistically different from zero (p =0.001). The 95% confidence intervals of the slope of the regression model between observed and predicted net swimming costs ranged from 0.07 to 0.13. This slope was significantly different from unity (p =0.001).

Table 4.4 Comparisons between the observed net swimming costs for given combinations of mean flow velocity ($\bar{u}$) and standard deviation of the flow velocity (u_{SD}) and the predictions of forced and spontaneous swimming model of Boisclair and Tang (1993) implemented with same mean flow velocity.

$\bar{u}$ ($cm \cdot s^{-1}$)	u_{SD} ($cm \cdot s^{-1}$)	Factor 1	Factor 2
18	5	1.9	6.6
18	8	2.4	5.0
23	5	2.6	4.5
23	8	4.2	2.8

Note: Factor 1 represents the factor by which the predictions of the forced swimming model underestimated observed net swimming costs. Factor 2 represents the factor by which spontaneous swimming model overestimated observed net swimming costs.

Net swimming costs predicted by the spontaneous swimming model of Boisclair and Tang (1993) always overestimated net swimming costs in turbulent flows (Figure 4.4). At the low flow velocity, the spontaneous swimming model overestimated the net swimming costs in a turbulent flow by a factor ranging from 6.6 (u_{SD} =5 $cm \cdot s^{-1}$) to 5.0 (u_{SD} =8 $cm \cdot s^{-1}$). The overestimation of the net swimming costs predicted by the spontaneous model was decreased to factors ranging from 4.5 (u_{SD} =5 $cm \cdot s^{-1}$) to 2.8 (u_{SD} =8 $cm \cdot s^{-1}$) at high flow conditions. The 95% confidence intervals of the intercept associated with the regression model between observed and predicted net swimming costs ranged from 7.11 to 9.15. The intercept of this regression model was significantly different from zero ($p = 0.001$). The 95% confidence interval of the slope of the relationship between observed and predicted net swimming costs ranged from 0.73 to 1.44. This slope was not significantly different from the expected value of 1 ($p > 0.05$).

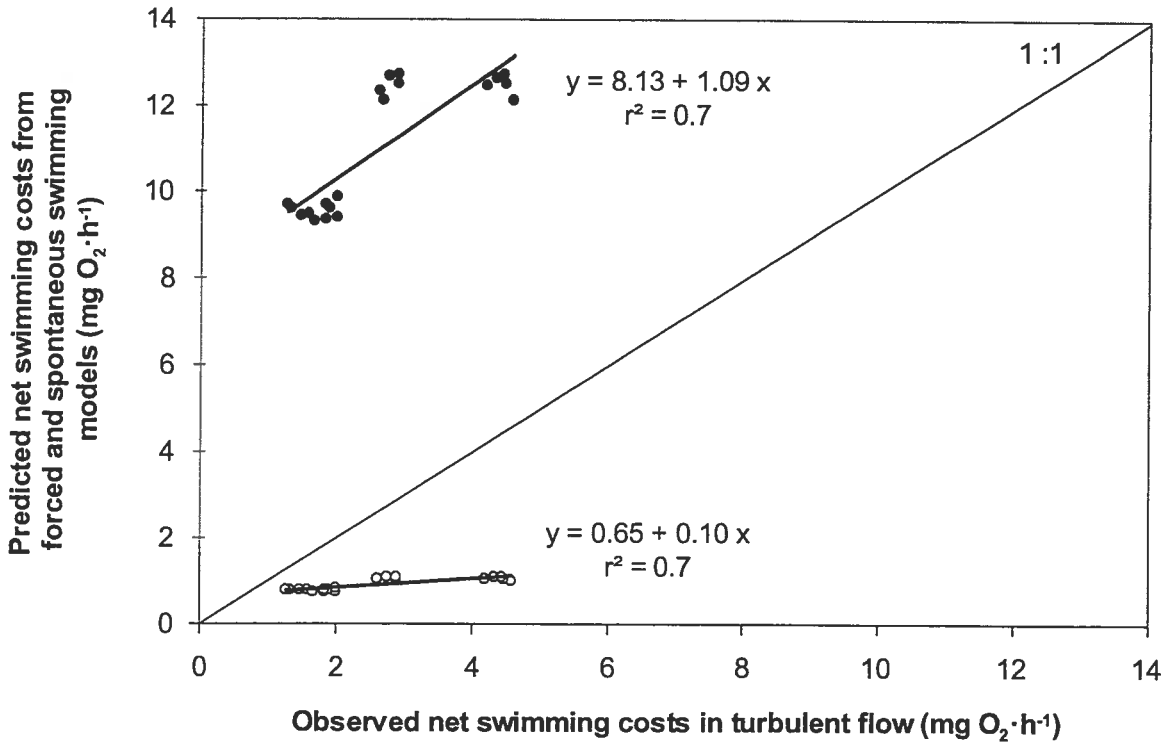

Figure 4.4 Comparison between the observed net swimming costs of juvenile Atlantic salmon (*Salmo salar*) of 10 g under four different turbulent conditions (two mean flow velocities $\bar{u}$ of 18 cm·s^{-1} and 23 cm·s^{-1} and two standard deviations u_{SD} of 5 cm·s^{-1} and 8 cm·s^{-1}) and the net swimming costs predicted by the forced (open circles) and the spontaneous (solid circles) swimming models of Boisclair and Tang (1993).

4.4 Discussion

Our analyses indicate that the net swimming costs of JAS in turbulent flow may significantly increase as mean flow velocity and standard deviation of the flow velocity increase. In our experiments, net swimming costs increased by an average factor of 1.5 as mean flow velocity increased from 18 cm·s^{-1} to 23 cm·s^{-1}. The effect of mean flow velocity on fish respiration rates is not surprising as it is imbedded in all swimming costs models currently available (Beamish 1978; Boisclair and Tang 1993; Tang et al. 2000). We also found that net swimming costs for a given mean flow velocity may increase with the standard deviation of the flow velocity. In our study, fish respiration rates increased, on average, by a factor of 2.1, as the standard

deviation of the flow velocity increased from 5 $cm \cdot s^{-1}$ to 8 $cm \cdot s^{-1}$. Our analyses also showed that the effect of increasing the intensity of the turbulence of flow may increase as mean flow velocity increases. As the standard deviation of the flow velocity increased from 5 $cm \cdot s^{-1}$ to 8 $cm \cdot s^{-1}$, net swimming costs of JAS increased by a factor of 1.3 at a mean flow velocity of 18 $cm \cdot s^{-1}$, and by a factor of 1.6 at a mean flow velocity of 23 $cm \cdot s^{-1}$.

Our work may be taken as an indication that not only mean flow velocity but also standard deviation of flow may be required to adequately estimate the cost of swimming under turbulent conditions. However, our data do not really allow us to fully evaluate the ultimate cause of the variation of fish respiration rates among our treatments. Although our methods focus mostly on the mean and the standard deviation of flow velocity, any other characteristic such as the number and the intensity of the flow events may affect the metabolic rate of fish. In our study, experimental treatments did not only vary in terms of mean and standard deviation of flow velocity, but also in terms of the number of events per minute (particularly the number of low-speed flow events; Table 4.2). In our study, among-experiments variability in flow structure was expressed by more low-speed flow events in high turbulence conditions (3-5/min) than in low turbulence conditions (2/min; high-speed flow events were always 5/min). Similarly, more events occurred under high velocity conditions (5 low-speed flow events/min) than under low velocity conditions (3 low-speed flow events/min). Because the descriptors of flow are interrelated, it is presently impossible, with the few data we have, to assess the relative effect of mean flow velocity, standard deviation of flow velocity, and the number of low- and high-speed flow events on net swimming costs. Our present contribution is limited to

providing estimates of the effect that turbulence may have on fish respiration rates, notwithstanding its ultimate cause.

The applicability of our results to field situations depends on the ability of our experimental design to reflect natural conditions found in rivers and streams, and on the validity of the assumptions we used to estimate net swimming costs. Activity metabolism is generally estimated using forced swimming experiments seeking to minimize heterogeneity of flow velocity and direction (Brett 1965; Beamish 1978) or using spontaneous activity experiments in absence of flow (Boisclair and Tang 1993; Krohn and Boisclair 1994; Tang and Boisclair 1995). Because rivers are characterized by temporally heterogeneous flow, we expected that using an experimental design that does not only allow flow to be present but to be varied may better represent natural flow conditions faced by the fish. Both mean and standard deviation of the flow velocity used during our experiments were chosen to represent a subset of the natural conditions encountered by JAS. The two experimental mean flow velocities ($\bar{u}$ =18 cm·s^{-1} and 23 cm·s^{-1}) are within the range of focal point and microhabitat velocities used by JAS (DeGraaf and Bain 1986; Morantz et al. 1987; Guay et al. 2000). The experimental standard deviations of 5 cm·s^{-1} and 8 cm·s^{-1} were adopted following field observations of habitat selected by JAS in the Sainte-Marguerite River (E.C. Enders and D. Boisclair, unpublished data). Natural flow conditions comprise realistic flow structures such as temporal successions of fast and slow moving flow events extending over the whole water column (Kirkbride and Ferguson 1995; Ferguson et al. 1996). In gravel-bed rivers, flow events lasting from 0.5 - 5 s have been shown to occur at 5 to 30 s intervals (Roy et al. 1999). Consequently, we controlled the electric current powering the pump that created a

pulsating flow such that our apparatus produced low-speed flow events of a mean duration of 1 s at 6 s intervals. Hence, we performed our experiments under combinations of mean flow velocity, standard deviation of the flow velocity, duration of flow events, and interval between flow events that are within the range found under natural conditions. However, our results do not cover the complete range of conditions that may be encountered in natural environments. Furthermore, flow characteristics other than those we studied may affect fish swimming costs. For instance, Webb (1993a) described that 'ground effects' created by solid structures, such as the walls of our swimming chamber, increase lift, reduce drag, and therefore decrease swimming costs. Fish from our experiments may have been subjected to such effects. In view of our objectives, the presence of ground effects may not affect the relevance of our results to field situations. In their natural habitat, JAS exhibiting their typical feeding behavior may spend most of their time in their sit-and-wait position just above the substrate. However, the difference between the ground effects perceived by fish in our swimming chamber and those experienced by fish under natural conditions, and the effect of such a difference on the applicability of our results to field situations, represents a more important issue for which we have no immediate solution. Similarly, because we measured flow velocity only in one central point of the swimming chamber, we cannot describe the form and size of the vortices that may have been present in our swimming chamber. Theoretically, the 'upstream' grid introduced in the swimming chamber should prevent the occurrence of large vortices or recirculation zones that would decrease the energy expenditure of fish (Tritton 1988). Although the existence of such recirculation zones in our swimming chamber should be assessed to better interpret our results, two lines of evidence suggest that JAS were not subjected to a significant effect of vortex. First,

negative streamwise flow velocities were not observed in our swimming chamber. This indicates that, during our experiments, JAS were not submitted to a counter-streamwise flow. Second, the vertical (V) and lateral (W) flow velocity components were highly variable (range = -31.41 $cm \cdot s^{-1}$ to 31.45 $cm \cdot s^{-1}$) and directionally unstable (from negative to positive values). This suggests that fish were not subjected to directionally stable conditions that characterize recirculation zones (Vogel 1994). Consequently, the cost of swimming estimated may not be representative of those incurred by JAS when they hold position on the downstream end of a rock (where vortices and recirculation zones are expected to occur). However, the respiration rates we obtained may adequately represent the net swimming costs against a turbulent flow (with similar mean and standard deviation of flow velocity) while JAS perform the attack phase of their feeding motions to capture prey items.

During our experiments JAS were continuously swimming over a 6 h period. However, in their natural environment, JAS may swim against a turbulent flow only during shorter time periods than those used in our experiments (attacks directed towards invertebrates that drift in the flow, aggressive interactions, habitat exploration). Although we recognize that the duration of our experiments may have been demanding to the fish, within-experiment variation in oxygen consumption rates during 30 min (Vo_2) ranged from 3.8 to 11.6%. Furthermore, we found no relationship between Vo_2 and time since the beginning of an experiment ($0.01 < r^2 < 0.134$; $0.24 < p < 1$). Hence, our experimental conditions did not appear to cause any functionally or statistically significant fatigue to the fish used.

The method used to estimate net swimming costs is based on the assumption that the standard metabolic rate (SMR) of Atlantic salmon is adequately represented by that of sockeye salmon of similar sizes (Brett and Glass 1973). The use physiological models developed for one species to predict bioenergetic attributes of another species may produce potentially misleading estimates (Ney 1993). Our use of the SMR data of sockeye salmon for Atlantic salmon was motivated by the absence of SMR data specific to Atlantic salmon, by the availability of a large data set for sockeye salmon, and by the taxonomic (both salmonids), morphological (body mass-length relation), physiological (preferred water temperature), and ecological (juvenile stages in riverine freshwater) similarities between both species. However, it may be hypothesized that SMR for similar sized fish held at a same water temperature vary among different salmonid species. To our knowledge, the only data that may allow us to test this hypothesis are the SMR data of Job (1955) for brook charr (*Salvelinus fontinalis*) ranging from 5 to 2000 g at 15°C. Job (1955) estimated SMR as the lowest hourly respiration rates of fish held in a rectangular respirometer during 24 h. Applying the SMR model of brook charr to the fish size used in our experiments, we obtained SMR values ranging from 1.02 to 1.12 mg $O_2 \cdot h^{-1}$. Corresponding values obtained with the model based on data collected for sockeye salmon, and used during our computations, ranged from 0.99 to 1.07 mg $O_2 \cdot h^{-1}$. The 2.4% to- 4.5% difference between SMR obtained for two different species of salmonids suggests that the use of the SMR model of sockeye salmon to predict the SMR of Atlantic salmon may have a minor effect on our estimates of net swimming costs.

Forced and spontaneous swimming models are presently the most commonly used models to estimate the net swimming costs of fish. Comparisons between predictions made by these models and our estimates of the cost of swimming under turbulent flow allowed us to assess the effect of turbulence of swimming energetics. However, it is useful to compare models that are subjected to similar assumptions. Three basic assumptions are shared by all swimming costs models. Firstly, all types of models assume that experimental conditions allow fish to swim in a manner that may mimic their swimming in the field. Experimental approaches differ with respect to the probability that this assumption may be true. For instance, during forced swimming experiments, fish are forced to swim against a flow of constant velocity and direction (no acceleration and no turns are allowed). Such flow is rarely present in the field. Therefore, fish may rarely swim at a constant speed and direction, whether against a flow, or in a body of water without any flow. In turbulent swimming experiments, fish are forced to swim against a turbulent flow, which does exist in the field. During spontaneous swimming experiments, fish control their swimming speed. They are also allowed to freely perform accelerations and turns. As such, spontaneous swimming models may be expected to be the closest to natural conditions for fish living in habitats that have no significant flow (lakes, ponds, etc). Secondly, all models assume that, within the range of the duration of the experiments performed, the length of an experiment (h) has no effect on the validity of fish respiration rates obtained (i.e. respiration rates per h estimated over 30 s is identical to respiration rates per h estimated over 6 h). Forced and turbulent swimming experiments are particularly susceptible to this assumption because experiments often require that fish swim continuously for hours, which may not correspond, to the natural behavior of most fish species. Both types of approaches assume that, if fish

continue to swim for the complete duration of an experiment, and if fish respiration rates do not significantly increase or decrease through time, then fish are not fatigued and their respiration rates adequately represent swimming costs under the experimental conditions. As such, when developing swimming costs models, combinations of swimming intensity and duration of the experiments are selected to avoid fatigue. Spontaneous swimming experiments are not affected by this assumption because fish are free to swim or to remain immobile. Thirdly, all models assume that swimming costs are adequately estimated by measuring oxygen consumption by fish. This assumption also presumes that the energy required to swim comes mostly from the aerobic metabolism. If anaerobic metabolism contributes to fish swimming costs, then the potential exists for oxygen consumption rates to underestimate actual swimming costs. However, the absolute or relative contribution of aerobic and anaerobic metabolism is difficult to establish and is rarely estimated. Yet, anaerobic metabolism could theoretically interfere with estimates of fish swimming costs obtained by measuring oxygen consumption by fish under forced, turbulent, or spontaneous swimming experiments. Indeed, even under spontaneous swimming experiments, fish may occasionally perform intense accelerations that may require anaerobic metabolism. The interference caused by anaerobic metabolism is circumvented by modulating the experimental flow velocities and the duration of the experiments to minimize the expression of anaerobic metabolism. It is expected that avoiding extreme velocities may minimize the use by fish of anaerobic metabolism. Furthermore, performing longer (few hours but without provoking fatigue) rather than shorter experiments (few minutes) may allow oxygen depletion estimated during the respirometry experiments to include the repayment of an oxygen debt incurred by the recourse to anaerobic metabolism.

Hence, the three approaches to estimate or model fish swimming costs rest on the same basic assumptions.

Generally, the three approaches employ the same strategy (selection of experimental flow velocities, assessment of trends of fish respiration rates during experiments, selection of the duration of experiments) to measure, avoid, and minimize the effects of these assumptions. Another element common to all three approaches is that fish respiration rates are modeled using fish mass, flow velocity, or fish swimming speed. This facilitates the comparison among models although it may be necessary for fish living in turbulent flows, as illustrated by our work, to add descriptors of the complexity of flow (e.g., standard deviation of flow) to this list of independent variables. Providing evidence that the inclusion of such descriptors in swimming costs models for fish living under turbulent conditions may not only be necessary, but also achievable, may constitute the most important contribution of our work. It is our contention that the comparisons we performed among the different models are justified not only from a fundamental perspective but also from a functional perspective. Although it may be conceptually obvious that using forced swimming models to estimate the cost of swimming for fish swimming against a turbulent flow may be incorrect, a number of recent studies used this approach because of the lack of quantitative information about the effect turbulence may have on fish swimming costs. The comparisons we performed among swimming models allow users of such models to readily assess the functional and quantitative consequences of our work on estimates produced by the most commonly used models.

The net swimming costs estimated under our experimental conditions were 1.9- to 4.2-fold larger than those predicted using a forced swimming model, and 4.2- to 6.6-fold smaller than those predicted by a spontaneous swimming model. The higher net swimming costs estimated under turbulent conditions relative to predictions made by forced swimming conditions are consistent with the suggestion of Webb (1982) and Boisclair and Tang (1993) that unsteady swimming (including changes in speed and direction) is more energetically costly than steady swimming (no changes in speed and direction). Changes in swimming speed and direction that must be performed under turbulent conditions may be expected to cause a substantial increase in the energetic costs compared to steady swimming at the same average speed. Adjustments undertaken by fish with their fins to maintain their position in the water column are also expected to increase swimming costs (Weatherley et al. 1982; Gauthier 1998; McLaughlin and Noakes 1998). The extensive use of fins provides stability but also increases drag (Webb 1993b) and, as illustrated by our work, it increases energy expenditure at a same mean flow velocity. McLaughlin and Noakes (1998) noted a temporal variability in the tail beat frequency and amplitude of young-of-the-year brook charr observed in a natural stream. They suggested that these adjustments corresponded to the fluctuations of the flow velocity, which may increase the energetic costs for swimming against a turbulent flow. Our results are consistent with their suggestion.

Net swimming costs predicted by the forced swimming model we used are expected to increase with swimming speed raised to a power of 1.21 (Boisclair and Tang 1993). An exponent greater than one suggests a relatively higher increase of the net swimming costs with a given increase of swimming speed. Therefore, it may be

hypothesized that the estimation of net swimming costs with instantaneous flow velocities instead of the mean flow velocity would improve the accuracy of the predictions made by the forced swimming model (e.g. peaks in flow velocities could lead to an important increase of the net swimming costs estimated using a model in which velocity has an exponent of 1.21). We tested this hypothesis by estimating the net swimming costs predicted by the forced swimming model using flow velocity data recorded at 25 Hz (Table 4.5). Our results indicated that the use of instantaneous flow velocity, instead of the mean flow velocity, increased net swimming costs predicted by the forced swimming model by 2 to 6%. This analysis confirms that the use of forced swimming models in bioenergetics modeling of riverine fish species may underestimate actual net swimming costs in turbulent flow even when these models are implemented with instantaneous measures of flow velocity.

Table 4.5 Comparisons between the net swimming costs (C_A) predicted by the forced swimming model of Boisclair and Tang (1993) implemented with the mean flow velocity (u_{SD}=0) and predictions of this model implemented with instantaneous flow velocities recorded at 25 Hz (u_{SD} =5 or 8 cm·s^{-1}).

$\bar{u}$ (cm·s^{-1})	u_{SD} (cm·s^{-1})	C_A (mg O_2·h^{-1})	Factor A
18	0	0.77	-
18	5	0.79	1.03
18	8	0.82	1.06
23	0	1.04	-
23	5	1.06	1.02
23	8	1.07	1.03

Note: Factor A represents the factor by which the predictions increased because of the use of the instantaneous instead of the mean flow velocities.

Our data suggests that the net swimming costs in a turbulent flow may be higher than predicted by forced swimming models but lower than expected when using spontaneous swimming models. In our study, the difference between actual net swimming costs and those predicted by the forced swimming model increased with the mean and the standard deviation of flow. Furthermore, the difference between

actual net swimming costs and those predicted by the spontaneous swimming model decreased with the mean and the standard deviation of flow. Because our laboratory experiments simulated flow conditions from the lower part of the turbulence spectrum that may be observed under natural environments, we anticipate that the difference between actual net swimming costs observed in our study and those predicted by the forced swimming model may be much lower than those that could be found in more extreme turbulent conditions. Similarly, we expect that the difference between actual net swimming costs observed in our study and those predicted by the spontaneous swimming model may be higher than those that could be found in more extreme turbulent conditions.

The major difference between the movements performed by fish during spontaneous swimming experiments and those observed under the turbulent conditions we used do not appear to reside in the standard deviation of fish swimming speed (or flow velocity) but in the intensity of the changes in direction. The variance of speed estimated during spontaneous swimming experiments generally range from 3.7 to 109 $cm^2 \cdot s^{-2}$ (Tang and Boisclair 1995; Tang et al. 2000). These values correspond to standard deviations of 1.9 to 10.5 $cm \cdot s^{-1}$. However, during spontaneous swimming experiments, fish perform turns ranging from 30.9° to 63.5° (Tang and Boisclair 1995). Such turns were not performed under the experimental conditions that we used. Hence, for a given swimming speed, lowest costs may be predicted by a forced swimming model (low standard deviation of the flow velocity and small angles of turns), intermediate costs may be predicted by a turbulent model developed under conditions similar to those used in our experiments (turbulent flow with intermediate levels of standard deviation of the flow velocity,

e.g., 5-8 $cm \cdot s^{-1}$, and small angles of turns), and the highest costs may be predicted with spontaneous models (high standard deviation of flow velocity and more pronounced angles of turns). This situation may indicate that, for a given mean flow velocity or swimming speed, forced, turbulent, and spontaneous swimming data obtained for increasing standard deviation of flow velocities or swimming speeds and increasing angles of turns may form a continuum of increasing net swimming costs. In the context of estimating the net swimming costs of JAS in the field, we speculate that such ranking may mean that the forced swimming model may be adequate to estimate the net swimming costs for fish facing flows of minimized heterogeneity (e.g., sit-and-wait position of fish near the substrate), that the turbulent swimming model may be adequate for fish inhabiting turbulent flow conditions, and that the spontaneous swimming models may be adequate for fish in more stringent conditions (complex swimming motions, high turbulence). Estimation of the net swimming costs of fish in turbulent flows may therefore require more than one model.

Our results suggest that bioenergetics models aimed at estimating the costs of habitat utilization by fish living in turbulent environments may require a description of the behavior of the fish, estimates of the mean and the standard deviation of the flow velocity, and swimming costs models in which the effects of the mean and the standard deviation of flow velocity are explicitly represented. Such approach should be extended to studies using video-observations (Trudel and Boisclair 1996; Aubin-Horth et al. 1999), radio tracking (Bourke et al. 1996; Ovidio 1999), and physiological telemetry (electromyograms; Korsmeyer et al. 1997; Dewar et al. 1999) in turbulent environments. We anticipate that models using the mean and the standard deviation of flow velocity may provide estimates of the costs of habitat

utilization by fish living in rivers that are more accurate than commonly used forced swimming models. As such, our study suggests that the use of models more adequately representing the cost of swimming against a turbulent flow may strongly affect estimates of the cost of swimming and the expected balance the benefits and costs of habitat utilization in turbulent environments.

5 THE COSTS OF HABITAT UTILIZATION OF WILD, FARMED, AND DOMESTICATED JUVENILE ATLANTIC SALMON (*SALMO SALAR*)[3]

Abstract

We compared the total swimming costs of wild, farmed (first generation progeny of wild progenitors from hatchery), and domesticated (seventh generation progeny of the Norwegian aquaculture strain) juvenile Atlantic salmon. Respirometry experiments were performed to assess total swimming costs of fish ranging from 3.95-16.11 g wet weight at a water temperature of 15°C. Fish were subjected to two turbulent flows (two standard deviations of flow velocity: 5 $cm \cdot s^{-1}$ and 8 $cm \cdot s^{-1}$, with a mean flow velocity of 23 cm s^{-1}) that corresponded to turbulence intensities (standard deviation/mean flow velocity) of 0.22 and 0.35, respectively. Total swimming costs were significantly affected by turbulence intensity and increased, on average, 1.4-fold as turbulence intensity increased. Total swimming costs were 2.4- to 4.0-fold higher than expected values predicted by forced swimming models developed under conditions that minimize flow heterogeneity. Total swimming costs of wild and farmed fish were not statistically different (average difference =6.7%). Hence, swimming costs models developed using farmed fish may be used to estimate swimming costs of wild fish. However, domesticated fish had total swimming costs 12.0% to 29.2% higher than wild or farmed fish. This may be related to domesticated fish having deeper bodies and smaller fins.

[3] Enders, E.C., D. Boisclair & A.G. Roy. The costs of habitat utilization of wild, farmed, and domesticated juvenile Atlantic salmon (*Salmo salar*). *Canadian Journal of Fisheries and Aquatic Sciences*. In preparation.
Contribution to the program of CIRSA.

5.1 Introduction

Numerous habitat models have utilized information about the environmental conditions used or avoided by juvenile Atlantic salmon (*Salmo salar*; JAS) to predict fish distribution patterns in rivers (Guay et al. 2000; Mäki-Petäys et al. 2002). Models based on environmental conditions used or avoided by fish allow the identification of habitat features that should be the focus of protection and restoration programs. Furthermore, these fish distribution models may be complemented by bioenergetics models designed to predict the net energy gain JAS may obtain from specific habitats (Hayes et al. 2000; Boisclair 2001). In suitable habitats, fish have a positive net energy gain between the energy acquired from their environment and that required for metabolic expenditures and physiological maintenance (Fausch 1984). Bioenergetics modeling involves the estimation of consumption, growth, metabolism, excretion, and egestion. The activity metabolism is the most important variable of the energy budget of fish exerting up to 40% of the energy intake (Brett and Groves 1979; Boisclair and Leggett 1989). Consequently, the precise quantification of the fish activity metabolism is of particular importance to obtain appropriate predictions of the net energy gain from bioenergetics models (Boisclair and Leggett 1989; Hansen et al. 1993; Ney 1993).

Swimming costs of stream-dwelling fish are generally estimated using forced swimming models (Hughes and Dill 1990; Sabo et al. 1996; Guensch et al. 2001). These models are derived from experiments conducted with fish swimming at a steady speed in a flume respirometer designed to minimize flow heterogeneity (Job 1955; Brett 1964; Beamish 1978). However, in their natural environment stream-dwelling fish are confronted by highly turbulent flow. In these environments,

turbulence is associated with a wide range of instantaneous velocities to which fish have to continuously adjust their swimming speed and their body position to maintain their location in the surrounding flow field. It has been demonstrated that turbulence affects the behavior and distribution of stream-dwelling fish. For example, sustained and critical swimming speeds of fish decreased with an increase of turbulence intensity, indicating that the energy expenditures are higher in turbulent flow (Pavlov et al. 2000). In contrast, young-of-the-year brook charr (*Salvelinus fontinalis*) have been shown to profit from turbulence by the use of flow velocity refuges (McLaughlin and Noakes 1998). Similarly, Liao et al. (2003) demonstrated that adult rainbow trout (*Oncorhynchus mykiss*) swimming through turbulent flow took advantage of the energy of vortices, resulting in a reduction of their muscle activity. The reduced muscle activity suggests that rainbow trout profit from the energy of the vortices, reducing the energetic cost of swimming.

In a preliminary study, we demonstrated that fish swimming costs under fluctuating flow velocities may be 2- to 4-fold higher than those predicted by forced swimming models (Enders et al. 2003). For practical reasons, the respirometry experiments were performed with fish of aquaculture origin. However, Fleming et al. (1994) demonstrated that cultured JAS diverged significantly from their principal wild founder population in body morphology, having smaller heads and fins, and narrower caudal peduncles. Cultured JAS also differed from wild fish in several other aspects including dominance and predator avoidance behavior (Einum and Fleming 1997; Johnsson et al. 2001). The morphological differences that exist between wild and aquaculture fish may also affect the applicability of swimming costs models developed using aquaculture fish to wild populations. This may, in turn,

affect estimates of the net energy gain and the habitat quality values generated by bioenergetics models (Ney 1993).

The objectives of our study were (1) to confirm the effect of flow turbulence on the energetic cost of swimming, (2) to quantify the differences that may exist among the total swimming costs of wild JAS, farmed JAS (first generation progeny from wild progenitors), and domesticated JAS (seventh generation progeny of a Norwegian aquaculture strain), and (3) to compare morphological variables among the different groups of fish. This study was designed to assess the applicability of respirometry models developed with cultured JAS to wild JAS.

5.2 Material and methods

We accomplished our objectives by performing respirometry experiments during which we subjected individual fish to two different types of turbulent flow characterized by the same mean flow velocity, but two different standard deviations of flow velocity. Experiments were therefore performed under two levels of turbulence intensity (standard deviation/mean flow velocity). Total swimming costs obtained for the two turbulence intensities were compared for four groups of fish that differed in geographical origin (Canada, Norway) and degree of domestication (wild, farmed, domesticated). All fish were adapted to a water temperature of 15°C for a period of three weeks before starting the respirometry experiments. The body mass of the fish used for our experiments ranged from 3.95-16.11 g wet (Table 5.1). Photographs of twenty individuals from each of the four fish groups were taken in order to measure thirty morphometric variables describing different features of their body dimensions.

Table 5.1 Number of respirometry experiments per flow condition for four groups of juvenile Atlantic salmon: wild fish, farmed fish from the Sainte-Marguerite River, farmed fish from the Imsa River, and domesticated fish; range of body mass; total swimming costs under low and high turbulence intensities with the same mean flow velocity of 23 $cm \cdot s^{-1}$ and two different standard deviations of 5 $cm \cdot s^{-1}$ and 8 $cm \cdot s^{-1}$.

Fish group	wild	farmed	farmed	domesticated
Population	Ste-Marguerite R.	Ste-Marguerite R.	Imsa River	Sunndalsøra
Experiments per flow condition	8	8	5	6
Body mass (g)	4.15 – 13.02	4.90 – 16.01	3.95 – 16.11	7.73 – 14.06
Total swimming cost (mg $O_2 \cdot h^{-1}$)				
under low turbulence intensity	2.10 – 4.40	2.68 – 6.00	2.11 – 6.59	3.99 – 6.25
under high turbulence intensity	2.83 – 7.21	3.74 – 8.00	2.67 – 8.02	5.24 – 8.29

5.2.1 Fish

We obtained juvenile Atlantic salmon (JAS) for our experiments from four different sources:

(1) Wild JAS from the Sainte-Marguerite River (Saguenay Region, Québec, Canada, 48°15' N, 69°55' W) were collected with a Smith-Root Inc.® backpack electroshocker (model 12-B, Vancouver, Washington, USA). Fish were returned to the laboratory at the Université de Montréal and kept in a 500 L Living Stream aquaria (model LSW 700, Frigid Units Inc., Toledo, Ohio, USA). Flow in these tanks was approximately 5 $cm \cdot s^{-1}$. Wild fish did not accept commercial pellets and were fed daily with red mosquito larvae (San Francisco Bay Brand®, Newark, California, USA).

(2) Farmed JAS from the crossing of wild progenitors that originated from the Sainte-Marguerite River were obtained from the Pisciculture de Tadoussac (operated by the Société de la Faune et des Parcs du Québec, Canada). The juveniles were transferred to the Université de Montréal and kept under conditions (tank and flow velocities) identical to those of wild fish. However, farmed fish from the Pisciculture de Tadoussac were fed daily with commercial food pellets (Corey Feed Mills Ltd., Fredericton, New-Brunswick, Canada).

(3) Farmed JAS from the crossing of wild progenitors that originated from the Imsa River were provided by the Norwegian Institute of Nature Research (NINA) Research Station at Ims (Rogaland, Norway, 58°59'N, 5°58'E). The fish were kept in 1 m^2 tangential flow tanks supplied with flow-through freshwater from the Imsa River. These fish were fed an excess of commercial food pellets (EWOS®, Bergen, Norway) using automatic feeders.

(4) Domesticated JAS that originated from the Norwegian National Breeding Program at Sunndalsøra (Aquagen, Norway) and were taken as eyed eggs to the NINA Research Station. The Sunndalsøra salmon were developed for the Norwegian fish farm industry and have bred selectively since 1971 to attain certain characteristic such as increased growth, delayed maturity, and disease resistance. The first generation fish were derived from forty different wild salmon populations. However, after four generations, the stock was dominated by individuals coming from only one to three populations characterized by fast-growing and late-maturing fish. The fish we studied were seventh generation of the first brood line (Gjedrem et al. 1991). The domesticated JAS were kept under conditions (tank, flow velocities, food) identical to those of farmed fish of the Imsa River.

5.2.2 Experimental design

The respirometry system consisted of a transparent Plexiglas® container (24 L; 60 cm x 20 cm x 20 cm) with a lid that could be hermetically sealed. The respirometer was placed in a water bath to maintain water temperature of 15°C during the experiments. The details of the experimental design are described in Enders et al. (2003) and are presented here only in a summarized version. The respirometer contained two pumps and a bottle-shaped swimming chamber. The

shape of the swimming chamber was selected to ensure that fish could not avoid the water flow during the experiments. The narrow neck of the swimming chamber was connected to pump 1 (Model 1750, Jacobs Canada Inc., Mississauga, Ontario) that generated the turbulent flow in the swimming chamber by recirculating water within the respirometer. The swimming chamber contained two grids. The grids consisted of nylon mesh 9 cm in diameter perforated with 2 mm x 2 mm holes. The grids were located in the 'upstream' and 'downstream' sections of the swimming chamber. The 'upstream' grid was used to produce a spatially uniform fine turbulence flow structure within the swimming chamber (Tritton 1988). The 'downstream' grid was designed to force the fish to remain in the swimming chamber without interfering with the flow. Pump 2 (Model 402, Powerhead, Montréal, Québec) served two purposes. Before an experiment, pump 2 was used to create water exchange between the respirometer and the aquarium, hence providing oxygenated water to the respirometer. During an experiment, pump 2 was used to transfer water from the respirometer to the oxygen meter. Fish swimming costs were quantified by measuring the oxygen depletion over time with an oxygen meter (model 565, Intab, Stenkullen, Sweden; $\pm$ 0.005 mg $O_2 \cdot L^{-1}$).

5.2.3 Characteristics of flow structures

Turbulence in the swimming chamber was created by modulating the electric current that powered pump 1. Four components of the electric current were adjustable: (1) the maximal electric current which determines the maximal flow velocity, (2) the minimal electric current which determines the minimal flow velocity, (3) the frequency of pulsation between a diminution of the electric current to introduce a pulsation of the water flow, and (4) the duration of the diminution of

the electric current to manipulate the duration of low- and high-speed flow conditions. Flow structures were quantified using an Acoustic Doppler Velocimeter (ADV, Sontek, San Diego, California, USA). The ADV allowed us to record the three orthogonal velocity components of the flow (streamwise, U; vertical, V; lateral, W) at a frequency of 25 Hz. The volume sampled by the ADV (0.25 cm^3) is located 5 cm away from its probe so that the perturbation of the measured flow by the probe is minimized. Turbulence was quantified at the beginning of the suite of experiments in Canada and at the beginning of the suite of experiments in Norway aimed at testing the effect of flow conditions on total swimming costs. Turbulence was quantified in the absence of fish to avoid interference caused by fish on the recordings. For every flow condition, a velocity time series was recorded for a period of 5 min. The ADV permitted us to define the settings of the components of the electric current that could create two different flow conditions determined by one mean streamwise flow velocitiy, $\bar{u}$ (23 $cm \cdot s^{-1}$) and two different standard deviations of the streamwise flow velocity, u_{SD} (low turbulence condition $= 5$ $cm \cdot s^{-1}$; high turbulence condition $= 8$ $cm \cdot s^{-1}$). This approach was employed to create two flows characterized by turbulence intensities (standard deviation/mean flow velocity) of 0.22 and 0.35. We calculated the mean and the standard deviation of the 5 min velocity time series measured at a frequency of 25 Hz. The two experimental flow structures were selected for our experiments because they occurred within the range of mean flow velocities (5 to 40 $cm \cdot s^{-1}$; DeGraaf and Bain 1986) and of standard deviations of flow velocity (4 to 14 $cm \cdot s^{-1}$) at the focal point of the JAS in nature (Enders et al., submitted to Journal of Fish Biology).

Stability and repeatability tests with three velocity time series recorded at the beginning and the end of a suite of experiments were conducted in a previous study. These tests demonstrated that our apparatus generates consistent and reproducible turbulent flow structures (Enders et al. 2003). The repeatability of each of the two experimental flow structures created by our apparatus was again tested using one-way analysis of variance (ANOVA). This ANOVA was performed to compare the mean streamwise flow velocities during the time series recorded before a suite of experimental observations. The repeatability of the standard deviations of the flow velocities was tested using the same approach, with Levene's test of the homogeneity of variance (SPSS Inc., Chicago, Illinois, USA).

5.2.4 Total swimming costs

We used a single fish per respirometry experiment. A fish was selected at random from our stock of experimental fish and was not fed for two days before the experiment to avoid increased metabolic rates associated with digestion (Brett and Groves 1979). Twenty-four hours before the beginning of an experiment, the fish was introduced into the swimming chamber to allow it to adapt to the experimental conditions. After the introduction of the fish into the swimming chamber, the respirometer was sealed without residual air bubbles. During this adaptation phase, pump 2 generated a water exchange between the respirometer and ambient water of the aquarium. At the beginning of the experiment, pump 2 was connected to the oxygen meter preventing an external water supply and pump 1 was started to create the turbulent flow structures in the swimming chamber. The initial oxygen concentration was measured at the beginning of the experiment and subsequently at every 30 min.

We monitored fish behavior during each experiment to ensure that fish were continuously swimming. Every 10 min, an image of the position held by the fish within the swimming chamber was automatically registered with a web cam (Sony Electronics Inc., Oradell, New Jersey, USA). In addition, during the last 30 min of the experiment, the fish was continuously filmed by a video camera (WV-BL602; Panasonic Canada Inc., Lachine, Québec). Hence, our procedure assumes that if a fish is always in a swimming position during a series of images registered at 10 min intervals, and if a fish swims continuously during the last 30 min of an experiment, it was continuously swimming throughout the experiment. Consequently, we assume that fish were continuously swimming against the flow structures created by our apparatus. An experiment ended after 6 h. No observation was made below 7.6 mg $O_2 \cdot L^{-1}$ to minimize the influence of low oxygen concentration on fish behavior (Beamish 1978). At the end of an experiment the fish was removed from the respirometer, anaesthetized (clove oil; 0.6 mg$\cdot L^{-1}$), weighed (g wet), and measured (TL cm). The biological oxygen demand (BOD) was determined within 6 h of an experiment using the same procedure but without fish.

The total oxygen consumption rate of the fish (Vo_2; mg $O_2 \cdot h^{-1}$) was estimated as

$$Vo_2 = \Delta O_2 / \Delta t \cdot V_W - BOD \tag{5.1}$$

where ΔO_2 is the difference in oxygen concentration between two successive oxygen concentration measurements (mg $O_2 \cdot L^{-1}$), Δt is the time interval of 0.5 h between two consecutive oxygen concentration measurements, V_W (22.6 L) is the volume of water in the respirometer excluding the volume of the pumps and swimming chamber, and

BOD is the biological oxygen demand by micro-organisms in the water (mg $O_2 \cdot h^{-1}$). Since we measured oxygen concentration within the swimming chamber at 30 min intervals over 6 h, we obtained twelve Vo_2 values per experiment. We then calculated the total swimming costs C_R as the mean of the Vo_2 values obtained for each experiment.

Prior to statistical analyses, total swimming costs and body masses were log transformed and the residuals were tested for normality using graphical probability plots and for homogeneity of variance using Levene's test. A two-way ANOVA was used to determine the effect of the fish groups and the turbulence intensities on the total swimming costs. During these analyses, body mass was used as a covariate. Scheffe's *post hoc* test was used to verify which of the four fish groups were significantly different. The two-way ANOVAs were performed using SuperANOVA 1.11 statistical packages (Abacus Concepts Inc., 1991).

5.2.5 Morphometric measurements

Fish from each treatment (n =20) were photographed on the left side of the body. Prior to photographing, each fish was anaesthetized (clove oil; 0.6 mg$\cdot L^{-1}$) and placed left side up on a moist, blue carpet that had two millimeter rulers along the lower and left edges. Anal, dorsal and caudal fins were erected and small pieces of white paper were placed under the pectoral and pelvic fins to increase their visibility. Images were taken using a tripod and a video camera (ES610 fitted with a 50 mm lens, Canon Canada Inc., Mississauga, Ontario) set at a fixed distance of 40 cm from the fish. The images were analyzed using the image analysis software SigmaScan Pro 5.0 (Statistical Solutions, Saugus, Massachusetts, USA). Spatial coordinates of

eighteen morphometric landmarks as described in Winans (1984) and Swain et al. (1991) were taken (Figure 5.1).

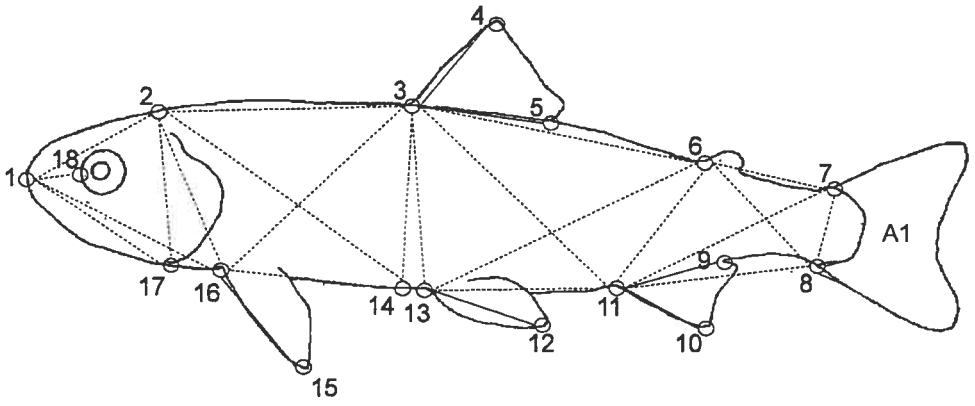

Figure 5.1 Location of eighteen landmarks (open circles), twenty-three trusses (dashed lines), six fin lengths (solid lines), and (A1) the caudal fin area. (1) Anterior tip of snout at upper jaw, (2) most posterior aspect of neurocranium, (3) origin of dorsal fin, (4) distal tip of dorsal fin, (5) insertion of dorsal fin, (6) origin of adipose fin, (7) anterior attachment of dorsal fin membrane from caudal fin, (8) anterior attachment of the ventral membrane from caudal fin, (9) insertion of anal fin, (10) distal tip of anal fin, (11) origin of anal fin, (12) distal tip of pelvic fin, (13) origin of pelvic fin, (14) point of the ventral surface of the body directly below the anterior dorsal fin origin, (15) distal tip of pectoral fin, (16) origin of pectoral fin, (17) posteriormost point of the maxilla, and (18) anteriormost edge of the orbit.

The eighteen morphometric landmarks were used to calculate twenty-three interconnected distance variables defining different aspects of the dimensions of a fish (subsequently referred to as truss measurement, Figure 5.1). The truss network is a series of measurements calculated between the landmarks that form a regular pattern of contiguous quadrilaterals or cells across the body. Compared to more conventional sets of measurements, the truss network has the advantage of providing an equal coverage of the entire body (Strauss and Bookstein 1982). In addition to the truss network, six fin measurements were calculated from the landmark coordinates and the caudal fin area was measured. Consequently, we obtained thirty morphometric variables describing different aspects of body dimensions. To measure the precision of the digitizing approach, ten individuals were measured five times.

The measurement error was always less than 0.5 mm (variations of 1.3% to 4.6% depending on the morphometric variable).

Principal components analysis was then used to describe the body shape independent of body size (Jolicoeur 1963). Therefore, all morphometric variables were log transformed. This procedure allows body size, which we are trying to control for during our comparative analyses, to become an additive component of every variable. In the analysis, the first principal component was expected to represent a combination of the morphometric variables correlated to the general body size and was therefore removed from the data set in order to control for body size. The dorsal fin height was the only morphometric variable that did not vary with body size. Variables that do not vary with body size dominate the subsequent shape components and artificially influence the importance of these variables. Therefore the dorsal fin height was omitted from the principal components analysis as suggested by Somers (1986). The loadings of the twenty-nine remaining size-corrected morphometric variables from the second and third principal components were used to compare the four fish groups. The significance of the morphological differences between the four groups was assessed using multivariate analysis of variance (MANOVA) followed by Scheffe's *post hoc* test.

5.3 Results

5.3.1 Characteristics of flow structures

The mean values of the streamwise flow velocities obtained for the two different turbulent conditions were consistent with the targeted value of 23 $cm \cdot s^{-1}$ (Table 5.2). The mean of the streamwise flow velocities ranged from 23.01 to 23.04

$cm \cdot s^{-1}$. Standard deviation of the streamwise flow velocity ranged from 5.13 to 5.15 $cm \cdot s^{-1}$ under low turbulent condition (target =5 $cm \cdot s^{-1}$). Corresponding values for the high turbulent condition (target = 8 $cm \cdot s^{-1}$) ranged from 7.99 to 8.07 $cm \cdot s^{-1}$. The turbulence intensity was 0.22 for the low turbulence condition and 0.35 for the high turbulence condition. The mean vertical flow velocities ranged from -0.15 to 0.92 $cm \cdot s^{-1}$ with the standard deviation of the vertical flow velocity ranging from 4.92 to 7.56 $cm \cdot s^{-1}$. The mean lateral flow velocities ranged from 0.09 to 0.33 $cm \cdot s^{-1}$ with the standard deviation of the lateral flow velocities ranging from 5.41 to 7.69 $cm \cdot s^{-1}$.

Table 5.2 Ranges of the mean flow velocity, standard deviation, minimum, and maximum of the streamwise U, vertical V, and lateral W flow velocity components ($cm \cdot s^{-1}$) under low and high turbulence intensities.

		U	V	W
Low turbulence intensity 0.22	mean	23.01 - 23.04	-0.04 - 0.92	0.09 - 0.10
	SD	5.13 - 5.15	4.92 - 5.09	5.41 - 5.59
	min	5.23 - 5.64	-27.64 - -21.89	-26.88 - -21.71
	max	34.98 - 37.58	21.84 - 29.73	28.19 - 28.23
High turbulence intensity 0.35	mean	23.01 - 23.04	-0.15 - -0.01	0.29 - 0.33
	SD	7.99 - 8.07	7.35 - 7.56	7.69 - 7.70
	min	0.17 - 0.90	-30.32 - 29.56	- 29.61 - -29.76
	max	44.85 - 46.91	29.52 - 30.34	29.95 - 32.45

The trace of the time series of the streamwise flow velocity for the two flow conditions clearly indicated that the flow created by our apparatus was turbulent (Figure 5.2). For the two turbulence conditions, the mean streamwise flow velocity, $\bar{u}$, did not vary significantly among the recordings performed for the four velocity time series (variation =0.1%, ANOVA, $F_{3,30003}$ =0.05, p =0.98). Similarly, for any given flow condition, the standard deviation of streamwise flow velocity, u_{SD}, obtained for the two velocity time series did not vary significantly (variation =0.4%,

Levene's statistic$_{1,15000}$ =2.50, p =0.12, variation =1.0%, Levene's statistic$_{1,15000}$ = 0.55, p =0.81, respectively). These results confirm our previous findings that the flow structures created by our apparatus were repeatable and stable (Enders et al. 2003).

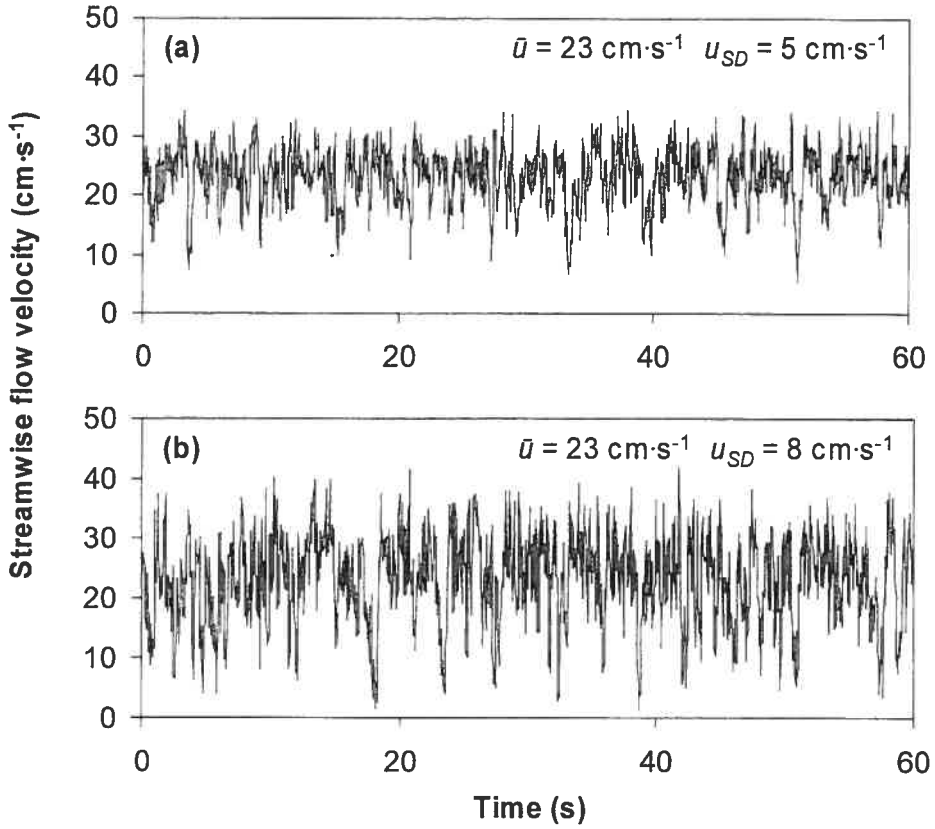

Figure 5.2 Velocity time series of 1 min (25 Hz) for the two different flow conditions with a mean flow velocity, $\bar{u}$, of 23 cm·s^{-1} and two standard deviations of the flow velocity, u_{SD}, of a) 5 cm·s^{-1}, and b) 8 cm·s^{-1}, in the swimming chamber in which juvenile Atlantic salmon swam during the respirometry experiments.

5.3.2 Total swimming costs

Total swimming costs depended on fish body mass and varied 4-fold among treatments (Figure 5.3). The predicted total swimming costs for a 10 g wild JAS held under low turbulence intensity (3.80 mg $O_2 \cdot h^{-1}$) was 45.9% lower than predicted value under high turbulence intensity (5.55 mg $O_2 \cdot h^{-1}$; Table 5.3). Total swimming costs differed between the four groups of fish (ANOVA, $F_{3,38}$ =7.2; p =0.0006) and increased with an increase of turbulence intensity ($F_{1,38}$ =127.0; p =0.0001) and body mass ($F_{1,38}$ =307.0; p =0.0001).

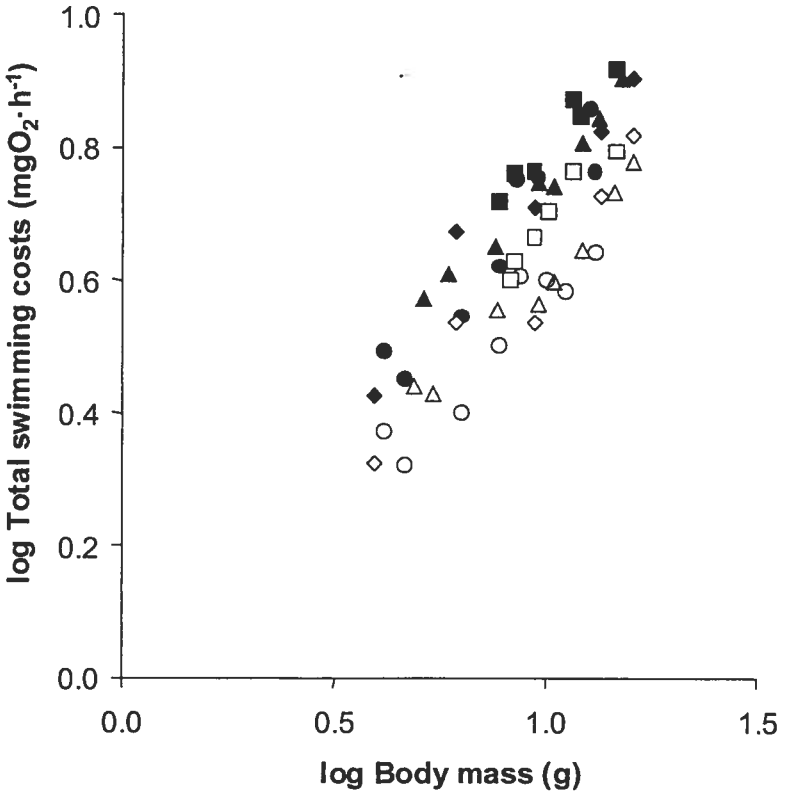

Figure 5.3 Total swimming costs of wild fish (●),farmed fish from the Sainte-Marguerite River (▲), farmed fish from the Imsa River (♦), and domesticated fish (■) under low turbulence intensity (open symbols) and high turbulence intensity (solid symbols).

The interaction terms between fish group, turbulence intensity, and body mass were not significant (0.66 <p <0.95), and indicates that the direction of the effect of

turbulence intensity and body mass on total swimming costs was similar among fish groups. Total swimming costs of wild fish were not significantly different from those of farmed fish (difference ranging from 2.3 to 11.2%, p =0.08). Similarly, the total swimming costs of the two groups of farmed fish (Sainte-Marguerite River and Imsa River) were not significantly different (p =0.73). However, the total swimming costs of wild fish differed significantly from domesticated fish (p = 0.0001). Total swimming costs predicted for a 10 g wild fish were 29.2% lower under low turbulence intensity and 15.2% lower under high turbulence intensity than the total swimming costs of domesticated fish (Figure 5.4). Total swimming costs predicted for a 10 g farmed fish were also significantly different from domesticated fish (p = 0.01). The total swimming costs of a 10 g farmed fish was 12.5% lower (high turbulence intensity) to 16.2% lower (low turbulence intensity) than a domesticated fish of the same mass.

Table 5.3 Total swimming costs and 95% confidence intervals of 10 g fish under two turbulence intensities characterized by the same mean flow velocity of 23 $cm \cdot s^{-1}$ and two different standard deviations of 5 $cm \cdot s^{-1}$ and 8 $cm \cdot s^{-1}$. Four fish groups were compared: wild fish, farmed fish from the Sainte-Marguerite River, farmed fish from the Imsa River, and domesticated fish. Observed total swimming costs were compared with predictions of a new forced swimming model developed.

Fish group	wild	farmed	farmed	domesticated
Population	Ste-Marguerite R.	Ste-Marguerite R.	Imsa River	Sunndalsøra
Total swimming costs ($mg\ O_2 \cdot h^{-1}$)				
under low turbulence	3.80	4.14	4.32	4.91
95% Confidence interval	[3.41-4.24]	[3.91-4.38]	[3.54-5.26]	[4.62-5.22]
Factor A	2.4	2.6	2.7	3.1
under high turbulence	5.55	5.70	5.65	6.39
95% Confidence interval	[4.91-6.27]	[5.48-5.93]	[4.74-6.73]	[6.13- 6.66]
Factor B	3.5	3.6	3.6	4.0

Note: The factor A represents the factor by which the predictions of the forced swimming model underestimated observed total swimming costs under low turbulence intensity and Factor B under high turbulence intensity.

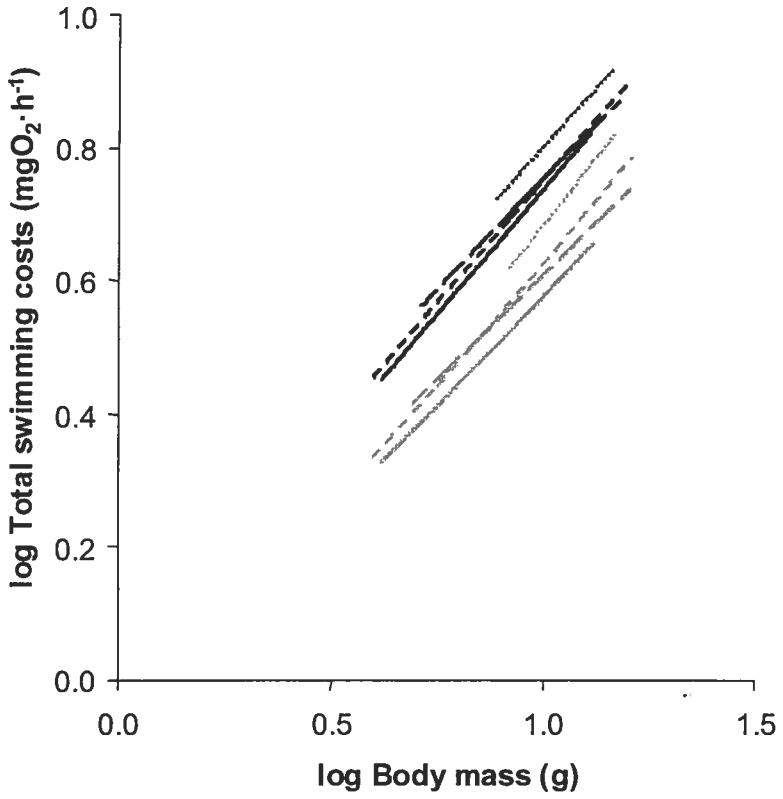

Figure 5.4 Regression lines representing the relationship between body mass and total swimming costs of wild fish (—), farmed fish from the Sainte-Marguerite River (- - -), farmed fish from the Imsa River (----), and domesticated fish (· · ·) under low turbulence intensity (shaded lines) and high turbulence intensity (solid lines).

5.3.3 Comparison of the morphometric variables for the four different fish groups

Principal components analysis indicated differences in body shape between the four groups of fish (Figure 5.5). The first principal component (PC1) summarized the strong correlation between the morphometric characters and the total body length ($r^2 = 0.88$, $p = 0.001$). The second and third principal components (PC2 and PC3) described the variation in body shape, statistically independent from total body length ($r^2 = 0.07$, $p = 0.15$ and $r^2 = 0.00$, $p = 0.86$, respectively). PC1 accounted for

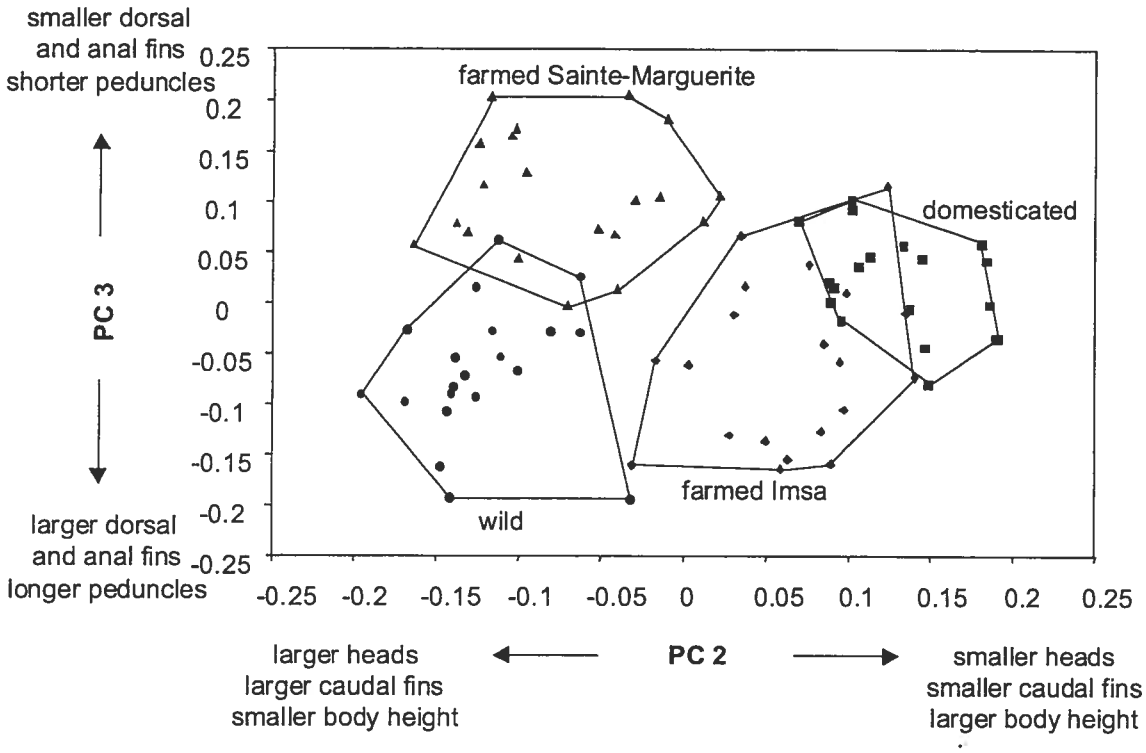

Figure 5.5 Principal components analysis of the morphometric variables of wild fish (●), farmed fish from the Sainte-Marguerite River (▲), farmed fish from the Imsa River (♦), and domesticated fish (■). Morphometric variables, which have loadings on the principal component axis 2 and 3, are noted and the arrows indicate the direction of the correlation.

76.3% of the total variance in the morphometric variables. PC2 explained 6.8% and PC3 accounted for 5.0% of the total variance in morphometric variables (Table 5.4). PC2 involved a contrast between body depth, caudal fin area, and measurements in the head region. Domesticated fish had positive scores on PC2 indicating a deep body shape with smaller caudal fins and smaller heads, whereas the wild fish and farmed fish from the Sainte-Marguerite River had negative scores on PC2, indicating slender bodies with greater caudal fins and larger heads. The body height of domesticated JAS was 7.9% to 8.6% larger than for wild JAS. The caudal fin and the head of domesticated JAS were on average 16.7% and 26.7% smaller than for wild JAS. In this respect, farmed fish from the Imsa River were intermediate between farmed fish from the Sainte-Marguerite River and domesticated fish. The

Table 5.4 Loadings of the morphometric variables along the first, second and third principal component axes. Morphometric variables are the distances between the landmarks numbered in Figure 5.1. The morphometric variables with important loadings (threshold =0.2) along PC2 are indicated in bold letters and along PC3 in italic letters.

Variable	PC1	PC2	PC3	Description
1 - 2	-0.137	**-0.217**	0.036	**forehead length**
2 - 17	-0.176	0.013	0.023	head depth 1
2 - 16	-0.175	0.020	0.096	head depth 2
2 - 14	-0.196	0.016	0.070	head to pelvic fin
2 - 3	-0.215	0.009	0.141	head to dorsal fin
3 - 16	-0.209	0.145	0.073	dorsal to pectoral fin
3 - 14	-0.207	**0.301**	0.067	**body depth**
3 - 13	-0.198	**0.226**	0.051	**dorsal to pelvic fin**
3 - 11	-0.198	0.013	0.052	dorsal to anal fin
3 - 6	-0.205	-0.146	0.022	dorsal to adipose fin
6 - 13	-0.201	0.015	0.032	pelvic to adipose fin
6 - 11	-0.199	0.143	-0.065	anal to adipose fin
6 - 8	-0.193	0.085	***0.209***	***adipose to caudal fin ventral insertion***
6 - 7	-0.174	-0.013	***0.217***	***adipose to caudal fin dorsal insertion***
7 - 11	-0.171	-0.053	0.004	caudal fin dorsal insertion to anal fin
7 - 8	-0.206	0.002	0.062	caudal fin dorsal to caudal fin ventral insertion
8 - 11	-0.180	-0.052	0.038	anal fin to caudal fin ventral insertion
11 - 13	-0.197	-0.057	0.149	pelvic fin insertion to anal fin insertion
13 - 16	-0.207	0.038	0.017	pectoral to pelvic fin
16 - 17	-0.132	**0.597**	0.144	**length between premaxilla and pectoral**
1 - 16	-0.139	-0.175	0.070	snout to below pectoral
1 - 17	-0.135	**-0.254**	0.015	**snout to below premaxilla**
1 - 18	-0.153	**-0.333**	-0.006	**snout to orbit**
3 - 5	-0.155	0.160	***-0.586***	***dorsal fin length***
10 - 11	-0.211	-0.023	-0.151	anal fin height
9 - 11	-0.166	0.105	***-0.641***	***anal fin length***
12 - 13	-0.193	-0.167	-0.050	pelvic fin length
15 - 16	-0.135	-0.082	-0.042	pectoral fin length
A1	-0.254	**-0.309**	-0.134	**caudal fin area**

four groups showed significant differences for the PC2 (MANOVA, $F_{3,79}$ =135.2; p <0.001). PC3 was defined by tail length, and dorsal and anal fin lengths. Farmed fish from the Sainte-Marguerite River scored positively on PC3 indicating shorter tail lengths and smaller dorsal and anal fin lengths whereas the wild fish and farmed fish from the Imsa River tended to score negatively on PC3, indicating longer tail lengths, and larger dorsal and anal fin lengths. The tail length of farmed JAS from the Sainte-Marguerite ranging from 4 g to 16 g was 19.3% to 17.9% shorter than for wild JAS. The dorsal and anal fin lengths of farmed JAS of the Sainte-Marguerite were on

average 26.6% and 3.4% smaller than for wild JAS. Domesticated fish did not score on PC3. Mean PC3 scores differed significantly between the four fish groups (MANOVA, $F_{3,79}$ =31.2; p <0.001). Scheffe's *post hoc* test showed that PC3 scores of wild JAS differed significantly from those of farmed and domesticated JAS ($p < 0.01$). The PC3 scores of farmed fish were significantly different from domesticated JAS ($p < 0.01$). However, the PC3 scores of the two groups of farmed JAS from the Sainte-Marguerite River and the Imsa River were not significantly different ($p = 0.98$).

5.4 Discussion

Our study confirms that the total swimming costs of JAS increase significantly with an increase in turbulence intensity. Total swimming costs increase by an average factor of 1.4 as standard deviation of the flow velocity increased from 5 $cm \cdot s^{-1}$ to 8 $cm \cdot s^{-1}$ and as turbulence intensity increased from 0.22 to 0.35. Furthermore, total swimming costs increased with body mass. The effect of body mass and mean flow velocity is well established and included in all swimming costs models currently available (Beamish 1978; Brett and Groves 1979; Farrell et al. 2003). However, our results indicated that descriptors of flow heterogeneity such as the standard deviation of the flow or the turbulence intensity may be required to adequately estimate the total swimming costs under turbulent flow conditions. JAS live in gravel-bed rivers characterized by highly turbulent flow. Estimates of swimming costs derived from experiments with minimized flow heterogeneity, such as forced swimming models, may therefore underestimate the actual cost of swimming of JAS in their natural environment. Enders et al. (2003) estimated the magnitude of the effect of turbulence on fish respiration rates by comparing the

swimming costs incurred by fish under turbulent flows and those predicted by the forced swimming model of Boisclair and Tang (1993). This analysis indicated that forced swimming models may underestimate swimming costs in turbulent flows by a factor ranging from 2 to 4. Such comparative analysis cannot be performed with the results of the present study because the models of Boisclair and Tang (1993) were developed to estimate net swimming costs (total respiration rate of unfed fish minus the standard metabolic rate of fish). In the present study, we estimated only the total swimming costs of unfed fish. Comparisons between total swimming costs and net swimming costs would be misleading. Calculations of net swimming costs from our data would have required an estimate of standard metabolic rate (SMR) for each fish group. Because such data do not exist for the four fish groups studied and because SMR may vary among fish of different origins within a species (Boily and Magnan 2002; Grisdale-Helland et al. 2002; Trudel et al. 2004), we did not perform the calculation of potentially misleading net swimming costs for our four fish groups. Consequently, in the present study, we estimated the magnitude of the effect of turbulence on fish respiration rates by developing a new forced swimming costs model. This model was based on the data set used by Boisclair and Tang (1993) with the exceptions that the dependent variable was not net swimming costs but total swimming costs, and that temperature was added as an independent variable. Indeed, before developing their model, Boisclair and Tang (1993) subtracted from published total swimming costs the SMR values provided in the papers used to perform the empirical analysis. Hence, the development of a new forced swimming model (Forced Total Swimming Costs; FTSC, mg $O_2 \cdot h^{-1}$) simply required the reversal of the computational approach used by Boisclair and Tang (1993). This procedure resulted in the development of the following FTSC model

(5.2) $$\log_{10} C_{FTSC} = 0.96 \log_{10} M + 0.23 \log_{10} \bar{u} + 0.67 \log_{10} T - 1.85$$

where C_{FTSC} is the total swimming costs under minimized flow heterogeneity (mg $O_2 \cdot h^{-1}$), M is the body mass of fish (g wet), $\bar{u}$ is the mean flow velocity ($cm \cdot s^{-1}$), and T the water temperature (°C). Body mass, contributed with 79% to most of the explained variance in the FTSC ($F_{3,114} = 162.35$, $R^2 = 0.81$, $p < 0.0001$). The new FTSC model predicted that the total swimming costs of a 10 g fish swimming at a speed of 23 $cm \cdot s^{-1}$, in a flow with minimized flow heterogeneity that characterizes forced swimming experiments, and at a water temperature of 15°C should be 1.58 mg $O_2 \cdot h^{-1}$ (95% confidence intervals: 1.35 – 1.85 mg $O_2 \cdot h^{-1}$). The total swimming costs we estimated for 10 g wild JAS swimming against our low and high turbulence intensities were respectively 2.4- (3.80 mg $O_2 \cdot h^{-1}$) and 3.5-fold (5.55 mg $O_2 \cdot h^{-1}$) higher than predicted by the new FTSC models (Table 5.4). Differences between the predictions by the FTSC model and our observations were more pronounced for domesticated JAS ranging from 3.1- (low turbulence intensity, 4.91 mg $O_2 \cdot h^{-1}$) to 4.0-fold (high turbulence intensity, 6.31 mg $O_2 \cdot h^{-1}$). Observations on fish behavior suggested that swimming in turbulent flow should increase the swimming costs of fish (McLaughlin and Noakes 1998; Pavlov et al. 2000). This study supported this suggestion showing a clear increase of the total swimming costs of 2.4- to 4.0-fold in flow of fluctuating velocities compared to swimming in steady flow conditions.

Our results indicated that total swimming costs of wild and farmed JAS were not significantly different. We therefore conclude that swimming costs models obtained using farmed fish can be employed to adequately estimate the swimming

costs of wild fish. However, total swimming costs of wild and farmed JAS differed significantly from the total swimming costs of domesticated JAS. The differences were larger between wild and domesticated JAS (15.2% to 29.2%) than between farmed and domesticated JAS (12.5% to 16.2%). These results suggest that swimming costs models developed with wild or farmed fish should not be applied to domesticated fish, and vice versa.

Four hypotheses may explain the difference between the total swimming costs of wild and domesticated JAS. First, this difference may result from a conditioning effect. Throughout their freshwater life, wild JAS are exposed to turbulent flow with mean focal point velocities of 5 to 40 $cm \cdot s^{-1}$ (DeGraaf and Bain 1986). When feeding on invertebrate drift, fish are exposed to even higher mean flow velocities of 10 to 120 $cm \cdot s^{-1}$ (Morantz et al. 1987). Therefore, wild JAS may be better conditioned to swim against the experimental flow than farmed or domesticated fish. Conditioning improves growth rate, food conversion efficiencies and changes condition factor and body composition (see Davison (1997) for review). Conditioning has also been shown to increase routine metabolism and to decrease total swimming costs (Bagatto et al. 2001). For example, zebrafish larvae (*Danio rerio*) conditioned to 5 $BL \cdot s^{-1}$ had a 45% increased routine metabolism compared to unconditioned fish. The observed increase in the routine metabolism may be explained by an actual conditioning effect causing an augmentation of the standard metabolic rate or by an increase of the routine activity level. However, conditioned fish swimming at 2 $BL \cdot s^{-1}$ had a 2.3-times lower total swimming costs than unconditioned fish (Bagatto et al. 2001). Also JAS increased their sprint performance when imposed to flows of 1 to 2 $BL \cdot s^{-1}$ (McDonald et al. 1998). Unconditioned JAS sustained swimming for 231 s in a flow

of 38 $cm \cdot s^{-1}$ (5-8 $BL \cdot s^{-1}$), whereas fish conditioned to 1 $BL \cdot s^{-1}$ sustained swimming for a longer period of 294 s, and fish conditioned to 2 $BL \cdot s^{-1}$ to an even more increased period of 324 s. Our findings that total swimming costs of wild JAS are lower than those of domesticated fish, regardless of the turbulence intensity, are consistent with the hypothesis that conditioning may have provided an advantage to wild fish (lower total swimming costs). However, farmed and domesticated JAS were raised and held in flow tanks characterized by identical flow velocities. Hence, despite similar conditioning, total swimming costs of farmed fish were significantly different from those of domesticated fish. In addition, although wild and farmed fish experienced different conditioning, we found no significant difference between total swimming costs of these two groups of fish. These comparisons may suggest that other variables may play a more important role than conditioning in determining swimming cost. An additional argument which may be put forward against the effect of conditioning in our experiments we did not observe any fatigue or exhaustion in the fish from the four groups during our experiments. JAS of all groups seemed to be in the physically capable of swimming continuously over a 6 h period. In their natural environment, JAS likely swim against turbulent flow during shorter time periods to attack invertebrate drift, to explore habitat, or to defend their territory. Therefore, the duration of the experiment may be seen as energetically demanding for the fish. However, fish from the four groups did not show any indication of exhaustion, such as drifting back against the downstream grid. Furthermore, we did not observe an increasing relationship between C_R and time since the beginning of an experiment ($0.00 < r^2 < 0.19$; $0.22 < p < 1.00$). Hence, our experimental conditions did not appear to cause any functionally or statistically significant fatigue to any of the fish groups during the experiment.

Second, differences in total swimming costs among fish groups may be due to differences in body composition among these groups (Kleiber 1975). Differences in body composition may be related to differences in diet among the fish groups we studied. Although we have no data regarding the body composition of the fish we studied, it may be hypothesized that this trait differed between wild and farmed or domesticated fish due to differences in diet, as wild fish were fed natural preys items, whereas farmed and domesticated fish were fed with commercial diets. This hypothesis is supported by the study of McDonald et al. (1998) who found 2.2-times higher lipid concentrations in aquaculture JAS than in wild JAS. Adipose tissue is metabolically inert relative to lean tissue and does not significantly contribute to the overall metabolism (Hayward 1965). Therefore, though the storage of lipids may raise the fish body mass, the standard metabolic rate may remain unchanged. Consequently, the storage of lipids may lead to a lower mass-specific standard metabolic rate. Goolish and Adelman (1987) demonstrated tissue-specific metabolic capacity using cytochrome-c oxidase activity as a measure of metabolic rate. Body tissue containing a small amount of lipid, such as muscles, had 7-times lower cytochrome-c oxidase activity than body tissue containing a higher amount of lipid, such as the hepatopancreas. However, in northern elephant seal pups (*Mirounga angustirostris*) adipose tissue mass was not correlated to the standard metabolic rate, although the concentration of body fat increased from 4% at birth to 48% by the 4th week (Rea and Costa 1992). These results may suggest that the possible differences in body composition among the four fish groups may have had only a minor effect on the total swimming costs. In this study, we observed the highest total swimming costs in domesticated JAS, who should have a higher lipid concentration than wild

JAS (McDonald et al. 1998), and therefore a lower standard metabolic rate (Hayward 1965).

Third, it may be hypothesized that differences in total swimming costs among the four groups of JAS may be due to SMR that differ among these groups. Variations of the standard metabolic rates between different fish species have been well established (Herrmann and Enders 2000; Steffensen 2002). Trudel et al. (2004) demonstrated that the standard metabolic rates may also vary depending on body mass and water temperature, from close to 0% to 200% among closely related species such as Pacific salmon (*Oncorhynchus* spp.). However, only a few studies have assessed the magnitude of within-species variation of SMR. Boily and Magnan (2002) concluded that there was a statistically significant difference between the SMR of brook charr (*Salvelinus fontinalis*) having different body shapes. The observed within-species variation in fish morphology may suggest that the differences in SMR among the four different groups of JAS may have influenced the total swimming costs.

Finally, the morphology of the domesticated JAS is known to have diverged from the wild form with the head becoming smaller, the body more robust, and rayed fins smaller (Fleming and Einum 1997). By contrast, wild fish have a more slender body shape and larger fins. Our work supports these findings, showing that domesticated fish have smaller heads, deeper bodies, and smaller caudal fins than wild fish. Increased total swimming costs may be imputed to morphological features that increase drag. The morphological variable that is most directly related to drag is the caudal fin area (Webb 1983). Our respirometry experiments and our

morphological analysis indicate that the fish group with the highest total swimming costs was also the fish group with the smallest caudal fins. This suggests that the morphological difference we found between wild, farmed, and domesticated fish may have had a minor effect on the drag and consequently, on the total swimming costs.

The observed changes in body morphology, which may lead to lower swimming performance, seem to be caused by the removal of predation pressure and by artificial selection. Salmon from Sunndalsøra were developed for the Norwegian fish farm industry and have been bred selectively since 1971 for seven generations. This has generated genetic changes in traits like body depth and fin size (Fleming et al. 1994). The first three generations of artificial selection were only directed to a rapid growth based on body mass (Gjedrem et al. 1991). After four generations of selection the Sunndalsøra salmon grew 77% faster than wild salmon from the principal founder population (Gjedrem 2000). Artificial selection for increased body mass may have resulted in the deeper body depth of domesticated fish (Gjerde and Schaeffer 1989). The relaxed selection for swimming performance is believed to result in a loss of hydrodynamic body shape combined with artificial rearing which is known to generate a high level of fin nipping (Abbott and Dill 1985) and erosion (Bosakowski and Wagner 1994).

The lower swimming performance of domesticated JAS resulting in higher costs of habitat utilization may ultimately reduce survival rate. The increasing numbers of escaped domesticated fish may affect the gene pools of wild fish populations if interbreeding between wild and domesticated fish occurs.

Consequently, this would lead to a decrease in the natural production. These possible effects of behavioral and physiological changes should be considered when farmed JAS are intentionally released to rebuild wild populations or when domesticated JAS escape unintentionally from commercial fish farms. Salmon from the Norwegian National Breeding Program have been exported to Australia, Canada, Chile, Ireland, Scotland, and the USA. More than 50% of the Atlantic salmon in the world's commercial fish farm industry originate from this program (Fleming et al. 2000). Our study provides additional support for the suggestion that the invasion of escaped domesticated salmon in natural environments may not only increase the competition for natural resources, but also result in the change in the genetic structure of wild populations, which may lead to a fitness decrease of wild salmon populations through a decrease in swimming efficiency against turbulent flow.

6 A MODEL OF SWIMMING COSTS IN TURBULENT FLOW FOR JUVENILE ATLANTIC SALMON (*SALMO SALAR*)[4]

Abstract

Juvenile Atlantic salmon (*Salmo salar*; JAS) live in rivers characterized by highly turbulent flows. In these environments, flow turbulence is associated with a wide range of instantaneous flow velocities which may affect the energetic costs of habitat utilization of JAS. The purpose of our work was to develop a swimming costs model for JAS which especially accounts for the effects of velocity fluctuations in turbulent environments. We estimated the total swimming costs of fish in a respirometer in which we produced five turbulent flow conditions, each characterized by a mean and a standard deviation of flow. We used the variables mean flow velocity, standard deviation of flow velocity, turbulence intensity (standard deviation/mean flow velocity), and turbulent kinetic energy to analyze the effect of turbulence on total swimming costs. Respirometry experiments were conducted at water temperatures of 10, 15 and 20°C with fish ranging in size between 4.3 to 17.6 g at three mean flow velocities (18, 23, 40 $cm \cdot s^{-1}$) and three standard deviations of flow velocity (5, 8, 10 $cm \cdot s^{-1}$). Our results confirmed that total swimming costs increased with an increase of water temperature, body mass, mean flow velocity, and standard deviation of flow velocity (R^2=0.93). Water temperature, body mass, mean flow velocity, and standard deviation of flow velocity contributed respectively 2%, 31%, 46%, and 14% to the explained variation in total swimming costs.

[4] Enders, E.C., D. Boisclair & A.G. Roy. A model of swimming costs in turbulent flow for juvenile Atlantic salmon (*Salmo salar*). *Canadian Journal of Fisheries and Aquatic Sciences*. In preparation. Contribution to the program of CIRSA.

6.1 Introduction

Bioenergetics models may be applied to assess fish habitat quality and spatial distribution of fish (Fausch 1984; Van Winkle et al. 1998; Nislow et al. 2000). In a habitat with favorable growth conditions, fish obtain a positive balance between the energetic gains through food consumption, the energetic costs for metabolism, and the losses from excretion and egestion (Fausch 1984; Hill and Grossman 1993; Sabo et al. 1996). Increased growth may lead to fitness advantages with respect to foraging abilities, competitive capacities (Hill and Grossman 1993; Cutts et al. 1998), overwinter survival (Cunjak and Therrien 1998; Morgan et al. 2000), and age of first reproduction (Hutchings and Jones 1998; Morgan et al. 2002). However, the precision of the predictions of bioenergetics models depends on the reliability of the sub-models used to adequately represent the different components of fish energy budget, (Hansen et al. 1993; Ney 1993). With up to 40% of the energy budget, the activity metabolism may be the most important component (Brett and Groves 1979; Boisclair and Leggett 1989). Consequently, the precise quantification of the activity metabolism is of great interest to obtain appropriate predictions from bioenergetics models (Boisclair and Leggett 1989; Hansen et al. 1993; Ney 1993).

Estimation of the activity metabolism requires the description of the movements performed by the fish in their natural environment (i.e. number, duration, and speed of movements) and the quantification of the energetic costs of performing these movements. Generally, the energy expenditures associated with movements of stream-dwelling fish are estimated by models derived from respirometry experiments with fish swimming at a steady speed in a flume designed to minimize flow heterogeneity (Job 1955; Brett 1964; Beamish 1978). However, in their natural

environment, stream-dwelling fish are often confronted with a highly turbulent flow. Studies have shown that the sustained and critical swimming speed of fish decreased with an increase of turbulence intensity (standard deviation/mean flow velocity) indicating that the energy expenditures are higher in turbulent flow (Pavlov et al. 2000). Similarly, young-of-the-year brook charr (*Salvelinus fontinalis*) have been observed to profit from turbulence by the use of flow velocity refuges (McLaughlin and Noakes 1998). Liao et al. (2003) demonstrated that adult rainbow trout (*Oncorhynchus mykiss*) profit from the energy of vortices reducing their muscle activity. However, the turbulent flow in gravel-bed rivers consists not only of spatially explicit turbulent flow structures like vortices caused by the river bed roughness, but also of temporally fluctuating large-scale flow structures (Kirkbride and Ferguson 1995; Buffin-Bélanger et al. 2000a; Roy et al. 2004). Large-scale flow structures which extend over the entire water column may be seen as a temporal succession of quasi-periodic pulses of high- and low-speed fluid lasting several seconds (Roy and Buffin-Bélanger 2001; Roy et al. 2004). The high-speed pulses are generally directed towards the river bed whereas the low-speed pulses develop towards the water surface. Measurements of these turbulent flow structures suggest that the flow velocity can change 3- to 8-fold relative to the mean flow velocity within 1 to 5 s (Roy et al. 1999). These large-scale flow structures vary in length between 3- and 5-times the water depth, and in width between 0.5- and 1-times the water depth (Roy et al. 2004). In a preliminary study, we showed that the cost of swimming in such a temporal fluctuating flow may be 2- to 4-times the value predicted by steady swimming models (Enders et al. 2003). However, the estimations of the energetic cost of swimming under turbulent flow conditions were performed using only a single water temperature and fish body mass. In the present study we

conducted experiments under a wider range of water temperature, body mass, mean flow velocity and standard deviation of flow velocity. We described turbulence with the help of three different variables: the standard deviation of flow velocity (u_{SD}); the turbulence intensity (*TI*); and the turbulent kinetic energy (*TKE*). The turbulent kinetic energy represents the sum of the variances of the three-dimensional flow velocity components per unit volume.

The objectives of this study were (1) to evaluate the effect of water temperature, fish body mass, mean flow velocity and variables describing turbulence (standard deviation of flow velocity, turbulence intensity, and turbulent kinetic energy) on the energetic cost of swimming in fish, and (2) to develop swimming costs models for fish swimming under turbulent flow conditions.

6.2 Material and methods

We attained our objectives by performing respirometry experiments during which we subjected individual fish to turbulent flow conditions. Respirometry experiments were conducted at 10, 15, and 20°C to test the effect of water temperature on the total swimming costs of fish. We performed eight experiments per combination of flow condition and water temperature with variable fish size. We measured total swimming costs under four turbulent flow conditions - the combinations of two means (18 and 23 $cm \cdot s^{-1}$) and two standard deviations of the flow velocity (5 and 8 $cm \cdot s^{-1}$). At 15°C we conducted another series of eight experiments at a turbulent flow condition characterized by a mean flow velocity of 40 $cm \cdot s^{-1}$ and a standard deviation of flow velocity of 10 $cm \cdot s^{-1}$.

6.2.1 Fish

We evaluated the energetic cost of swimming in a turbulent flow using juvenile Atlantic salmon (age 1+; *Salmo salar* L.; JAS). JAS are particularly suitable for this study because their natural habitat comprises riffle sections in gravel-bed rivers which are characterized by a highly turbulent flow. JAS are drift feeders and undertake feeding motions from the river bed towards the water surface to capture drifting invertebrates (Kalleberg 1958). During these motions, JAS experience rapid changes in flow velocities and structure.

JAS were provided by the Pisciculture de Tadoussac (operated by the Société de la Faune et des Parcs du Québec, Canada). These fish are the offspring from the crossing of wild genitors originating from the Sainte-Marguerite River (Saguenay Region, Québec, Canada). The juveniles were transferred to the Université de Montréal where they were kept in 500 L 'Living Stream' aquaria (LSW 700, Frigid Units Inc., Toledo, Ohio, USA). Fish were adapted for a period of one month at the targeted water temperatures (10, 15, and 20°C) before starting a series of the experiments. Fish were fed daily with commercial food pellets (Corey Feed Mills Ltd., Fredericton, New-Brunswick). The fish mass used for our respirometry experiments ranged from 4.3 to 17.6 g wet.

6.2.2 Respirometry

The details of the experimental design and procedure we employed are described in Enders et al. (2003). They are only summarized here. The respirometer consisted of a Plexiglas® box which could be hermetically sealed. The respirometer contained two pumps (further referred to as pumps 1 and 2) and a bottle-shaped

swimming chamber. The narrow neck of the swimming chamber was connected to pump 1 (Jacobs Canada Inc., Mississauga, Ontario) that generated the turbulent flow in the swimming chamber. Pump 2 (Powerhead, Montréal, Québec) transferred water from the respirometer to an oxygen meter (Intab, Stenkullen, Sweden). The energetic cost of swimming against a turbulent flow was quantified by measuring the oxygen depletion over time with the oxygen meter (±0.005 mg $O_2 \cdot L^1$).

6.2.3 Turbulent flow structure

The turbulent flow within the swimming chamber was created by modulating the electric current that powered pump 1. The flow structure within the swimming chamber was quantified using an Acoustic Doppler Velocimeter (ADV, Sontek, San Diego, California, USA). The structure of the turbulent flow created by pump 1 was measured in the absence of the fish to avoid interference caused by its body and movements. The ADV allowed us to record the three orthogonal velocity components of the flow (streamwise, U; vertical, V; lateral, W) at a frequency of 25 Hz. The ADV also permitted us to define the settings of the components of the electric current that could create five different flow conditions (Table 6.1). The flow conditions are characterized by a selected combination of three mean streamwise flow velocities $\bar{u}$ (low flow velocity =18 $cm \cdot s^{-1}$; medium flow velocity =23 $cm \cdot s^{-1}$; high flow velocity =40 $cm \cdot s^{-1}$) and three standard deviations of the streamwise flow velocity u_{SD} (low turbulence = 5 $cm \cdot s^{-1}$; medium turbulence = 8 $cm \cdot s^{-1}$; high turbulence = 10 $cm \cdot s^{-1}$). The settings for the five turbulent flow conditions were selected because they are situated within the range of mean flow velocities (5 to 40 $cm \cdot s^{-1}$; DeGraaf and Bain 1986; Guay et al. 2000) and of standard deviations of flow

velocity (4 to 14 $cm \cdot s^{-1}$) observed at the focal point of the JAS under natural conditions (Enders et al., submitted to Journal of Fish Biology).

Table 6.1 Mean flow velocity ($cm \cdot s^{-1}$), standard deviation of the flow velocity ($cm \cdot s^{-1}$), minimum and maximum values ($cm \cdot s^{-1}$) measured for the streamwise U, vertical V, and lateral W velocity components at five different flow conditions, turbulence intensity (TI; standard deviation u_{SD}/mean velocity $\bar{u}$), and turbulent kinetic energy (TKE; $g \cdot cm^{-1} \cdot s^{-2}$).

Velocity component	Low velocity low turbulence	Low velocity medium turbulence	Medium velocity low turbulence	Medium velocity medium turbulence	High velocity high turbulence
$\bar{u}$	18.1	18.3	23.1	23.1	40.7
u_{SD}	5.1	8.2	5.1	8.0	10.3
u_{min}	3.6	0.5	5.0	0.7	2.5
u_{max}	34.6	39.7	35.2	43.7	76.6
$\bar{v}$	0.1	0.0	0.0	0.0	-2.1
v_{SD}	4.9	7.0	5.0	7.4	14.8
v_{min}	-21.9	-24.8	-22.9	-29.9	-74.7
v_{max}	21.9	23.7	21.5	29.8	51.0
$\bar{w}$	0.2	0.1	0.0	0.3	3.1
w_{SD}	5.5	7.6	5.5	7.5	12.4
w_{min}	-21.9	-26.0	-27.4	-28.2	-49.4
w_{max}	23.3	26.6	26.5	30.7	56.0
TI	0.27	0.44	0.22	0.34	0.25
TKE	66.8	139.4	68.8	143.6	416.2

The flow structure was recorded during 5 min at the beginning and the end of a suite of respirometry experiments at a given flow condition and a given water temperature. This strategy was adopted to verify the stability and repeatability of the flow structures created by our apparatus for given settings of the components of the electric current that powered pump 1. The stability of the four experimental flow conditions was tested using Student t-test. Such t-tests were performed to compare the mean streamwise flow velocities recorded before and after a suite of experimental observations. The repeatability of the turbulent flow structure was tested using a one-way analysis of variance (ANOVA) comparing the mean streamwise flow velocities of the suites of experimental observations at different

water temperatures. During this analysis, the velocity time series obtained before and after a suite of experimental observations were used as replicates. The stability and repeatability of the standard deviations of the streamwise flow velocities were tested using the Levene's test of the homogeneity of variance using the same procedure.

From each flow condition we obtained the mean and the standard deviations for the streamwise U, the vertical V, and the lateral W velocity components. We also calculate the turbulence intensity (TI; standard deviation u_{SD}/mean velocity $\bar{u}$) of the streamwise velocity component. Finally, as we obtained from the ADV three velocity components, we calculated the turbulent kinetic energy (TKE; $g \cdot cm^{-1} \cdot s^{-2}$) including all three velocity components

$$TKE = 1 / n \sum_{i=1}^{n} 0.5 \rho (u_i'^2 + v_i'^2 + w_i'^2) \quad (6.1)$$

where n is the number of instantaneous velocity fluctuations (7500 measurements per velocity time series), ρ is the water density ($g \cdot cm^{-3}$), u_i', v_i', and w_i' ($cm \cdot s^{-1}$) represent the instantaneous velocity fluctuations of the three flow velocity components.

6.2.4 Total swimming costs

A fish was selected at random from our stock of experimental fish, kept separately, and not fed for two days before the experiment to avoid increased metabolic rates due to digestion (Brett and Groves 1979). The fish was introduced into the swimming chamber 24 h before the beginning of the experiment to allow it to adapt to the experimental conditions. The initial oxygen concentration was measured at the beginning of the experiment and subsequently at every 30 min until

the end of an experiment. We monitored fish behavior during each experiment using a web cam (Sony Electronics Inc., Oradell, New Jersey, USA) to ensure that fish were continuously swimming. An experiment ended after 6 h for the low and medium flow velocity experiments and after 3 h for the high flow velocity experiments. No observation was made below 7.6 mg $O_2 \cdot L^{-1}$ to minimize the influence of low oxygen concentration on the fish behavior (Beamish 1978). At the end of an experiment the fish was removed from the respirometer, anaesthetized (clove oil; 0.6 mg$\cdot L^{-1}$), weighed (g wet), and measured (TL cm). The biological oxygen demand (BOD) was determined within 3 h of an experiment using the same procedure but without fish. We estimated the total oxygen consumption rate (sum of standard metabolic rate plus net swimming costs) of fish (Vo_2; mg $O_2 \cdot h^{-1}$) as

$$Vo_2 = \Delta O_2 / \Delta t \cdot V_W - BOD \tag{6.2}$$

where ΔO_2 is the difference in oxygen concentration between two consecutive oxygen concentration measurements (mg $O_2 \cdot L^{-1}$), and Δt is the time interval of 0.5 h between two consecutive oxygen concentration measurements, V_W (L) is the volume of water in the respirometer excluding the volume of our pumps and swimming chamber, and BOD is the biological oxygen demand by micro-organisms in the water (mg $O_2 \cdot h^{-1}$). As we measured oxygen concentration within the swimming chamber at 30 min intervals over 3 h or 6 h, we obtained 6 or 12 Vo_2 values per experiment, respectively. We then calculated the mean (further referred to as total swimming costs C_R; mg $O_2 \cdot h^{-1}$) of the Vo_2 values obtained for each experiment.

Prior to statistical analyses, the obtained total swimming costs and body mass were log transformed and the residuals were tested for normality using graphical probability plots, and for homogeneity of variance using Levene's test. To test the effect of water temperature, mean flow velocity and standard deviation of flow velocity, a three-way ANOVA was applied to the data set of total swimming costs estimated at four turbulence flow conditions (combinations of two mean flow velocities of 18 and 23 $cm \cdot s^{-1}$ and two standard deviations of flow velocity of 5 and 8 $cm \cdot s^{-1}$). During this analysis, water temperature, mean flow velocity, and standard deviation of flow velocity were used as independent variables. Body mass was used as a covariate.

The relationship between water temperature, body mass, mean flow velocity, and turbulence (alternately represented by standard deviation of flow velocity, turbulence intensity, or turbulent kinetic energy), and total swimming costs were developed using multiple regression analyses. In a first series we performed three stepwise multiple regression analyses. In the first analysis we used water temperature, body mass, mean flow velocity, and standard deviation of flow velocity as independent variables. We replaced the mean flow velocity and the standard deviation of flow velocity in the second analysis by the turbulence intensity and in a third analysis by the turbulent kinetic energy. A second series of three stepwise multiple regression analyses was completed using experiments from three flow conditions ($\bar{u}$ = 18 $cm \cdot s^{-1}$, u_{SD} =5 $cm \cdot s^{-1}$; $\bar{u}$ = 23 $cm \cdot s^{-1}$, u_{SD} =8 $cm \cdot s^{-1}$; $\bar{u}$ = 40 $cm \cdot s^{-1}$, u_{SD} =10 $cm \cdot s^{-1}$) conducted at 15℃ to develop swimming costs models that include higher flow velocities. We then used the same combination of variables employed in the first series of multiple regression analyses. Consequently, in the fourth analysis

body mass, mean flow velocity, and standard deviation of flow velocity were used as independent variables. In the fifth analysis we used body mass and turbulence intensity. In the last analysis we replaced turbulence intensity by turbulent kinetic energy.

6.3 Results

6.3.1 Turbulent flow structure

The five different flow conditions were characterized by the targeted means (18, 23, and 40 $cm \cdot s^{-1}$) and standard deviations (5, 8, and 10 $cm \cdot s^{-1}$) of the flow velocity (Table 6.1). The mean streamwise flow velocities ranged from 18.1 to 18.3 $cm \cdot s^{-1}$ for the low flow condition, was equal 23.1 $cm \cdot s^{-1}$ under medium flow condition, and equal to 40.7 $cm \cdot s^{-1}$ under high flow condition (Figure 6.1). The standard deviation of the streamwise flow velocity was 5.1 $cm \cdot s^{-1}$, 8.0 to 8.2 $cm \cdot s^{-1}$, and 10.3 $cm \cdot s^{-1}$ for the low, medium, and high turbulence condition, respectively. The means of the vertical and lateral flow velocities were close to 0 $cm \cdot s^{-1}$ and the standard deviation of the vertical and lateral flow velocity ranged from 4.9 to 14.8 $cm \cdot s^{-1}$. The turbulence intensity of the five different flow conditions varied between 0.22 and 0.44. Turbulent kinetic energy increased from 66.8 $g \cdot cm^{-1} \cdot s^{-2}$ under low velocity and low turbulence condition to 416.2 $g \cdot cm^{-1} \cdot s^{-2}$ under high velocity and high turbulence condition (Table 6.1).

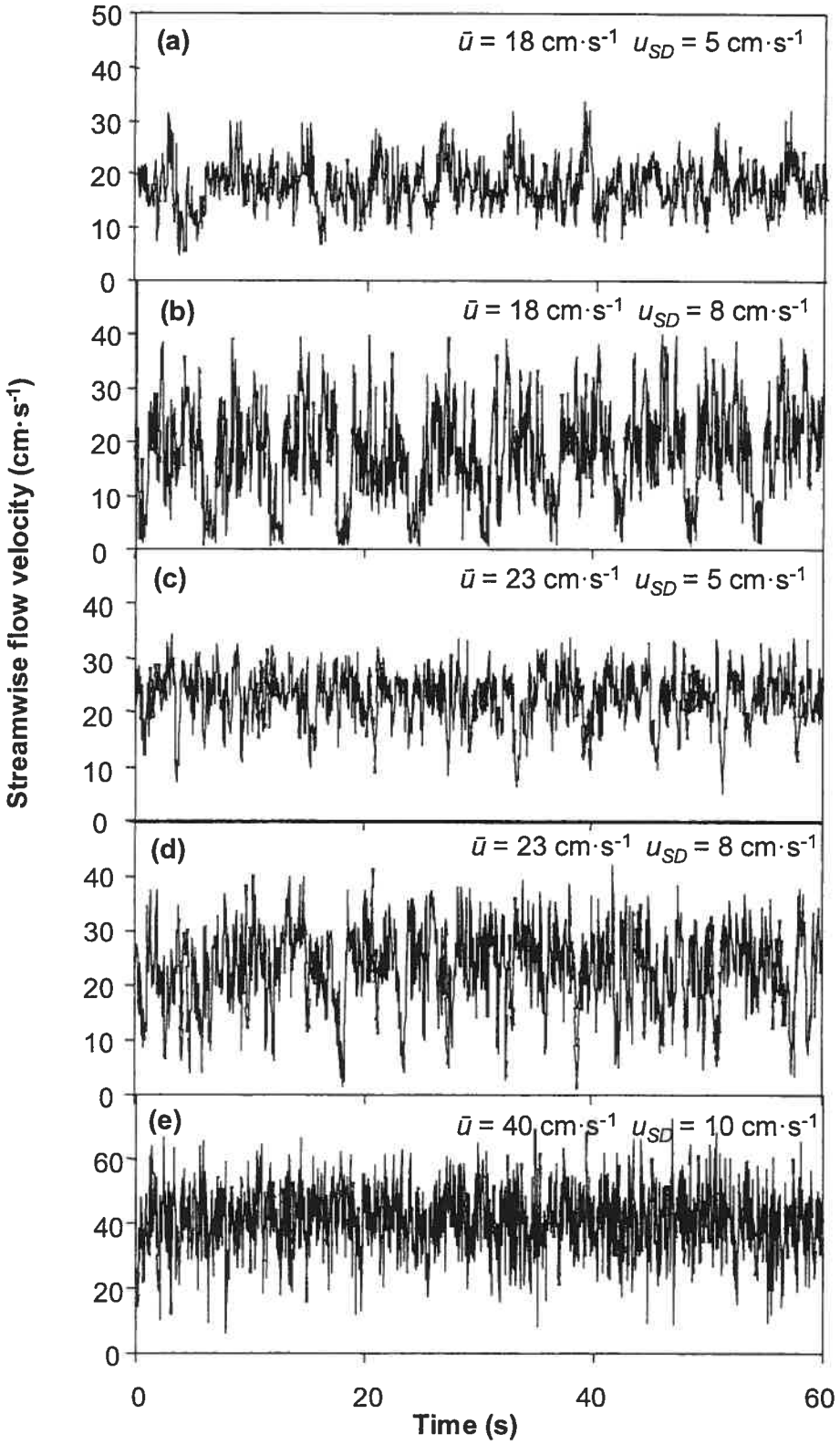

Figure 6.1 Velocity time series of 1 min (25 Hz) of the downstream flow velocity component (cm·s^{-1}) for the five different flow conditions in the swimming chamber in which juvenile Atlantic salmon swam during the respirometry experiments.

For any given flow condition, the mean streamwise flow velocity $\bar{u}$ and the standard deviation of streamwise flow velocity u_{SD} did not vary significantly among the two recordings performed before and after a suite of experimental observations (Stability test; $\bar{u}$: $0.42 < p < 0.98$, variation $= 0.0\text{-}0.3\%$; u_{SD}: $0.12 < p < 0.94$, variation $= 0.2\text{-}2.1\%$). Similarly, for the flow conditions used at different temperatures, the mean streamwise flow velocity $\bar{u}$ and the standard deviation of streamwise flow velocity u_{SD} obtained for the different suites of experimental observations did not vary significantly (Stability test; $\bar{u}$: $0.39 < p < 0.99$, variation $= 0.1\text{-}0.9\%$; u_{SD}: $0.17 < p < 0.69$, variation $= 0.1\text{-}2.3\%$). These results suggest that the flow structures created by our apparatus were stable and repeatable.

6.3.2 Total swimming costs

The total swimming costs varied 9.3-fold among our experiments, ranging from 1.6 mg $O_2 \cdot h^{-1}$ to 14.9 mg $O_2 \cdot h^{-1}$ (Table 6.2). As expected, we observed an increase in the total swimming costs with increasing water temperatures (Figure 6.2). At a given flow condition, the total swimming costs of a 10 g fish increased by 10.5% to 16.9% with an increase in water temperatures from 10 to 20°C. Similarly, at all flow conditions, we observed a positive relation between the total swimming costs and the body mass (Table 6.3). Under a given flow condition, a 15 g fish consumed twice the oxygen of a 5 g fish. The regression coefficients a ranged from -0.32 to 0.27 and the mass exponents b from 0.54 to 0.77 ($0.68 < r^2 < 0.97$; $p < 0.01$). We also observed an increase in the total swimming costs with mean flow velocity and standard deviation of flow velocity (Figure 6.3). The total swimming costs increased for a 10 g fish by 61.4% with an increase of the mean flow velocity from 18 to 23 $cm \cdot s^{-1}$ under low turbulent conditions, and by 52.9% under medium

turbulent conditions. With an increase of the standard deviation of the flow velocity from 5 to 8 $cm \cdot s^{-1}$, again for a 10 g fish, we observed an increase of the total swimming costs by 31.9% under low flow velocity and by 25.0% under medium flow velocities. The total swimming costs increased significantly with water temperature ($F_{2,83} = 17.55$; $p < 0.001$), with an augmentation of the mean flow velocity ($F_{1,83} = 650.62$; $p < 0.001$), and with an increase of the standard deviation of flow velocity ($F_{1,83} = 196.05$; $p < 0.001$). The interaction terms between temperature, mean flow velocity and standard deviation of flow velocity were not significant ($0.11 < p < 0.99$) indicating that the direction of the effects of water temperature, mean and standard deviation of flow velocity on the total swimming costs was similar among the different flow conditions.

Table 6.2 Number of respirometry experiments (n) per temperature and flow condition (selected combination of mean flow velocity $\bar{u}$ and standard deviation of the flow velocity u_{SD}), range of body mass (M) of fish used in the experiments and total swimming costs (C_R) measured in the corresponding turbulence flow condition.

n	Temperature (°C)	$\bar{u}$ ($cm \cdot s^{-1}$)	u_{SD} ($cm \cdot s^{-1}$)	M (g wet)	C_R ($mg\ O_2 \cdot h^{-1}$)
8	10	18	5	5.3 – 16.4	1.5 – 3.2
8	10	18	8	5.6 – 16.3	1.7 – 4.1
8	10	23	5	5.4 – 17.6	2.2 – 5.5
8	10	23	8	6.4 – 15.0	3.5 – 7.1
8	15	18	5	5.6 – 15.5	1.6 – 3.5
8	15	18	8	5.2 – 15.0	2.0 – 4.3
8	15	23	5	4.9 – 16.0	2.7 – 6.0
8	15	23	8	5.1 – 15.0	3.7 – 8.0
8	15	40	10	4.3 – 14.0	5.0 – 14.9
8	20	18	5	5.2 – 15.2	1.7 – 3.9
8	20	18	8	5.9 – 16.1	2.4 – 5.1
8	20	23	5	5.9 – 16.1	2.7 – 6.2
8	20	23	8	5.9 – 16.8	3.6 – 8.2

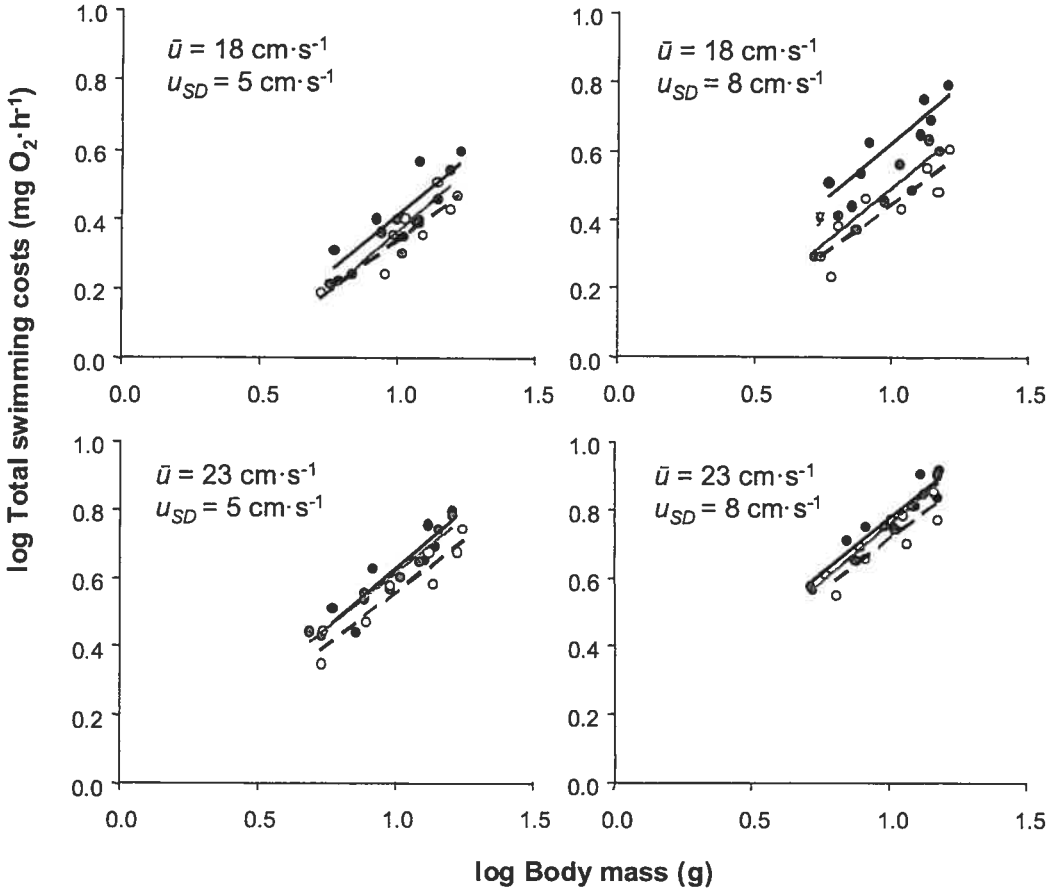

Figure 6.2 Total swimming costs of juvenile Atlantic salmon at four different flow conditions (combinations of two mean flow velocities $\bar{u}$ =18 and 23 cm·s^{-1} and two standard deviations u_{SD} =5 and 8 cm·s^{-1}) at 10°C (open symbols), 15°C (shaded symbols), and 20°C (solid symbols). Regression lines of the log linear relation between body mass and total swimming costs are presented.

Table 6.3 The total swimming costs (C_R) and the 95% confidence interval estimated for a 10 g fish under a given temperature and flow condition. Intercept a and regression coefficients b of the log linear relation between the body mass and the total swimming costs are given.

n	Temperature (°C)	$\bar{u}$ (cm·s^{-1})	u_{SD} (cm·s^{-1})	C_R (mg O$_2$·h^{-1})	95% C.I. (mg O$_2$·h^{-1})	a	b	r^2	p
8	10	18	5	2.2	[2.0 – 2.4]	-0.27	0.61	0.77	0.003
8	10	18	8	2.8	[2.5 – 3.2]	-0.15	0.60	0.76	0.003
8	10	23	5	3.6	[3.3 – 3.9]	-0.06	0.62	0.88	0.000
8	10	23	8	5.2	[4.7 – 5.7]	0.09	0.62	0.72	0.005
8	15	18	5	2.3	[2.1 – 2.5]	-0.32	0.69	0.82	0.001
8	15	18	8	3.1	[2-8 – 3.4]	-0.18	0.67	0.85	0.001
8	15	23	5	4.1	[3.9 – 4.4]	0.26	0.65	0.95	0.000
8	15	23	8	5.7	[5.5 – 5.9]	0.07	0.68	0.97	0.000
8	15	40	10	10.8	[9.4 – 12.5]	0.27	0.77	0.84	0.001
8	20	18	5	2.6	[2.2 – 3.0]	-0.25	0.66	0.68	0.007
8	20	18	8	3.4	[3.1 – 3.8]	-0.01	0.54	0.78	0.002
8	20	23	5	4.2	[3.7 – 4.7]	-0.06	0.68	0.79	0.002
8	20	23	8	5.9	[5.4 – 6.5]	0.13	0.64	0.84	0.001

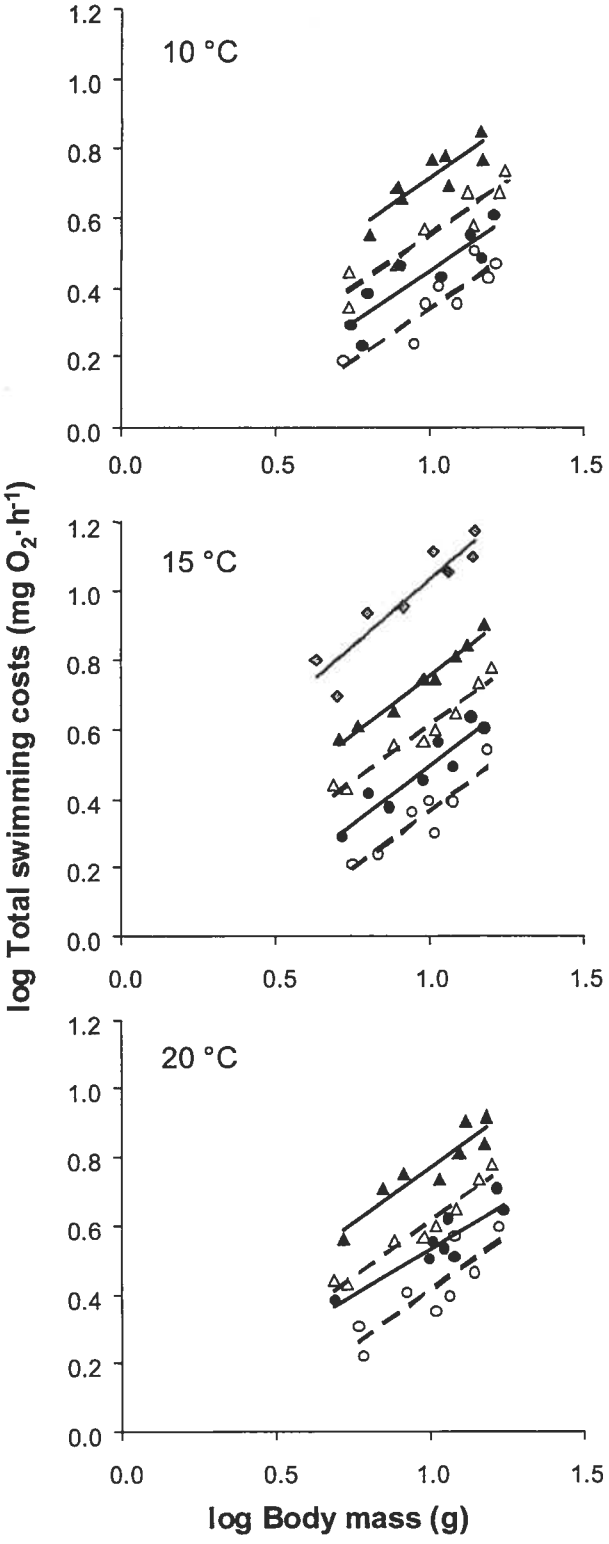

Figure 6.3 Total swimming costs of juvenile Atlantic salmon under low flow velocities (circle), medium flow velocities (triangle), and high flow velocities (rhombus) at water temperatures of 10, 15, and 20°C. The open symbols represent the low turbulence condition, the solid symbols the medium turbulence condition, and the shaded symbols the high turbulence condition. Regression lines of the log linear relation between body mass and total swimming costs are presented.

The results of our experiments allowed us to develop a relationship between water temperature, body mass, mean flow velocity, standard deviation of flow velocity, and total swimming costs (Table 6.4). The four variables explained a total of 93.4% of the variability in the total swimming costs ($F_{4,91} = 337.37$, $p < 0.001$). Water temperature explained 2%, body mass 31%, mean flow velocity 46%, and standard deviation of the flow velocity 14% of the variation in total swimming costs. In our second analysis turbulence intensity was not significantly correlated to total swimming costs. As a result, no model considering the turbulence intensity was developed. A three-variable model ($F_{3,92} = 29.41$, $p < 0.001$) using water temperature, body mass, and turbulent kinetic energy explained 49% of the variation in total swimming costs where water temperature explained 3%, body mass 31%, and turbulent kinetic energy 16% of the variation in total swimming costs.

The second series of multiple regression analyses were performed with a wider range of flow velocity at a constant water temperature of 15°C. The aim of this series of analyses was to develop models which predict total swimming costs under a wider range of mean flow velocities and standard deviations of flow velocity. A three-variable model was developed ($F_{3,20} = 317.63$, $R^2 = 0.98$, $p < 0.001$) where body mass, mean flow velocity, and standard deviation of flow velocity contributed, respectively, to 11%, 18%, and 69% of the variation in total swimming costs. We again observed no correlation between the turbulence intensity and the total swimming costs. However, body mass and turbulent kinetic energy increased to total swimming costs, resulting in a two-variable model ($F_{2,21} = 184.81$, $R^2 = 0.94$, $p <$

0.001) with body mass contributing 11% and turbulent kinetic energy 84% of the variation in total swimming costs.

Table 6.4 Four multiple regression models to estimate the total swimming costs (C_R; mg $O_2 \cdot h^{-1}$) in turbulent flow for juvenile Atlantic salmon using water temperature (°C), body mass (M; g wet), mean flow velocity ($\bar{u}$; $cm \cdot s^{-1}$), standard deviation of the flow velocity (u_{SD}; cm), and turbulent kinetic energy (TKE; $g \cdot cm \cdot s^{-2}$), as explanatory variables.

Turbulent swimming models	Contribution of variable					Model statistics		
	T	M	$\bar{u}$	u_{SD}	TKE	n	R^2	p
$\log C_R = 0.23 \log T + 0.64 \log M + 2.43 \log \bar{u} + 0.67 \log u_{SD} - 4.06$	0.02	0.31	0.46	0.14		96	0.93	<0.001
$\log C_R = 0.23 \log T + 0.64 \log M + 1.52 \log TKE - 4.06$	0.03	0.31			0.16	96	0.49	<0.001
At 15°C:								
$\log C_R = 0.72 \log M + 0.41 \log \bar{u} + 1.75 \log u_{SD} - 2.11$		0.11	0.18	0.69		24	0.98	<0.001
$\log C_R = 0.73 \log M + 0.87 \log TKE - 2.31$		0.11			0.83	24	0.94	<0.001

6.4 Discussion

Our analyses demonstrated that total swimming costs of JAS swimming in turbulent flow increased with water temperature, body weight, mean flow velocity, and standard deviation of flow velocity. With an increase of water temperature from 10°C to 20°C, total swimming costs of a 10 g JAS increased by 9.6% to 21.1% depending on the flow condition. Similarly, an increase in body mass from 5 g to 15 g led to an increase in the total swimming costs by a factor of 1.5 to 3.2. Our study further indicated that total swimming costs of JAS swimming in a turbulent flow increase as both mean flow velocity and standard deviation of the flow velocity increase. Total swimming costs increased by an average of 61.5% as mean flow velocity increased from 18 $cm \cdot s^{-1}$ to 23 $cm \cdot s^{-1}$. The effect of mean flow velocity on fish total swimming costs is incorporated in all swimming cost models currently available (Beamish 1978; Boisclair and Tang 1993; Tang et al. 2000). Our findings indicate that the energetic cost of swimming at a given mean flow velocity increased on average by 29.8% with an increase in the standard deviation of the flow velocity

from 5 $cm \cdot s^{-1}$ to 8 $cm \cdot s^{-1}$. Our work therefore indicates that not only mean flow velocity but also standard deviation of the flow velocity is required to adequately estimate the cost of swimming under turbulent conditions. The standard deviation of the flow velocity explained 14% of the variability in total swimming costs.

We suggest that estimates from commonly used forced swimming models may underestimate the actual total swimming costs of stream-dwelling fish. Because the forced swimming models are derived from experiments with minimized flow heterogeneity, they do not account for the increase in total swimming costs due to turbulence. In order to compare our observed values of total swimming costs with the predictions of the forced swimming model of Boisclair and Tang (1993), developed to estimate net swimming costs, we would have had to subtract the standard metabolic rate from the observed total swimming costs. In the absence of an appropriate model of standard metabolic rate of JAS at given water temperatures and body masses, we decided to develop a new forced swimming costs model from the data set of Boisclair and Tang (1993) with the total swimming costs as the dependent variable instead of the net swimming costs. Also, we added the water temperature as an independent variable which gave us the following model

$$\log_{10} C_{forced} = 0.67 \log_{10} T + 0.96 \log_{10} M + 0.23 \log_{10} \bar{u} - 1.85 \quad (6.3)$$

where C_{forced} is the total swimming costs under minimized flow heterogeneity (mg $O_2 \cdot h^{-1}$), T is the water temperature (°C), M is the fish body mass (g wet), and $\bar{u}$ is the mean flow velocity ($cm \cdot s^{-1}$). Although all variables were significant, body mass explained most (79%) of the variation in the total swimming costs ($F_{3,114} = 162.35$,

$R^2 = 0.81$, $p < 0.0001$). The model predicted total swimming costs of a 10 g fish swimming in minimized flow heterogeneity at a water temperature of 15°C and a swimming speed of 18 and 23 $cm \cdot s^{-1}$ should be 1.50 mg $O_2 \cdot h^{-1}$ and 1.58 mg $O_2 \cdot h^{-1}$, respectively. Under low turbulence conditions, the total swimming costs we estimated for 10 g JAS at 15°C were 2.0- to 2.7-times higher than predicted by the forced swimming model. The differences were more pronounced under medium turbulence conditions, ranging from 3.0- to 3.6-fold.

The increase in the actual total swimming costs under turbulent condition above those predicted by the forced swimming model corresponds to the assumption that unsteady swimming movements, such as changes in speed and active accelerations and decelerations, are energetically more costly than steady swimming movements at constant speed and direction (Webb 1983; Boisclair and Tang 1993; Kramer and McLaughlin 2001). In turbulent flow, fish have to adjust to the fluctuations in velocity and direction of flow by constantly moving their fins to maintain their position. These movements substantially increase the energetic costs of unsteady swimming above those of steady swimming for the same average swimming speed (Gauthier 1998; Tang et al. 2000).

Studies on several fish species have shown that turbulence intensity affects the performance of swimming. For example, roach (*Rutilus rutilus*) decreased their critical swimming speed by 44% in response to an increase in turbulence intensity of 0.05 (Pavlov et al. 2000). The authors suggested that the observed diminution of swimming performance resulted from an increase in swimming costs. Similarly, McLaughlin and Noakes (1998) observed an increase in tail beat frequency and

amplitude due to increased temporal and spatial heterogeneity of flow, suggesting an increase in swimming costs. Our works supports these suggestions showing that JAS experience an increase in swimming costs with increasing flow fluctuations. Flow velocity fluctuations are observed in salmon freshwater habitats like gravel-bed rivers. They are defined as large-scale flow structures. These large-scale flow structures are intermittent fluids of high velocity divided by fluids of low velocity. Measurements of these large-scale flow structures showed that the instantaneous velocities can change 3- to 8-fold relative to the mean velocity within seconds (Roy et al. 1999). The spatial length of these large-scale flow structures may vary between 3- and 5-times the water depth being relatively long against the width of 0.5- to 1-fold the water depth (Roy et al. 2004). The average frequency of occurrence of large-scale flow structures was nine events per minute and their duration lasted up to 5 s. Because of their size and duration, large-scale flow structures are likely to affect the swimming costs of JAS exposed to these fluctuations, as we demonstrated in our laboratory study.

In gravel-bed rivers, we also observe a variety of spatial flow structures such as vortices which are generated by the roughness of the river bed. Protruding obstacles like the 'home rocks' of JAS used as station holding positions during active foraging cause the formation of vortex shedding motions at the lee side of obstacles. Liao et al. (2003) demonstrated that adult rainbow trout may profit from the energy of vortices in a laboratory study. Fish changed their swimming patterns to slalom between the vortices resulting in a reduction of the axial muscle activity. Similarly, it has been suggested that adult sockeye salmon exploit recirculation zones during upriver spawning migration to minimize the energy expenditures (Hinch and Rand

1998; Standen et al. 2002). It is also known that schooling fish profit from the vortices generated by the leading fish (Vogel 1994). Sea bass (*Dicentrarchus labrax*) swimming at speed of 15 to 32 $cm \cdot s^{-1}$ in front of the fish school had a 9 to 14% higher tail beat frequency than the fish swimming in the rear (Herskin and Steffensen 1998). This behavior resulted in decrease of the total swimming costs of 9 to 23%.

The models of total swimming costs in turbulent flow presented in this study may be applied to estimate the energy expenditures that JAS would experience in situations where they swim against turbulent flow. These situations may include foraging attempts in the water column to capture drifting food particles or migrations between different habitats (e.g. changes between summer and winter habitat). The model may also be applied to non-territorial individuals that inhabit the spaces between territories (Martel 1996). Their foraging strategy differs from the commonly described station holding behavior of JAS. Non-territorial fish may minimize their energy expenditure related to territorial defense, but they may do so at the expense of increased swimming costs due to exposure to large-scale flow structures. It is anticipated that in situations where territorial JAS use home rocks in their typical sit-and-wait position near the substrate, no increase in the metabolic costs due to activity occurs (Facey and Grossman 1990). Similarly, in situations where JAS seek shelter in the interstices of the river bed substrate, especially during low water temperature, no increase in the swimming costs are anticipated (Cunjak 1988; Bremset 2000).

Bioenergetics models aiming to estimate the energetic costs of habitat utilization by stream-dwelling fish in turbulent environments may require both a description of the behavior of the fish in relation to turbulence, and swimming costs

models in which the effects of the flow turbulence are explicitly represented. We conclude that models using the mean and the standard deviation of flow velocity may provide estimates of the costs of the habitat utilization for stream-dwelling fish that are more accurate than the commonly used forced swimming models. Comprehension of the effects of turbulence on swimming costs may also be relevant to models developed for habitat restoration and management (Boisclair 2001) and to the design of migratory fish passages (Odeh et al. 2002; Guiny et al. 2003).

7 CONCLUSION GÉNÉRALE

Des questions intéressantes émergent des relations entre la biologie des poissons et la dynamique des fluides. Ces questions concernent l'adaptation du comportement des poissons à la structure de l'écoulement et l'influence de la turbulence sur le métabolisme d'activité des poissons. Dans cette thèse, nous avions comme objectifs spécifiques d'examiner l'ajustement du comportement des juvéniles du saumon atlantique aux structures turbulentes de l'écoulement en rivière à lit de gravier et d'analyser l'effet de la turbulence sur les coûts énergétiques de nage en laboratoire. Les résultats présentés dans cette thèse offrent des avenues de réponse à trois questions spécifiques : 1) le comportement des juvéniles du saumon atlantique varie-t-il en fonction des structures turbulentes à grande échelle ? 2) les coûts énergétiques de nage changent-ils en fonction de la température de l'eau, de la masse du poisson, de la vitesse et de l'intensité de la turbulence de l'écoulement ? et 3) le modèle de coûts énergétiques de nage obtenu à partir des poissons élevés en pisciculture s'applique-t-il à des poissons sauvages ?

7.1 Les coûts énergétiques de l'activité des juvéniles du saumon atlantique dans un écoulement turbulent

Les connaissances sur le comportement des poissons en nature ainsi que les coûts énergétiques de nage reliés à ce comportement sont des composantes essentielles de la modélisation bioénergétique. Certains aspects du comportement des poissons, en relation avec la turbulence de l'écoulement, sont déjà connus. En effet, la vitesse maximale de nage diminue avec une augmentation de l'intensité turbulente (écart-type/moyenne de vitesse) de l'écoulement (Pavlov et al. 2000). Il semble que

les poissons puissent utiliser les vortex présents dans un écoulement turbulent (Liao et al. 2003). Cependant, nous avons identifié une lacune dans les connaissances sur les interactions entre le comportement des poissons et les structures turbulentes à grande échelle qu'on retrouve dans l'écoulement des rivières à lit de gravier. De cette lacune découle en grande partie la supposition que l'on peut estimer les coûts énergétiques de nage des poissons de rivière à partir de la vitesse moyenne de l'écoulement. C'est le cas du modèle de nage forcée qui est fréquemment utilisé pour estimer les coûts énergétiques de nage des poissons de rivière. Il existe en ce moment peu de données qui permettent d'affirmer si ces modèles prédisent adéquatement les coûts énergétiques de nage dans un écoulement turbulent. Nous avons voulu vérifier si l'utilisation de la vitesse moyenne dans un modèle de nage forcée était adéquate pour estimer les coûts énergétiques de nage des poissons en rivière. Pour ce faire, nous devions améliorer nos connaissances sur l'ensemble des interactions entre, d'une part, la turbulence et le comportement du poisson et d'autre part, la turbulence et la physiologie du poisson.

Dans cette recherche, l'approche préconisée était double puisqu'elle visait non seulement à observer le comportement des poissons en milieu naturel mais aussi à estimer les coûts énergétiques de nage dans un écoulement turbulent en laboratoire. Cette approche a mené à un avancement important dans nos connaissances sur le métabolisme d'activité des juvéniles du saumon atlantique en fonction de la structure turbulente de l'écoulement. Les principaux résultats ont été résumés dans chacun des chapitres.

Au troisième chapitre, nous avons décrit en détail le comportement alimentaire des juvéniles du saumon atlantique dans un écoulement turbulent en rivière à lit de gravier. On retrouve des structures turbulentes à grande échelle dans ce type de rivière. Nous avons vérifié si la présence de ces structures entraîne une adaptation des poissons lors de leurs déplacements alimentaires. Dans cette perspective, nous avons analysé le comportement des juvéniles du saumon atlantique en relation avec la variabilité temporelle de l'écoulement en rivière. Nous avons proposé une nouvelle technique permettant de mesurer simultanément le comportement des poissons et la vitesse de l'écoulement. Nos observations ont montré que le comportement des juvéniles du saumon atlantique varie en fonction des caractéristiques de l'écoulement turbulent. Les poissons sont moins actifs et entreprennent moins de mouvements de longue distance quand l'intensité de la turbulence de l'écoulement augmente. De plus, la proportion de temps accordée à l'activité diminue avec une augmentation de la vitesse moyenne et de l'intensité de la turbulence. Cependant, les juvéniles du saumon atlantique ne semblent pas préférer les plus lentes structures turbulentes à grande échelle pour initier leurs mouvements, ce qui aurait pu être avantageux sur le plan énergétique. Les structures turbulentes à grande échelle sont en réalité des séquences de pulsations accompagnées d'accélération ou décélération marquées qui occupent toute la colonne d'eau. Ces structures peuvent durer jusqu'à cinq secondes (Roy et al. 2004). Nous n'avons pu mettre en évidence un lien direct entre l'amorce des mouvements alimentaires et les périodes de faibles vitesses d'écoulement, un comportement qui entraînerait une diminution des coûts énergétiques lies à l'activité. Nos simulations indiquent clairement que si les juvéniles du saumon atlantique profitaient des périodes de faible vitesse pour amorcer leurs mouvements, ils minimiseraient leurs coûts énergétiques

de nage de 20% lors des conditions de faible turbulence et de 31% lors des conditions de forte turbulence. L'absence de lien direct peut s'expliquer d'une part par la possibilité que la disponibilité de nourriture, sous forme de dérive, ait une influence sur l'initiation des déplacements alimentaires. Toujours à la recherche de gains énergétiques, les juvéniles du saumon atlantique pourraient initier un mouvement d'attaque alimentaire lors de période de forte vitesse d'écoulement lorsque le potentiel énergétique de la proie semble surpasser les coûts énergétiques liés à cette attaque. Dans un compromis entre les coûts et les gains énergétiques reliés au déplacement, il pourrait donc être avantageux pour les juvéniles du saumon atlantique de se déplacer pour attraper une particule même à une forte vitesse d'écoulement. D'autre part, l'absence de lien pourrait être causée par l'utilisation d'un modèle simplifié des structures turbulentes à grande échelle. En effet, classer l'écoulement en rivière en deux grand types de structures turbulentes ne permet peut-être pas de dégager l'influence du champ de vitesse sur le comportement du poisson. Conséquemment, nous n'avons pas pu isoler les variables de l'écoulement qui agissent comme déclencheurs de l'initiation des déplacements des juvéniles du saumon atlantique. Cette supposition se base sur des travaux récents qui ont montré que les structures turbulentes à grande échelle peuvent être très complexes et variables (Roy et al. 2004).

Nous avons ensuite estimé les coûts énergétiques de nage dans un écoulement turbulent (chapitre 4). Ces estimations ont été réalisées grâce à des expériences en laboratoire. Nous avons ainsi pu examiner l'effet de quatre conditions turbulentes sur les coûts énergétiques de nage. Le protocole expérimental a été conçu de façon à pouvoir étudier individuellement les effets de la vitesse moyenne et de l'écart type de

la vitesse de l'écoulement turbulent. Il est difficile d'isoler ces deux variables en nature. La première série d'expériences a été réalisée à une température de l'eau de 15℃ avec des poissons d'une masse de 10 g dans un écoulement turbulent en utilisant deux moyennes (18 $cm \cdot s^{-1}$ et 23 $cm \cdot s^{-1}$) et deux écart types de la vitesse de l'écoulement (5 $cm \cdot s^{-1}$ et 8 $cm \cdot s^{-1}$). Nos résultats ont confirmé que les coûts énergétiques de nage sont affectés par l'intensité de la turbulence. Il en ressort que pour une vitesse moyenne constante, les coûts énergétiques de nage ont augmenté par un facteur de 1.3 à 1.6 lorsque écart type passe de 5 à 8 $cm \cdot s^{-1}$. Les modèles de nage forcée sous-estiment les coûts réels de nage en écoulement turbulent par un facteur de 1.9 à 4.2, ce qui est considérable. Par ailleurs, les modèles de nage spontanée surestiment les coûts réels de nage par un facteur de 2.8 à 6.6. Ainsi, nous proposons que de nouveaux modèles où figurent de façon explicite la moyenne et l'écart type de la vitesse de l'écoulement sont requis pour estimer les coûts énergétiques de nage contre un écoulement turbulent.

Au cinquième chapitre, nous avons tenté de vérifier si nous pouvions utiliser les résultats obtenus en laboratoire avec des poissons élevés en pisciculture pour prédire les coûts énergétiques de nage des juvéniles sauvages. Dans cette perspective, nous avons mesuré les coûts énergétiques de nage des juvéniles du saumon atlantique évoluant dans deux conditions turbulentes différentes (une vitesse moyenne de 23 $cm \cdot s^{-1}$ et deux écart types de la vitesse de 5 $cm \cdot s^{-1}$ et 8 $cm \cdot s^{-1}$). Les expériences ont été effectuées avec des saumons sauvages, des saumons piscicoles de première génération et des saumons domestiques de septième génération. Les résultats confirment les conclusions obtenues au chapitre 3 et montrent que les coûts énergétiques varient selon l'intensité de la turbulence. Ainsi, pour une même vitesse

moyenne de l'écoulement, les poissons dépensent 1.4 fois plus d'énergie lorsque la turbulence augmente. Les coûts énergétiques de nage des juvéniles piscicoles sont similaires à ceux obtenus en utilisant des juvéniles sauvages. Les modèles des coûts énergétiques de nage développés pour les saumons piscicoles de première génération peuvent donc être utilisés pour estimer adéquatement les coûts énergétiques de nage des poissons sauvages. Cependant, les saumons domestiques diffèrent dans leur métabolisme d'activité des saumons sauvages et des saumons piscicoles de la première génération. Ces derniers ont des coûts énergétiques de nage de 15.2 à 29.2% plus élevés que les saumons sauvages et de 12.5 à 16.2% plus élevés que les saumons piscicoles. Plusieurs facteurs peuvent expliquer ces différences : l'entraînement des poissons, la composition corporelle, le taux de métabolisme standard et la morphométrie. Nous n'avons pu déterminer de manière définitive le rôle respectif de chacun de ces facteurs.

Finalement, nous avons présenté au sixième chapitre des expériences de quantification des coûts énergétiques de nage en relation avec d'autres variables comme la température, la masse corporelle, la vitesse moyenne et l'écart type de la vitesse. Ces expériences ont été effectuées dans le but de développer un modèle complet de coûts énergétiques de nage. Les expériences nous ont permis de formuler un modèle décrivant l'effet de la température, de la masse corporelle, de la vitesse moyenne et de l'écart type de la vitesse sur les coûts énergétiques de nage dans un écoulement turbulent. La température, la masse corporelle, la vitesse moyenne et l'écart type de la vitesse expliquent respectivement 2%, 31%, 46% et 14% de la variabilité des coûts énergétiques de nage. Les coûts énergétiques de nage

augmentent lorsque la température, la masse corporelle, la vitesse moyenne et l'écart type de la vitesse augmentent.

7.2 Originalité de la thèse

Nous nous sommes basés sur des travaux récents portant sur la connaissance en dynamique des fluides, notamment la caractérisation de la variabilité temporelle de l'écoulement turbulent en rivière (Buffin-Bélanger 2001; Roy et Buffin-Bélanger 2001; Roy et al. 2004), pour soulever des questions nouvelles concernant l'interaction entre les structures turbulentes à grande échelle et le comportement des poissons. L'intégration de la dynamique des fluides dans l'étude de l'écologie des poissons est prometteuse pour notre compréhension des liens entre le comportement et l'environnement dynamique des poissons. Cette voie semble attirer de plus en plus l'attention des chercheurs (Pavlov et al. 2000; Kemp et al. 2003; Liao et al. 2003).

Les études précédentes qui analysaient les liens entre la turbulence et la biologie se concentraient surtout sur l'effet de la turbulence sur la distribution des macroinvertébrés (Bouckaert et Davis 1998; Rempel et al. 2000). L'avantage de travailler sur les macroinvertébrés est que la plupart d'entre-eux sont relativement sédentaires, ce qui facilite la mesure de la vitesse de l'écoulement à l'endroit où l'organisme vit. À l'opposé, la difficulté de travailler avec des juvéniles du saumon atlantique réside dans le fait qu'ils se déplacent fréquemment et qu'il devient plus difficile de mesurer la vitesse d'écoulement à l'endroit précis où les juvéniles se trouvent. Il a donc été nécessaire de développer un nouveau protocole expérimental pour caractériser et quantifier simultanément la turbulence et le comportement des poissons en rivière. Ce protocole expérimental représente une des premières approches d'analyse de la relation entre la variabilité temporelle de l'écoulement et

le comportement des poissons lors de l'initiation du mouvement pour s'alimenter. L'échantillonnage à une haute résolution temporelle (20 et 25 Hz) de la vitesse d'écoulement jumelé à l'observation simultanée du comportement des poissons par enregistrement vidéo nous a permis d'analyser les vitesses instantanées au moment de l'initiation des mouvements des poissons (Chapitre 3).

Généralement, les coûts énergétiques de nage sont estimés à partir d'expériences dans lesquelles les poissons doivent nager contre un écoulement unidirectionnel à vitesse constante. Afin d'analyser l'effet de la turbulence sur les coûts énergétiques de nage, nous avons mis en place un protocole nouveau permettant de mesurer en laboratoire les coûts énergétiques de nage dans un écoulement turbulent. La création, inspirée des structures turbulentes à grande échelle du milieu naturel, d'un écoulement turbulent artificiel à l'intérieur d'un respiromètre nous a permis de mesurer les coûts énergétiques de nage des juvéniles du saumon atlantique dans des conditions similaires à celles de l'environnement naturel (Chapitre 4 à 6). La mise en œuvre de telles expériences respirométriques a rarement, sinon jamais été réalisée. Les expériences respirométriques nous ont permis non-seulement de quantifier les coûts énergétiques de nage dans un écoulement turbulent mais aussi d'isoler l'effet de la turbulence et de la vitesse moyenne sur les coûts énergétiques de nage. Nous avons également validé l'utilisation des poissons provenant de la pisciculture dans ces expériences. Les coûts énergétiques ne diffèrent pas significativement entre les poissons sauvages et les poissons piscicoles. Il est donc possible d'appliquer le modèle que nous avons développé à partir des connaissances acquises dans les chapitres précédents afin

d'estimer les coûts énergétiques de nage en écoulement turbulent des poissons sauvages.

7.3 Généralisation et application des résultats

Nous avons observé que la turbulence exerce un effet sur le comportement et sur les coûts énergétiques de nage des juvéniles du saumon atlantique en milieu naturel. La turbulence pourrait probablement avoir des effets sur le comportement et les coûts énergétiques de nage chez d'autres espèces de poisson vivant en rivière. Différents auteurs ont déjà souligné ces effets. Premièrement, pour une multitude d'espèces de poisson, notamment pour le gardon (*Rutilus rutilus*), le goujon (*Gobio gobio*), le meunier (*Leuciscus cephalus*), la perche (*Perca fluviatilis*), l'ombre (*Thymallus thymallus*) et le carassin (*Carassius carassius*), une augmentation de l'intensité turbulente a mené à une diminution de la vitesse de nage (Pavlov et al. 2000). Les auteurs ont proposé que la nage dans un écoulement turbulent mène à une augmentation des coûts énergétiques de nage, ce qui conduit à son tour à une diminution de la performance de nage. Deuxièmement, les juvéniles de l'omble de fontaine augmentent la fréquence et l'amplitude de leurs coups de queue lors d'une augmentation de l'hétérogénéité temporelle et spatiale de l'écoulement (McLaughlin et Noakes 1998). Les auteurs soupçonnent que ces résultats démontrent une augmentation des coûts énergétiques de nage lorsque la turbulence augmente. Troisièmement, les neuromastes sont une caractéristique universelle chez les poissons. Les neuromastes permettent aux poissons de ressentir les fluctuations de la vitesse de l'écoulement ambiant. La plupart des espèces de poisson devraient donc avoir la capacité de réagir à la turbulence de l'écoulement (Montgomery et al. 2002).

Cependant, il faut être prudent avant de généraliser tous les résultats de l'étude; aussi, nous désirons souligner ses limites. Les modèles développés à l'aide de la régression multiple afin d'estimer les coûts énergétiques de nage dans un écoulement turbulent devraient uniquement être appliqués en respectant les limites des variables auxquelles les poissons ont été confrontés. Ensuite, on ne devrait pas utiliser les paramètres du modèle pour estimer les coûts énergétiques de nage pour d'autres espèces. Finalement, il reste la question des circonstances où on peut appliquer le modèle. Celui-ci estime les coûts énergétiques de nage libre dans un écoulement turbulent. Or, la nage libre dans un écoulement turbulent ne représente qu'une portion de l'activité des juvéniles du saumon atlantique. Lorsque les juvéniles du saumon atlantique se cachent dans les interstices ou se placent au-dessus de leur roche-mère, on soupçonne qu'ils ne présentent pas d'augmentation du taux métabolique relié à l'activité (Facey et Grossman 1992). De plus, nous pensons que les juvéniles du saumon atlantique utilisent les zones de recirculation situées derrière leur roche-mère lorsqu'ils retournent, suite à un déplacement alimentaire, en position d'attente ; ceci diminuerait les coûts énergétiques de nage. Notre modèle s'applique cependant aux phases d'attaque des déplacements alimentaires, aux individus non territoriaux qui nagent librement dans l'écoulement et aux migrations entre les habitats estivaux et hivernaux. Nous avons décrit la proportion de temps que les juvéniles du saumon atlantique allouent à leur activité alimentaire estivale pendant le jour (chapitre 1). Cependant, le comportement des juvéniles du saumon atlantique varie selon une échelle journalière et saisonnière. Il sera donc nécessaire de développer un modèle qui décrit le patron d'activité des juvéniles du saumon atlantique afin d'estimer le temps que les juvéniles accordent à la nage contre un écoulement turbulent.

Ensuite, bien que le lien entre les coûts énergétiques de nage et la condition turbulente ait été montré, il n'en demeure pas moins que la majeure partie des données de cette thèse ont été recueillies dans les conditions artificielles du laboratoire. Il pourrait être délicat de transférer directement le modèle à des milieux naturels. Il serait subséquemment fort pertinent de valider l'effet des caractéristiques de l'écoulement turbulent sur les coûts énergétiques de nage décrits dans cette thèse en milieu naturel grâce aux méthodes de la télémétrie physiologique (éléctromyographie ou éléctrocardiographie).

Les résultats présentés dans cette thèse dépassent l'intérêt fondamental de la caractérisation du métabolisme d'activité des poissons dans un écoulement turbulent. En effet, nous proposons des interprétations nouvelles liées au métabolisme d'activité pour la modélisation bioénergétique. Premièrement, le chapitre 3 établit que les juvéniles du saumon atlantique ne semblent pas réagir à la variabilité temporelle de l'écoulement lors de l'initiation de leurs déplacements. Cependant, il faut considérer la vitesse moyenne et l'écart-type, choisis comme caractéristiques de l'écoulement turbulent, pour estimer le temps accordé par le poisson à l'activité. Deuxièmement, nos résultats nous permettent aussi de vérifier si l'utilisation des modèles de nage forcée est justifiée dans l'estimation des coûts énergétiques de nage des poissons en rivière. Le chapitre 4 montre que les modèles de nage forcée sous-estiment les coûts énergétiques de nage observés dans un écoulement turbulent. En conséquence, nous proposons d'utiliser le nouveau modèle des coûts énergétiques de nage dans un écoulement turbulent présenté au chapitre 6 afin d'estimer le métabolisme d'activité des poissons en rivière. Le modèle des coûts énergétiques développé dans le cadre de cette thèse diffère substantiellement des modèles de nage

forcée, une approche qui domine la bioénergétique depuis les années 60 et qui persiste toujours même si on possède aujourd'hui des modèles décrivant l'activité spontanée. Dans cette perspective, il importe que les connaissances acquises dans cette thèse soient utilisées dans les modèles bioénergétiques des poissons de rivière.

Les résultats de cette thèse pourront également être utiles lors de projets de restauration et de gestion des habitats fluviaux. La pression grandissante exercée sur les ressources naturelles a mené au développement d'approches permettant d'identifier les habitats clés pour les poissons. La restauration et la gestion des habitats fluviaux requièrent des modèles qui permettent de prédire les patrons de distribution et le gain énergétique net des poissons. Malgré l'attrait conceptuel des approches spatialement explicites, des outils fonctionnels ne pourront être obtenus qu'une fois leurs suppositions de base testées et leurs modèles validés. Notre étude sur le comportement des poissons et les conséquences énergétiques de ce comportement contribue à ce qu'à l'avenir, les critères bioénergétiques utilisés pour quantifier les coûts énergétiques de l'activité des poissons et ultimement définir la qualité de l'habitat des poissons ne soient plus basés sur des suppositions arbitraires mais bien sur des critères réels.

Cette thèse apporte aussi des connaissances pratiques dont on devra tenir compte lors de la conception des passes migratoires. La formidable capacité des salmonidés à franchir des obstacles naturels est largement reconnue. Cependant, les mouvements des salmonidés passant des obstacles artificiels ne sont pas encore très bien connus (Odeh et al. 2002; Guiny et al. 2003). Les passes migratoires sont souvent des composantes inhérentes aux barrages; elles permettent de dissiper

l'énergie de l'eau et de fournir un passage alternatif aux poissons. Le succès d'une passe migratoire est assuré lorsque les poissons en trouvent aisément l'entrée et que la passe exerce un effet positif sur la survie et l'énergétique des poissons. Afin de développer des passes migratoires mieux adaptées aux besoins, il est important de comprendre précisément la réponse comportementale et physiologique des poissons aux phénomènes hydrauliques et turbulents. Notre approche pourrait donc conduire à une sensibilisation des ingénieurs civils à l'importance de l'effet de la turbulence sur les coûts énergétiques de nage et conséquemment sur la survie et l'énergétique des poissons lors du passage d'une passe migratoire.

Malgré leur contribution importante, les résultats présentés dans cette thèse ne comblent qu'une partie les lacunes dans nos connaissances sur le comportement des poissons en relation avec l'écoulement turbulent en rivière. Il serait par exemple d'un grand intérêt d'étudier davantage l'initiation des mouvements des juvéniles du saumon atlantique non seulement en relation avec les structures turbulentes à grande échelle mais aussi avec la dispersion de la dérive, qui elle-même pourrait être affectée par la turbulence. On pourrait alors mieux comprendre le déclencheur de l'initiation des mouvements.

Les études qui se penchent sur les liens entre la dynamique des fluides et la biologie des poissons sont prometteuses. L'enthousiasme de cette nouvelle avenue de recherche se manifeste par la récente croissance du nombre d'articles portant sur la thématique de la turbulence liée à la distribution, au comportement et à la physiologie des poissons. Ces articles nous proposent quelques réponses mais soulèvent également beaucoup de questions...

8 BIBLIOGRAPHIE

Abbott, J.C. et L.M. Dill (1985) Patterns of aggressive attack in juvenile steelhead trout (*Salmo gairdneri*). *Canadian Journal of Fisheries and Aquatic Sciences* **42**: 1702-1706.

Acarlar, M.S. et C.R. Smith (1987) A study of hairpin vortices in a laminar boundary layer. Part 1. Hairpin vortices generated by a hemisphere protuberance. *Journal of Fluid Mechanics* **175**: 1-41.

Allen, P.A. (1997) Earth Surface Processes. Blackwell Science, London, 404 pp.

Amundsen, P.A., H.M. Gabler, T. Herfindal et L.S. Riise (2000) Feeding chronology of Atlantic salmon parr in subarctic rivers: consistency of nocturnal feeding. *Journal of Fish Biology* **56**: 676-686.

Armstrong, J.D. (1986) Heart rate as an indicator of activity, metabolic rate, food intake and digestion in pike, *Esox lucius* L. *Journal of Fish Biology* **29**: 207-221.

Armstrong, J.D. (1998) Relationships between heart rate and metabolic rate of pike - Integration of existing data. *Journal of Fish Biology* **52**: 362-368.

Armstrong, J.D., F.A. Huntingford et N.A. Herbert (1999) Individual space use strategies of wild juvenile Atlantic salmon. *Journal of Fish Biology* **55**: 1201-1212.

Arnold, G.P. et B.H. Holford (1995) A computer simulation model for predicting rates and scales of movement of demersal fish on the European continental shelf. *ICES Journal of Marine Science* **52**: 981-990.

Arnold, G.P., P.W. Webb et B.H. Holford (1991) The role of the pectoral fins in station-holding of Atlantic salmon parr (*Salmo salar* L.). *Journal of Experimental Biology* **156**: 625-629.

Aubin-Horth, N. (2002) Déterminismes de la variation à micro-échelle d'une stratégie de reproduction conditionnelle chez le saumon atlantique mâle. Dissertation, Université Laval, Québec, Canada. 148 pp.

Aubin-Horth, N., J. Gingras et D. Boisclair (1999) Comparison of activity rates of 1+yellow perch (*Perca flavescens*) from populations of contrasting growth rates using underwater video observations. *Canadian Journal of Fisheries and Aquatic Sciences* **56**: 1122-1132.

Bachman, R.A. (1984) Foraging behaviour of free-ranging wild and hatchery trout in a stream. *Transactions of the American Fisheries Society* **113**: 1-32.

Bagatto, B., B. Pelster et W.W. Burggren (2001) Growth and metabolism of larval zebrafish: effects of swim training. *Journal of Experimental Biology* **204**: 4335-4343.

Bainbridge, R. (1958) The speed of swimming of fish as related to size and to the frequency and amplitude of the tail beat. *Journal of Experimental Biology* **35**: 109-133.

Bardonnet, A. et J.L. Baglinière (2000) Freshwater habitat of Atlantic salmon (*Salmo salar*). *Canadian Journal of Fisheries and Aquatic Sciences* **57**: 497-506.

Beamish, F.W.H. (1978) Swimming capacity. *Dans* Fish Physiology - Locomotion. *Édité par* W.S. Hoar et J.R. Randall. Academic Press, New York. 101-187.

Berst, A.H. et G.R. Spangler (1972) Lake Huron: effects of exploitation, introductions, and euthrophication on the salmonid community. *Journal of Fisheries Research Board Canada* **28**: 877–887.

Bevelhimer, M.S. (2002) A bioenergetics model for white sturgeon *Acipenser transmontanus*: assessing differences in growth and reproduction among Snake River reaches. *Journal of Applied Ichthyology* **18**: 550-556.

Bohlin, T., C. Dellefors et I. Faremo (1986) Early sexual maturation of male sea trout and salmon - an evolutionary model and some particular implications. *Fisheries Board of the Swedish Institute of Freshwater Research Drottingholm Report* **63**: 17-25.

Boily, P. et P. Magnan (2002) Relationship between individual variation in morphological characters and swimming costs in brook charr (*Salvelinus fontinalis*) and yellow perch (*Perca flavescens*). *Journal of Experimental Biology* **205**: 1031-1036.

Boisclair, D. (1992) An evaluation of the stereocinematographic method to estimate fish swimming speed. *Canadian Journal of Fisheries and Aquatic Sciences* **49**: 523-531.

Boisclair, D. (2001) Fish habitat modeling: from conceptual framework to functional tools. *Canadian Journal of Fisheries and Aquatic Sciences* **58**: 1-9.

Boisclair, D. et W.C. Leggett (1989) The importance of activity in bioenergetics models applied to actively foraging fishes. *Canadian Journal of Fisheries and Aquatic Sciences* **46**: 1859-1867.

Boisclair, D. et P. Sirois (1993) Testing assumptions of fish bioenergetics models by direct estimation of growth, consumption, and activity rates. *Transactions of the American Fisheries Society* **122**: 784-796.

Boisclair, D. et M. Tang (1993) Empirical analysis of the influence of swimming pattern on the net energetic cost of swimming in fishes. *Journal of Fish Biology* **42**: 169-183.

Bosakowski, T. et E.J. Wagner (1994) Assessment of fin erosion by comparison of relative fin length in hatchery and wild trout in Utah. *Canadian Journal of Fisheries and Aquatic Sciences* **51**: 636-641.

Bouckaert, F.W. et J. Davis (1998) Microflow regimes and the distribution of macroinvertebrates around stream boulders. *Freshwater Biology* **40**: 77-86.

Bourke, P., P. Magnan et M.A. Rodriguez (1996) Diel locomotor activity of brook charr, as determined by radiotelemetry. *Journal of Fish Biology* **49**: 1174-1185.

Bovee, K.D. (1982) A guide to stream habitat analysis using the instream flow incremental methodology. *U.S. Fish and Wildlife Service* **FWS/OBS 82/26**

Bradshaw, P. (1985) An introduction to turbulence and its measurements. Pergamon Press, Oxford. 218 pp.

Brayshaw, A.C., L.E. Frostick et I. Reid (1983) The hydrodynamics of particle clusters and sediment entrainement in coarse alluvial channels. *Sedimentology* **30**: 137-143.

Bremset, G. (2000) Seasonal and diel changes in behaviour, microhabitat use and preferences by young pool-dwelling Atlantic salmon, *Salmo salar*, and brown trout, *Salmo trutta*. *Environmental Biology of Fishes* **59**: 163-179.

Brett, J.R. (1963) The energy required for swimming by young sockeye salmon with a comparison of the drag force on a dead fish. *Transaction of the Royal Society of Canada* **1**: 441-457.

Brett, J.R. (1964) The respiratory metabolism and swimming performance of young sockeye salmon. *Journal of Fisheries Research Board Canada* **21**: 1183-1226.

Brett, J.R. (1965) The relation of size to rate of oxygen consumption and sustained swimming speed of sockeye salmon (*Oncorhynchus nerka*). *Journal of Fisheries Research Board Canada* **22**: 1491-1501.

Brett, J.R. (1973) Energy expenditure of sockeye salmon, *Oncorhynchus nerka*, during sustained performance. *Journal of Fisheries Research Board Canada* **30**: 1799-1809.

Brett, J.R. et N.R. Glass (1973) Metabolic rates and critical swimming speeds of sockeye salmon (*Oncorhynchus nerka*). *Journal of Fisheries Research Board Canada* **30**: 379-387.

Brett, J.R. et D.D. Groves (1979) Physiological energetics. *Dans* Fish Physiology - Bioenergetics and Growth. *Édité par* W.S. Hoar, J.R. Randall et J.R. Brett. Academic Press, New York. 279-352.

Briggs, C.T. et J.R. Post (1997) Field metabolic rates of rainbow trout estimated using electromyogram telemetry. *Journal of Fish Biology* **51**: 807-823.

Buffin-Bélanger, T. (2001) Structure d'un écoulement turbulent dans un cours d'eau à lit graviers en presence d'amas de galets. Dissertation, Université de Montréal, Montréal, Canada. 242 pp.

Buffin-Bélanger, T., A.G. Roy et A.D. Kirkbride (2000a) On large-scale flow structures in a gravel-bed river. *Geomorphology* **32**: 417-435.

Buffin-Bélanger, T., A.G. Roy et A.D. Kirkbride (2000b) Vers l'intégration des structures de l'écoulement dans la dynamique d'un cours d'eau à lit de graviers. *Géographie Physique et Quaternaire* **54**: 105-117.

Casey, J.M. et R.A. Myers (1998) Near extinction of a large, widely distributed fish. *Science* **281**: 690-692.

Christie, W.J. (1972) Lake Ontario: effects of exploitation, introductions, and eutrophication on the salmonid community. *Journal of Fisheries Research Board Canada* **29**: 913–929.

Christie, W.J. (1974) Changes in the fish species composition of the Great Lakes. *Journal of Fisheries Research Board Canada* **31**: 827–854.

Church, M., M.A. Hassan et J.F. Wolcott (1998) Stabilizing self-organized structures in gravel-bed stream channels: Field experimental observations. *Water resources research* **34**: 3169-3179.

COSEWIC (2002) Canadian species at risk. Committee on the Status of Endangered Wildlife in Canada. 34 pp.

Cunjak, R.A. et J. Therrien (1998) Inter-stage survival of wild juvenile Atlantic salmon, *Salmo salar* L. *Fisheries Management and Ecology* **5**: 209-223.

Cunjak, R.J. (1988) Behaviour and microhabitat of young Atlantic salmon (*Salmo salar*) during winter. *Canadian Journal of Fisheries and Aquatic Sciences* **45**: 2156-2160.

Cutts, C.J., N.B. Metcalfe et A.C. Taylor (1998) Aggression and growth depression in juvenile Atlantic salmon - the consequences of individual variation in standard metabolic rate. *Journal of Fish Biology* **52**: 1026-1037.

Davis, N.D., K.W. Myers et Y. Ishida (1998) Caloric value of high-seas salmon prey organisms and simulated salmon ocean growth and prey consumption. *North Pacific Anadromous Fisheries Commission Bulletin* **1**: 146-162.

Davison, W. (1997) The effects of exercise training on teleost fish, a review of recent literature. *Comparative Biochemistry and Physiology A* **117**: 67-75.

DeGraaf, D.A. et L.H. Bain (1986) Habitat use by and preferences of juvenile Atlantic salmon in two Newfoundland rivers. *Transactions of the American Fisheries Society* **115**: 671-681.

Dehnhardt, G., B. Mauck, W. Hanke et H. Bleckmann (2001) Hydrodynamic trail-following in harbor seals (*Phoca vitulina*). *Science* **293**: 102-104.

Dempson, J.B., C.J. Schwarz, D.G. Reddin, M.F. O'Connell, C.C. Mullins et C.E. Bourgeois (2001) Estimation of marine exploitation rates on Atlantic salmon (*Salmo salar* L.) stocks in Newfoundland, Canada. *ICES Journal of Marine Science* **58**: 331-341.

Diana, J.S. (1980) Diel activity pattern and swimming speeds of Northern Pike (*Esox lucius*) in Lac Ste. Anne, Alberta. *Canadian Journal of Fisheries and Aquatic Sciences* **37**: 1454-1458.

Dingman, S.L. (1984) Fluvial hydrology. Freeman and Co, New York. 283 pp.

Ebersole, J.L., W.J. Liss et C.A. Frissell (2003) Thermal heterogeneity, stream channel morphology, and salmonid abundance in northeastern Oregon streams. *Canadian Journal of Fisheries and Aquatic Science* **60**: 1266-1280.

Einum, S. et I.A. Fleming (1997) Genetic divergence and interactions in the wild among native, farmed and hybrid Atlantic salmon. *Journal of Fish Biology* **50**: 634-651.

Elliott, J.M. (1967) Invertebrate drift in a Dartmoor stream. *Journal of Applied Ecology* **4**: 59-71.

Enders, E.C., D. Boisclair et A.G. Roy (2003) The effect of turbulence on the cost of swimming for juvenile Atlantic salmon (*Salmo salar*). *Canadian Journal of Fisheries and Aquatic Science* **60**: 1149-1160.

Enders, E.C. et J.-P. Herrmann (2003) Energy costs of spontaneous activity in horse mackerel quantified by a computerised imaging analysis. *Archive of Fishery and Marine Research* **50**: 205-219.

Everest, F.H. et D.W. Chapman (1972) Habitat selection and spatial interaction by juvenile Chinook salmon and Steelhead trout in two Idaho streams. *Journal of Fisheries Research Board Canada* **29**: 91-100.

Facey, D.E. et G.D. Grossman (1990) The metabolic cost of maintaining position for four north American stream fishes: Effects of season and velocity. *Physiological Zoology* **63**: 757-776.

Facey, D.E. et G.D. Grossman (1992) The relationship between water velocity, energetic costs, and microhabitat use in four North American stream fishes. *Hydrobiologia* **239**: 1-6.

Farrell, A.P., C.G. Lee, K. Tierney, A. Hodaly, S. Clutterham, M. Healey, S. Hinch et A. Lotto (2003) Field-based measurements of oxygen uptake and swimming performance with adult Pacific salmon using a mobile respirometer swim tunnel. *Journal of Fish Biology* **62**: 64-84.

Fausch, K.D. (1984) Profitable stream positions for salmonids: Relating specific growth rate to net energy gain. *Canadian Journal of Zoology* **62**: 441-451.

Fausch, K.D. (1993) Experimental analysis of microhabitat selection by juvenile steelhead (*Oncorhynchus mykiss*) and coho salmon (*O. kisutch*) in a British Columbia stream. *Canadian Journal of Fisheries and Aquatic Sciences* **50**: 1198-1207.

Fausch, K.D. et R.J. White (1986) Competition among juveniles of Coho salmon, brook trout, and brown trout in a laboratory stream, and implication for Great Lakes tributaries. *Transactions of the American Fisheries Society* **115**: 363-381.

Ferguson, R.I., A.D. Kirkbride et A.G. Roy (1996) Markov analysis of velocity fluctuations in gravel-bed rivers. *Dans* Coherent Flow Structures in Open Channels. *Édité par* P.J. Ashworth, S.J. Bennett, J.L. Best et S.J. Mclelland. John Wiley & Sons Ltd., Chichester. 165-181.

Fleming, I.A. et S. Einum (1997) Experimental tests of genetic divergence of farmed from wild Atlantic salmon due to domestication. *ICES Journal of Marine Science* **54**: 1051-1063.

Fleming, I.A., K. Hindar, I.B. Mjolnerod, B. Jonsson, T. Balstad et A. Lamberg (2000) Lifetime success and interactions of farm salmon invading a native population. *Proceedings of the Royal Society of London Series B: Biological Sciences* **267**: 1517-1523.

Fleming, I.A., B. Jonsson et M.R. Gross (1994) Phenotypic divergence of sea-ranched, farmed, and wild salmon. *Canadian Journal of Fisheries and Aquatic Sciences* **51**: 2808-2824.

Forstner, H. et W. Wieser (1990) Patterns of routine swimming and metabolic rate in juvenile cyprinids at three temperatures: analysis with a respirometer-activity-monitoring system. *Comparative Biochemistry & Physiology, B* **160**: 71-76.

Fraser, N.H.C., J. Heggenes, N.B. Metcalfe et J.E. Thorpe (1995) Low summer temperatures cause juvenile Atlantic salmon to become nocturnal. *Canadian Journal of Zoology* **73**: 446-451.

Fraser, N.H.C. et N.B. Metcalfe (1997) The costs of becoming nocturnal - Feeding efficiency in relation to light intensity in juvenile Atlantic salmon. *Functional Ecology* **11**: 385-391.

Fraser, N.H.C., N.B. Metcalfe et J.E. Thorpe (1993) Temperature-dependent switch between diurnal and nocturnal foraging in salmon. *Proceedings of the Royal Society of London - Series B: Biological Sciences* **242**: 135-139.

Fraser, P.J. et R.L. Shelmerdine (2002) Fish physiology: Dogfish hair cells sense hydrostatic pressure. *Nature* **415**: 495-496.

Friedland, K.D., L.P. Hansen et D.A. Dunkley (1998) Marine temperature experienced by post-smolt and the survival of Atlantic salmon, *Salmo salar* L., in the North Sea area. *Fish Oceanography* **7**: 22-34.

Friedland, K.D., L.P. Hansen, D.A. Dunkley et J.C. MacLean (2000) Linkage between ocean climate, post-smolt growth, and survival of Atlantic salmon (*Salmo salar* L.) in the North Sea area. *ICES Journal of Marine Science* **57**: 419-429.

Friedland, K.D., D.G. Reddin, J.R. McMenemy et K.F. Drinkwater (2003) Multidecadal trends in North American Atlantic salmon (*Salmo salar*) stocks and climate. *Canadian Journal of Fisheries and Aquatic Sciences* **60**: 563-583.

Fry, F.E.J. (1971) The effect of environmental factors on the physiology of fish. *Dans* Fish Physiology - Environmental Relations and Behavior. *Édité par* W.S. Hoar et J.R. Randall. Academic Press, New York. 1-98.

Gauthier, A. (1998) Modélisation des coûts de la nage spontanée des poissons. Mémoire de maîtrise, Université de Montréal, Montréal, Canada. 70 pp.

Ginot, V. et Y. Souchon (1995) Logiciel EVHA - Evaluation de l'habitat physiques des poissons en rivière. CEMAGREF et Ministère de l'Environment, Dir. de l'Eau, Lyon, Paris.

Gjedrem, T. (2000) Genetic improvement of cold-water fish species. *Aquaculture Research* **31**: 25-33.

Gjedrem, T., H.M. Gjoen et B. Gjerde (1991) Genetic origin of Norwegian farmed Atlantic salmon. *Aquaculture* **98**: 41-50.

Gjerde, B. et L.R. Schaeffer (1989) Body traits in rainbow trout. 2. Estimates of heritabilities and of phenotypic and genetic correlations. *Aquaculture* **80**: 25-44.

Godin, J.-G.J. et R.W. Rangeley (1989) Living in the fast lane: effects of cost of locomotion on foraging behaviour in juvenile Atlantic salmon. *Animal Behaviour* **37**: 943-954.

Goolish, E.M. et I.R. Adelman (1987) Tissue-specific cytochrome oxidase activity in largemouth bass: The metabolic costs of feeding and growth. *Physiological Zoology* **60**: 454-464.

Grant, J.W.A. et D.L.G. Noakes (1987) Movers and stayers: Foraging tactics of young-of-the-year brook charr, *Salvelinus fontinalis*. *Journal of Animal Ecology* **56**: 1001-1013.

Grass, A.J. (1971) Structural features of turbulent flow over smooth and rough boundaries. *Journal of Fluid Mechanics* **50**: 233-255.

Gries, G. et F. Juanes (1998) Microhabitat use by juvenile Atlantic salmon (*Salmo salar*) sheltering during the day in summer. *Canadian Journal of Zoology* **76**: 1441-1449.

Grisdale-Helland, B., B. Ruyter, G. Rosenlund, A. Obach, S.J. Helland, M.G. Sandberg, H. Standal et C. Roesjoe (2002) Influence of high contents of dietary soybean oil on growth, feed utilization, tissue fatty acid composition, heart histology and standard oxygen consumption of Atlantic salmon (*Salmo salar*) raised at two temperatures. *Aquaculture* **207**: 311-329.

Gross, M.R. (1998) One species with two biologies: Atlantic salmon (*Salmo salar*) in the wild and in aquaculture. *Canadian Journal of Fisheries and Aquatic Sciences* **55**: 131-144.

Guay, J.C., D. Boisclair, D. Rioux, M. Leclerc, M. Lapointe et P. Legendre (2000) Development and validation of numerical habitat models for juveniles of Atlantic salmon (*Salmo salar*). *Canadian Journal of Fisheries and Aquatic Sciences* **57**: 2065-2075.

Guensch, G.R., T.B. Hardy et R.C. Addley (2001) Examining feeding strategies and position choice of drift-feeding salmonids using an individual-based, mechanistic foraging model. *Canadian Journal of Fisheries and Aquatic Sciences* **58**: 446-457.

Guiny, E., J.D. Armstrong et D.A. Ervine (2003) Preferences of mature male brown trout and Atlantic salmon parr for orifice and weir fish pass entrances matched for peak velocities and turbulence. *Ecology Freshwater Fish* **12**: 190-195.

Hansen, L.P. et J.A. Jacobsen (2003) Origin and migration of wild and escaped farmed Atlantic salmon, *Salmo salar* L., in oceanic areas north of the Faroe Islands. *ICES Journal of Marine Science* **60**: 110-119.

Hansen, M.J., D. Boisclair, S.B. Brandt, S.W. Hewett, J.F. Kitchell, M.C. Lucas et J.J. Ney (1993) Applications of bioenergetics models to fish ecology and management - Where do we go from here ? *Transactions of the American Fisheries Society* **122**: 1019-1030.

Hartman, W.L. (1972) Lake Erie: effects of exploitation, environmental changes and new species on the fishery resources. *Canadian Journal Fisheries and Aquatic Sciences* **29**: 899-912.

Hassan, M.A. et I. Reid (1990) The influence of microform bed roughness elements on flow and sediment transport in gravel bed rivers. *Earth Surface Processes and Landforms* **15**: 739-750.

Hayes, J.W., J.D. Stark et K.A. Shearer (2000) Development and test of a whole-lifetime foraging and bioenergetics growth model for drift-feeding brown trout. *Transactions of the American Fisheries Society* **129**: 315-332.

Hayward, J.S. (1965) Metabolic rate and its temperature-adaptive significance in six geographic races of *Peromyscus*. *Canadian Journal of Zoology* **43**: 309-323.

Herrmann, J.-P. et E.C. Enders (2000) Effect of body size on the standard metabolism of horse mackerel. *Journal of Fish Biology* **57**: 746-760.

Herskin, J. et J.F. Steffensen (1998) Energy savings in sea bass swimming in a school - Measurements of tail beat frequency and oxygen consumption at different swimming speeds. *Journal of Fish Biology* **53**: 366-376.

Hill, J. et G.D. Grossman (1993) An energetic model of microhabitat use for rainbow trout and rosyside dace. *Ecology* **74**: 685-698.

Hinch, S.G. et P.S. Rand (1998) Swim speeds and energy use of upriver-migrating sockeye salmon *(Oncorhynchus nerka)* - Role of local environment and fish characteristics. *Canadian Journal of Fisheries and Aquatic Sciences* **55**: 1821-1831.

Hinch, S.G. et P.S. Rand (2000) Optimal swimming speeds and forward-assisted propulsion: energy-conserving behaviours of upriver-migrating adult salmon. *Canadian Journal of Fisheries and Aquatic Sciences* **57**: 2470-2478.

Höjesjö, J., J.I. Johnsson et M. Axelsson (1999) Behavioural and heart rate responses to food limitation and predation risk: an experimental study on rainbow trout. *Journal of Fish Biology* **55**: 1009-1019.

Hughes, N.F. (1992) Selection of positions by drift-feeding salmonids in dominance hierarchies: Model and test for Arctic grayling (*Thymallus arcticus*) in subarctic mountain streams, interior Alaska. *Canadian Journal of Fisheries and Aquatic Sciences* **49**: 1999-2008.

Hughes, N.F. et L.M. Dill (1990) Position choice by drift-feeding salmonids: Model and test for Arctic grayling (*Thymallus arcticus*) in subarctic mountain streams, interior Alaska. *Canadian Journal of Fisheries and Aquatic Sciences* **47**: 2039-2048.

Hutchings, J.A. et M.E.B. Jones (1998) Life history variation and growth rate thresholds for maturity in Atlantic salmon, *Salmo salar*. *Canadian Journal of Fisheries and Aquatic Sciences* **55**: 22-47.

ICES (2003) Report of the working group on North Atlantic salmon. International Council for the Exploration of the Sea. No. ICES CM 2003/ACFM:19 Ref.D,F,C. 301 pp.

Job, S.V. (1955) The oxygen consumption of *Salvelinus fontinalis*. *University of Toronto Biological Series* **61**: 1-39.

Johnsson, J.I. (2003) Group size influences foraging effort independent of predation risk: an experimental study on rainbow trout. *Journal of Fish Biology* **63**: 863-870.

Johnsson, J.I., J. Höjesjö et I.A. Fleming (2001) Behavioural and heart rate responses to predation risk in wild and domesticated Atlantic salmon. *Canadian Journal of Fisheries and Aquatic Sciences* **58**: 788-794.

Johnston, P. (2002) Facteurs de l'habitat physique influçant le comportement et la croissance des saumons atlantique juvéniles (*Salmo salar*) des rivières Petite rivière Cacapédia et Bonaventure (Gaspésie, Québec). Mémoire de maîtrise, Université du Québec, Québec, Canada. 102 pp.

Jolicoeur, P. (1963) The multivariate generalization of the allometric equation. *Biometrics* **19**: 497-499.

Jutila, E., E. Jokikokko et M. Julkunen (2003) Management of Atlantic salmon in the Simojoki river, northern Gulf of Bothnia: effects of stocking and fishing regulation. *Fisheries Research* **64**: 5-17.

Kalleberg, H. (1958) Observations in a stream tank of territoriality and competition in juvenile Atlantic salmon and trout (*Salmo salar* L. and *S. trutta* L.). *Fisheries Board of the Swedish Institute of Freshwater Research Drottingholm Report* **39**: 55-98.

Kaseloo, P.A., A.H. Weatherley, J. Lotimer et M.D. Farina (1992) A biotelemetry system recording fish activity. *Journal of Fish Biology* **40**: 165-179.

Kausch, H. (1968) Der Einfluß der Spontanaktivität auf die Stoffwechselrate junger Karpfen (*Cyprinus carpio* L.) im Hunger und bei Fütterung. *Archiv für Hydrobiologie* **33**: 263-330.

Keenleyside, M.H.A. et F.T. Yamamoto (1961) Territorial behaviour of juvenile Atlantic salmon (*Salmo salar* L.). *Behaviour* **19**: 139-169.

Kemp, P.S., D.J. Gilvear et J.D. Armstrong (2003) Do juvenile Atlantic salmon parr track local changes in water velocity? *River Research and Applications* **19**: 569-575.

Kerr, S.R. et R.A. Ryder (1997) The Laurentian Great Lakes experience - a prognosis for the fisheries of Atlantic Canada. *Canadian Journal of Fisheries and Aquatic Sciences* **54**: 1190-1197.

Kirkbride, A.D. (1993) Observations of the influence of bed roughness on turbulence structure in depth limited flows over gravel beds. *Dans* Turbulence: Persepectives on flow and sediment transport. *Édité par* N.J. Clifford, J.R. French et J. Hardisty. John Wiley & Sons Ltd, Chichester. 185-196.

Kirkbride, A.D. et R. Ferguson (1995) Turbulent flow structure in a gravel-bed river: Markov chain analysis of the fluctuating velocity profile. *Earth Surface Processes and Landforms* **20**: 721-733.

Kitchell, J.F., D.J. Stewart et D. Weininger (1977) Applications of a bioenergetics model to yellow perch (*Perca flavescens*) and walleye (*Stizostedion vitreum vitreum*). *Journal of the Fisheries Research Board Canada* **34**: 1922-1935.

Kleiber, M. (1975) The fire of life: an introduction to animal energetics. Wiley, New York. 453 pp.

Klemetsen, A., P.A. Amundsen, J.B. Dempson, B. Jonsson, N. Jonsson, M.F. O'Connell et E. Mortensen (2003) Atlantic salmon *Salmo salar* L., brown trout *Salmo trutta* L. and Arctic charr *Salvelinus alpinus* (L.): a review of aspects of their life histories. *Ecology of Freshwater Fish* **12**: 1-59.

Kline, S.J., W.C. Reynolds, F.A. Schraub et P.W. Runstadler (1967) The structure of turbulent boundary layers. *Journal of Fluid Mechanics* **30**: 741-773.

Knighton, D. (1998) Fluvial forms & processes - A new perspective. Arnold, London. 383 pp.

Koch, F. et W. Wieser (1983) Partitioning of energy in fish: Can reduction of swimming activity compensate for the cost of production? *Journal of Experimental Biology* **107**: 415-419.

Kramer, D.L. et R.L. McLaughlin (2001) The behavioral ecology of intermittent locomotion. *American Zoologist* **41**: 137-153.

Krebs, J.R. (1978) Optimal foraging: Decision rules for predators. *Dans* Behavioural ecology: An evolutionary approach. *Édité par* J.R. Krebs et N.B. Davies. Blackwell Scientific Publications, Oxford. 23-63.

Krohn, M., S. Reidy et S. Kerr (1997) Bioenergetic analysis of the effects of temperature and prey availability on growth and condition of northern cod (*Gadus morhua*). *Canadian Journal of Fisheries and Aquatic Sciences* **54**: 113-121.

Krohn, M.M. et D. Boisclair (1994) Use of a stereo-video system to estimate the energy expenditure of free-swimming fish. *Canadian Journal of Fisheries and Aquatic Sciences* **51**: 1119-1127.

Lapointe, M. (1992) Burst-like sediment suspension events in a sand bed river. *Earth surface processes and landforms* **17**: 253-270.

Lapointe, M.F., B. De Serres, P. Biron et A.G. Roy (1996) Using spectral analysis to detect sensor noise and correct turbulence intensity and shear stress estimates from EMCM flow records. *Earth Surface Processes and Landforms* **21**: 195-203.

Leclerc, M., A. Boudreault, J.A. Bechara et G. Corfa (1995) Two-dimensional hydrodynamic modelling - A neglected tool in the instream flow incremental methodology. *Transactions of the American Fisheries Society* **124**: 645-662.

Legendre, P. et L. Legendre (1998) Numerical ecology. Elsevier Science Publishers, Amsterdam. 853 pp.

Liao, J.C., D.N. Beal, G.V. Lauder et M.S. Triantafyllou (2003) Fish exploiting vortices decrease muscle activity. *Science* **302**: 1566-1569.

Lu, S.S. et W.W. Willmarth (1973) Measurements of the structure of the Reynolds stress in a turbulent boundary layer. *Journal of Fluid Mechanics* **60**: 481-511.

Lucas, M.C., J.D. Armstrong et I.G. Priede (1993) Use of physiological telemetry as a method of estimating metabolism of fish in the natural environment. *Transactions of the American Fisheries Society* **122**: 822-833.

Lucas, M.C., I.G. Priede, J.D. Armstrong, A.N.Z. Gindy et L.d. Vera (1991) Direct measurements of metabolism, activity and feeding behaviour of pike, *Esox lucius* L., in the wild, by the use of heart rate telemetry. *Journal of Fish Biology* **39**: 325-345.

MacCrimmon, H.R. et B.L. Gots (1979) World distribution of Atlantic salmon (*Salmo salar*). *Canadian Journal of Fisheries Research Board Canada* **36**: 422-457.

Mäki-Petäys, A., A. Huusko, J. Erkinaro et T. Muotka (2002) Transferability of habitat suitability criteria of juvenile Atlantic salmon (*Salmo salar*). *Canadian Journal of Fisheries and Aquatic Sciences* **59**: 218-228.

Martel, G. (1996) Growth rate and influence of predation risk on territoriality in juvenile coho salmon (*Oncorhynchus kisutch*). *Canadian Journal of Fisheries and Aquatic Sciences* **53**: 660-669.

Mathur, D., W.H. Bason, E.J. Purdy, Jr. et C.A. Silver (1985) A critique of the instream flow incremental methodology. *Canadian Journal of Fisheries and Aquatic Sciences* **42**: 825-831.

McDonald, D.G., C.L. Milligan, W.J. McFarlane, S. Croke, S. Currie, B. Hooke, R.B. Angus, B.L. Tufts et K. Davidson (1998) Condition and performance of juvenile Atlantic salmon (*Salmo salar*): effects of rearing practices on hatchery fish and comparison with wild fish. *Canadian Journal of Fisheries and Aquatic Sciences* **55**: 1208-1219.

McLaughlin, R.L. et D.L.G. Noakes (1998) Going against the flow - an examination of the propulsive movements made by young brook trout in streams. *Canadian Journal of Fisheries and Aquatic Sciences* **55**: 853-860.

Ménard, C. (1991) Utilisation de la vidéo pour mesurer les poissons *in situ*. Mémoire de maîtrise, Université de Montréal, Montréal, Canada. 88 pp.

Mills, D.D. (1989) Ecology and management of Atlantic salmon. Chapman & Hall, London 351 pp.

Mills, E.L., J.H. Leach, J.T. Carlton et C.L. Secor (1994) Exotic species and the integrity of the Great Lakes. *Bioscience* **44**: 666-669.

Misund, O.A. et A.K. Beltestad (1996) Target-strength estimates of schooling herring and mackerel using the comparison method. *ICES Journal of Marine Science* **53**: 281-284.

Moir, H.J., C. Soulsby et A.F. Youngson (2002) Hydraulic and sedimentary controls on the availability and use of Atlantic salmon (*Salmo salar*) spawning habitat in the River Dee system, north-east Scotland. *Geomorphology* **45**: 291-308.

Montgomery, J., G. Carton, R. Voigt, C. Baker et C. Diebel (2000) Sensory processing of water currents by fishes. *Philosophical Transactions of the Royal Society of London Series B: Biological Sciences* **355**: 1325-1327.

Montgomery, J.C., F. Macdonald, C.F. Baker et A.G. Carton (2002) Hydrodynamic contributions to multimodal guidance of prey capture behavior in fish. *Brain Behavior and Evolution* **59**: 190-198.

Moore, A., I.C. Russell et E.C.E. Potter (1990) The effects of intraperitoneally implanted dummy acoustic transmitters on the behaviour and physiology of juvenile Atlantic salmon, *Salmo salar* L. *Journal of Fish Biology* **37**: 713-721.

Morantz, D.L., R.K. Sweeney, C.S. Shirvell et D.A. Longard (1987) Selection of microhabitat in summer by juvenile Atlantic salmon (*Salmo salar*). *Canadian Journal of Fisheries and Aquatic Sciences* **44**: 120-129.

Morgan, I.J., I.D. McCarthy et N.B. Metcalfe (2000) Life-history strategies and protein metabolism in overwintering juvenile Atlantic salmon: growth is enhanced in early migrants through lower protein turnover. *Journal of Fish Biology* **56**: 637-647.

Morgan, I.J., I.D. McCarthy et N.B. Metcalfe (2002) The influence of life-history strategy on lipid metabolism in overwintering juvenile Atlantic salmon. *Journal of Fish Biology* **60**: 674-686.

Myers, R.A. et B. Worm (2003) Rapid worldwide depletion of predatory fish communities. *Nature* **423**: 280-283.

Nakagawa, H. et I. Nezu (1981) Structure of space-time correlations of bursting phenomena in an open-channel flow. *Journal of Fluid Mechanics* **104**: 1-43.

Ney, J.F. (1993) Bioenergetics modelling today: Growing pains on the cutting edge. *Transactions of the American Fisheries Society* **122**: 736-748.

Nezu, I. et H. Nakagawa (1993) Turbulence in open channel flows. A.A. Balkema, Rotterdam. 281 pp.

Nislow, K.H., C. Folt et M. Seandel (1998) Food and foraging behaviour in relation to microhabitat use and survival of age-0 Atlantic salmon. *Canadian Journal of Fisheries and Aquatic Sciences* **55**: 116-127.

Nislow, K.H., C.L. Folt et D.L. Parrish (2000) Spatially explicit bioenergetic analysis of habitat quality for age-0 Atlantic salmon. *Transactions of the American Fisheries Society* **129**: 1067-1081.

Noakes, D.J., R.J. Beamish et M.L. Kent (2000) On the decline of Pacific salmon and speculative links to salmon farming in British Columbia. *Aquaculture* **183**: 363-386.

Northcutt, R.G. (1997) Animal behaviour - Swimming against the current. *Nature* **389**: 915-916.

O'Brien, W.J. et J.J. Showalter (1993) Effects of current velocity and suspended debris on the drift feeding of Arctic grayling. *Transactions of the American Fisheries Society* **122**: 609-615.

Odeh, M., J.F. Noreika, A. Haro, A. Maynard, T. Castro-Santos et G.F. Cada (2002) Evaluation of the effects of turbulence on the behavior of migratory fish. Report to Bonneville Power Administration. No. Contract No., 00000022, Project No. 200005700. 55 pp.

Økland, F., B. Finstad, R.S. McKinley, E.B. Thorstad et R.K. Booth (1997) Radio-transmitted electromyogram signals as indicators of physical activity in Atlantic salmon. *Journal of Fish Biology* **51**: 476-488.

Orth, D.J. et O.E. Maughan (1982) Evaluation of the incremental methodology for recommending instream flows for fishes. *Transactions of the American Fisheries Society* **111**: 413-445.

Ott, J. (1988) Einführung in die Meereskunde. Ulmer, Stuttgart. 386 pp.

Ovidio, M. (1999) Cycle annuel d'activité de la truite commune (*Salmo trutta*) adulte: étude par radio-pistage dans un cours d'eau de l'Ardenne belge. *Bulletin Français de la Pêche et de la Pisciculture* **352**: 1-18.

Parrish, J.K. (1999) Using behavior and ecology to exploit schooling fishes. *Environmental Biology of Fishes* **55**: 157-181.

Pauly, D., V. Christensen, J. Dalsgaard, R. Froese et F.J. Torres (1998) Fishing down marine food webs. *Science* **279**: 860-863.

Pauly, D., V. Christensen, S. Guenette, T.J. Pitcher, U.R. Sumaila, C.J. Walters, R. Watson et D. Zeller (2002) Towards sustainability in world fisheries. *Nature* **418**: 689-695.

Pauly, D. et R. Watson (2003) Counting the last fish. *Scientific American* **289**: 42-47.

Pavlov, D.S., A.I. Lupandin et M.A. Skorobogatov (2000) The effects of flow turbulence on the behavior and distribution of fish. *Journal of Ichthyology* **40**: S232-S261.

Pedersen, J. (1996) Discrimination of fish layers using the three-dimensional information obtained by a split-beam echo-sounder. *ICES Journal of Marine Science* **53**: 371-376.

Pitcher, T.J. et P.J.B. Hart (1982) Fisheries ecology. Chapman & Hall, London. 414 pp.

Priede, I.G. et A.H. Young (1977) The ultrasonic telemetry of cardiac rhythms of wild free-living brown trout (*Salmo trutta* L.) as an indicator of bioenergetics and behaviour. *Journal of Fish Biology* **10**: 299-318.

Puckett, K.J. et L.M. Dill (1984) Cost of sustained and burst swimming to juvenile coho salmon (*Oncorhynchus kisutch*). *Canadian Journal of Fisheries and Aquatic Sciences* **41**: 1546-1551.

Puckett, K.J. et L.M. Dill (1985) The energetics of feeding territoriality in juvenile coho salmon (*Oncorhynchus kisutch*). *Behaviour* **92**: 97-111.

Rader, R.B. (1997) A functional classification of the drift: Traits that influence invertebrate availability to salmonids. *Canadian Journal of Fisheries and Aquatic Science* **54**: 1211-1234.

Rand, P.S. et D.J. Stewart (1998) Prey fish exploitation, salmonine production, and pelagic food web efficiency in Lake Ontario. *Canadian Journal of Fisheries and Aquatic Sciences* **55**: 318-327.

Rea, L.D. et D.P. Costa (1992) Changes in standard metabolism during long-term fasting in northern elephant seal pups (*Mirounga- angustirostris*). *Physiological Zoology* **65**: 97-111.

Reddin, D.G. et K.D. Friedland (1999) A history of identification to continent of origin of Atlantic salmon (*Salmo salar* L.) at west Greenland. *Fisheries Research* **43**: 221-235.

Regier, H.A. et W.L. Hartman (1973) Lake Erie's fish community: 150 years of cultural stresses. *Science* **180**: 1248-1255.

Rempel, L.L., J.S. Richardson et M.C. Healey (2000) Macroinvertebrate community structure along gradients of hydraulic and sedimentary conditions in a large gravel-bed river. *Freshwater Biology* **45**: 57-73.

Reynolds, O. (1883) An experimental investigation of the circumstances which determine whether the motion of water shall be direct or sinous, and the law of resistance in parallel channels. *Philosophical Transactions of the Royal Society of London* **174**: 935-982.

Richards, K.S. (1976) The morphology of riffle-pool sequences. *Earth Surface Processes and Landforms* **1**: 71-88.

Rimmer, D.M., U. Paim et R.L. Saunders (1983) Autumnal habitat shift of juvenile Atlantic salmon (*Salmo salar*) in a small river. *Canadian Journal of Fisheries and Aquatic Sciences* **40**: 671-680.

Rinberg, D. et H. Davidowitz (2000) Do cockroaches 'know' about fluid dynamics ? *Nature* **405**: 756.

Rowan, D.J. et J.B. Rasmussen (1996) Measuring the bioenergetic cost of fish activity in situ using a globally dispersed radiotracer (^{137}Cs). *Canadian Journal of Fisheries and Aquatic Sciences* **53**: 734-745.

Roy, A.G., P.M. Biron, T. Buffin-Bélanger et M. Levasseur (1999) Combined visual and quantitative techniques in the study of natural turbulent flows. *Water Resources Research* **35**: 871-877.

Roy, A.G. et T. Buffin-Bélanger (2001) Advances in the study of turbulent flow structures in gravel-bed rivers. *Dans* Gravel-Bed River V. *Édité par* M.P. Mosley. New Zealand Hydrological Society, New Zealand. 375-397.

Roy, A.G., T. Buffin-Bélanger et S. Deland (1996) Scales of turbulent coherent flow sructures in a gravel-bed river. *Dans* P.J. Ashworth, S.J. Bennett, J.L. Best et S.J. Mclelland, eds. *Coherent Flow Structures in Open Channels*. John Wiley & Sons Ltd., Chichester: Pages 147-164

Roy, A.G., T. Buffin-Bélanger, H. Lamarre et A.D. Kirkbride (2004) Size, shape and dynamics of large-scale turbulent flow structures in a gravel-bed river. *Water Resources Research.* **500:** 1-27.

Sabo, M.J., D.J. Orth et E.J. Pert (1996) Effect of stream microhabitat characteristics on rate of net energy gain by juvenile smallmouth bass, *Micropterus dolomieu*. *Environmental Biology of Fishes* **46**: 393-403.

Scarenecchia, D.L. (1984) Climatic and oceanic variations affecting yield of Icelandic stocks in Atlantic salmon (*Salmo salar*). *Canadian Journal of Fisheries and Aquatic Sciences* **41**: 917-935.

Scherrer, B. (1984) Biostatistique. Gaëtan Morin, Montreal. 850 pp.

Schindler, D.W. (2001) The cumulative effects of climate warming and other human stresses on Canadian freshwaters in the new millennium. *Canadian Journal of Fisheries and Aquatic Sciences* **58**: 18-29.

Schurmann, H. et J.F. Steffensen (1994) Spontaneous swimming activity of Atlantic cod *Gadus morhua* exposed to graded hypoxia at three temperatures. *Journal of Experimental Biology* **197**: 129-142.

Sirois, P. et D. Boisclair (1995) The influence of prey biomass on activity and consumption rates of brook trout. *Journal of Fish Biology* **46**: 787-805.

Smit, H. (1965) Some experiments on the oxygen consumption of goldfish (*Carassius auratus*) in relation to swimming speed. *Canadian Journal of Zoology* **43**: 623-633.

Somers, K.M. (1986) Multivariate allometry and removal of size with principal components analysis. *Systematic Zoology* **35**: 359-368.

Spoor, W.A. (1946) A quantitative study of the relationship between the activity and oxygen consumption of goldfish, and its application to the measurement of respiratory metabolism in fishes. *Biological Bulletin* **91**: 312-325.

Standen, E.M., S.G. Hinch, M.C. Healey et A.P. Farrell (2002) Energetic costs of migration through the Fraser River Canyon, British Columbia, in adult pink (*Oncorhyncus gorbuscha*) and sockeye (*Oncorhynchus nerka*) salmon as assessed by EMG telemtery. *Canadian Journal of Fisheries and Aquatic Sciences* **59**: 1809-1818.

Steffensen, J.F. (2002) Metabolic cold adaptation of polar fish based on measurements of aerobic oxygen consumption: fact or artefact? Artefact! *Comparative Biochemistry & Physiology, A* **132**: 789-795.

Stephens, D.W. et J.R. Krebs (1986) Foraging theory. Princeton University Press, Princeton. 247 pp.

Stewart, D.J. et M. Ibarra (1991) Predation and production by salmonine fishes in Lake Michigan, 1978-88. *Canadian Journal of Fisheries and Aquatic Sciences* **48**: 909-922.

Stewart, D.J., D. Weininger, D.V. Rottiers et T.A. Edsall (1983) An energetics model for lake trout, *Salvelinus namaycush*: Application to the Lake Michigan population. *Canadian Journal of Fisheries and Aquatic Sciences* **40**: 681-698.

Stradmeyer, L. et J.E. Thorpe (1987a) Feeding behaviour of wild Atlantic salmon, *Salmo salar* L., parr in mid- to late summer in a Scottish river. *Aquaculture and Fisheries Management* **18**: 33-49.

Stradmeyer, L. et J.E. Thorpe (1987b) The responses of hatchery-reared Atlantic salmon, *Salmo salar* L., parr to pelletted and wild prey. *Aquaculture and Fisheries Management* **18**: 51-61.

Strauss, R.E. et F.L. Bookstein (1982) The truss: Body form reconstruction in morphometrics. *Sytematic Zoology* **31**: 113-135.

Sureau, D. et J.P. Lagardere (1991) Coupling of heart rate and locomotor activity in sole, *Solea solea* (L.), and bass, *Dicentrarchus labrax* (L.), in their natural environment by using ultrasonic telemetry. *Journal of Fish Biology* **38**: 399-405.

Swain, D.P., B.E. Riddell et C.B. Murray (1991) Morphological differences between hatchery and wild populations of coho salmon (*Oncorhynchus kisutch*): Environmental versus genetic origin. *Canadian Journal of Fisheries and Aquatic Sciences* **48**: 1783-1791.

Tang, M. et D. Boisclair (1995) Relationship between respiration rate of juvenile brook trout (*Salvelinus fontinalis*), water temperature, and swimming characteristics. *Canadian Journal of Fisheries and Aquatic Sciences* **52**: 2138-2145.

Tang, M., D. Boisclair, C. Menard et J.A. Downing (2000) Influence of body weight, swimming characteristics, and water temperature on the cost of swimming in brook trout (*Salvelinus fontinalis*). *Canadian Journal of Fisheries and Aquatic Sciences* **57**: 1482-1488.

Theodorsen, T. (1952) Mechanism of turbulence. *Proceedings of the 2nd Midwestern Conference on Fluid Mechanics*, Ohio State University, Columbus: 1-18.

Tritton, D.J. (1988) Physical fluid dynamics. Clarendon Press, Oxford. 519 pp.

Trudel, M. et D. Boisclair (1996) Estimation of fish activity costs using underwater video cameras. *Journal of Fish Biology* **48**: 40-53.

Trudel, M., D.R. Geist et D.W. Welch (2004) Modeling the oxygen consumption rates in Pacific salmon and steelhead trout: an assessment of current models and practices. *Transactions of the American Fisheries Society* **133**: 326-348.

Van Winkle, W., H.I. Jager, S.F. Railsback, B.D. Holcomb, T.K. Studley et J.E. Baldrige (1998) Individual-based model of sympatric populations of brown and rainbow trout for instream flow assessment - Model description and calibration. *Ecological Modelling* **110**: 175-207.

Vehanen, T. (2003) Adaptive flexibility in the behaviour of juvenile Atlantic salmon: short-term responses to food availability and threat from predation. *Journal of Fish Biology* **63**: 1034-1045.

Vehanen, T., P.L. Bjerke, J. Heggenes, A. Huusko et A. Mäki-Petäys (2000) Effect of fluctuating flow and temperature on cover type selection and behaviour by juvenile brown trout in artificial flumes. *Journal of Fish Biology* **56**: 923-937.

Vogel, S. (1994) Life in moving fluid: The physical biology of flow. Princeton University Press, Princeton, N.J. 467 pp.

Wankowski, J.W.J. (1979) The role of food particle size in the growth of juvenile Atlantic salmon, *Salmo salar*. *Journal of Fish Biology* **14**: 351-370.

Wardle, C.S. et J.W. Kanwisher (1974) The significance of heart rate in free swimming cod, *Gadus morhua*: Some observations with ultra-sonic tags. *Marine Behavioural Physiology* **2**: 311-324.

Weatherley, A.H., S.C. Rogers, D.G. Pincock et J.R. Patch (1982) Oxygen consumption of active rainbow trout, *Salmo gairdneri* Richardson, derived from electromyograms obtained by radiotelemetry. *Journal of Fish Biology* **20**: 479-489.